Motor Compensation During Lower Limb Pedaling After Stroke

Brice Thomas Cleland
Marquette University

MOTOR COMPENSATION DURING LOWER LIMB PEDALING AFTER STROKE

by

Brice T. Cleland, B.S., M.S.

A Dissertation submitted to the Faculty of the Graduate School,
Marquette University,
in Partial Fulfillment of the Requirements for
the Degree of Doctor of Philosophy

Milwaukee, Wisconsin

August 2018

ABSTRACT
MOTOR COMPENSATION DURING LOWER LIMB PEDALING AFTER STROKE

Brice T. Cleland, B.S., M.S.

Marquette University, 2018

Long-term motor dysfunction in the lower limb is common after stroke. One potential contributor is motor compensation, a behavior in which functions originally performed by the paretic limb are performed by the non-paretic limb. Compensation in chronic stroke may contribute to long-term motor dysfunction by limiting functional ability, impairing future recovery, and eliciting maladaptive neuroplasticity. The purpose of this dissertation was to describe the impact of compensation on motor function and brain activation during lower limb pedaling and identify elements that produce this behavior.

To achieve this purpose, we evaluated muscle activation and motor performance when compensation was prevented. During unilateral pedaling, paretic muscle activation increased but motor performance deteriorated. During bilateral uncoupled pedaling, paretic muscle activation further increased. However, subjects were unable to coordinate movements of the legs, and motor performance further deteriorated. These results suggest that compensation improves motor performance but limits paretic motor output. Because motor performance was worse during bilateral uncoupled than unilateral pedaling, impaired interlimb coordination may be a primary factor leading to compensation. As a follow-up, we determined whether altered interlimb spinal reflex pathways contribute to impaired interlimb coordination after stroke. Interlimb cutaneous reflexes were elicited during pedaling, and we assessed whether the amplitude was altered. Interlimb reflex was altered, particularly in bifunctional muscles and at pedaling transitions. Reflex alterations were correlated with impairments in interlimb coordination and compensation. These data suggest that stroke-related changes in interlimb reflex pathways undermine interlimb coordination. Finally, we assessed whether altered motor commands and performance, such as seen with compensation, are related to decreased pedaling-related brain activation after stroke. Brain activation was measured during volitional pedaling and during passive pedaling, when between-group differences were minimized. Between-group differences in brain activation persisted during passive pedaling, suggesting that altered motor commands and pedaling performance do not account for reduced brain activation after stroke.

Overall, these studies provide insight into rehabilitative interventions that may decrease long-term motor dysfunction in the lower limb after stroke. One potential strategy is to enhance paretic muscle activity by preventing compensation while simultaneously employing efforts to improve interlimb coordination, possibly by manipulating interlimb reflex pathways.

ACKNOWLEDGMENTS

Brice T. Cleland, B.S., M.S.

There are so many people to thank for helping me along the path to complete this dissertation. First, none of this would have been possible without the guidance of my advisor, Dr. Sheila Schindler-Ivens. I have learned so much from you through the process of writing fellowship applications, designing experiments and collecting data, and organizing findings into manuscripts. I will apply the lessons I've learned throughout the rest of my career in academia. More importantly, you have been my most valuable mentor for both my personal and professional life. I cannot thank you enough for your support, encouragement, and friendship over the last five years.

I would like to thank my committee members, Dr. Allison Hyngstrom, Dr. Derek Kamper, and Dr. Brian Schmit, for their feedback and support through this process. You have provided unique and helpful perspectives on my work and pushed me to improve my understanding and conveyance of the work included in this dissertation. I can see how time and energy intensive it is to serve on a dissertation committee, and I am so grateful that you were willing to invest those resources in me.

There is an army of current and former lab members who helped me complete this work. Most of all, I would like to thank Brett Arand, Mary Asma, and Nutta-on Promjunyakul. Brett and Nutta-on (Oiy), thank you so much for the extensive amount of time you spent helping me acclimate to the pedaling device and fMRI procedures when I first came to the lab. Mary, thank you for your incredible help collecting and analyzing data for Chapter 4 of this document. I would like to thank Tamicah Gelting and Jan Struhar for their help collecting data for Chapter 2 of this document. Finally, thank you to Domenic Busa, Jiao Fan, Tianyu Jiang, Ben Rappaport, Tom Ruopp, Christine Smith, Amanda Waldera, and Sam Wojcinski for all of your help over the last several years. Besides help with the scientific work in the lab, all of you have been great friends.

There are a variety of other individuals who have helped me throughout this effort. Thank you to Dr. Sandra Hunter for your feedback throughout the dissertation process. Thank you to Dr. Steve Kautz for your assistance in preparing my pre-doctoral fellowship and for your help during the piloting phase of one of the projects. Thank you to Dr. Taly Gilat-Schmidt for reviewing my comprehensive exam. I also want to thank my fellow CTRH students, particularly those in the "Agraphia" writing group for your support and encouragement. Thank you to the CTRH faculty and staff for your essential support. Additionally, this work would not have been possible without the support of the American Heart Association Pre-Doctoral Fellowship.

Finally, I want to thank my family and friends for their love and support for many years more than this dissertation has taken. Thank you Mom, Dad, Chris, Cecilia, and the whole Harling family. Most of all, thank you to my wife Alyssa. You have adapted your life to fit my professional career goals for the last 7 years. You have endured countless hours of practice talks, many triumphs and frustrations, and the typical graduate student guilt about not doing enough work. Thank you, and I love you.

TABLE OF CONTENTS

LIST OF TABLES

LIST OF FIGURES

ABBREVIATIONS

AFNI	Analysis of Functional NeuroImages
AFO	ankle foot orthosis
AM	adductor magnus
ANOVA	Analysis of Variance
BA6	Brodmann's area 6
BF	biceps femoris
BMI	body mass index
BOLD	blood-oxygenation-level dependent contrast
Cb	cerebellum
CIMT	constraint-induced movement therapy
COM	center of mass
COV	coefficient of variation
CPG	central pattern generator
CRP	continuous relative phase
EEG	electroencephalography
EMG	electromyography
FM/FMA	Fugl Meyer Assessment
fMRI	functional magnetic resonance imaging
fNIRS	functional near infrared spectroscopy
FOV	field of view
LI	laterality index
M1S1	primary motor and sensory cortices
MEP	motor evoked potential
MG	medial gastrocnemius
MI	modulation index
MR	magnetic resonance
MRI	magnetic resonance imaging
MVC	maximal voluntary contraction
PCI	phase coordination index
PET	positron emission tomography
PMC	premotor cortex
PT	perceptual threshold
rCBF	regional cerebral blood flow
RF	rectus femoris
RPM	revolutions per minute
ROI	region of interest
RT	radiating threshold
rTMS	repetitive transcranial magnetic stimulation
SICI	short-interval intracortical inhibition
SOL	soleus
SM	semimembranosus
SMA	supplementary motor area
SMC	sensorimotor cortex

ST	semitendinosus
T1	longitudinal relaxation time constant
T2	transversal spin-spin decay time constant
T2*	transversal decay time constant
TA	tibialis anterior
tDCS	transcranial direct current stimulation
TE	echo time
TES	transcranial electrical stimulation
TMS	transcranial magnetic stimulation
TR	repetition time
VL	vastus lateralis
VM	vastus medialis

CHAPTER 1: LITERATURE REVIEW

1.1 Introduction

A stroke is an injury to the brain caused by a lack of blood flow to brain tissue (ischemia) or bleeding from the vasculature into the surrounding brain tissue (hemorrhage). Approximately 795,000 individuals in the U.S.A. are affected by stroke each year, and 7.2 million living individuals have previously had a stroke (Benjamin et al., 2017). In many of these individuals, stroke affects areas that are directly or indirectly involved in motor commands. Consequently, many stroke survivors exhibit motor impairments, including weakness or paralysis of the limbs contralateral to the damaged hemisphere. It is estimated that up to 88% of stroke survivors experience motor impairments of the upper and lower limb during the initial period after stroke (Bonita & Beaglehole, 1988). Motor deficits in the lower limb are particularly detrimental because they are strongly related to disability (Desrosiers et al., 2003).

Over the first 6 months after stroke, substantial recovery of strength, function, and ability to perform activities of daily living occurs in the lower limb (Duncan et al., 1994; L. Jørgensen & Jacobsen, 2001; Mayo et al., 1999; Skilbeck, Wade, Hewer, & Wood, 1983; Wade, Wood, & Hewer, 1985). A meta-analysis by Hendricks et al. (2002) found that ~65% of stroke survivors experience some degree of motor recovery in the lower limb within the acute and sub-acute stages. Despite this initial stage of recovery, many stroke survivors have persistent lower limb motor impairments. For example, after discharge from rehabilitation, 36% of stroke survivors are still unable to walk independently (H. S. Jørgensen, Nakayama, Raaschou, & Olsen, 1995). In addition,

walking speed in chronic stroke is often below that required for community ambulation (Desrosiers et al., 2003). These persistent lower limb deficits restrict independence and prevent the performance of activities of daily living.

The persistence of motor deficits in chronic stroke suggests that lower limb rehabilitation techniques have been inadequate. For example, a recent meta-analysis found that body-weight supported treadmill training elicits improvements in walking, but these improvements are often not clinically relevant (Mehrholz, Thomas, & Elsner, 2017). A limitation to the development of more effective rehabilitation techniques is our lack of knowledge about what factors contribute to long-term motor dysfunction after stroke. One potential contributor to long-term motor dysfunction in the lower limb is motor compensation, a behavior in which functions originally performed by the paretic limb are performed by the non-paretic limb. Motor compensation can facilitate acute recovery but often persists chronically despite recovery of paretic motor function. This is problematic because this behavior may limit functional ability, impair future recovery of paretic motor function, and elicit neuroplastic changes that reinforce these negative effects, thus contributing to long-term motor dysfunction (Levin, Kleim, & Wolf, 2009).

Therefore, additional knowledge about compensation may be imperative for developing more successful rehabilitation strategies. This project sought to describe how compensation is related to motor function and brain activation during lower limb pedaling and identify elements that cause this behavior to persist chronically. Pedaling was used as the experimental paradigm because of its similarities with walking. Both tasks involve rhythmic, bilateral flexion and extension across multiple joints and muscle groups. At the same time, pedaling does not require body-weight support or balance,

allowing the performance of unilateral tasks and the performance of tasks that challenge coordination. This chapter provides a literature review of topics critical for understanding the work included in this dissertation. First, motor compensation after stroke is characterized. Next, elements that may contribute to chronic motor compensation after stroke are defined and discussed. These elements include paretic motor impairments, impaired interlimb coordination, and learned non-use. Finally, we discuss the relation between compensation and movement-related brain activation. Specific aims and hypotheses follow.

1.2 Motor compensation after stroke

Broadly, motor compensation after stroke describes the phenomenon whereby functions of the paretic limb are "taken over, replaced, or substituted by different end effectors or body segments" (Levin et al., 2009). In this dissertation, I focus on a form of compensation where the non-paretic limb performs these functions. It is assumed that this behavior occurs because of impaired or neglected function of the paretic limb. I also focus on involuntary, not deliberate manifestations of this phenomenon.

Compensation has been repeatedly observed in the upper limb, where the non-paretic limb performs tasks normally executed by the paretic limb, including reaching and other activities of daily living (Castro, 1977; Nudo & Milliken, 1996; Rinehart, Singleton, Adair, Sadek, & Haaland, 2009; Vega-González & Granat, 2005). Overall, real-world everyday use is lower in the paretic than the non-paretic upper limb, regardless of handedness (Han et al., 2013; Sterr, Freivogel, & Schmalohr, 2002). Compensation is also prevalent during lower limb tasks. For example, during standing, the non-paretic

limb bears more weight and contributes more to postural control than the paretic limb (Geurts, de Haart, van Nes, & Duysens, 2005; Roerdink, Geurts, de Haart, & Beek, 2009). When rising from a chair, stroke survivors bear more weight on their non-paretic limb and are unaware of this asymmetry (Briere, Lauziere, Gravel, & Nadeau, 2010).

During bilateral, locomotor movements of the lower limb, compensation is signified by kinetic asymmetries between limbs. When walking, the non-paretic limb produces less braking and more propulsive force, work, impulse, and power than the paretic limb (Bowden, Balasubramanian, Neptune, & Kautz, 2006; Olney, Griffin, Monga, & McBride, 1991; Raja, Neptune, & Kautz, 2012; Turns, Neptune, & Kautz, 2007). Overall, the non-paretic limb accounts for ~60% of the total work or power produced throughout the walking cycle. There are corresponding kinetic asymmetries at specific phases of the walking cycle. At toe-off, kinetic energy is lower in the paretic limb and higher in the non-paretic limb as compared to controls (G. Chen, Patten, Kothari, & Zajac, 2005). During pre-swing, net joint moments are decreased in the paretic limb, particularly because of decreased ankle plantarflexion work and power (G. Chen & Patten, 2008; Peterson, Hall, Kautz, & Neptune, 2010). During lower limb pedaling, the non-paretic limb produces more net mechanical work than the paretic limb, resulting from less braking and more propulsion (Alibiglou & Brown, 2011; Brown & Kautz, 1998; Brown, Kautz, & Dairaghi, 1997; H. Y. Chen, Chen, Chen, Fu, & Wang, 2005; De Marchis et al., 2015; Kautz & Brown, 1998; Landin, Hagenfeldt, Saltin, & Wahren, 1977; Perell, Gregor, & Scremin, 1998).

Kinetic asymmetries between the paretic and non-paretic limb during walking are associated with kinematic asymmetries. In terms of spatial kinematics, paretic limb

progression is often accomplished with pelvic hiking and circumduction of the paretic limb and increased bilateral hip flexion (Allen, Kautz, & Neptune, 2011; G. Chen et al., 2005; Knutsson & Richards, 1979). Key findings at individual joints include: 1) paretic knee flexion is decreased at toe-off and during swing but increased at heel strike and stance, often resulting in hyperextension; 2) paretic hip flexion is decreased at heel strike but increased at toe-off; and 3) ankle plantarflexion is increased at heel strike and midswing but decreased at toe-off (Burdett, Borello-France, Blatchly, & Potter, 1988; G. Chen et al., 2005; Knutsson & Richards, 1979). Temporally, stroke survivors have a longer swing time and shorter stance time in the paretic limb as compared to the non-paretic limb and controls (Brandstater, de Bruin, Gowland, & Clark, 1983; G. Chen et al., 2005; A. L. Hsu, Tang, & Jan, 2003; C. M. Kim & Eng, 2003; Olney et al., 1991; von Schroeder, Coutts, Lyden, Billings, & Nickel, 1995). These kinematic asymmetries are correlated with kinetic asymmetries and likely occur to retain balance amid impaired paretic support and propulsion (C. M. Kim & Eng, 2003; Olney & Richards, 1996).

A major assumption of many of these studies is that kinetic asymmetries during bilateral locomotor movements of the lower limb are representative of compensation. However, kinetic asymmetries could result from decreased motor output from the paretic limb without a compensatory increase in motor output from the non-paretic limb. If true, compensation would be an erroneous term to describe kinetic asymmetries. Nevertheless, some evidence suggests that the non-paretic limb has a higher output than it would if motor output from the paretic limb were not decreased. During walking, plantarflexor moments are larger and electromyography (EMG) amplitude is larger in several muscles in the non-paretic limb than in controls, including at times when the muscle is not

normally active (Allen et al., 2011; Raja et al., 2012). In many pedaling studies, control and stroke subjects pedaled against the same workload. Therefore, when the non-paretic limb performs >50% of the net work, it is performing greater absolute work than each limb in controls. These studies have shown that the non-paretic limb produces at least 62% more work than each limb in controls (Alibiglou & Brown, 2011; Brown & Kautz, 1998; Brown et al., 1997; Kautz & Brown, 1998). Overall, these findings support the argument that compensation is an appropriate description of asymmetries between the paretic and non-paretic limb during bilateral locomotor movements of the lower limb.

Compensation is common during acute stroke. During this time, motor deficits in the paretic limb are the greatest, partly because of transient effects distant to the site of the stroke, termed diaschisis (Feeney & Baron, 1986). Because of motor deficits in the paretic limb, compensatory motor patterns are often adopted to help quickly improve motor function. For example, in rats, the use of novel movement patterns helps restore the success of reaching movements (Alaverdashvili, Foroud, Lim, & Whishaw, 2008; Gharbawie & Whishaw, 2006). In humans, the adoption of compensatory strategies is essential for upper limb motor recovery in many stroke survivors (Nakayama, Jørgensen, Raaschou, & Olsen, 1994). Accordingly, compensation is often reinforced in acute stroke rehabilitation because it is effective at restoring function, particularly in more impaired individuals (Levin et al., 2009; O'Sullivan, Schmitz, & Fulk, 2014). Although compensation may have beneficial effects acutely, the persistence of motor compensation into the chronic phase of stroke may have negative effects.

Negative effects of compensation

First, compensation may limit functional ability. Stroke survivors walk slower than controls, and those with the least paretic plantarflexion (most compensation) walk the slowest (Brandstater et al., 1983; Lin, Yang, Cheng, & Wang, 2006; Nadeau, Gravel, Arsenault, & Bourbonnais, 1999; Patterson et al., 2008). Similarly, individuals with more asymmetrical overall force production during walking have slower walking speeds (Bowden et al., 2006; C. M. Kim & Eng, 2003). The converse is also true; individuals with increased contribution from the paretic limb and less compensatory activation in the non-paretic limb have faster walking speeds (Hall, Peterson, Kautz, & Neptune, 2011). Training-induced improvements in walking speed are driven by an increase in paretic—not non-paretic—propulsion (Hsiao, Awad, Palmer, Higginson, & Binder-Macleod, 2015). One specific strategy that offsets decreased paretic propulsion during walking after stroke is increased bilateral hip flexion (G. Chen & Patten, 2008). Use of this compensatory strategy is associated with slower maximal walking velocity and decreased ability to modulate walking velocity (Jonkers, Delp, & Patten, 2009; Nadeau et al., 1999; Patterson et al., 2008). Specifically, stroke survivors who increase hip flexion to compensate for poor paretic plantarflexion have an impaired ability to modulate stance or swing time, and thus have impaired ability to increase walking speed (Jonkers et al., 2009). Besides walking speed, kinetic asymmetries during walking and pedaling are associated with a higher degree of hemiparesis and poorer function (Bowden et al., 2006; Brown et al., 1997; De Marchis et al., 2015).

Second, compensation may elicit neuroplasticity that reinforces compensatory behaviors and reduces future recovery of paretic motor ability. In monkeys, the recovery

of skilled hand use after an infarct largely occurs through compensatory movements (Friel & Nudo, 1998; Hoffman & Strick, 1995). Simultaneously, the cortical territory for skilled hand use shrinks, and the cortical territory for more proximal movements expands (Nudo & Milliken, 1996). In rats, dendritic branching, axonal growth, and synapse number are decreased in the ipsilesional hemisphere and increased in the contralesional hemisphere after a cortical lesion (Biernaskie & Corbett, 2001; Bury & Jones, 2002; Jones, Kleim, & Greenough, 1996; Jones & Schallert, 1994; Napieralski, Butler, & Chesselet, 1996; Stroemer, Kent, & Hulsebosch, 1995). These neural adaptations occur naturally after a cortical lesion but are enhanced by training or by increased use of the non-paretic limb (Bury & Jones, 2002; Jones & Schallert, 1994). These neuroplastic changes may reinforce compensation and impair future recovery of paretic motor function. For example, rats who perform reach training with the non-paretic limb after a cortical lesion have poorer reaching performance with the paretic limb (Allred, Maldonado, Hsu And, & Jones, 2005). In addition, reach training with the non-paretic limb impairs motor re-learning in the paretic limb and enhances motor learning in the non-paretic limb (Allred & Jones, 2008; Allred et al., 2005; Bury & Jones, 2002).

Third, compensatory motor patterns are less efficient. For example, because of the decrease in propulsion and postural support from the paretic limb, walking is often accomplished with the kinematic changes described above, such as pelvic hiking or circumduction of the paretic limb (G. Chen et al., 2005; Knutsson & Richards, 1979). These alterations in walking kinematics contribute to increased energy cost of walking, independent of walking speed (Finley & Bastian, 2017; Olney, Monga, & Costigan, 1986; Platts, Rafferty, & Paul, 2006; Zamparo, Francescato, De Luca, Lovati, & di

Prampero, 1995). Increased energy cost of movements may reduce independence and increase physical inactivity and fatigue.

Surprisingly, despite the negative effects of chronic compensation, this behavior is prevalent during locomotor movements of the lower limb in chronic stroke. Chronic compensation is also surprising because diaschisis has been resolved by the chronic stage, and there has been at least some restoration of function in the paretic limb. Several findings suggest that the paretic limb has regained function, and chronic compensation may not be necessary to ensure good task performance. During quiet standing, R. W. Bohannon and Larkin (1985) have shown that people with stroke bear approximately 40% of their body weight on the paretic limb. Yet, when asked to shift their weight, they can bear up to 70% body weight on the paretic limb. During walking, when chronic stroke survivors are asked to take long steps with their paretic limb, muscle activity increases, and forward propulsion increases by 319% in the paretic limb (Clark, Neptune, Behrman, & Kautz, 2016). Going from self-selected to a fast walking speed produces a 28% increase in propulsion in the paretic limb (Hsiao, Awad, Palmer, Higginson, & Binder-Macleod, 2016). During pedaling, increases in workload or changes in posture can elicit an increase in the mechanical work performed by the paretic limb (Brown & Kautz, 1998; Brown et al., 1997). Therefore, it is important to understand the elements that cause compensation to persist in chronic stroke despite the restoration of function and the consequences of this behavior.

1.3 Contributing elements to compensation

There are several potential reasons why compensation might persist during chronic stroke. Potential reasons include 1) residual motor impairments in the paretic limb and 2) impaired interlimb coordination. Both might impair task performance when the contribution from the paretic limb is increased. If true, compensation might occur because it decreases the impact of these impairments, allowing the maintenance of task performance. Another potential reason is that learned nonuse leads to compensation despite the ability to successfully perform the task with greater contribution from the paretic limb (paretic limb is neglected). These possibilities are discussed below.

1.3.1 Paretic motor impairments

Numerous motor impairments in the paretic limb might lead to impaired task performance when the contribution from the paretic limb is increased during locomotor tasks in the lower limb. Strength and power deficits in the paretic limb have been described in every major lower limb muscle group, including the hip flexors, hip extensors, hip abductors, knee extensors, knee flexors, ankle dorsiflexors, and ankle plantarflexors (Allen et al., 2011; Richard W Bohannon & Andrews, 1995; Harris, Polkey, Bath, & Moxham, 2001; Klein, Brooks, Richardson, McIlroy, & Bayley, 2010; Klein, Power, Brooks, & Rice, 2013; Newham & Hsiao, 2001; Sanchez, Acosta, Lopez-Rosado, Stienen, & Dewald, 2017). Decreased strength and power may limit the ability of the paretic limb to perform key aspects of locomotion (e.g. advance the limb or support the weight of the body), leading to decrements in task performance. For instance,

many stroke survivors are unable to properly advance the paretic limb despite near maximal activation of their paretic plantarflexors during walking (Allen et al., 2011; G. Chen & Patten, 2008; Nadeau et al., 1999). This suggests that plantarflexor weakness impairs the ability of the paretic limb to successfully participate in the task.

The mechanisms underlying decreased force and power in the paretic limb are both muscular and neural. At the muscular level, lean tissue mass is decreased by ~5% in the lower limb (English, McLennan, Thoirs, Coates, & Bernhardt, 2010). In the thigh, cross sectional area is decreased by ~15%. There is a concomitant increase in the amount of intramuscular fat in the lower limb (Ryan, Buscemi, Forrester, Hafer-Macko, & Ivey, 2011; Ryan, Dobrovolny, Smith, Silver, & Macko, 2002). The reduction in lean tissue mass and increase in intramuscular fat is thought to result from several interrelated processes, including immobilization, disuse, and neural effects of stroke (Gracies, 2005). Since the primary determinant of force and power production is the number of cross bridges in parallel, these alterations after stroke are impactful (Enoka, 2008).

At the neural level, stroke leads to changes in motor unit number and firing properties that contribute to decreased force and power production. There are fewer motor units in the paretic than the non-paretic hand and forearm, and firing properties are affected in the remaining units (Arasaki et al., 2006; Li, Wang, Suresh, Rymer, & Zhou, 2011; Lukacs, 2005; Lukács, Vécsei, & Beniczky, 2008; McComas, Sica, Upton, & Aguilera, 1973). Mean, minimum, and maximum motor unit firing rates are lower, and the motor unit recruitment range is compressed in the paretic tibialis anterior (TA) and biceps brachii (Chou, Palmer, Binder-Macleod, & Knight, 2013; Gemperline, Allen, Walk, & Rymer, 1995; Rosenfalck & Andreassen, 1980). During walking, motor units

for the TA have a lower peak firing rate in the paretic than the non-paretic limb (Frontera, Grimby, & Larsson, 1997). Overall, altered firing rates and motor unit recruitment in the paretic limb may result from decreased corticomotor drive to the paretic limb, as found in the plantarflexors (Palmer, Zarzycki, Morton, Kesar, & Binder-Macleod, 2017).

Several studies have used the interpolated twitch technique to test for impairments in the ability to voluntarily activate the muscle in stroke survivors. During this technique, a supra-maximal electrical stimulus is applied to the nerve or muscle while a maximal voluntary contraction (MVC) is performed. Additional force produced by the stimulation represents a deficit in the ability to voluntarily activate the muscle (Shield & Zhou, 2004). Several studies using this technique have demonstrated that stroke survivors have a diminished ability to voluntarily activate the paretic musculature, including the elbow flexor, knee extensor, and plantarflexor muscles (Harris et al., 2001; Klein et al., 2010; Klein et al., 2013; Newham & Hsiao, 2001; Riley & Bilodeau, 2002). Deficits in voluntary activation could exacerbate limitations to force and power production.

Post-stroke alterations at the muscular and neural level are reflected in the reduction in EMG activity in the paretic limb. During walking, EMG activity is lower in multiple muscles in the paretic compared to the non-paretic limb and controls, including the TA, medial gastrocnemius (MG), vastus medialis (VM), rectus femoris (RF), vastus lateralis (VL), semitendinosus (ST), biceps femoris (BF), adductor longus, gluteus medius, and gluteus maximus (Frontera et al., 1997; Gray, Pollock, Wakeling, Ivanova, & Garland, 2015; Hirschberg & Nathanson, 1952; Knutsson & Richards, 1979; Raja et al., 2012). For example, EMG in the TA is nearly 10X smaller in the paretic than the non-paretic leg (Frontera et al., 1997). During pedaling, RF, BF, and semimembranosus (SM)

activation is lower in the paretic than the non-paretic limb (Brown et al., 1997; H. Y. Chen et al., 2005).

Even when force/power and the extent of muscle activation is maintained, alterations in the phasing of muscle activity could also impair the performance of cyclical locomotor movements involving the paretic limb. During walking, EMG phasing is altered in TA, BF, MG, soleus (SOL), and RF (Allen, Kautz, & Neptune, 2014; Den Otter, Geurts, Mulder, & Duysens, 2006, 2007; Gray et al., 2015; Knutsson & Richards, 1979; Peterson et al., 2010). Coactivation is greater for BF/RF, BF/MG, and RF/MG in the paretic limb during walking, which could also impair performance (Den Otter et al., 2007; Knutsson & Richards, 1979; Lamontagne, Richards, & Malouin, 2000). During pedaling, RF, BF, and SM activity is phase-advanced and VM activity is prolonged in the paretic limb (Kautz & Brown, 1998). These abnormalities in muscle phasing are associated with decreased net paretic propulsion/work during walking and pedaling (Allen, Kautz, & Neptune, 2013; Kautz & Brown, 1998; Turns et al., 2007).

Overall, strength and power are reduced (with muscular and neural causes), and the phasing of muscle activation is altered in the paretic limb after stroke. These paretic motor impairments might worsen the performance of cyclical locomotor movements of the lower limb when the paretic contribution to the task is increased. For example, paretic motor deficits may limit the ability to advance the limb or support the weight of the body. Thus, instead of experiencing impaired locomotor performance because of paretic motor impairments, compensation may occur to maintain task performance.

1.3.2 Impaired interlimb coordination

Another factor that might contribute to chronic compensation after stroke is impaired interlimb coordination. Interlimb coordination is the organized functioning of multiple limbs performing a motor task with a shared goal (Swinnen & Duysens, 2004). This is achieved through the mutual influence of the sensorimotor state of each limb on the other involved limbs. Interlimb coordination can be operationalized as the "spatiotemporal relationships between kinematic, kinetic, and physiological variables of two or more limbs" (Shirota et al., 2016). Interlimb coordination is thought to be important during lower limb locomotor movements, helping signal phase transitions, maintain stability, and respond to perturbations (Swinnen & Duysens, 2004; Zehr & Stein, 1999). Consequently, impairments in interlimb coordination after stroke might harm performance during locomotor tasks.

Besides the countless examples of coordinated kinematic, kinetic, and physiological variables between limbs during locomotor movements (e.g. Sousa, Silva, Santos, Sousa, & Tavares, 2013), many studies have demonstrated interlimb coordination through the application of mechanical perturbations. In spinal cats and humans, walking on a split-belt treadmill with the belts moving at different speeds produces an adaptation of the muscle activity and spatiotemporal characteristics to the activity in the contralateral limb (Dietz, Zijlstra, & Duysens, 1994; Forssberg, Grillner, Halbertsma, & Rossignol, 1980; Halbertsma, 1983; Reisman, Block, & Bastian, 2005). Application of a mechanical perturbation to one leg evokes an alteration in the muscle activity, kinematics, and kinetics of the contralateral leg (Berger, Dietz, & Quintern, 1984; Dietz, Horstmann, & Berger, 1989; Dietz, Quintern, Boos, & Berger, 1986; Eng, Winter, & Patla, 1994).

During pedaling, spatiotemporal patterns of muscle activation and force generation in a pedaling limb are altered when the contralateral limb is performing pedaling, rhythmic contractions, or sustained isometric contractions (Kautz, Brown, Van der Loos, & Zajac, 2002; Ting, Kautz, Brown, & Zajac, 2000; Ting, Raasch, Brown, Kautz, & Zajac, 1998). Muscle activation and force generation also adapt to changes in the phasing between pedals (Alibiglou, López-Ortiz, Walter, & Brown, 2009).

Although research into this area is sparse, there are a few studies that provide insight into alterations of interlimb coordination during lower limb movements after stroke. Dietz & Berger (1984) tested the response to a surface tilt perturbation during standing in individuals with spastic paresis. Responses in the paretic leg were delayed after a perturbation of either leg, and response amplitude was decreased in both limbs after a perturbation of the paretic leg. When performing ankle tracking movements, EMG phasing in the paretic limb is worse when the task is performed bilaterally as compared to unilaterally (Tseng & Morton, 2010). EMG phasing and accuracy in the non-paretic limb also is impaired by concurrently performing tracking movements with the paretic limb (Madhavan, Rogers, & Stinear, 2010; Tseng & Morton, 2010). During hip flexion and extension, torque production in the paretic limb is phase advanced, with a greater effect during bilateral as compared to unilateral movement (Hyngstrom, Onushko, Chua, & Schmit, 2010).

There are also some studies that shed light on how interlimb coordination during locomotion is altered after stroke. During walking, interlimb phasing is abnormal and more variable in stroke compared to controls (Meijer et al., 2011; Roerdink, Lamoth, Kwakkel, van Wieringen, & Beek, 2007). Stroke survivors also have abnormal responses

in the contralateral limb to perturbations in the ipsilateral limb during walking (Berger et al., 1984; Krasovsky, Lamontagne, Feldman, & Levin, 2013). During pedaling, interlimb effects are enhanced in stroke survivors, particularly in bifunctional muscles involved in pedaling transitions (Kautz et al., 2002; Kautz & Patten, 2005; Kautz, Patten, & Neptune, 2006; Rogers, Stinear, Lewis, & Brown, 2011). Kautz & Patten (2005) found that when both the non-paretic and paretic limb participate in pedaling, motor impairments in the paretic limb are the most pronounced. Unilateral pedaling in one leg induces muscle activity in the contralateral leg, and this effect is greater in stroke survivors than controls (Kautz et al., 2006). Overall, these studies provide evidence that interlimb coordination is impaired during lower limb movements after stroke.

Impairments in interlimb coordination after stroke could result from alterations in the control of several neural pathways. Specifically, coordination between legs during locomotion is thought to be mediated through supraspinal, spinal central pattern generator (CPG), and interlimb sensory reflex pathways (Swinnen & Duysens, 2004). Propriospinal pathways from the upper limbs also play a role in enabling interlimb coordination during tasks involving both the arms and legs. Besides direct impairments in any of these pathways, there is evidence that descending supraspinal neuromodulation and/or modulation by CPG circuity also contribute to the control of interlimb coordination. These factors can affect signals important for interlimb coordination that exist in multiple pathways. The accumulation of evidence suggests that interlimb coordination is redundantly controlled through these pathways. Thus, it is likely that each of these pathways is involved to some extent in interlimb coordination and may contribute to impairments after stroke. Below I discuss these various pathways.

Descending supraspinal signals may be important for interlimb coordination. Descending supraspinal signals may have bilateral effects through ipsilateral uncrossed pathways, branched bilateral pathways, and/or interhemispheric interactions between motor regions within the cortex (Carson, 2005). Ipsilateral, uncrossed projections facilitate the ipsilateral influence of neural signals that have their primary effect contralaterally. As much as 30% of corticospinal tract fibers descend ipsilaterally, where they synapse at multiple levels, including onto ipsilateral motoneurons (Jankowska & Edgley, 2006). The reticulospinal and vestibulospinal tracts (which receive inputs from the cortex) also have direct and indirect projections to ipsilateral limb motoneurons.

After stroke, it has been suggested that use of ipsilateral projections is enhanced to aid in the restoration of function of the paretic limb (Jankowska & Edgley, 2006). Enhancement of these ipsilateral pathways or bilateral branched pathways might also impair interlimb coordination. Several studies support a role of ipsilateral supraspinal input for interlimb coordination and alterations in this pathway after stroke. Paretic EMG phasing gets worse during pedaling when the non-paretic limb is also pedaling or performing static contractions (Kautz & Patten, 2005; Rogers et al., 2011). Impaired paretic phasing occurs regardless of whether the movements of the limbs are in-phase or antiphase. Therefore, the negative influence of the non-paretic on the paretic limb seems to be related to the supraspinal commands associated with activation of the non-paretic limb. Similarly, greater descending ipsilateral conductivity is associated with worse performance during antiphase ankle movements after stroke (Madhavan et al., 2010). These effects could be mediated through a number of the pathways described above, including ipsilateral uncrossed and bilateral crossed pathways. Abnormal

interhemispheric interactions may also mediate these effects and impair interlimb coordination. Multiple studies have found that the non-lesioned hemisphere inhibits the primary motor cortex in the lesioned hemisphere (Murase, Duque, Mazzocchio, & Cohen, 2004; Traversa, Cicinelli, Pasqualetti, Filippi, & Rossini, 1998).

Despite evidence for a role of supraspinal input for interlimb coordination, steady-state locomotion still occurs in spinal (various levels) and decerebrate cats with only small changes in interlimb coordination (Duysens & Pearson, 1976; Forssberg & Grillner, 1973). The primary change in spinal cats is that step timing between hindlimbs becomes more variable (Eidelberg, Story, Meyer, & Nystel, 1980; Kato, Murakami, Yasuda, & Hirayama, 1984). These results suggest that descending supraspinal input plays a role in interlimb coordination but is not essential.

Another pathway that may be important for interlimb coordination involves the interconnections between spinal central pattern generators (CPGs) in the spinal cord. Commissural interneurons connect CPGs controlling each limb, likely providing neural information that is important for coordination between limbs (Butt, Lebret, & Kiehn, 2002; Swinnen & Duysens, 2004). There are no known studies that evaluate alterations in these pathways after stroke, likely because of the difficulty of isolating them. Despite the theoretical importance of interlimb CPG pathways for interlimb coordination, Kato (1988) found that a longitudinal lumbar myelotomy minimally impacted interlimb coordination during walking in spinal cats. This suggests that commissural connections between CPGs (at least at the lumbar level) are not essential for interlimb coordination.

A third pathway that may be involved in interlimb coordination involves interlimb sensory reflex pathways. Interlimb sensory reflex pathways are thought to be important

for interlimb coordination because of the effects of altered sensory information on walking. When one limb is deafferented in chronic spinal and decerebrate cats, stepping becomes unstable and more variable when one limb is deafferented (Giuliani & Smith, 1987; Grillner & Zangger, 1984). In humans with spinal cord injury, locomotor patterns are more normal with the addition of limb loading and hip joint sensory information (Dietz, Müller, & Colombo, 2002). Similarly, bilateral antiphase hip flexion and extension enhances reflex effects that support bilateral coordination in individuals with spinal cord injury (Onushko & Schmit, 2007). Other studies have used electrical stimulation to demonstrate a role for interlimb sensory reflex pathways in interlimb coordination. Electrical stimulation applied to the hindlimb elicits coordinated responses in both hindlimbs during walking in spinal, decerebrate, and intact cats (Duysens, 1977; Duysens & Loeb, 1980; Duysens, Loeb, & Weston, 1980; Forssberg, Grillner, & Rossignol, 1977; Gauthier & Rossignol, 1981). Cutaneous stimulation applied during human walking and running also elicits coordinated responses in both limbs (Duysens, Tax, van der Doelen, Trippel, & Dietz, 1991; Duysens, Trippel, Horstmann, & Dietz, 1990; Tax, Van Wezel, & Dietz, 1995; Van Wezel, Ottenhoff, & Duysens, 1997; Yang & Stein, 1990). Despite evidence for a role of interlimb reflex pathways in interlimb coordination, coordinated, phasic muscle activity is present in both limbs during stepping in cats that have been spinalized and had dorsal column dissection (Grillner & Zangger, 1979). As with the other pathways, these results suggest that interlimb sensory reflexes play a role in interlimb coordination but are not essential.

Several studies suggest that interlimb sensory pathways are affected by stroke. In the upper limb, afferent information from the non-paretic limb elicits normal responses in

the paretic limb at a latency consistent with spinal pathways (Dietz & Schrafl-Altermatt, 2016). In contrast, afferent information from the paretic limb elicits abnormal responses in the non-paretic limb. During hip flexion and extension, reflex-related torque production in the paretic limb is more phase advanced during bilateral antiphase movements as compared to unilateral movement (Hyngstrom et al., 2010). During walking, a perturbation of either limb during swing phase elicits delayed interlimb reflexes in stroke compared to control subjects (Sharafi, Hoffmann, Tan, & Y, 2016). Zehr & Loadman (2012) have also found that reflex amplitude is altered in the paretic limb in several muscles when cutaneous stimulation is applied to the non-paretic limb. Consequently, altered control of these sensory reflex pathways may contribute to impaired interlimb coordination after stroke.

Overall, as with paretic motor deficits, impairments in interlimb coordination may degrade performance of cyclical locomotor movements of the lower limb. Specifically, deficits in interlimb coordination involving supraspinal, spinal, or afferent pathways could negatively affect phase transitions, the maintenance of stability, and responses to perturbations. Accordingly, instead of experiencing poorer locomotor performance because of impairments in interlimb coordination, compensation may be employed to maintain performance. Similarly, poor interlimb coordination may make it difficult to produce force and increase the metabolic cost of locomotion, leading to compensation (Sousa & Tavares, 2015).

1.3.3 Learned nonuse

Compensation after stroke might also occur because of learned non-use. Learned non-use is a phenomenon whereby stroke survivors can produce voluntary movement with the paretic limb but fail to do so spontaneously in real world situations (see Taub, Uswatte, Mark, & Morris, 2006 for review). Learned non-use emerges when initial attempts to use the paretic limb are unsuccessful, while use of the non-paretic limb enables goal-directed movement. Thus, stroke survivors learn not to use the paretic limb. This behavior becomes habitual, and in the chronic state, people with stroke do not recognize that the paretic limb has regained function and become useful again. Ultimately, this results in disproportionately more compensation than expected as a result of the actual stroke-related damage (Taub, 2012; Taub et al., 1993). The theory behind learned non-use was developed based on similar findings in deafferented primates (Taub, 1976). Although different operational definitions are used, in its purest form, learned non-use requires the ability to acutely increase the use of the paretic limb while maintaining good performance (Sunderland & Tuke, 2005).

There are some reports that potentially support the existence of learned non-use after stroke. In the upper limb, stroke survivors have low spontaneous use of the paretic limb during reaching and steering but can acutely increase use of the paretic limb if required to do so (Han et al., 2013; Johnson, Paranjape, Strachota, Tchekanov, & McGuire, 2011; Sterr et al., 2002). As discussed earlier, stroke survivors can also increase paretic limb use during quiet standing, walking, and pedaling (R. W. Bohannon & Larkin, 1985; Brown & Kautz, 1998; Brown et al., 1997; Clark et al., 2016; Hsiao et al., 2015). Although these studies demonstrate that paretic limb use can be acutely increased, they all report deficits in performance with the paretic limb. Consequently, the

reduced use of the paretic limb might occur because these paretic motor deficits impair the performance of the task, not because of learned nonuse (Sunderland & Tuke, 2005).

Other potential support for learned non-use comes from the multitude of studies demonstrating the effectiveness of constraint-induced movement therapy (CIMT). CIMT is a rehabilitation technique that restricts non-paretic limb use while intensive training of the paretic limb is undertaken (Taub, Uswatte, & Pidikiti, 1999). This therapy improves performance and increases spontaneous use of the paretic upper limb (Miltner, Bauder, Sommer, Dettmers, & Taub, 1999; Taub et al., 1993; Wolf, Lecraw, Barton, & Jann, 1989). In the lower limb, there have been few attempts at applying CIMT-like strategies. In one case, a splint was applied to the non-paretic limb in conjunction with physical therapy (Numata, Murayama, Takasugi, & Oga, 2008). After only two days, function improved in the paretic leg. Kahn & Hornby (2009) found some short-term and long-term changes in gait symmetry when stroke survivors performed unilateral step training.

However, the improvements that result from CIMT are only partly from reversal of learned non-use. For example, Taub et al. (1993) found that the paretic limb had regained ~50% of its total recovery by the end of the first day of training. The remaining recovery likely involved some motor (re)learning. Correspondingly, CIMT has also been shown to elicit neuroplastic adaptations including a shift of activation towards the affected hemisphere and increased motor map size (Dong, Winstein, Albistegui-DuBois, & Dobkin, 2007; Liepert, Uhde, Gräf, Leidner, & Weiller, 2001; Sawaki et al., 2008; Schaechter et al., 2002). CIMT-induced improvements in motor function were associated with increased functional magnetic resonance imaging (fMRI) activity in the ipsilesional premotor cortex (PMC) and secondary somatosensory cortex (Johansen-Berg et al.,

2002). These neuroplastic changes suggest that CIMT has a motor learning effect in addition to potentially reversing learned non-use.

1.4 Motor compensation & brain activation

In section 1.3, I considered potential contributing elements to chronic motor compensation. In this section, I consider the relation between motor compensation and brain activation. As discussed above, one of the potential negative effects of compensation is that it may elicit neuroplasticity that reinforces compensatory behaviors and reduces future recovery of paretic motor ability. In humans, functional neuroimaging studies abound that demonstrate altered movement-related brain activation that may be indicative of neuroplasticity. Most of these studies have used fMRI or positron emission tomography (PET) to investigate alterations in brain activation during movements of the upper limb. In acute and subacute stroke, the dominant findings have been that brain activation is more bilateral and more common in secondary motor areas such as the supplementary motor cortex (SMA), PMC, cingulate, and cerebellum (Cb) during movements of the paretic compared to the non-paretic upper limb (Calautti, Leroy, Guincestre, & Baron, 2001; Calautti, Leroy, Guincestre, Marié, & Baron, 2001; Cao, D'Olhaberriague, Vikingstad, Levine, & Welch, 1998; Carey, Abbott, Egan, Bernhardt, & Donnan, 2005; Chollet et al., 1991; Cramer et al., 1997; Marshall et al., 2000; Ward, Brown, Thompson, & Frackowiak, 2003b; Weiller, Chollet, Friston, Wise, & Frackowiak, 1992). In chronic stroke, movement-related brain activation becomes more like controls, but is still abnormal (Rehme, Eickhoff, Rottschy, Fink, & Grefkes, 2012). During finger, wrist, and elbow movements of the paretic limb, chronic stroke survivors

show more bilateral activation than during movements of the non-paretic limb (Calautti, Leroy, Guincestre, Marié, et al., 2001; Marshall et al., 2000; Nelles et al., 1999; Rehme, Fink, von Cramon, & Grefkes, 2011; Szameitat, Shen, Conforto, & Sterr, 2012).

Studies investigating lower limb movements after stroke have also found evidence of altered brain activation. In subacute and chronic stroke, paretic knee flexion/extension is associated with greater bilateral activation and activation in atypical brain areas, as compared to movements of the non-paretic limb (Y. H. Kim et al., 2006; Luft et al., 2005). During ankle dorsiflexion of the paretic limb, chronic stroke survivors have reduced overall brain activation compared to controls (Dobkin, Firestine, West, Saremi, & Woods, 2004). Additionally, a shift of activation to the contralesional hemisphere during paretic ankle dorsiflexion is correlated with worse functional ability (Enzinger et al., 2009; Enzinger et al., 2008).

Fewer studies have evaluated brain activation during locomotor movements after stroke because of the difficulty of performing these tasks during fMRI or PET. However, some investigators have used functional near infrared spectroscopy (fNIRS) to evaluate changes in blood flow during walking. Miyai et al. (2002) found increased brain activation in the contralesional sensorimotor cortex (SMC), SMA, pre-SMA, and PMC in stroke compared to control subjects during body-weight supported treadmill walking. Other investigators have evaluated brain activation during pedaling, which is more amenable to fMRI and PET environments. Using this paradigm, Promjunyakul, Schmit, & Schindler-Ivens (2015) found that stroke survivors have a decreased volume of brain activation compared to healthy controls across all regions of the cortex. Lin, Chen, & Lin

(2013) found that brain activation was generally higher in the contralesional than the ipsilesional hemisphere during pedaling after stroke.

In most of these studies, altered movement-related brain activation after stroke is suggested to result from neuroplastic changes. For example, as discussed above, many have suggested that increased activation of the contralesional hemisphere represents increased use of ipsilateral projections. However, changes in movement-related brain activation after stroke may also result from changes in volitional motor commands and motor performance associated with compensation. For example, kinetic, kinematic, and muscle activation profiles of walking are altered with compensation after stroke (e.g. Bowden et al., 2006; Den Otter et al., 2007; Knutsson & Richards, 1979). These changes may be associated with different patterns of brain activation. For instance, Promjunyakul et al. (2015) found that pedaling-related brain activation volume after stroke was highest in individuals with the least compensation. Consequently, these changes in volitional motor commands and motor performance associated with compensation confound the neuroplastic interpretation of functional brain imaging data (for review see Baron et al., 2004; Krakauer, 2007). Although inter-dependent, it is important to differentiate these causes of altered movement-related brain activation after stroke because this information could guide rehabilitation efforts.

1.5 Specific Aims

The purpose of this dissertation was to describe how compensation is related to motor function and brain activation during lower limb pedaling and identify elements that cause this behavior to persist chronically. To this end, Aim 1 (Chapter 2) of this

dissertation evaluated compensation during pedaling post-stroke and how it is related to potentially contributing elements: paretic motor impairments, impaired interlimb coordination, and learned nonuse. Finding evidence that interlimb coordination may contribute to compensation, Aim 2 (Chapter 3) of this dissertation determined whether altered interlimb sensory reflex pathways are associated with impaired interlimb coordination and compensation during pedaling after stroke. Finally, Aim 3 (Chapter 4) of this dissertation determined whether reduced pedaling-related brain activation post-stroke can be explained by compensation or neuroplasticity. Specific aims and hypotheses are presented below. Figure 1.1 provides a visual framework for the specific aims and their interrelations.

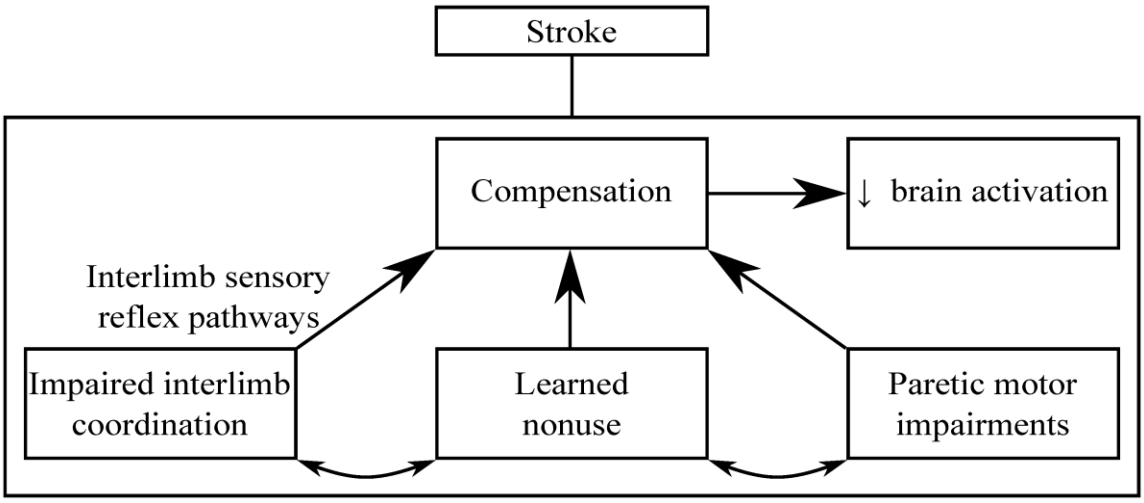

Figure 1.1. Framework for specific aims. After stroke, compensation occurs during lower limb pedaling. Aim 1 of this dissertation evaluated whether paretic motor impairments, impaired interlimb coordination, and/or learned nonuse are related to compensation. As depicted, these elements have mutual influences. Finding evidence that impaired interlimb coordination is related to compensation, Aim 2 determined whether altered interlimb reflex pathways are associated with impaired interlimb coordination and compensation. Because of the potential impact of compensation on neuroplasticity, Aim 3 determined whether decreased pedaling-related brain activation after stroke can be explained by altered volitional motor commands and pedaling performance (as seen during compensation).

Aim 1: Evaluate muscle activation and pedaling performance when compensation is prevented with unilateral and bilateral uncoupled pedaling, and determine whether paretic motor impairments, impaired interlimb coordination, or learned nonuse may contribute to compensation after stroke.

Subjects performed conventional, unilateral, and bilateral uncoupled pedaling. During unilateral and bilateral uncoupled pedaling, the pedals on our custom device were mechanically decoupled. For bilateral uncoupled pedaling, subjects were asked to pedal with both legs while attempting to maintain an antiphase relation between the pedals. Muscle activation and pedaling performance (i.e. rate, smoothness, and phasing) were measured. Compensation was measured as the percent mechanical work of pedaling performed by the paretic limb during conventional pedaling.

Hypothesis 1: If paretic motor impairments contribute to compensation, then pedaling performance would deteriorate during paretic unilateral pedaling as compared to conventional pedaling.

Hypothesis 2: If impaired interlimb coordination contributes to compensation, then pedaling performance would deteriorate in both limbs during bilateral uncoupled as compared to conventional and unilateral pedaling.

Hypothesis 3: If pure learned nonuse contributes to compensation, then paretic muscle activation would increase during unilateral and bilateral uncoupled pedaling, with minimal difference in performance as compared to conventional pedaling.

Aim 2: Determine whether interlimb cutaneous reflexes are altered during pedaling after stroke and whether alterations are associated with impaired interlimb coordination and compensation.

Stroke and control subjects performed conventional pedaling while electrical stimulation was applied to the sural nerve of the paretic and non-paretic limb. The amplitude of interlimb cutaneous reflexes was considered at different pedaling positions. In addition, interlimb coordination was measured as the ability to maintain an antiphase pedal relation during bilateral uncoupled pedaling, and compensation was measured as the proportion of pedaling work performed by the paretic limb. The relation between these measures of interest was assessed.

Hypothesis 1: The amplitude of interlimb cutaneous reflexes would be altered in stroke as compared to control subjects.

Hypothesis 2: If altered interlimb sensory reflex pathways are associated with impaired interlimb coordination and compensation, then 1) interlimb cutaneous reflex amplitude would be correlated with interlimb coordination during bilateral uncoupled pedaling, and 2) interlimb cutaneous reflex amplitude would be correlated with the proportion of pedaling work performed by the paretic limb during conventional pedaling.

Aim 3: Determine whether reduced pedaling-related brain activation after stroke can be explained by altered volitional motor commands and pedaling performance, as assessed with passive vs. volitional pedaling.

Stroke and control subjects performed volitional and passive pedaling during fMRI. During volitional pedaling, subjects used their own voluntary muscle activity to pedal. During passive pedaling, subjects relaxed and allowed an experimenter to move their limbs. The passive condition eliminated motor commands to pedal and minimized between-group differences in pedaling performance, which are altered by compensation. Thus, remaining differences in brain activation are likely reflective of neuroplastic changes.

Hypothesis: If volitional motor commands and pedaling performance contribute to reduced pedaling-related brain activation post-stroke, then: 1) between-group differences would be reduced during passive as compared to volitional pedaling and 2) brain activation would be different between passive and volitional pedaling.

1.6 Instrumentation and methods

Several experimental techniques were used to fulfill the aims of this dissertation. Although some techniques are generally well known, such as measuring muscle activity with EMG, other techniques like cutaneous reflexes and functional magnetic resonance imaging may not be as familiar. Thus, below, I provide background information about these techniques.

1.6.1 Cutaneous reflexes

To determine whether altered interlimb sensory reflexes contribute to impaired interlimb coordination and compensation during pedaling after stroke, we elicited interlimb cutaneous reflexes. Cutaneous reflexes involve the activation of skin mechanoreceptors (i.e. free nerve endings, Merkel disks, Pacinian corpuscles, Meissner corpuscles, Ruffini endings). Cutaneous reflexes include the flexor or withdrawal reflex (initiated by flexor reflex afferents) in response to nociceptive input and cutaneomuscular reflexes, which are responses involved in non-nociceptive movements (Pierrot-Deseilligny & Burke, 2012). It is thought that the primary role of cutaneous reflexes during locomotion is to preserve balance and stability (Zehr & Stein, 1999).

To experimentally elicit cutaneous reflexes, investigators electrically stimulate purely (or mostly) sensory nerves. Commonly stimulated nerves in the lower extremity are the sural, superficial peroneal, and posterior tibial nerves. These nerves are stimulated at the medial or lateral malleolus or the dorsum of the foot. Cutaneous reflexes have been elicited with a variety of different stimulation parameters (unless otherwise noted, information in this section is summarized from Brooke et al., 1997). Because the stimulated nerves are typically pure sensory nerves, stimulation intensity is based upon perception. Most studies evaluate either the perceptual threshold (PT)—when stimulation is first perceived—or the radiating threshold (RT)—when stimulation radiates away from the site of stimulation into the innervation area of the respective nerve. Because of the variability of perceptual responses, most studies reassess the PT or RT at multiple timepoints throughout a session to confirm stability of the threshold. To elicit reflexes,

stimulation intensity is then set at some multiple (usually 2-4 X) of the PT or RT. Stimulation can be nociceptive or non-nociceptive, with responses dependent on the intensity. A variety of different number of pulses, pulse durations, and stimulation frequencies have been used. However, because of the difficulty of eliciting measurable responses, most studies have used multiple pulses of short duration applied at a high intensity (Pierrot-Deseilligny & Burke, 2012).

Following stimulation, reflex responses in the muscle are measured with EMG (information in this section is summarized from: Brooke et al., 1997). In response to cutaneous stimulus in one lower limb, reflex responses have been measured in the ipsilateral limb, contralateral limb, and both of the upper limbs, although most studies have focused on ipsilateral responses in the stimulated limb. In this study, we focused on responses in the contralateral limb. Unlike reflexes such as the H-reflex, responses to cutaneous stimulation are typically less synchronized, more variable, and smaller. Consequently, multiple trials are often acquired and muscle activity during control trials is subtracted from the average stimulated trial.

Studies have quantified the onset latency and amplitude of cutaneous reflex responses. The latency of responses is normally determined with respect to the first pulse of stimulation. In electrical stimulation trials, the determination of onset latency is difficult because of the large variability. Additionally, the qualification of onset latency is subjective; a delayed onset latency could mean that the same reflex response was delayed in the group of interest or that the response of interest was missing. Because of these issues, many studies quantify the amplitude instead. The amplitude of responses is normally evaluated as the mean or integral of the EMG response. Some studies evaluate

reflexes within fixed latency intervals, while others select custom reflex latencies based on the observed responses. Fixed intervals allow for easier comparison across trials and muscles and simplify the evaluation of reflex responses. Custom reflex intervals can provide a more accurate representation of complex responses, but potentially introduce bias and decrease the ability to compare different responses.

Cutaneous reflexes may travel through several different pathways. At short latencies, cutaneous reflexes are mediated through spinal pathways. At longer latencies, these reflexes may be mediated through supraspinal or spinal pathways. For cutaneous reflexes to have a transcortical pathway, it has been estimated that a minimal latency of 85 – 90 ms is required (Nielsen, Petersen, & Fedirchuk, 1997). Some studies have suggested that there is a strong possibility that supraspinal structures are involved in long latency responses to cutaneous stimulation (Delwaide & Crenna, 1984; Pierrot-Deseilligny & Burke, 2012). This contention is supported by several studies using transcranial magnetic stimulation (TMS). Cutaneous stimulation of the sural nerve facilitates ipsilateral motor evoked potentials (MEPs) during early and middle swing phase of walking in the TA and BF and inhibits MEPS during late swing (Christensen, Morita, Petersen, & Nielsen, 1999; Pijnappels, Van Wezel, Colombo, Dietz, & Duysens, 1998). The response resulting from the combination of cutaneous stimulation and TMS is greater than the algebraic sum of each stimulation independently (Pijnappels et al., 1998). Additionally, facilitation does not occur with transcranial electrical stimulation, suggesting convergence at a cortical level (Christensen et al., 1999).

Despite the case for the supraspinal mediation of cutaneous reflexes, reflexes at a latency < 85 ms likely follow a spinal pathway. Longer latency reflexes may also follow

a spinal pathway. Support for a spinal pathway for cutaneous reflexes comes from work in spinalized or decerebrate cats and from work showing the phasic modulation of these reflexes. In chronic spinal cats and decerebrate cats, phase dependent interlimb reflex responses are elicited in response to cutaneous input during walking (Duysens, 1977; Duysens & Pearson, 1976; Forssberg, Grillner, & Rossignol, 1975; Gauthier & Rossignol, 1981). The existence of interlimb reflexes in spinal and decerebrate cats suggests that supraspinal regions are not essential for cutaneous reflexes. There is also evidence in humans that spinally mediated reflexes can occur, even at longer latencies. In individuals with spinal cord injury, reflex responses can occur up to 450 ms after stimulation (Roby-Brami & Bussel, 1987).

Cutaneous reflexes that follow a spinal pathway may be modulated by supraspinal inputs. For example, the corticoreticular-reticulospinal system is likely involved in interlimb coordination Matsuyama et al. (2004). The motor cortex inputs onto the reticular formation, and neural signals descend to the contralateral spinal cord through the reticulospinal tract. These projections synapse on commissural interneurons that have a tight coupling with the contralateral spinal cord. Because these interneurons are thought to be involved in CPG activity, this pathway is likely involved in modulating interlimb reflexes. Ipsilateral uncrossed and branched crossed projections from the cortex and from subcortical regions also synapse onto commissural interneurons, allowing another means for supraspinal regions to influence interlimb reflexes (Carson, 2005; Jankowska & Edgley, 2006).

Regardless of the pathway that they follow, cutaneous reflexes are thought to be modulated by central pattern generator (CPG) pathways. Like spinal and decerebrate cats,

cutaneous reflexes are phase gain controlled during walking in intact cats (Duysens & Loeb, 1980; Duysens et al., 1980; Duysens & Stein, 1978). In humans, cutaneous reflexes are phase dependent during rhythmic locomotor tasks such as walking, running, and pedaling in the contralateral and ipsilateral limb, but not during static contractions (Berger et al., 1984; Brown & Kukulka, 1993; Dietz et al., 1986; Duysens, Tax, Trippel, & Dietz, 1992, 1993; Duysens et al., 1990; Lamont & Zehr, 2006; Mileva, Green, & Turner, 2004; Tax et al., 1995; Van Wezel et al., 1997; Yang & Stein, 1990; Zehr, 2005; Zehr, Hesketh, & Chua, 2001; Zehr, Komiyama, & Stein, 1997). These studies also document several cutaneous reflex reversals in humans during walking and running. Reflex signals may be premotoneuronally facilitated or inhibited by the CPG or incorporated directly into the CPG, perhaps at the level of the commissural interneuron (Duysens et al., 1992; Forssberg et al., 1977).

1.6.2 Functional magnetic resonance imaging

To address whether reduced pedaling-related brain activation after stroke can be explained by altered volitional motor commands and pedaling performance, we measured brain activation with fMRI, a specialized form of magnetic resonance imaging (MRI). MRI is a brain imaging technique that measures electromagnetic energy given off by protons in the brain when a radiofrequency pulse is applied within a strong magnetic field. fMRI expands on this basic concept by measuring changes in MRI signal from physiological processes associated with neuronal activity.

When placed inside a magnetic resonance (MR) scanner, hydrogen atoms (i.e. protons) in the body align with the magnetic field of the scanner in a parallel or anti-

parallel orientation (information for this paragraph is summarized from: Huettel, Song, & McCarthy, 2009). These protons precess about the magnetic field, with randomly distributed phases. Consequently, the magnetic vector of these protons is aligned with the magnetic field of the scanner (longitudinal magnetization), but there is no measurable magnetic vector perpendicular to the magnetic field (transversal magnetization). In order to produce a measurable signal, a radio frequency pulse is introduced. This radio frequency pulse causes some protons to move to a higher energy (anti-parallel) orientation. The radio frequency pulse also aligns the precession phases of protons, yielding a transversal magnetic vector. When the radio frequency pulse is turned off, protons gradually return to their baseline state—longitudinal relaxation. The time constant for longitudinal relaxation is called T1 recovery. T1 differs between tissue types because of different susceptibilities to energy transfer from protons as they undergo longitudinal relaxation.

At the same time that longitudinal relaxation occurs, proton precession gradually returns to random phasing—transversal relaxation (information for this paragraph is summarized from: Huettel et al., 2009). Transversal relaxation occurs for two primary reasons. First, the magnetic fields of each proton influence nearby protons, affecting their precession frequencies. This is termed spin-spin relaxation. The time constant for transversal spin-spin relaxation is called T2 decay. Second, local external magnetic field inhomogeneities cause differences in precession frequency along the length of the bore. When the spin-spin interactions and magnetic field inhomogeneities are considered together, the decay of transversal magnetization is termed T2* decay. While there is a transversal magnetic vector, the resulting release of electromagnetic energy and change in

magnetic flux induces an electrical current in an antenna that is measured by the MR scanner. In order to produce images from MR signals, slice selection, frequency encoding, and phase encoding are used. These involve applying spatial gradients along the z, x, and y directions, respectively. These gradients allow 2D slice sampling and alter precession frequency based on location within the slice. Depending on parameter selection by the experimenter, the temporal resolution of MRI is normally on the order of mm (with a sampling time vs. resolution tradeoff).

Different tissues in the body have different proton density, yielding different rates of T1 and T2* decay (information for this paragraph is summarized from: Huettel et al., 2009). To exploit these differences, MRI scanning parameters are manipulated to provide images that detail tissues of interest. The two key parameters that are manipulated are: 1) repetition time (TR) – the time between excitatory RF pulses, and 2) echo time (TE) – the time between an excitation pulse and data acquisition. Generally, these parameters are selected to maximize tissue differences in T1 recovery for anatomical images (T1-weighted). In contrast, functional image data use parameters that maximize tissue differences in T2* decay (T2*-weighted).

fMRI builds upon the basic concepts of MRI by measuring changes in MRI signal associated with a phenomenon of interest—neuronal activation. Neuronal activation increases the energy demand of neurons. The vascular system responds to this demand by increasing the supply of blood (functional hyperemia), and thus oxygen and glucose, to the cells (unless otherwise noted, information for this paragraph is summarized from: Huettel et al., 2009). Instead of only providing enough oxygen and glucose to meet neuronal demand, there is a compensatory oversupply of blood and these substrates (Fox

& Raichle, 1986). Of these substrates, oxygen is of interest for fMRI. The hemoglobin molecules that bind to oxygen have different magnetic properties when they are oxygenated vs. deoxygenated. Oxygenated hemoglobin has no magnetic moment, and deoxygenated hemoglobin has a relatively large magnetic moment. Because deoxygenated hemoglobin has a magnetic moment, it distorts the magnetic field, increasing the rate of T2* decay, and decreasing MRI signal. This is termed blood-oxygenation-level dependent (BOLD) contrast. During neuronal activation, although hemoglobin becomes deoxygenated, the compensatory oversupply of blood actually causes the MRI signal to increase.

As described, the BOLD contrast is an indirect measure of neuronal activation that is directly impacted by both changes in blood oxygenation and blood flow (Heeger & Ress, 2002; Logothetis, 2008). Because of this indirect relation, the BOLD hemodynamic response has several unique characteristics. First, there is often an initial dip in BOLD signal resulting from the accumulation of deoxygenated hemoglobin prior to a large rise in local blood flow (Vanzetta & Grinvald, 1999). Second, there is a delayed rise in the BOLD response with respect to the onset of neuronal activity (DeYoe, Bandettini, Neitz, Miller, & Winans, 1994). The BOLD signal first increases ~2 seconds and reaches a peak ~5 seconds after onset. It takes a similar amount of time for the BOLD signal to decline after termination of neuronal activity. The slow time course of the hemodynamic response limits the temporal resolution of fMRI to the order of seconds.

CHAPTER 2: IMPAIRED INTERLIMB COORDINATION IS RELATED TO ASYMMETRIES DURING PEDALING AFTER STROKE

2.1 Introduction

In people with stroke, the work of locomotion and other functional behaviors of the lower limbs is accomplished primarily by the non-paretic lower limb. For example, during walking, the non-paretic limb generates approximately 60% of the work or power for forward translation (Bowden et al., 2006; Olney et al., 1991; Turns et al., 2007). These and other asymmetric movement strategies are useful in acute stroke because they enable goal directed behavior despite paralysis or severe weakness of the stroke-affected limb (O'Sullivan et al., 2014). However, repeated and prolonged use of the non-paretic limb instead of the paretic limb is associated with altered cortical representation and worsened movement of the paretic limb, limited functional recovery, and impaired quality of life (Allred & Jones, 2008; Allred et al., 2005; Jonkers et al., 2009; Mayo, Wood-Dauphinee, Cote, Durcan, & Carlton, 2002; Nadeau et al., 1999). Nevertheless, asymmetric contributions (non-paretic > paretic) to bilateral lower limb movements persist in chronic stroke even when the paretic limb has regained considerable motor function (R. W. Bohannon & Larkin, 1985; Brown & Kautz, 1998; Brown et al., 1997; Clark et al., 2016; Hsiao et al., 2016). This behavior is curious because walking, standing, and other functional lower limb movements are inherently bilateral and offer many opportunities to use the paretic limb. This study examined the possibility that motor impairments of the paretic limb and impaired interlimb coordination contribute to this phenomenon.

Asymmetric contributions to bilateral lower limb movements in chronic stroke may be due to residual impairment in motor output of the paretic limb. Even well recovered stroke survivors exhibit weak descending drive to spinal motor neurons (Palmer et al., 2017) and impaired motoneuronal rate coding (Chou et al., 2013; Frontera et al., 1997). Muscles on the stroke-affected side of the body have reduced cross sectional area (English et al., 2010) and lower force generating ability, as compared to normal (Richard W Bohannon & Andrews, 1995; Klein et al., 2010; Newham & Hsiao, 2001). The paretic limb also displays abnormal muscle phasing, whereby muscle activity is initiated and terminated at inappropriate phases in the movement cycle (Den Otter et al., 2007; Kautz & Brown, 1998; Knutsson & Richards, 1979). These impairments may prevent the stroke-affected limb from producing adequate torque, in the correct direction, at the appropriate point in the movement cycle to advance the limb or support the weight of the body for locomotion. Consequently, contributions from the partially recovered limb may not enhance movement, or may even impair movement, causing asymmetries to persist.

Even if the paretic limb can produce sufficient and appropriately phased motor output unilaterally, it may be unable to do so in a reciprocal alternating fashion with the non-paretic limb as required for locomotion. During hip flexion and extension, reflex-related torque production in the paretic limb is more abnormal during bilateral than unilateral movement (Hyngstrom et al., 2010). Kautz and Patten (2005) have shown that stroke survivors can produce adequate muscle force to rotate the crankshaft during unilateral pedaling with the paretic limb, but the timing of muscle activation is less appropriate when the non-paretic limb pedals at the same time. Moreover, interlimb

phasing is abnormal and more variable during walking in stroke as compared to control subjects (Meijer et al., 2011; Roerdink et al., 2007). Hence, the tendency to perform bilateral lower limb movements primarily with the non-paretic limb may be a strategy to reduce the undesirable impact of the paretic limb on the non-paretic limb or to reduce the need to coordinate the output of the two limbs.

The goal of this study was to better understand relationships among paretic motor impairment, impaired interlimb coordination, and asymmetric contributions to bilateral movements of the lower limbs in chronic stroke. To this end, we compared conventional, unilateral, and bilateral uncoupled pedaling in people with chronic stroke and age-matched controls. Pedaling involves continuous, reciprocal, multi-joint movement of both limbs, and therefore is a useful model of functional lower limb movement. During conventional pedaling, the right and left crank arms are mechanically coupled by a solid crank shaft, allowing forces applied to one side to be transferred to the other. People with stroke can pedal with minimal contributions from the paretic limb. Thus, conventional pedaling exposes asymmetric contributions to bilateral lower limb movement like those seen during walking. Because pedaling does not require body weight support, it can be done unilaterally. Each limb can be examined in isolation without the confounding influence of the contralateral limb. Thus, unilateral pedaling exposes paretic motor impairments. When the crankshaft is split into a left and right half, as was done during the bilateral uncoupled condition, pedaling can be performed bilaterally with no mechanical connection between the pedals. This task requires that each limb rotate its respective crankshaft and that the two limbs maintain a 180° phase relationship. Thus, by comparing unilateral and bilateral uncoupled pedaling in stroke survivors and controls,

we were able to distinguish motor impairments of the paretic limb from impairments in interlimb coordination. We then examined the relationship between these impairments and asymmetry during conventional pedaling. Direct relationships with asymmetry would provide support for the hypothesis that residual impairments in motor output of the paretic limb and interlimb coordination play a role in asymmetric contributions to bilateral lower limb movement in chronic stroke. Portions of this work have been presented previously in abstract form (Cleland, Gelting, Arand, Struhar, & Schindler-Ivens, 2016; Sheila Schindler-Ivens, Arand, & Cleland, 2016).

2.2 Methods

Participants

Twenty-one individuals with chronic stroke and eleven age-matched controls participated. All were free of neurological disease or injury other than stroke. All provided written informed consent in accordance with the Declaration of Helsinki and the Institutional Review Boards at Marquette University and the Medical College of Wisconsin. See Table 2.1 for participant demographics.

	Control (n = 11)	Stroke (n = 21)
Age (years)	64 (7)	60 (11)
Sex (M/F)	3/8	13/8
Time since stroke (years)		9.2 (3.7), Range: 1.7 – 15.8
Stroke type (ischemic/hemorrhagic)		16/5
Stroke location (cortical/sub-cortical)		12/9
Paretic limb (L/R)		12/9
$FM_{LEtotal}$ (max: 96)		79 (9), Range: 61 – 91
$FM_{LEmotor}$ (max: 34)		25 (6), Range: 15 – 33
FM_{LEsens} (max: 12)		10 (3), Range: 2 – 12
FM_{LEbal} (max: 10)		7 (1), Range: 6 – 9
FM_{LErom} (max: 20)		18 (3), Range: 14 – 20
FM_{LEpain} (max: 20)		20 (0)
Walking velocity (m/s)		0.83 (0.33)

Table 2.1. Participant demographics. Demographic characteristics for the stroke and control group. Values are Mean (SD). $FM_{LEtotal}$: Fugl Meyer Assessment total score; $FM_{LEmotor}$: motor score; FM_{LEsens}: sensory score; FM_{LEbal}: balance score; FM_{LErom}: range of motion score; FM_{LEpain}: pain score.

Clinical measures

People with stroke underwent a battery of assessments to characterize sensory and motor impairment of the lower limbs. Tests included the 8m comfortable walk test for walking velocity and the lower extremity Fugl-Meyer Assessment ($FM_{LEtotal}$), which was subdivided into motor ($FM_{LEmotor}$), sensory (FM_{LEsens}), balance (FM_{LEbal}), range of motion (FM_{LErom}), and pain (FM_{LEpain}) components. $FM_{LEmotor}$ included tests for reflex activity, synergy, and coordination. FM_{LEsens} included light touch and proprioception. Values are reported in Table 2.1.

Equipment and procedures

All participants performed conventional, unilateral, and bilateral uncoupled pedaling. Tasks were enabled by a custom-designed, split-crank pedaling device. See Figure 2.1. As the name suggests, the crankshaft of the device was split into a left and right half. The two halves could be fastened together with a coupler to create a

conventional, unitary crankshaft. Or, the coupler could be removed to eliminate the mechanical connection between the pedals. Importantly, each half of the crankshaft turned an eccentric pulley that enabled unilateral pedaling despite no mechanical contribution from the contralateral limb. Recall that during conventional pedaling, forces applied by the downstroke limb counteract forces generated by the upstroke limb that tend to retard forward crank progression (Kautz & Neptune, 2002). If the contribution from the downstroke limb is not simulated, unilateral pedaling is difficult to accomplish, even in people without stroke. During the downstroke of the pedaling cycle, the eccentric pulley stretched an elastic band. Energy stored in the band was released during the upstroke to help return the limb to the top-dead-center position, thus simulating the contribution of the contralateral limb. The stiffness of the eccentric pulley system was adjusted on an individual basis to achieve unilateral pedaling, as described below. During conventional pedaling, the coupler was in place to hold the right and left pedals in a fixed position 180° apart. Because the feet were secured to the pedals and the non-paretic limb was mechanically coupled to the paretic limb it could compensate for impaired paretic motor output. During unilateral and bilateral uncoupled pedaling, the coupler was removed, and there was no mechanical connection between the right and left pedals. Thus, to perform unilateral pedaling, the paretic limb had to rotate its crankshaft without a mechanical contribution from the non-paretic leg. Moreover, during bilateral uncoupled pedaling, the two limbs had to work in a coordinated fashion to maintain a 180° phase relationship.

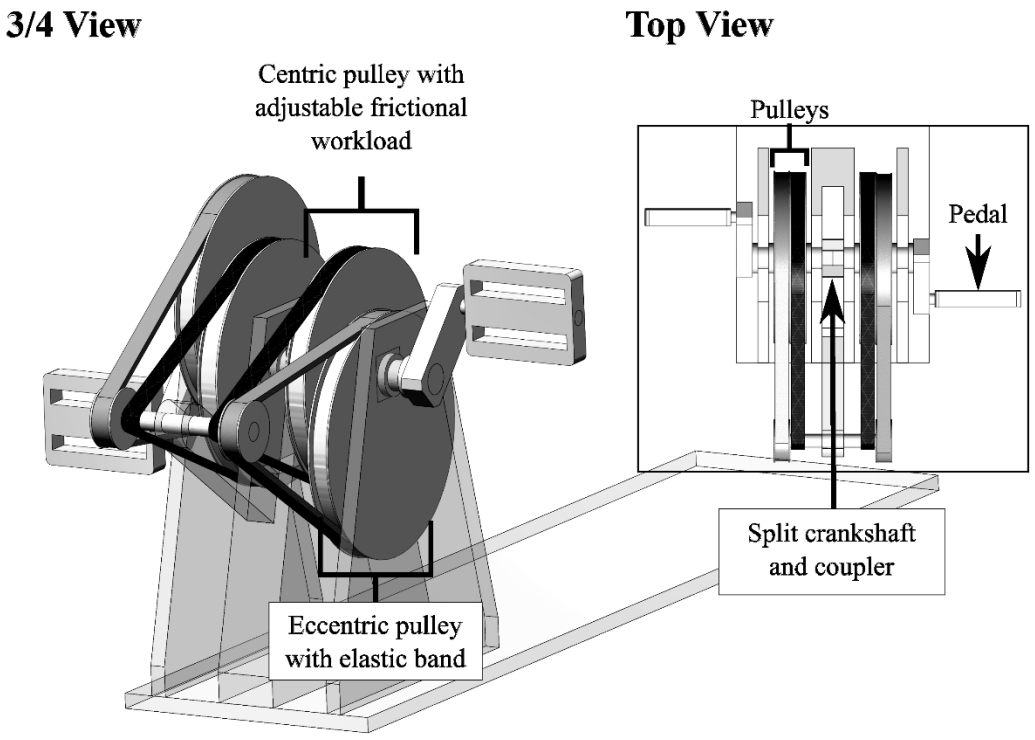

Figure 2.1. Pedaling device with split crankshaft. The top view depicts the split crankshaft and coupler. The coupler allowed conventional pedaling when fastened in place and unilateral or bilateral uncoupled pedaling when removed. The ¾ view depicts the pulley systems of the pedaling device. An eccentric pulley with elastic band was used during unilateral and bilateral uncoupled pedaling to simulate the contribution from the contralateral downstroke limb during conventional pedaling. The elastic band was stretched during the downstroke of the pedaling cycle, and energy stored in the band was released during the upstroke. A centric pulley applied an adjustable frictional workload.

Each participant completed a setup and a test session. During both sessions, participants lay supine with their feet secured to the pedals with a strap around the heel and the dorsum of each foot. Feet were secured to the pedals because many stroke survivors could not otherwise keep their paretic foot on the pedal. The ankle could still move freely. The skin was prepped, and muscle activity was recorded bilaterally from the tibialis anterior (TA), rectus femoris (RF), biceps femoris (BF), and medial gastrocnemius (MG) as described by Hermens, Freriks, Disselhorst-Klug, and Rau (2000). These muscles were selected because pilot work showed that they were prime

movers in supine pedaling with the custom device. Reference electrodes were placed on the medial malleolus.

The purpose of the setup session was to identify an elastic load on the eccentric pulley system that approximated the downstroke contribution of the contralateral limb and enabled unilateral pedaling. Loads were adjusted by changing the number of elastic bands arranged in parallel around the eccentric pulley. Up to six loads were examined on the right and left limb. Loads were presented in order of decreasing stiffness. After a load was in place, participants were asked to pedal forward with their right (or left) limb. During the setup session, participants also performed conventional pedaling. Here, the instruction was to pedal forward with both limbs. Bilateral uncoupled pedaling was not performed during the setup session.

Elastic loads for unilateral pedaling were selected by observing pedaling performance to rule out excessively low and high loads and then by analyzing pedaling velocity quantitatively. During the setup session, excessively low loads were identified visually as those with inadequate elastic force to return the limb to top-dead-center (i.e. the limb got stuck in upstroke). Excessively high loads were identified by observation as those that were so stiff that a) participants were unable to accomplish the downstroke or b) the limb raced back to top-dead-center such that participants or experimenters felt like it was moving uncontrollably. Typically, after eliminating excessively low and high loads, two or three loads remained. At this point, we computed the mean pedaling velocity as a function of crank position for all remaining loads. The difference between these values and analogous values recorded during conventional pedaling was computed.

The elastic load with the smallest mean difference in pedaling velocity from conventional pedaling was selected. Loads were selected for the right and left leg individually.

During the test session, participants performed conventional, unilateral, and bilateral uncoupled pedaling. The elastic loads identified from the setup session were used for unilateral and bilateral uncoupled pedaling. During bilateral uncoupled pedaling, participants were asked to pedal forward using both limbs and to keep the limbs 180° apart as in conventional pedaling. Instructions for unilateral and conventional pedaling were the same as in the setup session.

For each pedaling condition in each session, a 45-sec exposure period was provided after which 60-sec of data were collected. During the exposure period, we repeated the instructions and gave verbal feedback. During the 60-sec data collection, neither instructions nor feedback were provided. Pedaling was performed with and without an auditory pacing cue at 45 RPM. When cues were used, participants were asked to match their pedaling rate to the cue. When cues were not used, they were asked to pedal at a comfortable rate. Pedaling conditions and pacing cues were counterbalanced to avoid ordering effects. During all conditions, participants were able to see the movement of the pedals.

In addition to the eccentric pulley system, each half of the crankshaft of the custom device was connected to a centric pulley capable of providing an adjustable frictional workload. See Figure 2.1. Rotary optical encoders (MR318, Micronor Inc., Newbury Park, CA) were used to measure the position of the crankshaft. One encoder was connected to each half of the crankshaft via a chain and sprocket assembly. Fiber optic cables carried signals from each encoder to controller units (MR310, Micronor Inc.,

Newbury Park, CA). The zero position of the crank cycle (i.e. top-dead-center) was defined for each limb as the position where the crank arm was parallel to the plinth and the foot was nearest the hip. EMG was recorded with bipolar surface electrodes (Bagnoli-8, Delsys Inc., Natick, MA, Inc.) Signals were amplified 10 X at the electrode site before remote differential amplification (common mode rejection ratio 92 dB, gain 1,000 X, frequency response 20–450 Hz). Position and EMG signals were sampled at a rate of 2000 Hz using a 16-bit analog-to-digital convertor and data acquisition software (micro 1401 mk II, Spike 2, Cambridge Electronic Designs, UK) housed on a desktop computer.

Data processing and dependent variables

Position data were low pass filtered at 20 Hz, and the derivative of the position trace was computed to obtain pedaling velocity. EMG data were rectified and low pass filtered at 25 Hz. Velocity and EMG data were referenced to the crank position in 1° increments as described previously (S. Schindler-Ivens, Brown, & Brooke, 2004). Ensemble averages were created for each subject and condition. From these data, we computed the mean and coefficient of variation (COV) of pedaling velocity. Both values served as quantitative measures of pedaling performance, with COV of velocity providing a measure of smooth, continuous crank progression. In cases where group- or condition-related changes in mean and/or COV of velocity were detected, we examined the velocity traces to determine the pedaling position(s) where these changes occurred. Ensemble averaged velocity data for each subject were smoothed and the derivative of velocity was calculated. Points of interest were identified by zero crossings of velocity and acceleration data.

For the bilateral uncoupled condition, we computed the mean and COV of continuous relative phase (CRP), defined as the absolute value of the difference in position between the right and left crankshaft as a function of time. We adapted methods from Plotnik, Giladi, and Hausdorff (2007) to calculate phase coordination index (PCI), which incorporates aspects of both the mean (phase accuracy) and COV of CRP (phase consistency). As shown in the equation, PCI was obtained by summing the COV of CRP and the mean of the minimum absolute difference from a 180° phase relation. Thus, PCI evaluates the accuracy and consistency of interlimb phasing. The accuracy term was normalized to 180° to convert to the same units as the consistency term. Plotnik et al. (2007) suggest that PCI represents a distinct feature of gait because it is not strongly correlated with other common measures such as gait symmetry, speed, and variability.

$$\text{PCI}\ (\%) = \left[\frac{\sigma(\text{CRP})}{\mu(\text{CRP})} \times 100\right] + \left[\frac{\mu(|\text{CRP-180}|)}{180} \times 100\right]$$

Mean EMG amplitude and EMG modulation index (MI) were computed for each muscle across conditions and subjects. MI was computed as the difference between maximum and minimum EMG amplitude as a percent of maximum EMG amplitude (i.e., [EMGmax – EMGmin] / EMGmax * 100). Between-group and between-limb comparisons of EMG amplitude are difficult in pedaling because a normalization factor, such as an M-wave or background EMG, is not available. For example, a maximal EMG value measured at one joint position is not an appropriate normalization factor for muscle activity at different joint positions (Mirka, 1991). Hence, MI was used to compare muscle activity between groups and limbs. Given that muscles are phasically active in pedaling,

we reasoned that limbs and/or groups with higher muscle output would also display higher values for MI. Mean EMG amplitude and MI were used for within-limb comparisons of muscle activity across conditions.

Percent mechanical work performed by the paretic limb during pedaling was assessed using a pedaling device with a solid crankshaft (PowerTower with EMC Ergometric Multi Cycle attachment, Total Gym, San Diego, CA) and equipped with force and position sensors (force: Delta 660-60, ATI Industrial Automation, Apex, NC; position: BEI Model EX116-1024-2, BEI Sensors, Thousand Oaks, CA). The device and methods for quantifying work have been described previously (Fuchs, Sanghvi, Wieser, & Schindler-Ivens, 2011; Kautz & Brown, 1998; S. Schindler-Ivens et al., 2008). In brief, participants' feet were secured to the pedals with straps around the heel and dorsum of the foot, and they pedaled with an auditory pacing cue at 45 RPM against a moderate load. We measured the forces applied to each pedal and the position of the crank and the pedals. Offline, we computed the forces oriented tangentially to the crank arm because these forces create a torque that produces angular rotation of the crank. Data were referenced to the crank angle and ensemble averaged. The area under the resulting curve yielded the mechanical work done by the limb. Positive and negative areas were computed to measure the propulsive (positive area) and retarding (negative area) work of each limb. Percent work done by the paretic limb [propulsive [%Work(+)], retardant [%Work(-)], and net [%Work(net)]] were computed as: Work(paretic)/Work(total)*100, where Work(paretic) was the work done by the paretic limb and Work(total) was the sum of the work done by both legs. A value of 50% indicated equal sharing of the work between limbs, as is typical for able-bodied individuals.

Statistics

All data were tested for normality using the Shapiro Wilk test. Data used for between-group comparisons were tested for equality of variances using the Levene's test. Non-parametric statistics were used for variables that were non-normal or had unequal between-group variances. All statistical tests used SPSS Statistics 22.0 (International Business Machines Corporation, New York, NY), and $P < 0.05$ was accepted as significant.

Within- and/or between-group comparisons were performed for mean and COV of velocity, PCI, phase accuracy, phase consistency, mean EMG amplitude, and EMG MI. Between group comparisons were performed with independent sample t-tests and Mann-Whitney U tests. Within group comparisons were performed with paired sample t-tests and Wilcoxon signed rank tests. In controls, there were no between-limb differences for any measure of velocity or EMG ($P > 0.10$); so, the average of the limbs was used. We used one sample t-tests and Wilcoxon signed rank tests to 1) compare mean velocity to the rate of the auditory cue, and 2) compare %Work(+), %Work(-), and %Work(net) to a fixed value of 50%. Pearson and Spearman correlations were used to examine the relationship between %Work(net) and COV of velocity, PCI, change in mean EMG amplitude, and change in EMG MI between conditions. We also tested the correlations between these variables and walking velocity, $FM_{LEtotal}$, $FM_{Lemotor}$, and FM_{LEsens}. Variables that were significantly correlated with %Work(net) were entered into a stepwise linear regression with backward elimination to predict the dependent variable %Work(net). Variables were removed from the model in succession if the significance of the F value was the greatest of remaining variables and was ≥ 0.10. To further describe

pedaling performance during bilateral uncoupled pedaling, we calculated the time relative position and velocity for the average revolution of each limb. For every complete revolution (0 – 360 degrees) of each limb, we determined the mean position and velocity at every 1/500th of each revolution and averaged these 500 data points across all revolutions. We also calculated the time relative position and velocity for the contralateral limb during the average revolution of the ipsilateral limb. See Appendix A for detailed analysis methods for this study.

2.3 Results

Group mean (SD) values and significance tests for velocity, EMG, and interlimb phasing are provided in Tables 2.2 and 2.3. Representative examples of pedaling behavior across groups and conditions are shown in Figures 2.2 and 2.3. Group results for EMG are shown in Figures 2.5, 2.6, and 2.7. An additional group velocity figure is shown in Appendix A, Figure A.1.

Pedaling velocity		**Conventional**			**Unilateral**			**Bilateral Uncoupled**		
Mean (deg/s)		*Control*		*Stroke*	*Control*	*Non-Paretic*	*Paretic*	*Control*	*Non-Paretic*	*Paretic*
		270 (1)		288 (48)	273 (6)	286 (43)	264 (45)[bc]	274 (14)	226 (72)[acde]	204 (61)[acde]
COV (%)		11 (6)		11 (4)	11 (6)	12 (7)	25 (14)[abc]	23 (10)[cd]	51 (28)[acd]	65 (28)[abcd]
EMG		*Control*	*Non-Paretic*	*Paretic*	*Control*	*Non-Paretic*	*Paretic*	*Control*	*Non-Paretic*	*Paretic*
MI (%)	*TA*	58 (17)	64 (23)	60 (27)	74 (12)[c]	71 (18)	75 (20)[c]	75 (10)[c]	75 (14)[c]	75 (19)[c]
	RF	79 (11)	79 (15)	54 (26)[ab]	83 (11)	83 (7)	70 (23)[bc]	87 (8)[cd]	87 (8)[cd]	76 (20)[bcd]
	MG	77 (8)	77 (19)	55 (23)[ab]	77 (12)	68 (24)[c]	56 (22)[ab]	81 (7)[c]	81 (13)[cd]	66 (20)[abcd]
	BF	81 (11)	75 (15)	51 (28)[ab]	72 (13)	56 (22)[ac]	54 (23)[a]	78 (10)	87 (9)[acd]	62 (24)[abcd]
Mean amplitude (μV)	*TA*	1.9 (1.7)	4.0 (5.2)	6.7 (6.3)	5.0 (3.7)[c]	6.7 (5.6)[c]	20.8 (17.6)[c]	5.9 (6.0)[c]	16.5 (3.2)[cd]	21.1 (21.5)[c]
	RF	3.2 (2.8)	5.2 (5.4)	2.8 (4.2)	7.0 (4.1)[c]	10.4 (10.5)[c]	8.2 (9.1)[c]	7.7 (4.8)[c]	10.6 (12.9)[c]	9.2 (12.0)[c]
	MG	5.6 (2.7)	9.5 (9.4)	2.3 (2.3)	4.7 (2.4)	6.7 (8.4)[c]	2.7 (3.2)	7.7 (3.3)[cd]	14.6 (13.8)[cd]	4.5 (5.3)[cd]
	BF	4.1 (2.5)	4.4 (5.3)	2.4 (3.2)	2.4 (1.7)[c]	2.3 (3.4)[c]	2.1 (3.2)	4.1 (2.6)[d]	13.0 (20.4)[cd]	4.0 (4.5)[cd]
		[a] $p < 0.05$ vs. control [b] $p < 0.05$ vs. non-paretic			[a] $p < 0.05$ vs. control [b] $p < 0.05$ vs. non-paretic [c] $p < 0.05$ unilateral vs. conventional			[a] $p < 0.05$ vs. control [b] $p < 0.05$ vs. non-paretic [c] $p < 0.05$ bilat. uncoupled vs. conventional [d] $p < 0.05$ bilat. uncoupled vs. unilateral [e] $p < 0.05$ rate vs. 270 deg/s		

Table 2.2. Velocity and muscle activity across conditions and between groups. The top section shows mean and coefficient of variation of velocity for the stroke and control group during conventional pedaling and for controls, the non-paretic limb, and the paretic limb during unilateral and bilateral uncoupled pedaling. The bottom section shows EMG modulation index and mean amplitude for controls, the non-paretic limb, and the paretic limb during all conditions. Comparisons between groups/limbs were not performed for EMG mean amplitude. Significance notations for each condition are shown below each respective column. Values are Mean (SD). BF: biceps femoris; COV: coefficient of variation; EMG: electromyography; MG: medial gastrocnemius; MI: modulation index; RF: rectus femoris; TA: tibialis anterior.

	Control	Stroke			
		All	*Slowing (n = 10)*	*Pausing (n = 6)*	*Unstructured (n = 5)*
Phase accuracy (%)	18 (5)	39 (12)*	34 (12)	43 (9)	46 (9)
Phase consistency (%)	15 (5)	43 (16)*	34 (16)	50 (11)	53 (10)
PCI (%)	32 (10)	82 (27)*	68 (28)	93 (19)	98 (19)

Table 2.3. Interlimb phasing and coordination. Values are shown for phase accuracy and phase consistency, which are summed to produce values for PCI. Higher values represent worse performance. The stroke group had worse phase accuracy and phase consistency, and thus worse interlimb coordination as represented by PCI. Interlimb phasing and coordination values are also shown for three stroke subgroups as identified by pedaling strategy during the bilateral uncoupled condition. Values are Mean (SD). PCI: phase coordination index. *$P < 0.05$.

Velocity, work, and interlimb phasing

During conventional pedaling, both groups displayed continuous, forward crank progression (Figures 2.2A and 2.3A, B, C). There were no between-group differences in the mean or COV of pedaling velocity ($P > 0.10$). In both groups, mean pedaling velocity was not significantly different from the pace of the auditory cue ($P > 0.10$). Consistent with asymmetric contributions to bilateral lower limb movement post-stroke, the paretic limb performed 41 (8)% of the positive work, 64 (12)% of negative work, and 16 (24)% of the net mechanical work of pedaling.

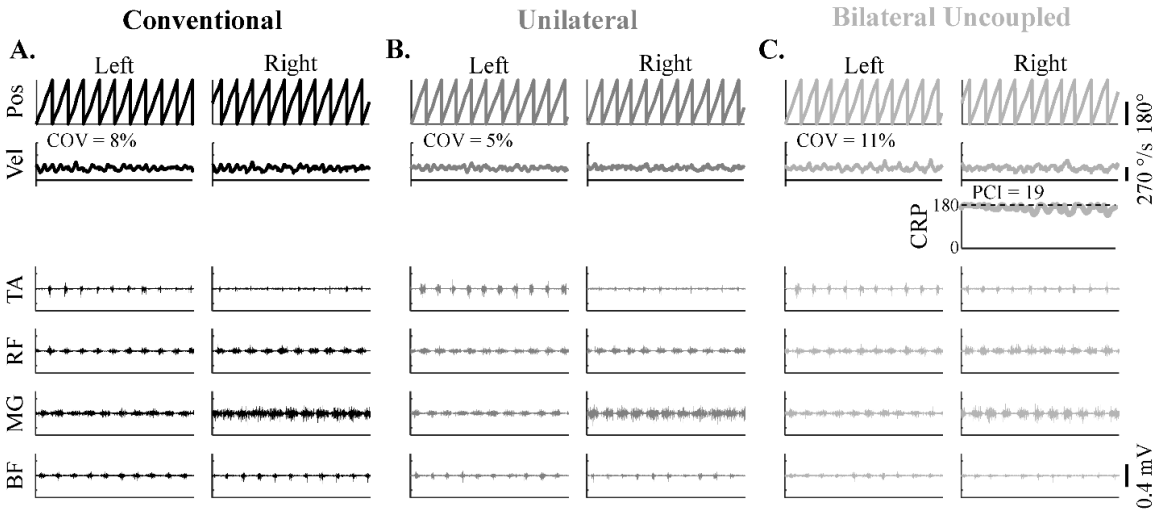

Figure 2.2. Representative data from one control participant. Position, velocity, and EMG data are shown for A) conventional (black lines), B) unilateral (dark gray lines), and C) bilateral uncoupled (light gray lines) pedaling for both the left and right limb. For bilateral uncoupled pedaling, continuous relative phase is also shown. The time interval of data shown (~13.7 sec) is the same across conditions. For unilateral pedaling, data for each leg are shown together despite being from different conditions. COV of velocity and PCI values that are displayed represent those values calculated for the entire data collection period. BF: biceps femoris; COV: coefficient of variation of velocity; CRP: continuous relative phase; MG: medial gastrocnemius; PCI: phase coordination index; Pos: position; RF: rectus femoris; TA: tibialis anterior.

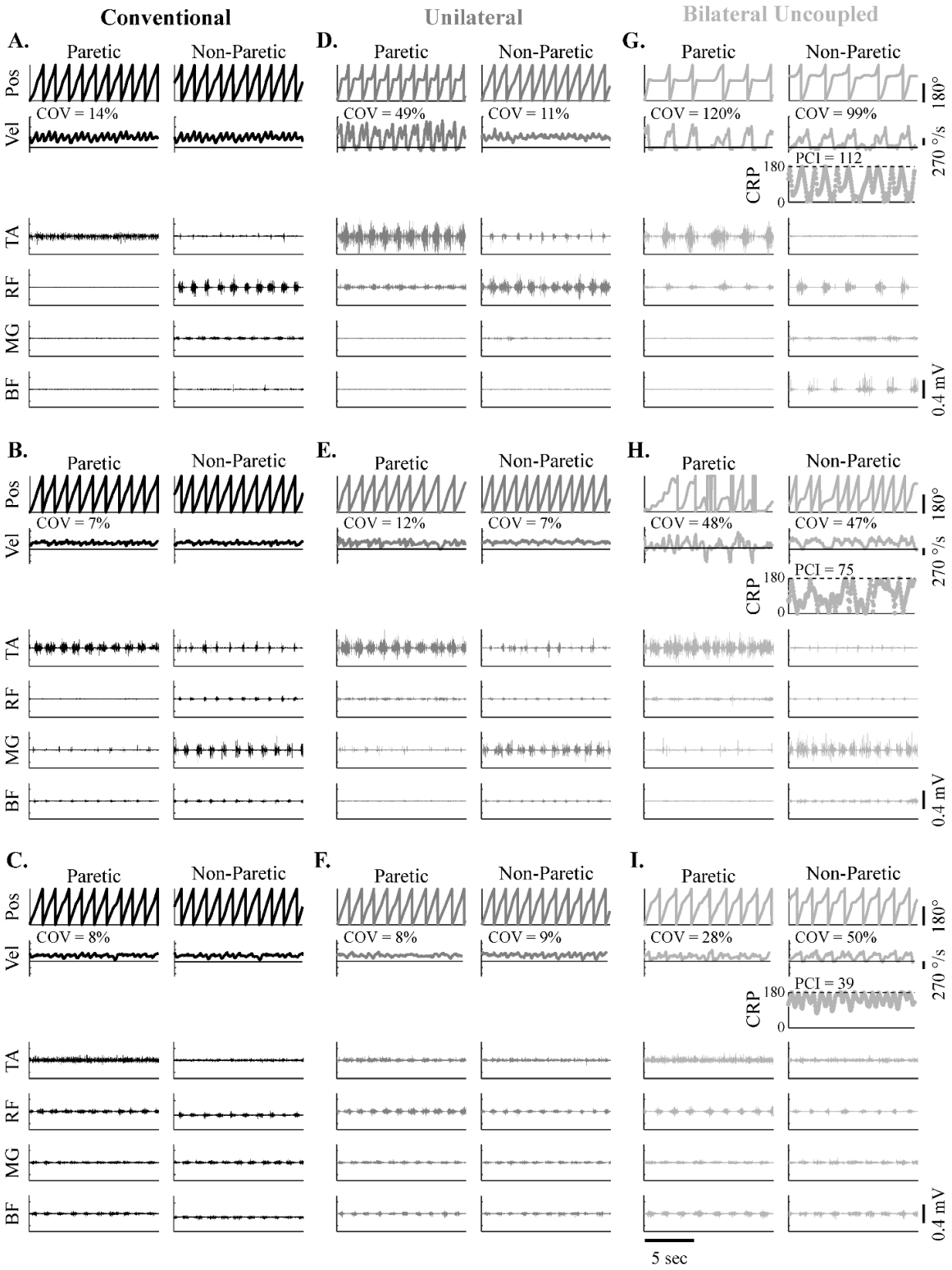

Figure 2.3. Representative data from three participants with stroke. Position, velocity, and EMG data are shown for A-C) conventional (black lines), D-F) unilateral (dark gray lines), and G-I) bilateral uncoupled (light gray lines) pedaling for both the paretic and non-paretic limb. One representative example is shown from each of the three subgroups identified during unilateral and bilateral uncoupled pedaling. For bilateral uncoupled pedaling, continuous relative phase is also

shown. The time interval of data shown (~13.7 sec) is the same across conditions. For unilateral pedaling, data for each leg are shown together despite being from different conditions. COV of velocity and PCI values that are displayed represent those values calculated for the entire data collection period. BF: biceps femoris; COV: coefficient of variation of velocity; CRP: continuous relative phase; MG: medial gastrocnemius; PCI: phase coordination index; Pos: position; RF: rectus femoris; TA: tibialis anterior.

During unilateral pedaling, the mean and COV of pedaling velocity were not different from conventional pedaling in the control group and the non-paretic limb of people with stroke ($P \geq 0.13$). However, in the paretic limb, mean velocity during unilateral pedaling decreased, and COV of velocity increased ($P \leq 0.006$). Both values were significantly different from the non-paretic limb during unilateral pedaling ($P \leq 0.01$). COV of velocity was significantly higher than for unilateral pedaling in controls ($P < 0.001$). Decreased mean velocity and increased COV in the paretic limb during unilateral pedaling were due to a transient decline in pedaling velocity during the extension-to-flexion phase transition (Figure 2.3D, E, F). On average, velocity began to decrease at 127 (32) deg in the pedaling cycle, reached a nadir of 165 (86) deg/sec at 202 (26) deg, and returned to baseline at 293 (36) deg. However, there was considerable inter-individual variation in the behavior of the paretic limb with respect to velocity fluctuations during unilateral pedaling. In most participants (n = 10, Figure 2.3E), the rate of forward crank progression decreased. In others (n = 6, Figure 2.3D), there was a pause and/or a brief reversal in pedaling direction. In the remaining individuals with stroke (n = 5, Figure 2.3F), there was little to no change in mean velocity. Individuals with stroke who were less successful with unilateral pedaling had more motor impairment as shown by a significant correlation between subgroup (no change, slow, stop/backward), Fugl-Meyer score, and walking velocity ($FM_{LEtotal}$: $R^2 = 0.23$, $P = 0.03$; $FM_{LEmotor}$: $R^2 = 0.28$, $P = 0.01$; walking velocity: $R^2 = 0.55$, $P < 0.001$).

During bilateral uncoupled pedaling, control participants rotated each crankshaft forward in a manner consistent with the representative example in Figure 2.2C. Mean pedaling velocity was not different from the other two conditions ($P \geq 0.33$); COV of velocity increased significantly from conventional and unilateral pedaling ($P < 0.001$). Increased COV was due to variations in velocity across the pedaling cycle. On average, velocity rose to 385 (55) deg/s at 148 (22) deg and declined to 182 (50) deg/s at 281 (43) deg. See Figure 2.4A. Because the downstroke limb moved faster than the upstroke limb, neither the accuracy nor the consistency of interlimb phasing was ideal. This observation is reflected in group mean values for PCI, phase accuracy, and phase consistency (Table 2.3).

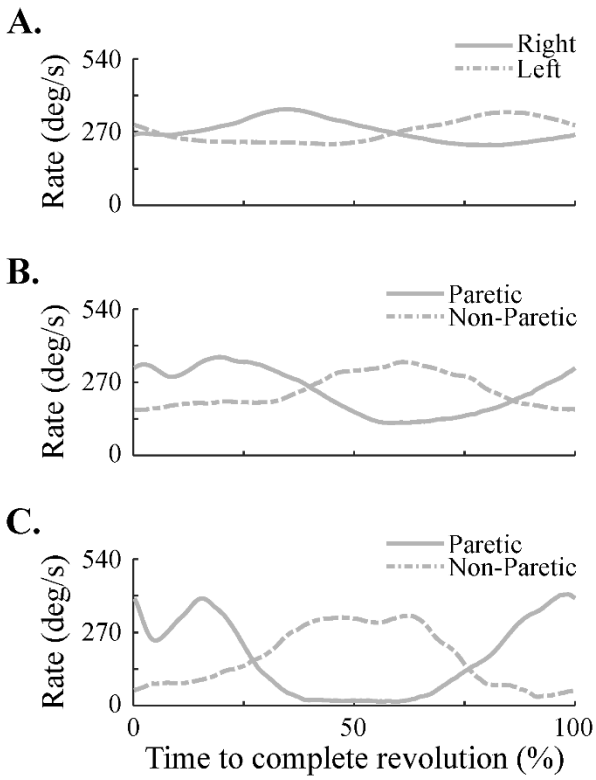

Figure 2.4. Time relative velocity during bilateral uncoupled pedaling. Average time relative velocity profiles for the right or paretic limb (solid lines) and for the left or non-paretic limb (dashed lines) are shown for A) the control group, B) the stroke subgroup who displayed an exaggerated version of the control strategy, and C) the stroke subgroup where one limb stopped pedaling while the other advanced the crank. Time relative velocity was determined by calculating the mean velocity at every 1/500th of every complete revolution (0 – 360 degrees). The resulting time relative velocity data were averaged across all revolutions and subjects within the group or subgroup of interest. The time relative velocity for the contralateral limb during the average revolution of the ipsilateral limb was determined in the same way with respect to complete revolutions of the ipsilateral limb.

When people with stroke performed bilateral uncoupled pedaling, mean pedaling velocity in the paretic and non-paretic limb was significantly lower than the control group ($P \leq 0.04$), the other pedaling conditions ($P \leq 0.005$), and the auditory cue ($P \leq 0.02$). COV of velocity in both limbs increased beyond the values for the control group and the other pedaling conditions ($P \leq 0.003$). COV of velocity was higher in the paretic than the non-paretic limb ($P = 0.01$). PCI during bilateral uncoupled pedaling in people with stroke was significantly higher than in controls ($P < 0.001$). Elevated PCI was due to

changes in phase accuracy and phase consistency, both of which were significantly different from control values ($P < 0.001$). Unlike control participants who displayed a uniform strategy for bilateral uncoupled pedaling, people with stroke exhibited a range of behaviors that contributed to the observed deficits in velocity and interlimb phasing. Most stroke participants (n = 10) displayed an exaggerated version of the control strategy wherein velocity rose to 373 (122) deg/s at 138 (31)° and declined to 71 (34) deg/s at 245 (44)°. As with the control group, the downstroke limb moved faster than the upstroke limb. See Figure 2.4A, B and 2.3I. In 6 people with stroke, one limb stopped pedaling while the other advanced the crank. In these individuals, forward crank progression stopped at 195 (18) deg in the pedaling cycle, while the contralateral limb moved from 217 (49) degrees in the pedaling cycle to 25 (88) degrees. This behavior alternated between limbs. See Figure 2.4C and 2.3G. The remaining 5 stroke survivors had considerable difficulty with bilateral uncoupled pedaling. As shown in the representative example in Figure 2.3H, some would complete more than one revolution of one crank while holding stationary or occasionally rotating the other crank. Crank rotations were often incomplete and interrupted by the backward crank progression. There was no repeatable pattern of motor output and no evidence of a reciprocal, alternating strategy between limbs. As seen in unilateral pedaling, individuals with stroke who were less successful with bilateral uncoupled pedaling had more motor impairment as shown by a significant correlation between subgroup (slow, stop, unstructured) and Fugl-Meyer score ($FM_{LEtotal}$: $R^2 = 0.36$, $P = 0.004$; $FM_{LEmotor}$: $R^2 = 0.36$, $P = 0.004$).

Muscle activity

During conventional pedaling, control participants showed no significant between-limb difference in MI for any muscle examined ($P > 0.06$). In people with stroke, MI in the RF, BF, and MG was lower in paretic than non-paretic limb and control limbs ($P \leq 0.01$). There was no difference in MI between the paretic, non-paretic, and control TA ($P \geq 0.35$). See Figures 2.5 and 2.6.

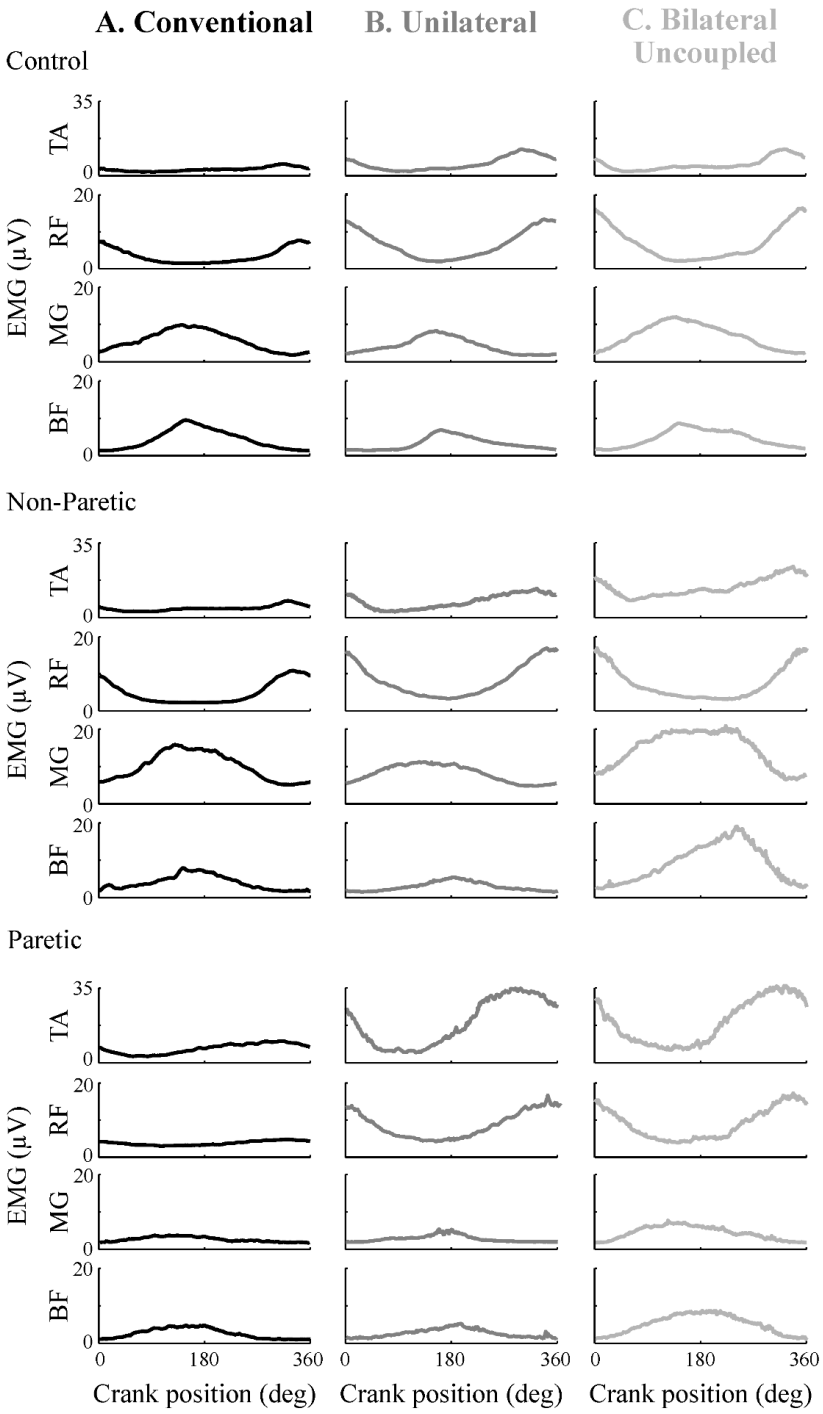

Figure 2.5. Average EMG data across both groups and all conditions. Ensemble average EMG data are shown for A) conventional (black lines), B) unilateral (medium gray lines), and C) bilateral uncoupled (light gray lines) pedaling. Data from four muscles are displayed for controls (top row), the non-paretic limb (middle row), and the paretic limb (bottom row). For unilateral pedaling, data for each leg are shown together despite being from different conditions. BF: biceps femoris; EMG: electromyography; MG: medial gastrocnemius; RF: rectus femoris; TA: tibialis anterior.

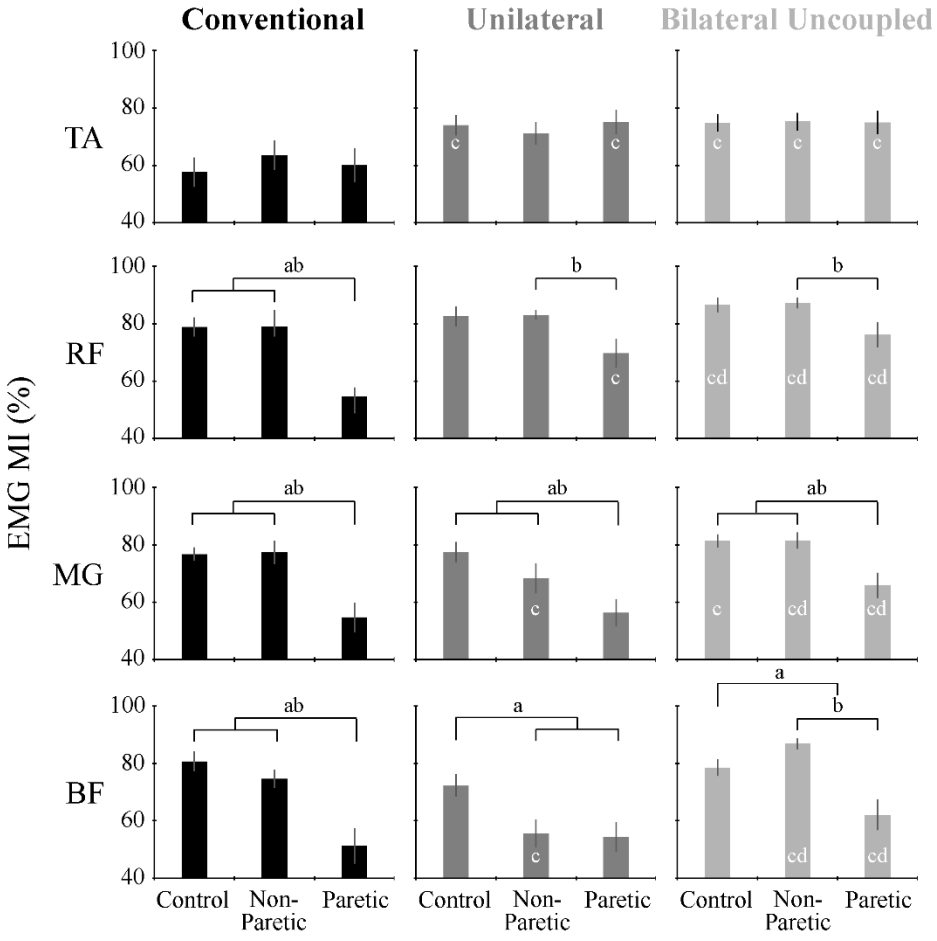

Figure 2.6. EMG modulation index across both groups and all conditions. Modulation index is shown for conventional (left column, black bars), unilateral (middle column, medium gray bars), and bilateral uncoupled pedaling (right column, light gray bars). Values are shown for all four muscles and from controls, the non-paretic limb, and the paretic limb. Differences between groups and limbs are indicated by significance lines. Differences between conditions are indicated by letters within the bars. Nomenclature for significance lettering is provided. BF: biceps femoris; EMG: electromyography; MG: medial gastrocnemius; RF: rectus femoris; TA: tibialis anterior.

During unilateral pedaling, both groups displayed significantly higher mean EMG in TA and RF as compared to conventional pedaling ($P \leq 0.009$, Figure 2.7). MI in the paretic TA and RF was higher during unilateral pedaling than in conventional pedaling ($P \leq 0.03$); values did not differ from the control group ($P \geq 0.11$, Figure 2.6). MI in the

paretic RF remained significantly lower than in the non-paretic RF ($P = 0.02$). Also, during unilateral pedaling, mean EMG decreased in the BF of control and non-paretic limbs and in the MG of the non-paretic limb ($P \leq 0.01$). There was no change in the mean EMG in the paretic MG and BF ($P \geq 0.52$). MI in the paretic MG remained below the control and non-paretic values ($P \leq 0.02$). In the paretic BF, MI was lower than the control group ($P = 0.02$) but not different from the non-paretic limb ($P = 0.59$).

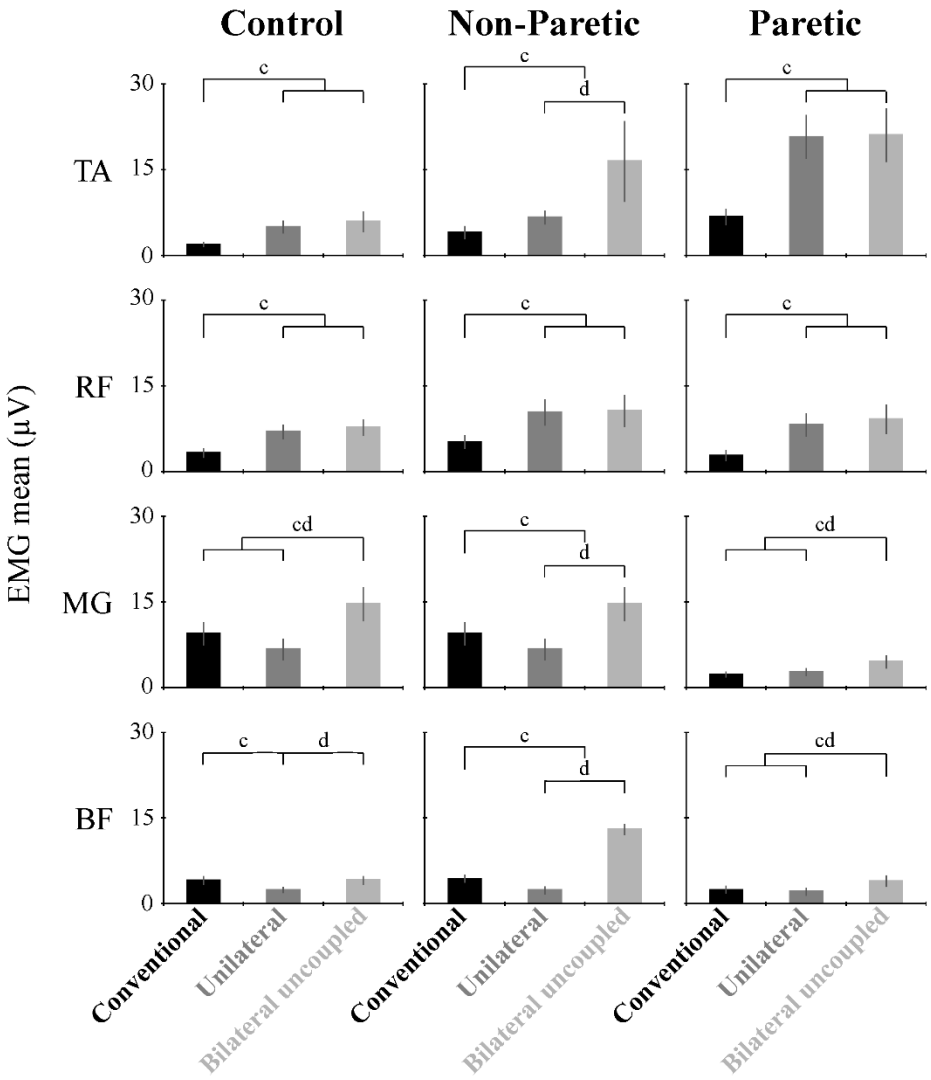

[c]p < 0.05 vs. conventional
[d]p < 0.05 vs. unilateral

Figure 2.7. Mean EMG amplitude across both groups and all conditions. Mean EMG amplitude is shown for controls (left column), non-paretic limb (middle column), and paretic limb (right column). Values are shown for all four muscles and during conventional (black bars), unilateral (medium gray bars), and bilateral uncoupled (light gray bars) pedaling. Differences between conditions (within a group or limb) are indicated by significance lines. No differences between groups were calculated for this independent measure. Nomenclature for significance lettering is provided. BF: biceps femoris; EMG: electromyography; MG: medial gastrocnemius; RF: rectus femoris; TA: tibialis anterior.

During bilateral uncoupled pedaling, mean EMG amplitude in the paretic, non-paretic, and control MG and BF was higher than during unilateral pedaling ($P \leq 0.01$). Mean EMG in these muscles was also higher than during conventional pedaling for all

cases ($P \leq 0.007$) except the control BF ($P = 0.43$). MI in the paretic and non-paretic MG and BF was higher than in conventional and unilateral pedaling ($P \leq 0.04$). However, in the paretic limb, these values were still lower than in control and non-paretic limbs ($P \leq 0.03$). In the non-paretic BF, MI was higher than controls ($P = 0.03$). Regardless of group, mean EMG amplitude in the RF did not increase beyond values observed during unilateral pedaling ($P \geq 0.12$). However, MI in the paretic, non-paretic, and control RF was significantly higher than during unilateral pedaling ($P \leq 0.02$). MI in the paretic RF was significantly lower than in the non-paretic RF ($P = 0.008$). Regarding the TA, only the non-paretic limb displayed a significant increase in mean EMG as compared to unilateral pedaling ($P < 0.05$).

Relationships with mechanical work and clinical measures

In the stroke group, %Work(net) was significantly correlated with PCI (R = -0.67, $P = 0.003$) and with COV of velocity in the paretic limb during unilateral (R = - 0.50, $P = 0.04$) and bilateral uncoupled (R = -0.54, $P = 0.02$) pedaling. %Work(net) was not significantly correlated with the change in mean EMG amplitude or EMG MI in the paretic limb between unilateral and conventional pedaling ($P \geq 0.15$). When the three significantly correlated variables were entered into a stepwise linear regression with backward elimination, only PCI made a significant contribution to the prediction of %Work(net) (F = 13, $R^2 = 0.44$, $P = 0.003$). If we forced the model to include both PCI and COV of velocity during unilateral pedaling with the paretic limb, there was no improvement in the model (F = 7, adjusted $R^2 = 0.42$, $P = 0.006$).

With respect to functional measures, $FMA_{LEtotal}$ was positively correlated with %Work(net) ($R^2 = 0.45$, $P = 0.003$) and negatively correlated with PCI ($R^2 = 0.50$, $P < 0.001$), but was not correlated with COV of velocity in the paretic limb during unilateral pedaling. Likewise, $FMA_{LEmotor}$ was also positively correlated with %Work(net) ($R^2 = 0.50$, $P = 0.001$) and negatively correlated with PCI ($R^2 = 0.61$, $P < 0.001$). Walking speed was positively correlated with %Work(net) ($R^2 = 0.28$, $P = 0.02$) and negatively correlated with PCI ($R^2 = 0.23$, $P = 0.03$). FM_{LEsens} was not significantly correlated with any outcome measure of pedaling performance.

Self-paced vs. auditory cued trials

COV of velocity, PCI, mean EMG amplitude, and EMG MI did not differ between self-paced and auditory cued trials ($P \geq 0.09$). Mean pedaling velocity was faster during self-paced than auditory cued trials ($P < 0.001$). PCI, mean EMG amplitude, and EMG MI were not different between experimental and exposure trials ($P \geq 0.27$). COV of velocity was lower during the experimental as compared to exposure trials ($P < 0.001$).

2.4 Discussion

The aim of this study was to better understand why asymmetric contributions (non-paretic > paretic) to bilateral lower limb movements persist in chronic stroke. We considered that motor impairment of the paretic limb and impaired interlimb coordination may contribute. A novel, split-crank pedaling device enabled conventional, unilateral, and bilateral uncoupled pedaling. Unilateral and bilateral uncoupled pedaling were performed to identify and distinguish between impairments in paretic motor output and

interlimb coordination. Conventional pedaling served as a nominal condition to which the other conditions were compared; it also provided measures of asymmetry during continuous, reciprocal, flexion and extension movements involving both lower limbs. While we found evidence of both impairments, results suggest that impaired interlimb coordination may be a more important factor than paretic motor impairment in chronic asymmetry. Below we discuss these findings in the context of prior work, examine physiological underpinnings, and consider implications for rehabilitation.

Conventional pedaling

Consistent with prior reports (Alibiglou & Brown, 2011; Brown & Kautz, 1998; H. Y. Chen et al., 2005; De Marchis et al., 2015; Kautz & Brown, 1998; Landin et al., 1977; Perell et al., 1998; Promjunyakul et al., 2015), conventional pedaling exposed asymmetries in mechanical work and muscle activity in the stroke group that were not apparent in controls. In the current study, the paretic limb of people with stroke produced only 16% of the net mechanical work for crank rotation. Muscle activity in RF, MG, and BF was significantly less modulated in the paretic limb than in the non-paretic and control limbs. While quantitative comparisons of EMG amplitude between the paretic and non-paretic limbs were not made, visual inspection of the data revealed many examples in which no task-related EMG was observed in the paretic limb during conventional pedaling. See Figure 3A. These observations support the conclusion that conventional pedaling is accomplished primarily by the non-paretic limb in people with stroke. They also suggest that pedaling is a useful model for functional lower limb

movements, such as walking, in which the non-paretic limb generates most of the work (Bowden et al., 2006; Olney et al., 1991; Turns et al., 2007).

Regarding the ability to accomplish the task, people with stroke performed conventional pedaling as rapidly and smoothly as controls. Both groups matched the rate of the auditory cue, and there were no between-group differences in COV of velocity. These observations suggest that the strategy that stroke survivors used, albeit asymmetric, was sufficient to meet the demands of conventional pedaling. Moreover, groups were well matched with respect to task completion during the nominal condition.

Unilateral pedaling

When the paretic limb performed unilateral pedaling, task performance was worse than during the conventional condition. Importantly, no such decline in performance was observed during unilateral pedaling in the control group or the non-paretic limb of people post-stroke. We conclude that these deficits represent stroke-related motor impairment in the paretic limb. Specifically, unilateral pedaling with the paretic limb was slower and less smooth than conventional pedaling. Deficits were driven by a transient decline in pedaling rate, a pause in forward crank progression, and/or a reversal of pedaling direction during the extension-to-flexion phase transition. Impairments in paretic motor output were not related to power generation, which occurs during the downstroke (Neptune & van den Bogert, 1998). Rather, performance deficits expressed during unilateral pedaling were due to difficulty executing the extension-to-flexion phase transition when the limb transitions from the downstroke (where power is generated) to the upstroke (where recovery occurs). During this transition, which is also known as the

posterior transition, the hip extends while the knee flexes so that the whole limb translates posterior with respect to the trunk. EMG data support that motor output associated with the posterior transition was impaired. EMG activity in the paretic BF was significantly less modulated than in controls, and BF EMG amplitude did not increase from conventional to unilateral pedaling. If we assume that BF is representative of other hamstring muscles involved in the posterior transition (Raasch & Zajac, 1999), we can conclude that insufficient activation of these muscles contributes to the paretic lower limb movement impairments seen in unilateral pedaling.

Unilateral pedaling also provides compelling evidence that the paretic limb has motor ability that is neither evident nor fully utilized during conventional pedaling. Mean EMG amplitude in the paretic TA and RF increased approximately threefold from conventional to unilateral pedaling. Values for MI in these muscles also increased, with the MI for the TA reaching control values. Thus, the tendency not to use the paretic limb in conventional pedaling (or to use it less than in unilateral pedaling) may represent learned non-use, a phenomenon whereby stroke survivors can move the paretic limb but fail to do so spontaneously, in real world situations (see Taub et al., 2006 for review). Learned non-use emerges when attempts to use the paretic limb are unsuccessful and use of the non-paretic limb results in effective, goal directed movement. Conventional pedaling provides an ideal environment for learned non-use. Through the mechanical connection between limbs and by securing the feet to the pedals, motor output from the non-paretic limb can compensate for deficits in the paretic limb and produce crank rotation. If the task is successfully accomplished in this way, there is no reward for using the paretic limb. Thus, stroke survivors learn to use the non-paretic limb over the paretic

limb. Although learned nonuse may explain a portion of the increased motor output in the paretic limb, some have suggested that pure learned non-use requires the ability to acutely increase the motor output of the paretic limb while maintaining good task performance (Sunderland & Tuke, 2005). We found that pedaling velocity was slower and more variable during unilateral pedaling with the paretic limb. Thus, in its purest form, learned nonuse may not fully explain increased motor output from the paretic limb.

Bilateral uncoupled pedaling

Participants in the control group were successful with bilateral uncoupled pedaling as evidenced by no change in mean pedaling velocity, as compared to conventional or unilateral pedaling. However, COV of velocity increased in controls during bilateral uncoupled pedaling. This effect was driven by a decrease in pedaling velocity during the posterior transition; this suggests that controls had more difficulty with this phase transition during bilateral uncoupled pedaling than during the other two conditions. That these changes occurred during bilateral uncoupled but not unilateral pedaling suggests that the posterior transition is more difficult to execute when simultaneous and coordinated output of both limbs is required. These data also provide insight into how neurologically intact individuals alter their pedaling strategy to fulfill the demands of bilateral uncoupled pedaling. To keep pace with the auditory cue, the control group adjusted their pedaling rate in each limb. Pedaling rate was above average in the downstroke and below average during upstroke. Because pedaling involves simultaneous and reciprocal movement of both limbs, these adjustments could be achieved only by coordinating the output of the two limbs. Thus, bilateral uncoupled pedaling exposed

decrements in pedaling performance that represent challenges to interlimb coordination, but it also provided evidence that people without stroke can overcome this challenge with a strategy reliant on interlimb coordination.

In the stroke group, bilateral uncoupled pedaling revealed evidence of impaired interlimb coordination. Observations from this condition also suggest that impaired interlimb coordination is a more substantial impediment to bilateral movement than paretic motor impairment alone. People with stroke were less successful at bilateral uncoupled pedaling than controls. During this condition, the stroke group was unable to match the rate of the auditory cue. Crank progression was less smooth, and interlimb phasing was less appropriate than in control participants. Some stroke survivors slowed their pedaling rate during the posterior transition while the contralateral limb moved more rapidly through downstroke. Others stopped pedaling during the posterior transition while they advanced the other limb, and some were wholly unable to achieve any sort of bilaterally coordinated movement of the limbs. Those who slowed or stopped one limb while advancing the other were most successful with the task. Their strategy resembled the one employed by controls wherein participants adjusted pedaling rate in each limb so that they could slow down for the posterior transition and still achieve the desired mean pedaling velocity. The observation that most stoke participants displayed behaviors similar to controls (e.g. slowing during posterior transition) suggests that they have some residual ability to produce reciprocally coordinated movement of the lower limbs and that they have access to the same neural resources for interlimb coordination as controls. However, because stroke survivors were less successful than controls with bilateral uncoupled pedaling (e.g. stopping, slowing more than controls), our data also suggest that

strategies available for interlimb coordination and their underlying mechanisms are degraded in chronic stroke. The observation that some people with stroke displayed no evidence of interlimb coordination during the bilateral uncoupled condition and were unable to move the limbs in a reciprocal, alternating fashion further supports this conclusion. Neural circuits responsible for interlimb coordination may be severely disrupted in these individuals.

Most deficits in pedaling performance across both groups occurred near the posterior transition of the pedaling cycle. In controls, pedaling velocity became more variable during bilateral uncoupled pedaling, largely because each limb slowed as it navigated the posterior transition. Most stroke survivors slowed or stopped near the posterior transition during this condition. Furthermore, most stroke survivors slowed or stopped near the posterior transition during unilateral pedaling. These findings suggest that the pedaling device does not perfectly simulate the mechanics of conventional pedaling. From a design standpoint, the elastic bands used to help move the limb through the upstroke offer the most resistance near the posterior transition. Nevertheless, because pedaling performance was only impaired in the stroke group, this condition can still provide insight into paretic motor impairments. Deficits in unilateral pedaling performance may occur because the mechanics of the device accentuate post-stroke alterations in activation of muscles involved in the posterior transition. Namely, excitation is phase advanced in BF and semimembranosus, making the posterior transition more difficult (Kautz & Brown, 1998). Because both groups had deficits in pedaling performance during bilateral uncoupled pedaling, the device mechanics likely have a larger effect during this condition. This coincides with previous work that has

shown altered muscle activation and increased braking torque during bilateral as compared to unilateral pedaling in both stroke survivors and controls (Kautz, Duncan, Perera, Neptune, & Studenski, 2005; Ting et al., 2000; Ting et al., 1998). However, limitations of the device likely do not negate the conclusions from this study. The mechanics required to perform unilateral and bilateral uncoupled pedaling were the same for each limb. Thus, differences in muscle activation and pedaling performance likely result from the coordination of movements of each limb. Although changes in muscle activity during unilateral and bilateral uncoupled pedaling as compared to conventional pedaling may have resulted from altered mechanics, any increase in muscle activity still suggests that the paretic limb had residual, unused motor ability.

Of note, pedaling performance in the non-paretic limb was impaired during bilateral uncoupled as compared to unilateral pedaling. Similarly, both limbs experienced performance deficits during bilateral uncoupled pedaling in the control group. These findings suggest that impaired interlimb coordination causes performance deficits in both limbs. In healthy controls, the bilateral influence of the sensorimotor state of one limb on the contralateral limb has been demonstrated during pedaling (Alibiglou et al., 2009; Ting et al., 2000; Ting et al., 1998). After stroke, it has been suggested that interlimb effects are enhanced, potentially through supraspinal disinhibition (Kautz & Patten, 2005; Kautz et al., 2006). Interestingly, performance of the non-paretic limb becomes worse and more similar to the paretic limb during bilateral movements of the upper limb (Dickstein, Hocherman, Amdor, & Pillar, 1993; Rice & Newell, 2001; Steenbergen, Hulstijn, de Vries, & Berger, 1996). Some of these authors have suggested that the non-paretic limb

adapts its motor performance to allow better interactions with the paretic limb. Such an effect might constrain the limbs to function as a unit to maximize performance bilaterally.

Interlimb coordination vs. paretic motor impairment

In this study, we detected stroke-related performance deficits during unilateral and bilateral uncoupled pedaling. These data suggest that both paretic motor impairment and deficiencies in interlimb coordination may contribute to reduced use of the paretic limb and asymmetric contributions to conventional pedaling. It is plausible that difficulty completing the posterior transition with paretic limb alone could contribute to asymmetry. Indeed, the paretic and non-paretic limbs are mechanically coupled, and the feet are secured to the pedals in conventional pedaling, and torque applied by the non-paretic limb can compensate for inadequate contributions from the paretic limb. The result may be reduced use of the paretic limb. The observation that COV of velocity during unilateral pedaling was associated with asymmetry further supports this conclusion. However, our data also strongly suggest that impaired interlimb coordination is a more important factor in asymmetry than paretic motor impairment alone. Most people with stroke displayed some deficiencies in unilateral pedaling, but all could produce repeated crank rotations. Hence, the inability to produce adequate torque in the correct direction at the correct time to rotate the crank cannot explain asymmetry. In contrast, not all stroke survivors could do bilateral uncoupled pedaling. Those who could produce reciprocal movement during this task displayed more substantial performance deficits than in unilateral pedaling. Finally, once a regression model accounted for movement deficits in bilateral uncoupled pedaling, impairments associated with unilateral

pedaling made no further contribution to the prediction of asymmetry during conventional pedaling. Together, these observations suggest that asymmetric work during conventional pedaling is due to the inability to coordinate the output of the paretic and non-paretic limbs, especially during the extension to flexion (i.e. posterior) phase transition.

There are several neural pathways that are thought to contribute to interlimb coordination between the legs. These pathways include supraspinal and interlimb sensory reflex pathways (Swinnen & Duysens, 2004). In addition, commissural interneurons connect CPGs controlling each limb, likely providing neural information that is important for coordination between limbs (Butt et al., 2002; Swinnen & Duysens, 2004). However, there is little information about alterations in these pathways after stroke. For tasks involving both the upper and lower limbs, propriospinal pathways also play a role in enabling interlimb coordination between the legs. Besides stroke-related changes directly within these pathways, supraspinal and CPG signals may modulate interlimb coordination through these pathways (Duysens et al., 1992; Matsuyama et al., 2004). The potential contributions of supraspinal and interlimb sensory reflex pathways to impaired interlimb coordination after stroke are discussed.

Descending supraspinal signals may have bilateral effects through ipsilateral uncrossed pathways and/or branched bilateral pathways. Ipsilateral uncrossed pathways and branched bilateral pathways both synapse at multiple levels onto ipsilateral motoneurons and interneurons (Carson, 2005; Jankowska & Edgley, 2006). Both pathways allow information contained in crossed neural signals to have bilateral effects. Reticulospinal and vestibulospinal tracts also have direct and indirect projections to

ipsilateral motoneurons that could facilitate interlimb coordination. Furthermore, neural output from each hemisphere of the brain may be coordinated through interhemispheric connections at various levels (Carson, 2005). Alterations at any of these levels could contribute to impairments in interlimb coordination.

After stroke, multiple studies suggest that descending supraspinal signals are altered and contribute to impaired interlimb coordination. When the non-paretic limb performs static contractions or pedaling, regardless of the timing of activation, paretic EMG phasing gets worse during pedaling (Kautz & Patten, 2005; Rogers et al., 2011). These findings suggest that the cause of impairment is descending commands associated with movement of the non-paretic limb. Consistent with this explanation, stroke survivors who are worse at bilateral antiphase ankle movements also have greater descending ipsilateral conductivity (Madhavan et al., 2010). These effects could be mediated through any of the pathways described above. Multiple studies have also found alterations in interhemispheric interactions after stroke. TMS and effective connectivity studies have demonstrated that the non-lesioned hemisphere inhibits motor areas in the lesioned hemisphere (Grefkes, Nowak, et al., 2008; Murase et al., 2004; Traversa et al., 1998). In acute and subacute stroke, resting interhemispheric connectivity is decreased in homologous sensorimotor regions, which is associated with worse motor performance (Carter et al., 2010; Carter et al., 2012). Thus, abnormal interhemispheric interactions may contribute.

Interlimb sensory reflex pathways are also thought to be important for interlimb coordination. Stepping in chronic spinal and decerebrate cats becomes unstable and more variable when one limb is deafferented (Giuliani & Smith, 1987; Grillner & Zangger,

1984). In humans with spinal cord injury, limb loading and hip joint sensory information facilitates a more normal locomotor pattern (Dietz et al., 2002). Also, in persons with spinal cord injury, bilateral antiphase hip flexion and extension enhances reflex effects that support bilateral coordination (Onushko & Schmit, 2007). Furthermore, electrical stimulation applied to the hindlimb elicits a coordinated bilateral response during walking in spinal and decerebrate cats (Duysens, 1977; Forssberg et al., 1977; Gauthier & Rossignol, 1981). In a similar manner, stimulation applied during human walking and running also elicits coordinated responses in both limbs (Duysens et al., 1991; Tax et al., 1995; Van Wezel et al., 1997; Yang & Stein, 1990). There are some observations that suggest that interlimb sensory reflex pathways are affected by stroke and may contribute to impaired interlimb coordination. During walking, swing phase perturbation to either limb elicits delayed interlimb reflexes in stroke compared to control subjects (Sharafi et al., 2016). Cutaneous stimulation applied to the non-paretic limb elicits altered reflex amplitude in the paretic limb at points in the walking cycle in TA, MG, VL, and BF (Zehr & Loadman, 2012).

Application to walking and clinical significance

Residual paretic motor impairments and impaired interlimb coordination are also evident during walking. The paretic limb is weaker in most, if not all, muscles of the lower limb than the non-paretic limb (for example see Richard W Bohannon & Andrews, 1995). Muscle weakness can have a profound functional impact; many stroke survivors cannot advance the paretic limb appropriately, even with near maximal plantarflexor activation (Allen et al., 2011; G. Chen & Patten, 2008; Nadeau et al., 1999). Poor muscle

activation may result from abnormal motor unit firing characteristics and or decreased corticomotor drive (Frontera et al., 1997; Palmer et al., 2017). EMG phasing is also abnormal during walking after stroke (Den Otter et al., 2007; Gray et al., 2015; Knutsson & Richards, 1979). These phasing deficits are associated with decreased paretic propulsion (Allen et al., 2013; Turns et al., 2007). There is also evidence of impaired interlimb coordination during walking after stroke. Heel strike phasing is abnormal and more variable in stroke compared to control subjects (Meijer et al., 2011; Roerdink et al., 2007). Stroke survivors have abnormal and/or delayed responses in the contralateral limb to perturbations in the ipsilateral limb during standing and walking (Berger et al., 1984; Dietz & Berger, 1984; Krasovsky et al., 2013). In a related task involving the stroke-affected lower limb, phasing of muscle activity in the paretic limb is worse during antiphase ankle movement of the non-paretic limb as compared to unilateral movement (Tseng & Morton, 2010). Task accuracy is also impaired in both the paretic and non-paretic limb when performing antiphase ankle tracking (Madhavan et al., 2010; Tseng & Morton, 2010). Overall, as seen in this study during pedaling, there is evidence of paretic motor impairments and impaired interlimb coordination after stroke during walking. Future work may evaluate the relative influence of each factor to asymmetric contributions to walking.

During both unilateral and bilateral uncoupled pedaling, we identified a wide variety of responses across stroke participants. Variability of responses is evident in the representative examples (Figure 3) and in the large standard deviations for measures such as mean pedaling velocity. To help organize these findings we identified three subgroups during both unilateral and bilateral uncoupled pedaling based on the pedaling strategy

used during each condition. We also considered whether stroke-related motor function was related to these subgroups, as might be expected. We found that subgroups defined during both unilateral and bilateral uncoupled pedaling were correlated with Fugl-Meyer total and motor scores; individuals with greater difficulty achieving the task had poorer motor function. Greater difficulty during unilateral pedaling was also correlated with slower walking velocity. These findings suggest that both paretic motor deficits and impaired interlimb coordination are important for overall motor function. Interestingly, unilateral and bilateral subgroup classification was not correlated ($R^2 = 0.12$, $P = 0.13$). Although no participant had better pedaling performance during bilateral uncoupled than unilateral pedaling, having greater performance impairments during unilateral pedaling was not predictive of having greater performance impairments during bilateral uncoupled pedaling. It is likely that the influence of paretic motor deficits and impaired interlimb coordination varies on a subject-by-subject basis. However, conclusions must be tempered because comparisons were made between artificial subgroups, not across a continuous variable.

In this study, we found evidence that TA retains substantial motor output in chronic stroke. Mean EMG activation in TA and MI both increased substantially during unilateral as compared to conventional pedaling. Muscle activation was also high during bilateral uncoupled pedaling. These findings are interesting because TA is typically one of the last muscles to recover, and exhibits substantial impairment, including reduced activation during walking (Knutsson & Richards, 1979). The large activation of TA during unilateral and bilateral uncoupled pedaling raises the possibility that these tasks could be used to improve spontaneous TA activity during functional movements of the

lower limb. Such an effect could positively influence functional recovery. However, motor output in TA may be contingent upon the activation of a flexion synergy; muscle activation in TA occurs with a similar phasing as in RF. Consequently, the rehabilitative benefits and detriments of training in-synergy or out-of-synergy movements must be considered. For example, promoting flexion synergies might be useful during the swing phase of walking, but be detrimental during other lower limb tasks.

The results from this study have implications for clinical rehabilitation of lower limb movement after stroke. Asymmetrical contributions to pedaling may promote optimal pedaling performance, but also yield an underutilization of paretic motor ability. Therefore, addressing the causes of asymmetries during pedaling may enhance paretic motor output while maintaining pedaling performance. In this study, we found evidence that both paretic motor impairments and impaired interlimb coordination contribute to asymmetry. Thus, rehabilitative interventions likely must address both causes to elicit improvement.

Limitations

There are several limitations to this study. First, the participants with stroke who participated in this study had relatively high levels of function. All individuals could function in the community and were able to participate in the study. In people who are lower functioning, paretic motor impairment be a more important contributor to asymmetry (e.g. the paretic limb is paralyzed). Second, our measures of asymmetry are imperfect. MI is an indirect measurement of the amplitude of muscle activity but was used because of limited ability to normalize EMG responses. Percent mechanical work

was evaluated on a different pedaling device than was used to assess interlimb coordination and paretic motor impairment. Different devices were used because the bike with a split crankshaft was not instrumented to measure force/torque. Thus, mechanical work symmetry on the instrumented device may not directly relate to the value of that construct on the other device. However, because many studies have described asymmetries during pedaling, it is likely that a similar result would have been found on the split-crank bike.

Impaired proprioception may have contributed to our results. Specifically, the inability to maintain an antiphase relation between the pedals may have resulted from an inability to sense the position of the leg, not interlimb coordination. However, subjects were positioned so they could see their feet while pedaling, and we did not find a relation between FM_{LEsens} and any measure of pedaling performance. These results suggest that impaired proprioception did not contribute to deficits in bilateral uncoupled pedaling. Differential levels of upper limb motor activity also may have affected our results. It is well documented that motor activity in the upper limb has a significant impact on motor activity in the lower limb (for review see Zehr, Hundza, & Vasudevan, 2009). Although we did not collect any upper limb data, anecdotally, we did not observe any noticeable upper limb motor activity in any participant.

The primary conclusion from this study was that impaired interlimb coordination may be a more important factor than paretic motor impairment in chronic asymmetry. This conclusion has several caveats. First, bilateral activation may exacerbate paretic motor impairments by increasing coactivation, demands for stabilization, etc. Second, task performance may have been impaired during bilateral uncoupled pedaling merely

because the task is more complex. The authors would argue that both represent aspects of interlimb coordination. However, this is our interpretations, and thus our conclusions may be under-representing the effect of paretic motor impairments and over-emphasizing the effect of impaired interlimb coordination on chronic asymmetries during pedaling after stroke.

CHAPTER 3: ALTERED INTERLIMB CUTANEOUS REFLEXES ARE RELATED TO INTERLIMB COORDINATION AND COMPENSATION DURING PEDALING AFTER STROKE

3.1 Introduction

The organized functioning of multiple limbs performing a motor task with a shared goal is termed interlimb coordination (Swinnen & Duysens, 2004). Interlimb coordination is thought to be important during lower limb locomotor movements because it supports phase transitions, the maintenance of stability, and responses to perturbations (Swinnen & Duysens, 2004; Zehr & Stein, 1999). Several studies have demonstrated that interlimb coordination is altered during lower limb locomotor movements after stroke. During hip flexion and extension, torque production in the paretic limb is more abnormal during bilateral than unilateral movement (Hyngstrom et al., 2010). During pedaling, phasing of paretic muscle activity and force development is abnormal when the non-paretic limb also pedals or performs isometric contractions (Kautz & Patten, 2005; Rogers et al., 2011). During walking, the phasing between heel strikes is abnormal and more variable in stroke compared to control participants (Meijer et al., 2011; Roerdink et al., 2007).

Recently, our lab found further evidence of impaired interlimb coordination during pedaling after stroke. Using a custom pedaling device that removes the mechanical connection between pedals, participants were asked to simultaneously move each leg while maintaining an antiphase relation between the pedals (bilateral uncoupled pedaling). Unlike controls, stroke participants were unable to maintain an antiphase relation between the pedals, and velocity and smoothness of pedaling deteriorated as

compared to unilateral and conventional pedaling. Motor performance was so poor in some participants that they were unable to successfully rotate either pedal. We also found that individuals with greater impairments in interlimb coordination produced a lower percentage of the mechanical work of pedaling with the paretic limb. Thus, interlimb coordination is impaired after stroke, and this may contribute to asymmetrical contributions to pedaling. Because of its impact on motor behavior, it is important to understand what factors contribute to impaired interlimb coordination after stroke.

Stroke-related alterations at a supraspinal or spinal level may affect neural pathways important for interlimb coordination, including supraspinal, spinal central pattern generator (CPG), and interlimb sensory reflex pathways (Swinnen & Duysens, 2004). Of these, much previous work has focused on interlimb sensory reflex pathways. During walking in spinal, decerebrate, and intact cats, tactile or electrical input applied to the hindlimb elicits a coordinated response in both hindlimbs (Duysens, 1977; Duysens & Loeb, 1980; Duysens et al., 1980; Forssberg et al., 1977; Gauthier & Rossignol, 1981). Similarly, in human walking and running, gait obstruction and cutaneous nerve stimulation evoke coordinated responses in both legs (Berger et al., 1984; Dietz et al., 1986; Eng et al., 1994; Tax et al., 1995; Van Wezel et al., 1997). These findings in cats and humans support an important role for interlimb sensory pathways in the control of interlimb coordination. Thus, insight into the how the control of interlimb sensory pathways is altered after stroke can be gained through the evaluation of interlimb sensory reflexes. These reflexes can also provide insight into how the control of other pathways important for interlimb coordination may be altered after stroke.

However, few studies have evaluated interlimb sensory reflexes after stroke. Kloter, Wirz, and Dietz (2011) evaluated interlimb cutaneous reflexes in the upper limb in response to stimulation of the non-paretic and paretic lower limb. They found that interlimb reflexes in the non-paretic upper limb are blunted. Other studies have evaluated interlimb cutaneous reflexes in the upper limb following stimulation of the contralateral upper limb. During rhythmic opening/closing of the hand and during arm cycling, interlimb cutaneous reflexes are abnormal in both limbs, with a stronger effect in the non-paretic limb (Schrafl-Altermatt & Dietz, 2016; Zehr, Loadman, & Hundza, 2012). These findings suggest that there is abnormal processing of sensory information from the paretic upper limb. In the lower limb, few studies have investigated interlimb cutaneous reflexes after stroke, particularly during locomotor movements. Zehr and Loadman (2012) found that cutaneous stimulation applied to the non-paretic limb elicited altered reflex amplitude in several paretic muscles.

The purpose of this study was to determine whether interlimb sensory reflexes are altered during pedaling after stroke and whether alterations are associated with impaired interlimb coordination. We elicited interlimb cutaneous reflexes with stimulation of the sural nerve and quantified the response amplitude. Interlimb coordination was assessed during bilateral uncoupled pedaling and quantified as the accuracy and consistency of maintaining an antiphase relation between the pedals. We hypothesized that stroke survivors would have abnormal interlimb cutaneous reflex amplitudes which would scale with impairments in interlimb coordination. Based on our previous findings, we also hypothesized that abnormalities in the amplitude of interlimb cutaneous reflexes would be associated with asymmetric contributions to pedaling propulsion. To test this

hypothesis, we quantified the percent propulsive pedaling work performed by the paretic limb during conventional pedaling. As an exploratory analysis, we also quantified interlimb coordination and propulsion symmetry during walking. Inter-relations between sensorimotor function, interlimb cutaneous reflexes, interlimb coordination, and symmetry during pedaling and walking were explored.

3.2 Methods

Participants

22 individuals with chronic stroke and 15 age-matched controls participated in the study. Subjects were free of medical illness and neurological disease or injury except for stroke. Study procedures were approved by the Institutional Review Board at Marquette University, and all subjects provided written informed consent.

Clinical measures

Stroke-related sensorimotor function of the lower limbs was assessed with multiple tests. Self-selected walking velocity was assessed with the 8m comfortable walk test. Stroke-related sensorimotor function was assessed with the lower extremity Fugl-Meyer Assessment ($FM_{LEtotal}$), which was subdivided into motor ($FM_{LEmotor}$), sensory (FM_{LEsens}), balance (FM_{LEbal}), range of motion (FM_{LErom}), and pain (FM_{LEpain}) sub-components. Balance was assessed with the Berg Balance Scale. Values and participant demographics are presented in Table 3.1.

Variable	Stroke (N = 22)	Control (N = 15)
Age (years)	61 (11)	67 (8)
Sex (male/female)	12/10	7/8
Height (cm)	174 (11)	172 (10)
Mass (kg)	84 (16)	79 (15)
BMI	28 (4)	27 (5)
Time since stroke (years)	12 (6), Range: 1 – 25	
Stroke type (ischemic/hemorrhagic)	18/4	
Stroke location (cortical/sub-cortical)	14/8	
Paretic limb (left/right)	13/9	
Walking vel. (m/s)	0.87 (0.30)	
Berg balance (max: 56)	47 (8)	
$FM_{LEtotal}$ (max: 96)	79 (9)	
$FM_{LEmotor}$ (max: 34)	25 (6)	
FM_{LEsens} (max: 12)	10 (3)	
FM_{LEbal} (max: 10)	7 (1)	
FM_{LErom} (max: 20)	18 (3)	
FM_{LEpain} (max: 20)	20 (0)	

Table 3.1. Participant demographics and clinical measures. Demographic characteristics are shown for the stroke and control group. Results from clinical tests of sensorimotor impairment are shown for the stroke group. Values are Mean (SD). BMI: body mass index; $FM_{LEtotal}$: Fugl Meyer Assessment total score; $FM_{LEmotor}$: motor score; FM_{LEsens}: sensory score; FM_{LEbal}: balance score; FM_{LErom}: range of motion score; FM_{LEpain}: pain score.

Interlimb cutaneous reflexes

During conventional, bilateral pedaling, interlimb cutaneous reflexes were elicited with electrical stimulation applied to the sural nerve of each limb at eight positions in the pedaling cycle [45, 90, 135, 180, 225, 270, 315, 360°]. Stimulation at these pedaling positions was applied across 4 x ~10 minute bouts of continuous pedaling. Within each bout, stimulation was applied at two of the eight pedaling positions, randomly selected for each limb. At each pedaling position, data were collected from 60 total trials: 15 stimulation and 15 control trials X two limbs. Thus, across eight pedaling positions, there were 480 trials. For each trial, we randomized the limb receiving stimulation (left or right), trial type (stimulation or control), and pedaling position (of the two positions

tested within the respective bout). During control trials, no stimulation was applied. There was a minimum time of 3.8 seconds between consecutive trials (>2 revolutions). Across both groups, stimulation was applied within 0.5 (0.07)° of the target position. For all pedaling, participants were asked to pedal with an auditory pacing cue at 45 RPM, but rate was not monitored in real time. Rest was given between pedaling bouts as needed.

Interlimb cutaneous reflexes were evoked with non-noxious constant current stimulation (DS7A, Digitimer, Ft. Lauderdale, FL, USA) to the sural nerve at the midway point between the lateral malleolus and the Achilles tendon. Stimulation consisted of 5 x 1 ms pulses at a frequency of 300 Hz. Stimulation intensity was selected as a multiple of the radiating threshold (RT) that produced EMG responses in the contralateral limb but was not painful. For all participants, the absolute intensity of stimulation was the same between limbs. In controls, the absolute intensity for both limbs was determined from the limb with the lowest RT; in stroke participants, the intensity for both limbs was determined from the non-paretic limb. RT was determined prior to pedaling and was defined as the intensity at which there was distinct radiation of the stimulus into the foot. To determine RT, the feet were strapped into the pedals with the crank arm for the target limb fixed at top dead center position. Stimulation pulses were applied with gradually increasing intensity until RT was reached. RT was reassessed between the second and third pedaling bout to ensure that relative stimulation intensity was consistent throughout the experiment. All electrical stimuli were delivered with disposable, 2 cm electrodes (Neuroline 720, Ambu, Ballerup, Denmark) secured to the skin with tape and elastic wrap.

Pedaling was performed on a custom-designed pedaling device (Figure 3.1) that allowed supine pedaling against a frictional load applied through a pulley system. This pedaling device has a bisected crankshaft that was coupled with the pedals in an antiphase orientation to allow conventional, bilateral pedaling. Rotary optical encoders (MR318, Micronor Inc., Newbury Park, CA) measured crankshaft position. Fiber optic cables carried position signals from the encoders to controller units (MR310, Micronor Inc., Newbury Park, CA). Top dead center position (0°), was defined for each crank arm as the position where the foot was nearest to the hip and the crank arm was parallel with the plinth. Participants' feet were secured to the pedals with a strap around the heel and the top of each foot because many stroke survivors could not keep their paretic foot on the pedal without these straps. Electromyography (EMG) data were recorded bilaterally from the biceps femoris (BF), medial gastrocnemius (MG), rectus femoris (RF), semitendinosus (ST), soleus (SOL), tibialis anterior (TA), vastus medialis (VM), and vastus lateralis (VL). The skin was prepared using isopropyl alcohol, and electrodes were applied at recommended locations (Hermens et al., 2000). A common reference electrode was placed on the medial malleolus. Electrodes were secured using tape and elastic bandages. EMG data were sampled with a band-pass filter (20 – 450 Hz) at a gain of 10,000 using an amplifier system (Bagnoli-8, Delsys Inc., Natick, MA).

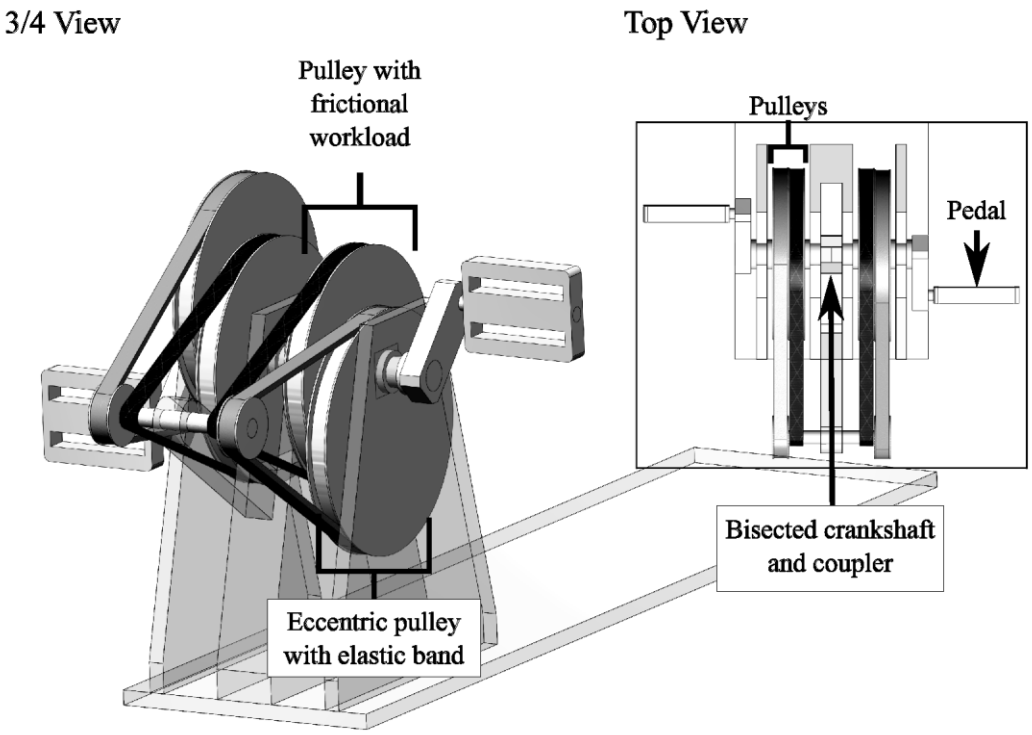

Figure 3.1. Pedaling device with bisected crankshaft. The top view depicts the bisected crankshaft and coupler. With the coupler in place, interlimb cutaneous reflexes were tested during conventional pedaling. With the coupler removed, interlimb coordination was tested during bilateral uncoupled pedaling. The ¾ view depicts the pulley systems of the pedaling device. A pulley with frictional workload was used to provide resistance during all pedaling. An eccentric pulley system with elastic bands was used during bilateral uncoupled pedaling to simulate the forces provided by the contralateral leg during conventional pedaling. Optical encoders (not pictured) measured crankshaft position.

EMG data were detrended, rectified, and crank referenced. To assess background muscle activity, EMG were extracted from complete revolutions (0 - 360°) that were uncontaminated by cutaneous stimulation. Revolutions were considered contaminated if stimulation occurred during that revolution or during the preceding revolution. The resulting EMG data were ensemble averaged. EMG modulation was quantified with modulation index (MI), defined as (EMGmax – EMGmin) / EMGmax * 100). EMG MI was used because it allows between-group comparisons of muscle activation without the associated errors caused by normalizing muscle activity during a cyclical task to a maximal value at a single joint position (Mirka, 1991).

To quantify reflex activity, EMG were extracted for the time period 0 – 150 ms after stimulation. For control trials, EMG were extracted for the time period 0 – 150 ms after the target pedaling position was attained. For each pedaling position in each leg, EMG from all stimulation trials were averaged together, and EMG from all control trials were averaged together. The average response from control trials was subtracted from the average response from stimulation trials to reveal reflex activity at each pedaling position. To quantify cutaneous reflex amplitude, the integral was calculated from this difference curve (stimulation – control) for the time interval 65 – 150 ms. Reflexes prior to 65 ms were disregarded because they were infrequent and often contaminated by stimulus artifact. The reflex response in most muscles terminated at or before 150 ms, so this was chosen as the longer latency cutoff. Using standardized cutoff periods facilitated comparisons between groups and limbs. To account for automatic gain control, reflex amplitude was normalized to the integral during control trials for the time interval 65 – 150 ms, calculated at each pedaling position. Eq. 1 shows the processing steps to quantify normalized reflexes.

$$\text{Eq. 1: Normalized reflexes} = \frac{\int_{65ms}^{150ms}[\mu(\text{stimulation trials}) - \mu(\text{control trials})]}{\int_{65ms}^{150ms}\mu(\text{control trials})} \times 100\%$$

Interlimb coordination during pedaling

To assess interlimb coordination, the bisected crankshaft on our pedaling device was mechanically uncoupled, allowing each pedal to function independently. Participants were instructed to perform bilateral uncoupled pedaling—pedal forward with both legs simultaneously and maintain an antiphase (180°) relation between the left and right

pedals. One 45 second exposure trial and one 60 second data collection trial were performed. Verbal feedback was provided during the exposure trial but not during data collection. Pedaling was performed with an auditory pacing cue at 45 RPM. Position was measured for both halves of the crankshaft, and top dead center position was defined separately for each crank arm as described above.

To facilitate bilateral uncoupled pedaling, an eccentric pulley system was used to mimic the mechanical work performed by the contralateral limb (see Figure 3.1). During the downstroke of the ipsilateral limb, elastic bands around the eccentric pulley system are stretched and store energy, which is released during the upstroke. The elastic load on the eccentric pulley system was determined during a separate session as described in Chapter 2. Briefly, subjects performed unilateral pedaling separately with each limb while up to six elastic loads were applied. The elastic load used during bilateral uncoupled pedaling was selected as the load that was adequate to allow pedaling and elicited an average velocity profile that was most similar to that seen during conventional pedaling.

Position data were used to characterize interlimb coordination during bilateral uncoupled pedaling. The continuous relative phase (CRP) of the crankarms was calculated as the minimum absolute difference between the position of the crankarms at every timepoint. Adapting methods from Plotnik et al. (2007), we calculated the phase coordination index ($PCI_{pedaling}$) from CRP data:

$$PCI_{pedaling}\ (\%) = \left[\frac{\sigma(CRP)}{\mu(CRP)} \times 100\%\right] + \left[\frac{\mu(|CRP\text{-}180|)}{180} \times 100\%\right]$$

$PCI_{pedaling}$ provides a composite measure of the accuracy (mean normalized difference from 180°) and consistency (coefficient of variation of CRP) of phasing. Larger values represent worse interlimb coordination. $PCI_{pedaling}$ was the primary outcome measure of interlimb coordination during pedaling.

Symmetry of mechanical work during pedaling

Mechanical work performed by each limb was assessed using a pedaling device with a solid crankshaft attached to a rigid backboard oriented at 40° from horizontal (PowerTower with EMC Ergometric Multi Cycle attachment, Total Gym, San Diego, CA, USA). This device and the methods for quantifying mechanical work have been described previously (Fuchs et al., 2011; Kautz & Brown, 1998; S. Schindler-Ivens et al., 2008). Briefly, participants' feet were secured to the pedals with straps around the heel and top of the foot, and they pedaled for 2 minutes with an auditory pacing cue at 45 RPM against a moderate load. Forces applied to each pedal were measured with 6-degree of freedom force transducers (Delta 660-60, ATI Industrial Automation, Apex, NC, USA), and position of the crankshaft and the pedals were measured with optical encoders (BEI Model EX116-1024-2, BEI Sensors, Thousand Oaks, CA, USA). Mechanical work data were collected from 19 stroke participants. Data were excluded from 3 participants because of loss to follow-up.

Torque contributing to angular rotation of the crankshaft (tangential with respect to the crank arm) was calculated. Data were referenced to crankshaft position and ensemble averaged. Positive area under the resulting curve represented propulsive work, negative area under the curve represented braking work, and the difference between

propulsion and braking was net work. Percent work done by the paretic limb ($\%Propulsion_{pedaling}$, $\%Braking_{pedaling}$, and $\%Net_{pedaling}$) was computed as: Work(paretic)/Work(total)*100, where Work(paretic) was the work done by the paretic limb and Work(total) was the sum of the work done by both legs. A value of 50% indicated equal sharing of the work between limbs. $\%Propulsion_{pedaling}$ was used as the primary outcome measure of symmetry during pedaling.

Interlimb coordination and propulsive symmetry during walking

Participants walked at a self-selected comfortable walking speed on a split belt instrumented treadmill (FIT, Bertec Corporation, OH, USA). Two 60 second trials were performed. Bilateral ground reaction forces in the vertical (GRFz), anterior/posterior (GRFx), and left/right (GRFy) directions were measured with force plates under each belt. A safety harness with no body-weight support was worn. Although encouraged to walk without support, participants were permitted to use handrails as needed to ensure safety. Walking data were analyzed from a subset of stroke survivors (n = 15). Data were excluded from 7 participants because of loss to follow-up (n = 3), safety limitations that precluded treadmill walking (n = 3), and equipment malfunction (n = 1). 80 (30) strides were analyzed per participant. Data were excluded from one significant outlier.

Heelstrike events were identified as the timepoints when GRFz exceeded 15 N. To measure interlimb coordination during walking, heelstrike events were used to calculate PCI, as detailed in Plotnik et al. (2007). First, the discrete relative phase (φ_i) between the paretic (tP) and non-paretic (tNP) limb was calculated for from the timing of every ith heelstrike.

$$\varphi i = \frac{\mathrm{tP}i - \mathrm{tNP}i}{\mathrm{tNP}(i+1) - \mathrm{tNP}i} \times 360°$$

Discrete relative phase is the paretic step time divided by the non-paretic stride time. Using discrete relative phase data, we calculated the mean discrete relative phase and $PCI_{walking}$:

$$\text{PCI (\%)} = \left[\frac{\sigma(\varphi i)}{\mu(\varphi i)} \times 100\%\right] + \left[\frac{\mu(|\varphi i - 180°|)}{180°} \times 100\%\right]$$

As during pedaling, $PCI_{walking}$ provides a composite measure of the accuracy (mean normalized difference from 180°) and consistency (coefficient of variation of discrete relative phase) of phasing. Higher values represent worse interlimb coordination.

Propulsive and braking impulse performed by each limb were also measured for each participant. Using GRFx data, propulsive and braking impulse were defined as the force-time integral for anteriorly and posteriorly directed forces, respectively. Percent impulse done by the paretic limb ($\%Propulsion_{walking}$ and $\%Braking_{walking}$) was computed, as described above. $PCI_{walking}$ was used as the primary outcome measure of interlimb coordination, and $\%Propulsion_{walking}$ was used as the primary outcome measure of symmetry during walking. Additional analyses and results related to walking can be found in Appendix B.

Statistics

All data were tested for normality using the Shapiro Wilk test. Data used for between-group comparisons were tested for equality of variances with the Levene's test. Non-parametric statistics were used for non-normal or inhomogeneous variables. For all ANOVAs, the Greenhouse-Geisser correction was used in cases where sphericity was violated. All statistical tests used SPSS Statistics 22.0 (International Business Machines Corporation, New York, NY), and $P < 0.05$ was accepted as significant.

In the control group, there were no differences for interlimb cutaneous reflex amplitude, EMG MI, RT, or relative stimulation intensity between the left and right leg, so values were averaged. Interlimb cutaneous reflex amplitudes were compared between the paretic and non-paretic limb with separate ANOVAs for each muscle [within subject factors of limb (2 levels) and pedaling position (8 levels)]. Reflex amplitude was also compared between the paretic limb and controls and between the non-paretic limb and controls using separate ANOVAs for each muscle [between subject factor of group (2 levels), within subject factors of pedaling position (8 levels)]. In the event of a significant interaction, reflex amplitude was compared between groups (paretic vs. control OR non-paretic vs. control) at every pedaling position with independent samples t-tests and Mann Whitney U tests or between limbs (paretic vs. non-paretic) with paired samples t-tests and Wilcoxon signed-rank tests. Because we had low power to detect effects and variability was high, we also tested reflexes between groups and between limbs if there was a main effect for limb or pedaling position.

Background EMG MI, phase accuracy, phase consistency, $PCI_{pedaling}$, RT, and relative stimulation intensity were compared between and/or within groups for each muscle. Between group comparisons (control vs. paretic and control vs. non-paretic, or

control vs. stroke) were performed with independent samples t-tests and Mann Whitney U tests; within group comparisons (paretic vs. non-paretic and right vs. left) were performed with paired samples t-tests and Wilcoxon signed-rank tests. Pedaling rate was compared between groups and across bouts with a mixed ANOVA [within subject factor of bout (4 levels) and between subject factor of group (2 levels)]. RT was compared between limbs and over time with a separate repeated measures ANOVA for each group [within subject factors of limb (2 levels) and time (2 levels)]. Percent work and impulse values performed by the paretic limb were compared with 50% and mean discrete relative phase was compared with 180° using one-sample t-tests and Wilcoxon signed-rank tests.

Relations between interlimb cutaneous reflex amplitude, interlimb coordination (PCI), propulsive symmetry (percent work and impulse), and clinical measures (FM scores, Berg, and walking velocity) were tested with Pearson and Spearman correlations. Only muscles that had between or within group differences were included in correlational analyses. If there was a main effect of group or limb, average reflex amplitude across all pedaling positions was used in correlational analyses; if there was an interaction effect, reflex amplitudes at pedaling positions with post-hoc differences were used.

3.3 Results

Background EMG activity

Group average background EMG activity for all muscles are shown for controls, the non-paretic limb, and the paretic limb in Figure 3.2. The biarticular RF was active during the transition from flexion to extension (anterior transition) and the biarticular BF, ST, and MG were active during the transition from extension to flexion (posterior

transition). The uniarticular VM, VL, and SOL were active primarily during extension. The uniarticular TA was active during two periods: during extension prior to the posterior transition and during flexion. The overall pattern of modulation of EMG activity appeared to be similar between controls, the non-paretic limb, and the paretic limb. However, EMG modulation in the paretic limb was smaller in MG, VM, RF, VL, ST, and BF as compared to controls and the non-paretic limb ($P \leq 0.01$, except for BF compared to controls: $P = 0.07$). EMG modulation was also smaller in the paretic TA as compared to the non-paretic limb ($P = 0.03$). In contrast, EMG modulation was not different between the non-paretic limb and controls for any muscle ($P \geq 0.09$). See Table 3.2.

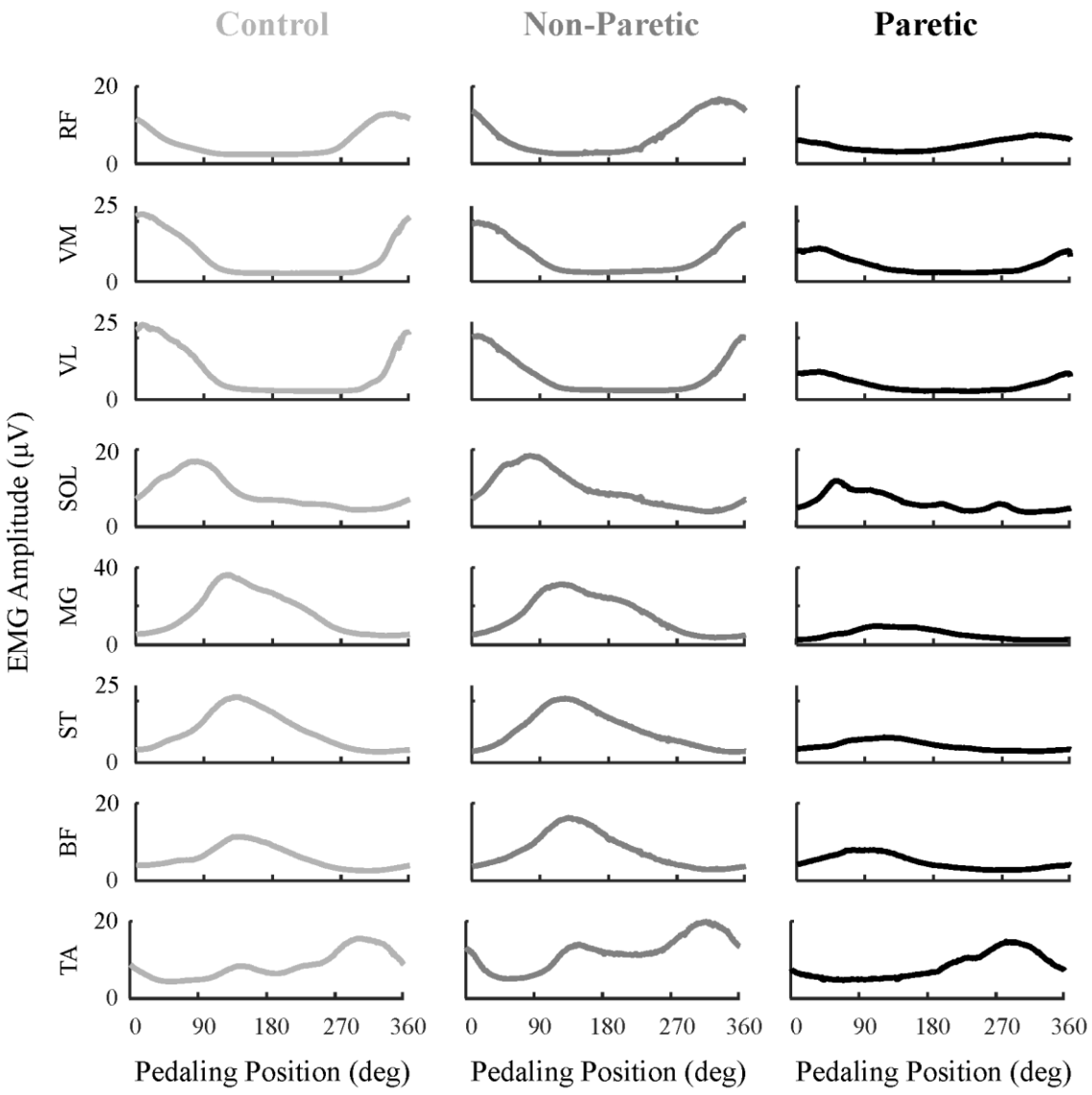

Figure 3.2. Background muscle activity during conventional pedaling. Group average EMG activity for controls (light gray), the non-paretic limb (medium gray), and the paretic limb (black). RF – rectus femoris; VM – vastus medialis; VL – vastus lateralis; SOL – soleus; MG – medial gastrocnemius; ST – semitendinosus; BF – biceps femoris; TA – tibialis anterior.

Muscle	Modulation Index (%)		
	Control	*Non-Paretic*	*Paretic*
RF	80 (12)	83 (9)	58 (21)*†
VM	83 (12)	82 (16)	62 (26)*†
VL	83 (10)	84 (16)	67 (25)*†
SOL	77 (11)	80 (17)	75 (17)
MG	86 (13)	88 (7)	70 (19)*†
ST	83 (13)	87 (8)	65 (18)*†
BF	73 (18)	79 (13)	65 (14)*
TA	71 (16)	80 (13)	69 (17)*

Table 3.2. EMG modulation index. Modulation index (%) is shown for controls, the non-paretic, and the paretic limb for all eight muscles. Modulation index was defined as (EMGmax – EMGmin) / EMGmax * 100). Values are Mean (SD). BF: biceps femoris; MG: medial gastrocnemius; RF: rectus femoris; SOL: soleus; ST: semitendonosus; TA: tibialis anterior; VM: vastus medialis; VL: vastus lateralis. $^{*}P < 0.05$ paretic vs. non-paretic, $^{\dagger}P < 0.05$ paretic vs. control.

Interlimb cutaneous reflexes

Representative examples of interlimb cutaneous reflexes are shown in Figure 3.3. Mean reflex amplitude at each pedaling position is shown in Figure 3.4 for controls, the non-paretic limb, and the paretic limb. In both figures, the pedaling position represents the position of the contralateral limb when stimulation was applied to the ipsilateral limb. For example, the reflex amplitude at 90° for the paretic limb represents the reflex response in the paretic limb to stimulation applied to the non-paretic limb at its 270° position. During conventional pedaling, the pedals are always 180° out of phase, so the paretic limb was at its 90° position in this example. In addition, note that although the data is shown at particular pedaling positions, the reflex amplitude was measured at a latency of 65 – 150 ms, which was 24 (6)° – 55 (11)° after the target pedaling position was attained. Most reflex responses were < 20% of the EMG amplitude during control trials, and there was a considerable amount of interindividual variability.

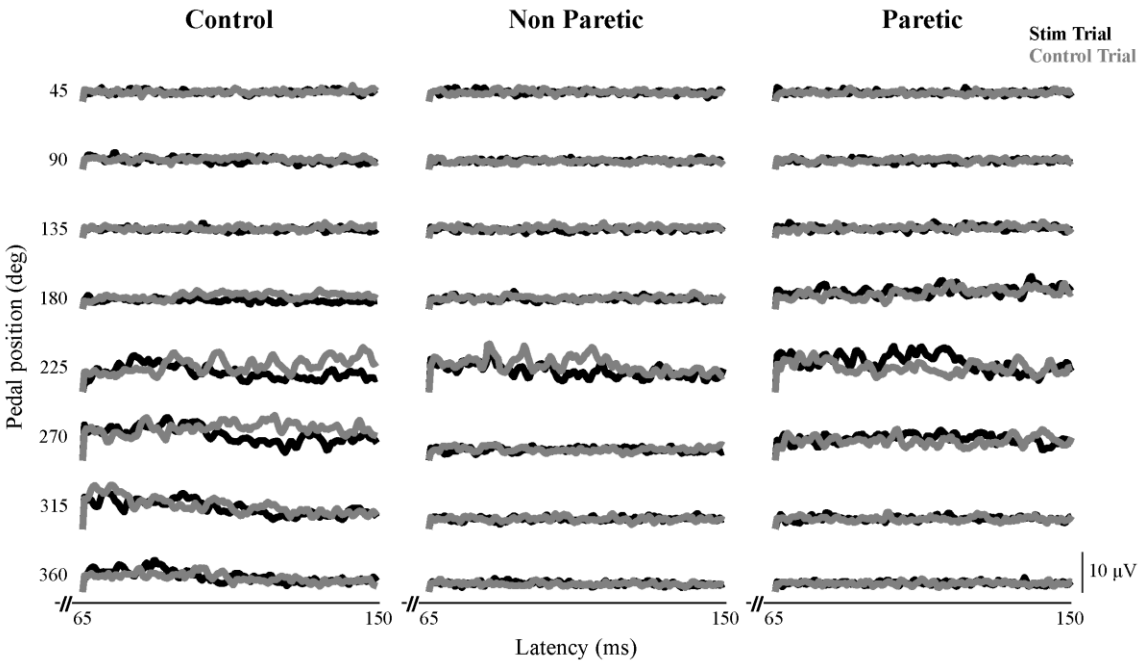

Figure 3.3. Representative examples of interlimb cutaneous reflexes. Rectus femoris EMG activity from stimulation (black lines) and control trials (gray lines) for one limb in a control subject and from both the paretic and non-paretic limb in a stroke subject. Data are shown for 65 – 150 ms after stimulation or the attainment of the target position; the stimulus artifact and any early reflexes are not shown. Responses are shown at 8 pedaling positions, which are 180° offset from the target position of the contralateral limb. For example, the data point at 45° for the paretic limb represents the interlimb cutaneous reflex amplitude in response to stimulation applied to the non-paretic limb when it was at 225°. Differences between the stimulation and control EMG represent reflex activity.

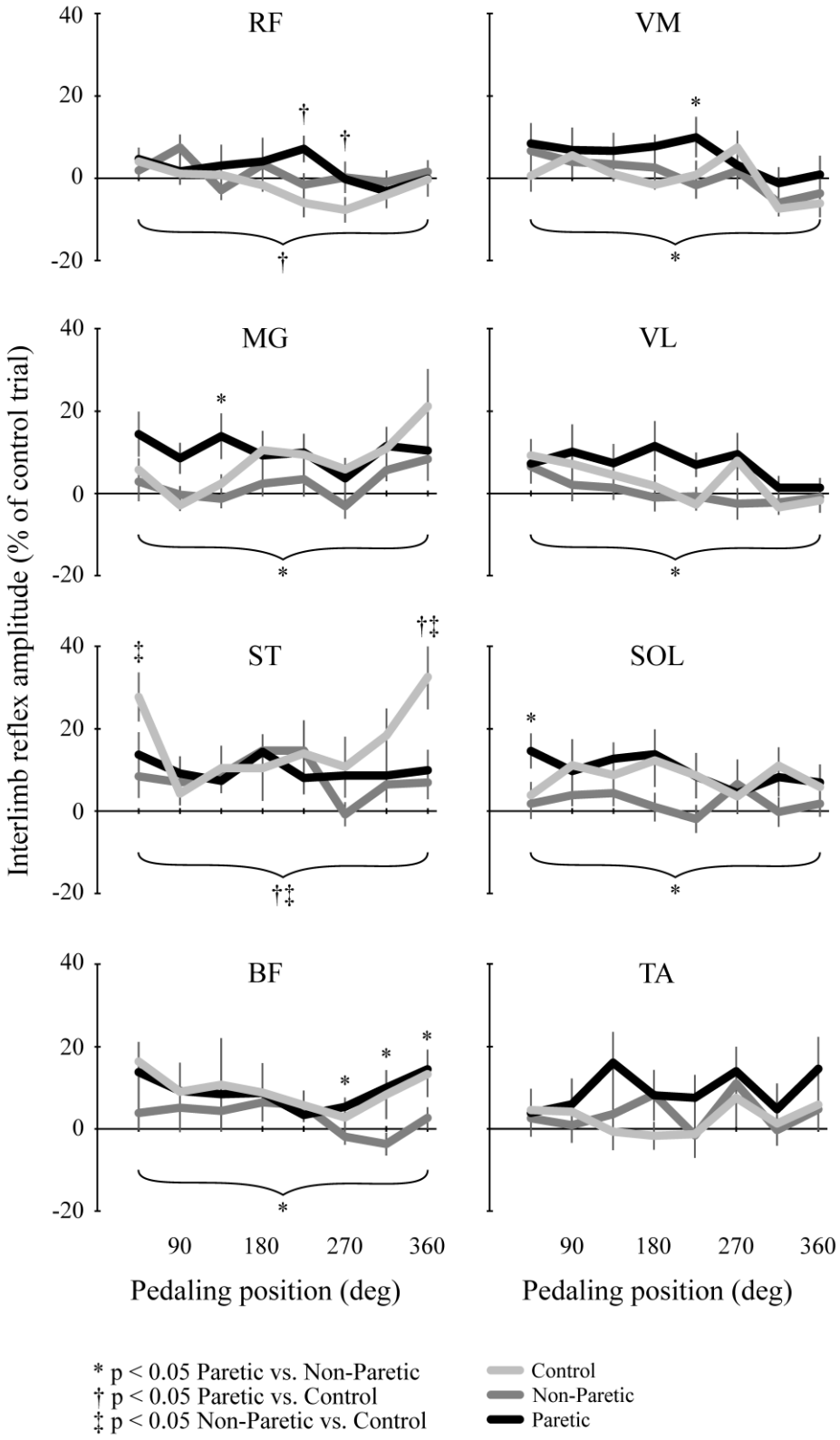

Figure 3.4. Group average interlimb cutaneous reflex amplitude. Interlimb cutaneous reflex amplitude is shown for controls (light gray), the non-paretic (medium gray), and the paretic (black) limb across the pedaling cycle. Reflex amplitude is the mean EMG value of the reflex

curve (stimulation trials – control trials) occurring from 65 – 150 ms after stimulus. Pedaling position represents the pedaling position of the limb of interest when stimulation was applied to the contralateral limb. For example, the data point at 180° for the paretic limb represents the interlimb cutaneous reflex amplitude in response to stimulation applied to the non-paretic limb when it was at 360°. Reflexes were normalized to the EMG amplitude during the same window from control trials. Error bars are standard error. RF – rectus femoris; VM – vastus medialis; VL – vastus lateralis; SOL – soleus; MG – medial gastrocnemius; ST – semitendinosus; BF – biceps femoris; TA – tibialis anterior. $^{*}P < 0.05$ paretic vs. non-paretic, $^{\dagger}P < 0.05$ paretic vs. control, ‡$P < 0.05$ non-paretic vs. control.

Differences in reflex responses between groups and between the paretic and non-paretic limb are shown in Figure 3.4. Compared to controls, reflexes were more facilitated in the paretic RF ($P < 0.05$). Post-hoc analyses revealed that reflexes were more facilitated at 225° and 270° ($P \leq 0.04$). In ST, reflexes were less facilitated in the paretic and non-paretic limb than in controls ($P \leq 0.04$), and there was an angle X limb interaction ($P \leq 0.03$). This interaction occurred because reflexes were significantly less facilitated in the paretic and non-paretic limb than in controls at 360° ($P = 0.02$) and 45° (non-paretic: $P = 0.02$; paretic: $P = 0.09$), but not different at other positions. Within the stroke group, there was a main effect of limb in SOL, MG, VM, VL, and BF ($P \leq 0.05$) whereby reflexes were more facilitated in the paretic than the non-paretic limb. Post-hoc analyses revealed between limb differences in SOL at 45° ($P = 0.02$), MG at 135° ($P = 0.02$), VM at 225° ($P < 0.05$), and BF at 270°, 315°, and 360° ($P < 0.05$).

Differences in interlimb cutaneous reflexes were not a result of differences in pedaling rate, threshold intensity, or stimulation intensity. The mean pedaling rate of 53 (9) RPM was not different between groups ($P = 0.46$) or across bouts ($P = 0.29$), and there was no interaction ($P = 0.73$). RT was consistent throughout each session for both groups ($P \geq 0.11$), was not different between the paretic and non-paretic limb ($P = 0.10$) or the left and right limb ($P = 0.79$), and there was no group X bout interaction ($P \geq$

0.21). In control subjects, stimulation was applied at 2.9 (1.8) X RT for both limbs (between limb, $P = 0.79$). In stroke, absolute stimulation intensity was not different between the paretic and non-paretic limb, and relative stimulation intensity was not different ($P = 0.07$) between the non-paretic [2.4 (1.0) X RT] and paretic [2.0 (1.2) x RT] limb. Relative stimulation intensity was also not different from controls for the non-paretic ($P = 0.73$) or paretic limb ($P = 0.12$).

Interlimb coordination and symmetry

Stroke subjects had worse interlimb coordination than control subjects during bilateral uncoupled pedaling. Phase accuracy, phase consistency, and $PCI_{pedaling}$ were larger in the stroke than the control group (Table 3.3; $P < 0.001$). Stroke subjects also showed evidence of pedaling work asymmetry. Propulsive, braking, and net mechanical pedaling work were higher in the non-paretic than the paretic limb, and thus $\%Propulsion_{pedaling}$, $\%Braking_{pedaling}$, and $\%Net_{pedaling}$ deviated from 50% (Table 3.3; $P \leq 0.001$). Impairments in interlimb coordination and asymmetries were also evident during walking. Mean discrete relative phase deviated from 180° ($P = 0.002$). Values for phase accuracy, phase consistency, and $PCI_{walking}$ are included in Table 3.3. The paretic limb produced more braking and less propulsive impulse ($P = 0.001$), even in the subset of subjects who did not use handrails ($P = 0.04$). See Table 3.3.

Pedaling			
	Paretic	*Non-Paretic*	*%Work(paretic)*
Propulsive work (Nm)	34 (7)	49 (16)	42 (8)†
Braking work (Nm)	-25 (7)	-15 (6)	62 (12)†
Net work (Nm)	9 (10)	34 (19)	21 (24)†
		Stroke	*Control*
Phase accuracy (%)		37 (12)*	18 (5)
Phase consistency (%)		40 (16)*	15 (5)
PCI (%)		77 (28)*	32 (10)
Walking			
	Paretic	*Non-Paretic*	*%Impulse(paretic)*
Propulsive impulse (Ns)	5 (5)	11 (4)	30 (16)†
Braking impulse (Ns)	-9 (5)	-6 (5)	66 (18)†
		Stroke	
Relative phasing (°)		168 (14)	
Phase accuracy (%)		8 (7)	
Phase consistency (%)		5 (1)	
PCI (%)		13 (7)	

Table 3.3. Assessments of interlimb coordination and pedaling symmetry during pedaling and walking. Values are Mean (SD). PCI: phase coordination index. $^{*}P < 0.05$ stroke vs. control, $^{\dagger}P < 0.05$ compared to 50%, $^{\ddagger}P < 0.05$ compared to 180°.

Relations between variables

Reflex amplitude in ST was associated with interlimb coordination and symmetry. Less facilitation in both the paretic and non-paretic ST around the anterior transition (average reflex amplitude at 360° and 45°) was associated with a larger $PCI_{pedaling}$ and a smaller $\%Propulsion_{pedaling}$ and $\%Propulsion_{walking}$ ($P < 0.05$). Less facilitation in the paretic limb was also associated with a larger $PCI_{walking}$ ($P = 0.001$). Figure 3.5 shows correlations with ST reflex amplitude in the paretic limb. Reflex amplitude in ST around the anterior transition was also correlated with clinical measures of sensorimotor function. Specifically, more facilitation in both the paretic and non-paretic ST was correlated with a larger $FM_{LEtotal}$ score ($P \leq 0.02$). More facilitation in the paretic ST was also correlated with a larger $FM_{LEmotor}$ score ($P = 0.02$), while more facilitation in the

non-paretic ST was correlated with a larger FM_{LEbal} score ($P = 0.004$), a larger Berg Balance Score ($P = 0.008$), and a faster walking speed ($P = 0.002$). Measures of interlimb coordination and symmetry were significantly related, even when measured during different tasks. Interlimb coordination and symmetry during both pedaling and walking were correlated with $FM_{LEtotal}$ and $FM_{LEmotor}$ ($P \leq 0.004$). $PCI_{pedaling}$ and $\%Propulsion_{walking}$ were correlated with the Berg Balance ($P = 0.02$), and $PCI_{pedaling}$ was also correlated with self-selected walking speed ($P = 0.03$). See Table 3.4 for all correlation coefficients.

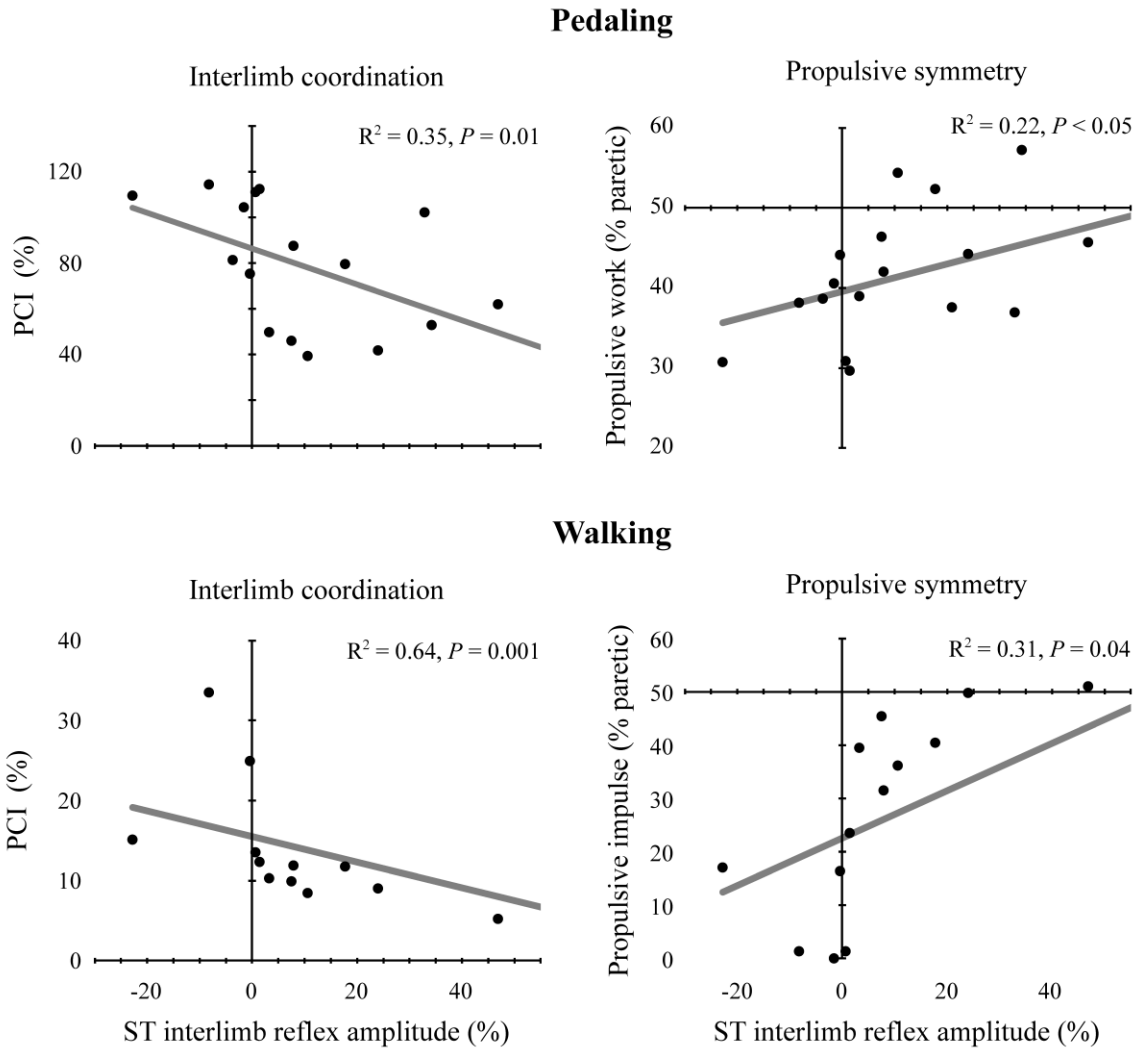

Figure 3.5. Relation of interlimb cutaneous reflexes with interlimb coordination and propulsive symmetry during pedaling and walking. The top row shows correlations during pedaling; the bottom row shows correlations during walking. Interlimb cutaneous reflex amplitudes are from paretic ST at the anterior transition (360 and 45°). PCI is the primary measure of interlimb coordination, and percent propulsion performed by the paretic limb is the primary measure of propulsive symmetry. Individual data points are represented by black dots. Gray line is the line of best fit. Correlations were performed with Pearson or Spearman correlations. R^2 and *P* values are presented for each correlation. PCI – phase coordination index; ST – semitendinosus.

	$ST_{paretic}$	$ST_{non\text{-}paretic}$	$PCI_{pedaling}$	$PCI_{walking}$	$\%Propulsion_{pedaling}$	$\%Propulsion_{walking}$
$ST_{non\text{-}paretic}$	0.45					
$PCI_{pedaling}$	-0.59*	-0.56*				
$PCI_{walking}$	-0.80**	-0.39	0.72*			
$\%Propulsion_{pedaling}$	0.47*	-0.61*	-0.71*	-0.68*		
$\%Propulsion_{walking}$	0.56*	0.59*	-0.75*	-0.89**	0.57*	
$FM_{LEtotal}$	0.57*	0.61*	-0.84**	-0.77*	0.70*	0.80**
$FM_{LEmotor}$	0.57*	0.46	-0.82**	-0.72*	0.70*	0.72*
FM_{LEbal}	0.44	0.66*	-0.34	-0.08	0.16	0.39
Berg Balance	0.29	0.63*	-0.58*	-0.35	0.37	0.61*
Walking speed	0.12	0.69*	-0.52*	-0.17	0.27	0.39

Table 3.4. Correlations between interlimb coordination, symmetry, and function. Correlation coefficients for relations between measures during pedaling and walking. PCI is the primary measure of interlimb coordination, and %Propulsion is the primary measure of compensation. Fugl-Meyer scores represent stroke-related disability, Berg Balance Score represents deficits in balance, and walking speed represent lower extremity function. Coefficients are from Pearson correlations for normally distributed variables and Spearman correlations for non-normally distributed variables. $FM_{LEtotal}$: Fugl-Meyer Assessment lower extremity total score; $FM_{LEmotor}$: motor subscore; FM_{LEbal}: balance subscore; PCI: phase coordination index. $ST_{paretic}$: average reflex amplitude in the paretic ST at 45° and 360°; $ST_{non\text{-}paretic}$: average reflex amplitude in the non-paretic ST at 45° and 360°. *$P < 0.05$, **$P < 0.001$.

3.4 Discussion

In this study, we found evidence of altered interlimb cutaneous reflexes during lower limb pedaling after stroke. Stroke-related alterations were observed in bifunctional muscles that aid in the transitions between flexion and extension (ST and RF). Abnormalities in ST were correlated with impaired interlimb coordination and reduced paretic propulsion during pedaling and walking. Thus, these changes in interlimb reflexes may reflect important alterations in the supraspinal and/or spinal control of interlimb coordination. Changes in interlimb coordination and propulsion were consistent across multiple locomotor tasks and related to sensorimotor function.

Interlimb cutaneous reflexes

In this study, we found that reflexes in ST at the anterior transition (360° and 45°) were less facilitated in both the paretic and non-paretic limbs as compared to controls. Because of the reflex latency, facilitation of ST at the anterior transition in controls affected muscle activity during the downstroke. This is an appropriate response to cutaneous perturbation in the contralateral limb, promoting hip extension and aiding a shift of loading from the limb experiencing cutaneous input to the contralateral limb. Facilitation at this part of the pedaling cycle was missing in the stroke group, which may impair contralateral responses to perturbation. Interestingly, reflexes were less facilitated at the anterior transition in BF than ST in controls, and responses were similar between these muscles for stroke participants. In controls reflexes near the anterior transition in ST were at least 42% larger than reflexes at other muscle-position combinations. The variability at these positions was like the variability at other positions and in other muscles, and there were no apparent outliers. Furthermore, at both positions, half of the participants had reflex amplitudes above the mean value. These high amplitude responses in controls suggest that the contralateral reflex response to cutaneous stimulation is particularly important when the stimulated limb is transitioning from extension to flexion, and ST is a primary facilitator of this response. ST may be the primary facilitator instead of BF because they have a differential role in rotation of the hip. Facilitation of ST and not BF near the anterior transition could promote internal rotation, allowing better hip extension during the downstroke.

In RF, interlimb cutaneous reflexes were more facilitated in the paretic limb than in controls. Although we did not detect a significant limb X angle interaction, this main

effect for limb appears to be a result of differences near the posterior transition. Post-hoc comparisons revealed that there were between group differences at 225° and 270°, with a reflex reversal at 225°; reflexes were facilitated in the paretic limb but inhibited in controls. VM and VL also appear to demonstrate similar differences between the paretic limb and controls, which reached significance in VM at 225°. The facilitation of these muscles at this phase in the paretic limb may contribute to maladaptive knee extension during the upstroke. Interestingly, reflexes in RF did not mirror those in ST and BF. ST and BF were facilitated near the anterior transition, but RF was inhibited at the posterior transition. These differences suggest that contralateral reflex responses to cutaneous sensory input are position and muscle dependent. Corresponding with these findings, Zehr and Loadman (2012) found that interlimb reflexes in VL were facilitated at end stance in the paretic limb but inhibited in controls during walking. Moreover, reflexes in VL and BF were not mirrored, supporting the muscle and position dependence of reflexes.

We also measured reflex differences between the paretic and non-paretic limb. Reflexes were more facilitated in the paretic VM, VL, MG, SOL, and BF than the non-paretic limb. In VM and VL, reflexes in the non-paretic limb resembled those in controls. Thus, differences between the paretic and non-paretic limb were most prominent near the posterior transition. Facilitation of MG and SOL was most prominent during the downstroke, which would promote activation of these muscles during the downstroke and near the posterior transition, when they are more active. This change might occur because of the low background activation of these muscles during this part of the pedaling cycle, as expressed by the low MI in this study. Finally, in BF, reflexes in the paretic limb

resembled those in controls. Differences between the paretic and non-paretic limb in BF were most pronounced during the upstroke and near the anterior transition. Thus, these differences resemble those seen between the stroke and control group in ST. Other studies have also found that interlimb reflexes in the non-paretic limb are generally blunted. When stimulation is applied to either lower limb during walking, reflexes in the non-paretic upper limb are blunted (Kloter et al., 2011). Similarly, stimulation to the paretic limb during bilateral rhythmic opening/closing of the hand elicits blunted reflex responses in the non-paretic upper limb (Schrafl-Altermatt & Dietz, 2016). Blunted responses in the non-paretic limb may reflect abnormal processing of sensory information from the paretic limb. Some potential causes of altered processing are discussed below.

Alterations of interlimb cutaneous reflexes after stroke may occur at a spinal level. In particular, the early portion (i.e. up to 85-90 ms after stimulation) of cutaneous reflex responses likely follows an oligosynaptic or polysynaptic spinal pathway (Nielsen et al., 1997; Pierrot-Deseilligny & Burke, 2012), although longer latencies may also be spinally mediated; interlimb reflexes have been observed up to 450 ms after stimulation in humans with spinal cord injury (Roby-Brami & Bussel, 1987). One example of spinally mediated alterations of interlimb cutaneous reflexes after stroke is that individuals with chronic stroke have less short latency (40 – 60 ms post-stimulus) interlimb inhibition in the contralateral soleus of both limbs than controls (Stubbs, Nielsen, Sinkjær, & Mrachacz-Kersting, 2012). There are other examples of altered sensory reflex processing in the spinal cord after stroke. For example, spasticity after stroke may involve reciprocal facilitation instead of reciprocal inhibition, facilitation of group II sensory input, and decreased presynaptic inhibition (Crone, Johnsen, Biering-

Sørensen, & Nielsen, 2003; Marque, Simonetta-Moreau, Maupas, & Roques, 2001; Morita, Crone, Christenhuis, Petersen, & Nielsen, 2001).

Interlimb reflex changes after stroke may result from altered modulation by central pattern generator (CPG) circuitry. The control of locomotion is thought to be primarily driven by the activity in CPGs, which likely involves the modulation of pathways important for interlimb coordination (for review see Dietz, 2003). In spinal, decerebrate, and intact cats, interlimb cutaneous reflexes are phase gain controlled during walking (Duysens, 1977; Duysens & Loeb, 1980; Duysens et al., 1980; Duysens & Pearson, 1976; Duysens & Stein, 1978; Forssberg et al., 1975; Gauthier & Rossignol, 1981). Likewise, in humans, cutaneous reflexes are not modulated during static contractions, but are phase dependent during rhythmic locomotor movements (Berger et al., 1984; Dietz et al., 1986; Tax et al., 1995; Van Wezel et al., 1997; Zehr, Hesketh, et al., 2001). Together, these findings support the hypothesis that interlimb reflexes are modulated by CPG circuitry. Modulation may occur through direct incorporation of interlimb sensory signals into the CPG or through premotoneuronal modulation (Duysens et al., 1992; Forssberg et al., 1977). Altered interlimb cutaneous reflexes after stroke might result from changes in the CPG modulation of interlimb signals.

Altered sensory processing in the spinal cord may result from changes in the supraspinal modulation of spinal pathways. For example, the corticoreticular-reticulospinal system synapses on commissural interneurons that have a tight coupling with the contralateral spinal cord and thus, likely modulates signals important for interlimb coordination (Matsuyama et al., 2004). Ipsilateral projections from the cortex and from subcortical regions also synapse onto commissural interneurons, allowing

another means for supraspinal regions to influence interlimb signals (Jankowska & Edgley, 2006). An effect of central nervous system injury on supraspinal modulation of spinal pathways is supported by multiple findings. In individuals with spinal cord injury, but not in controls, stimulation of mixed nerves elicits interlimb reflexes at rest (Calancie, 1991). After stroke, pedaling in one limb results in greater evoked muscle activity in the contralateral limb than in controls (Kautz et al., 2006). During unilateral pedaling of the paretic limb, if the non-paretic limb also pedals or performs isometric contractions, the phasing of paretic muscle activity and force production are altered (Kautz & Patten, 2005; Rogers et al., 2011). Disinhibition or facilitation of pathways that control interlimb coordination may contribute to these findings. After stroke, disinhibition of spinal pathways has been postulated to result from the loss of spinal inhibition through the dorsal reticulospinal tract (under cortical control), but maintenance or enhancement of facilitation through the medial reticulospinal and vestibulospinal tracts (independent of the cortex) (Trompetto et al., 2014).

Alterations of interlimb cutaneous reflexes after stroke may also partly occur from direct effects at a supraspinal level. It is estimated that a minimal latency of 85 – 90 ms is required in order for interlimb reflexes to have a transcortical pathway (Nielsen et al., 1997). In addition, several studies suggest that cutaneous reflexes are facilitated at a cortical level (Christensen et al., 1999; Pijnappels et al., 1998). Therefore, at least some portion of the measured reflexes could involve a supraspinal path. Consequently, stroke-related damage to supraspinal structures might directly affect the processing of sensory information traveling through these supraspinal pathways, leading to altered control of interlimb signals.

Despite evidence of alterations after stroke, there is evidence that interlimb reflexes are relatively well preserved in this population. During walking, Zehr and Loadman (2012) found no differences in interlimb cutaneous reflexes between the paretic limb and controls in 94% of the muscle-phase combinations (30/32 observations). During arm cycling, Zehr et al. (2012) found no differences between the paretic or non-paretic limb as compared to controls in 87% of muscle-position combinations (104/120 observations). In our study, we only detected differences between stroke and control groups in two of eight muscles, and differences in these muscles appeared to be restricted to a fraction of the pedaling positions. The general preservation of reflexes is surprising because it is contrary to what has been found in other types of reflexes after stroke. For example, H-reflex amplitude in VM and SOL is increased across all pedaling positions in stroke survivors compared to controls (Fuchs et al., 2011; S. Schindler-Ivens et al., 2008). These opposing findings might result from varying control of different reflex pathways. For example, H-reflexes are attenuated by passive pedaling, but cutaneous reflexes are not, suggesting a differential influence of peripheral afferent signals (Brooke et al., 1997; Brooke, McIlroy, & Collins, 1992; Brooke, McIlroy, Staines, Angerilli, & Peritore, 1999).

Interlimb coordination and symmetry

In this study, we found that stroke survivors had impairments in interlimb coordination during locomotion. During bilateral uncoupled pedaling, PCI (accuracy and consistency of phasing) was worse in stroke than control subjects. During walking, stroke survivors were unable to maintain a 180° phase relation between the legs, and PCI was

higher than has been reported previously in healthy controls (Meijer et al., 2011). These impairments in interlimb coordination are consistent with previous observations during locomotor movements after stroke. During bilateral hip flexion and extension, reflex-related torque production in the paretic limb is phase advanced, and more so than during unilateral movement (Hyngstrom et al., 2010). During pedaling, phasing of paretic EMG and force is abnormal when the non-paretic limb is also volitionally activated (Kautz & Patten, 2005; Rogers et al., 2011). During walking, heel strikes are not antiphase and are more variable in stroke than control subjects (Meijer et al., 2011; Roerdink et al., 2007). Moreover, contralateral responses to perturbations of the ipsilateral limb are delayed, have an abnormal amplitude, and represent a different control strategy during standing and walking in stroke survivors compared to controls (Berger et al., 1984; Dietz & Berger, 1984; Krasovsky et al., 2013). Impairments in interlimb coordination have also been observed during antiphase ankle tracking movements (Madhavan et al., 2010; Tseng & Morton, 2010).

We also found that individuals with stroke have between limb asymmetries in the work of pedaling and walking. During pedaling, the paretic limb only produced 21% of the net mechanical work, with less propulsive and more braking work. During walking, propulsive impulse was lower and braking impulse was higher in the paretic than the non-paretic limb. These findings are consistent with numerous other descriptions of asymmetries during pedaling and walking (Bowden et al., 2006; H. Y. Chen et al., 2005; De Marchis et al., 2015; Kautz & Brown, 1998; Olney et al., 1991; Perell et al., 1998; Turns et al., 2007).

Association between interlimb reflexes and interlimb coordination

Although interlimb cutaneous reflexes were generally unchanged after stroke, the few stroke-related changes in interlimb cutaneous reflexes may reflect important alterations in the supraspinal and/or spinal control of interlimb coordination. The majority of these interlimb reflex changes aligned with pedaling transitions between flexion and extension phases. Previous studies have indicated that transitional phases during locomotion are important for interlimb coordination. During walking, step-to-step transitions rely on interlimb coordination to retain the center of mass within the base of support and are the primary contributor to metabolic costs (Donelan, Kram, & Kuo, 2002; Sousa & Tavares, 2015). During pedaling, muscle activity increases in bifunctional muscles (RF, BF, and semimembranosus (SM)) when the contralateral limb is also active (Kautz et al., 2002). This increase in muscle activity generated by the contralateral limb may facilitate the smooth execution and coordination of pedaling transitions.

Other studies have found stroke-related impairments in interlimb coordination near transitions during locomotion. During walking, Sousa et al. (2013) found that interlimb effects were reduced during step-to-step transitions as compared to controls. During pedaling, inappropriate muscle activity in the paretic RF and SM is exacerbated by activity in the non-paretic limb (Kautz & Brown, 1998; Kautz & Patten, 2005; Rogers et al., 2011). Problems with transitional phases of pedaling after stroke may be related to changes in the complexity of motor control. Clark, Ting, Zajac, Neptune & Kautz (2010) found that patterns of muscle coordination during walking were less complex in stroke compared to control. Decreased complexity was associated with more muscle coactivation and poorer locomotor performance. Demonstrating the potential effect of

decreased locomotor complexity on interlimb coordination, Raasch and Zajac (1999) used modeling to demonstrate that forward crank progression is not possible when the control of biarticular muscles is combined with either the flexion or extension group (i.e. bifunctional muscles only contribute to flexion or extension). When this happens, each limb gets stuck near the transition from extension to flexion. Interestingly, our lab previously demonstrated that some stroke survivors exhibit this deficit during bilateral uncoupled pedaling.

Providing further support for an association between impaired interlimb coordination and altered interlimb cutaneous reflexes at pedaling transitions, we found that these constructs were correlated. Individuals with less facilitation in ST at the anterior transition (greater deviation from controls) had worse interlimb coordination during both pedaling and walking. Similarly, individuals with less facilitation in ST at the anterior transition (greater deviation from controls) produced less propulsion with the paretic limb during both pedaling and walking. Acknowledging the limitations of correlations analyses, these findings suggest that alterations in interlimb reflexes may reflect abnormal supraspinal or spinal control of interlimb coordination, particularly at pedaling transitions.

Previous results from our lab suggest that asymmetrical contributions to pedaling after stroke may be related to impairments in interlimb coordination. In the current study, we confirmed this finding by showing direct relations between worse interlimb coordination and greater asymmetry during both pedaling and walking. Bowden et al. (2006) also found a strong correlation between force symmetry during pedaling and walking trials. Thus, we hypothesize that asymmetrical contributions to pedaling may be

employed to maintain good performance despite impairments in interlimb coordination. Another possibility is that poor control of interlimb coordination makes it difficult to produce force and increases metabolic cost, leading to asymmetrical contributions to locomotion (Sousa & Tavares, 2015). As supported by correlational analyses, abnormal control of interlimb sensory signals may contribute to impaired interlimb coordination and the resulting asymmetry.

Besides altered control of interlimb sensory pathways, as found in the current study, alterations in descending supraspinal pathways may also contribute to impaired interlimb coordination (Swinnen & Duysens, 2004). For example, paretic EMG phasing is more impaired during pedaling when the non-paretic limb is also pedaling or performing static contractions (Kautz & Patten, 2005; Rogers et al., 2011). Impaired paretic phasing occurs regardless of whether movements are in-phase or antiphase, suggesting that this interlimb effect is related to supraspinal commands associated with activation of the non-paretic limb. Similarly, stroke survivors with greater descending ipsilateral conductivity, have worse performance during antiphase ankle movements (Madhavan et al., 2010). Descending supraspinal signals may contribute to impaired interlimb coordination after stroke through pathways that allow neural signals to have bilateral effects: ipsilateral uncrossed pathways, branched bilateral pathways, and/or interhemispheric interactions between motor regions within the cortex (Carson, 2005). Multiple studies have shown impaired interhemispheric interactions after stroke, whereby the non-lesioned hemisphere inhibits the primary motor cortex in the lesioned hemisphere (Murase et al., 2004; Traversa et al., 1998). Our results in interlimb cutaneous reflexes may provide insight into altered control of descending supraspinal pathways because they

share several common sources of modulation. Namely, both interlimb sensory pathways and descending supraspinal pathways may be affected by direct damage to supraspinal structures and/or changes in CPG modulation.

Sensorimotor function and rehabilitation after stroke

Individuals with better sensorimotor function had fewer interlimb reflex abnormalities (at the anterior transition in the paretic ST), better interlimb coordination, and better symmetry during pedaling and walking. Thus, these constructs (interlimb reflexes, interlimb coordination, and symmetry) may reflect the overall level of function. Associations were found with motor scores, balance, and walking speed. In terms of interlimb reflexes, more normal amplitude in the paretic limb was associated with improved motor performance. This finding supports an important role of contralateral sensory signals for paretic motor function. More normal reflexes in the non-paretic limb were correlated with better balance and a faster walking speed. This association may reflect the importance of sensory signals from the paretic limb for promoting an appropriate response in the non-paretic limb to maintain balance. Thus, interlimb reflex abnormality may have important implications for motor function, balance, and walking. This also raises the possibility that rehabilitative techniques aimed at improving interlimb coordination and/or symmetry may have beneficial effects for sensorimotor function.

Our results suggest that pedaling provides a good model of walking, particularly with respect to the constructs of symmetry and interlimb coordination. Corresponding measures of propulsive symmetry and interlimb coordination recorded during pedaling and walking were correlated. Furthermore, propulsive symmetry and interlimb

coordination were correlated, even when measured during a different locomotor task. Overall, these findings support a strong relation between constructs measured during pedaling and measured during walking.

Limitations

There are a several limitations to the statistical approaches used in this study. Because the variability of reflex responses was large, and the sample size was relatively small, we lacked power to detect some effects. Thus, although we used a more conservative statistical approach to evaluating interlimb reflexes (ANOVAs), we also liberally tested for between group and between limb differences in the absence of a significant angle X limb interaction. Although this approach allowed us to more fully evaluate for differences, it also increases the risk of Type 1 error. Another consideration is that conclusions about the relations between interlimb cutaneous reflexes, interlimb coordination, symmetry, and stroke-related function are largely based on correlational analyses. Thus, the proposed directionalities of these relations are hypothetical.

Our analysis techniques for interlimb cutaneous reflexes also have some limitations. The use of a fixed reflex interval (65 – 150 ms) has benefits and drawbacks. In instances when both facilitation and inhibition occur, the amplitude within this latency window cannot detect the complexity of the reflex response. Additionally, reflex responses may not optimally fit into the selected timeframe. However, a fixed reflex interval was used because it facilitates comparisons between groups. In most muscles evaluated in this study, the distinct reflex response was encompassed by the selected interval. In this study, we also did not evaluate the onset of reflex activity because of the

difficulty of objectively interpreting these results considering the variability and multi-phasic nature of the reflexes. For example, consider a reflex response that appears to be delayed. This reflex response might represent an actual delay, but it might also be a different portion of the reflex response mediated through an entirely different pathway.

Despite normalizing reflexes to control trials, the measured responses could have been affected by background muscle activity. Throughout the pedaling cycle, each muscle had periods of relatively low and high levels of activity. While at a relatively low level of activity (e.g. resting state) interlimb sensory input may have been needed just for motor units to reach the threshold for a response. Thus, even relatively high levels of interlimb sensory input may have elicited reflexes with a small amplitude. Conversely, while at a relatively high level of activity, the motor unit threshold for activation would have already been met. At these times, responses to any interlimb sensory input may have been greater than when the muscle is in a resting state.

Previous work has shown that upper limb activity can influence reflex responses in the lower limb. For example, phase modulation of cutaneous reflexes and amplitude of H-reflexes and stretch reflexes during pedaling with the lower limb are altered when the upper limb also performs rhythmic pedaling (Balter & Zehr, 2007; Barzi & Zehr, 2008; Mezzarane, Nakajima, & Zehr, 2014). We did not measure muscle activity in the upper limb, so our results may have been affected by differential levels of activity. Anecdotally, no visible upper limb muscle activation was noted in our participants, and no participants performed rhythmic movement with the upper limb. Most participants pedaled with their arms resting at their sides or crossed over their chest and abdomen. Thus, it is unlikely that upper limb activity influenced our results.

CHAPTER 4: BRAIN ACTIVATION DURING PASSIVE AND VOLITIONAL PEDALING AFTER STROKE

4.1 Introduction

There are many examples of altered movement-related brain activation in individuals with post-stroke hemiparesis. Changes in the extent, intensity, and location of brain activation have been observed during upper and lower limb movements, in acute and chronic stroke survivors, before and after rehabilitation (Bosnell et al., 2011; Calautti, Leroy, Guincestre, & Baron, 2001; Cramer et al., 1997; Dobkin et al., 2004; Enzinger et al., 2008; Y. H. Kim et al., 2006; Miyai et al., 2003; Miyai et al., 2002; Ward, Brown, Thompson, & Frackowiak, 2003a; Ward et al., 2003b; Weiller et al., 1992). Such changes in brain activation are often attributed to stroke-related neuroplastic phenomena (for review see Calautti & Baron, 2003). This interpretation of human neuroimaging data is supported by observations from non-human animal studies. Experimentally induced brain lesions in rat and mouse alter the excitability of remaining neural connections, induce dendritic sprouting, and lead to axonal outgrowth (Biernaskie & Corbett, 2001; Bury & Jones, 2002; Carmichael, Wei, Rovainen, & Woolsey, 2001; Dancause et al., 2005; Qü et al., 1998; Schiene et al., 1996). Hence, it is plausible that similar neural adaptations occur in human and manifest as altered brain activation as measured during functional imaging.

While neuroplasticity is a credible and attractive explanation for altered movement-related brain activation post-stroke, it is also possible that these observations are a result of changes in volitional motor commands and motor performance. Numerous studies provide evidence of altered kinetic, kinematic, and muscle activation profiles

during paretic limb movement (Bowden et al., 2006; Cirstea & Levin, 2000; Cruz, Waldinger, & Kamper, 2005; Knutsson & Richards, 1979). Such changes in motor commands and motor performance are difficult to control, and they confound the interpretation of functional brain imaging data (for review see Baron et al., 2004; Krakauer, 2007). For example, cross-sectional studies that demonstrate altered brain activation during index finger opposition and hand gripping after stroke also report unintended movements of other digits and of the paretic wrist and elbow (Ward et al., 2003b; Weiller et al., 1992). Even the pioneering work of Miyai et al. (2003; 2002) that showed lateralized and elevated cortical activation during hemiparetic walking was unavoidably confounded by stroke-related changes in the spatiotemporal characteristics of the gait cycle, such as decreased swing phase symmetry. Indeed, neuroplastic adaptations to stroke, altered motor commands, and changes in motor performance are concurrent, inter-dependent processes that are difficult to distinguish. Hence, the meaning of altered movement-related brain activation after stroke is still unclear.

Recently, our group was compelled to consider explanations for altered brain activation during hemiparetic lower limb movement. We used functional magnetic resonance imaging (fMRI) to examine brain activation during pedaling in people with and without stroke (Promjunyakul et al., 2015). People with stroke displayed reduced pedaling-related brain activation volume as compared to age-matched controls. While changes in the structure or function of the stroke-affected brain could explain these findings, other possible contributors include alterations in motor commands and differences in pedaling performance. Specifically, asymmetries in pedaling performance, whereby the non-paretic limb performs more than half of the work of pedaling, are well

documented after stroke and result in a more unilateral pedaling strategy as compared to controls (Brown & Kautz, 1998; Perell et al., 1998). This pedaling strategy may help explain our results, as brain activation is lower during unilateral as compared to bilateral movement (Grefkes, Eickhoff, Nowak, Dafotakis, & Fink, 2008; Noble, Eng, & Boyd, 2014). Moreover, a post-hoc, exploratory analysis revealed an association between brain activation volume and work accomplished by the paretic limb; volume increased with increased work from the paretic limb (Promjunyakul et al., 2015).

The purpose of this study was to determine whether reduced pedaling-related brain activation post-stroke can be explained by altered volitional motor commands and pedaling performance. We used fMRI to compare brain activation during volitional and passive pedaling. During volitional pedaling, subjects used their own voluntary muscle activity to pedal. During passive pedaling, they relaxed and allowed an experimenter to move their limbs. The passive condition eliminated motor commands to pedal and minimized between-group differences in pedaling performance (e.g. muscle activity, kinematics, symmetry). We hypothesized that, if volitional motor commands and pedaling performance contribute to reduced pedaling-related brain activation post-stroke, then between-group differences would be reduced during passive as compared to volitional pedaling. Additionally, brain activation would be different for volitional and passive pedaling. We also examined the feasibility of minimizing muscle activity for passive pedaling, which was necessary for testing our hypothesis. Portions of this work have been presented previously in abstract form (Cleland & Schindler-Ivens, 2015).

4.2 Methods

Subjects

Forty-five individuals (22 stroke, 23 control) were enrolled and screened for passive pedaling. All were free from 1) neurological disease or injury, except stroke, 2) contraindications to fMRI, and 3) medical conditions that could affect brain function or make it unsafe to pedal. Stroke and control subjects were matched for age (mean (SD); stroke: 62 (12), range = 33 – 83 years; control: 62 (12), range = 21 – 77; $P = 0.93$). All stroke survivors had sustained their stroke at least 1.5 years prior to participating. There were 10 cortical, 9 subcortical, and 3 unclassified strokes. Strokes were classified as cortical if the lesion included any part of the cerebral cortices. This classification included small, localized lesions of the gray matter and large lesions that extended into neighboring white matter. Strokes were classified as subcortical if they were restricted to regions outside the cerebral cortices. Stroke location was determined from MRI or, for subjects who did not advance to MRI, from the medical record. Subjects whose stroke location was unclassified were those who did not advance to MRI and had missing or incomplete medical records. Stroke subjects underwent the lower limb portion of the Fugl-Meyer Assessment and the 8-m comfortable walk test. Subjects were considered hyperreflexic if their seated reflex score from the Fugl-Meyer was ≤ 1. See Table 4.1. All subjects provided written informed consent; procedures were approved by Institutional Review Boards at Marquette University and the Medical College of Wisconsin.

	Stroke					Control				
Variable	**Enrolled Subjects**	**Not Passive**	**Passive**	**Scanned**	**fMRI Analysis**	**Enrolled Subjects**	**Not Passive**	**Passive**	**Scanned**	**fMRI Analysis**
N	22 (9 F)	12 (3 F)	10 (6 F)	8 (4 F)	5 (3 F)	23 (14 F)	9 (4 F)	14 (10 F)	11 (8 F)	10 (7 F)
Age (years)	62 (12)	60 (13)	64 (11)	64 (8)	68 (7)	62 (12)	61 (17)	63 (7)	64 (7)	65 (7)
Sex (M/F)	13/9	9/3	4/6	4/4	2/3	9/14	5/4	4/10	3/8	3/7
Height (cm)	174 (9)	175 (8)	173 (10)	175 (10)	174 (12)	170 (10)	174 (13)	168 (7)	169 (8)	168 (8)
Mass (kg)	87 (18)	91 (21)	83 (14)	85 (14)	81 (13)	77 (13)	77 (16)	76 (12)	75 (12)	73 (11)
BMI	29 (6)	30 (7)	28 (4)	28 (4)	27 (4)	26 (4)	25 (4)	27 (4)	26 (4)	26 (3)
Time since stroke (years)	8 (4)	8 (5)	8 (3)	8 (3)	8 (4)					
Stroke location (C/SC/UN)	10/9/3	4/5/3	6/4/0	6/2/0	3/2/0					
Paretic limb (L/R)	12/10	6/6	6/4	5/3	2/3					
Walking vel. (m/s)	0.76 (0.37)	0.89 (0.38)	0.63 (0.34)	0.68 (0.32)	0.77 (0.36)					
FMA total (96)	79 (8)	81 (9)	76 (8)	76 (8)	77 (10)					
FMA motor (34)	24 (5)	26 (5)	23 (6)	23 (6)	24 (7)					
FMA sensory (12)	9 (3)	10 (2)	9 (4)	9 (4)	8 (5)					
FMA balance (10)	7 (1)	8 (1)	7 (1)	7 (1)	6 (0)					
FMA ROM (20)	18 (2)	18 (2)	18 (2)	18 (2)	18 (2)					
FMA pain (20)	20 (0)	20 (0)	20 (0)	20 (0)	20 (0)					
Hyperreflexic (Y/N/NA)	13/5/4	5/4/3	8/1/1	7/1/0	4/1/0					

Table 4.1. Descriptive characteristics of subjects who participated in different steps of the study. Values are Mean (SD). M/F, male/female; C/SC/UN, cortical/subcortical/unknown; L/R, left/right; Y/N/NA, yes/no/not assessed; FMA, Fugl Meyer Assessment; ROM, range of motion.

Pedaling device

The pedaling device has been described previously and validated for fMRI (Mehta, Verber, Wieser, Schmit, & Schindler-Ivens, 2009, 2012; Promjunyakul et al., 2015). In brief, the pedaling device was a direct-drive apparatus constructed of non-metallic materials that provided a light frictional workload. An MRI-compatible rotary optical encoder (MR318, Micronor, Inc., Newbury Park, CA) coupled to the crankshaft measured the position of the crankshaft across the pedaling cycle. Zero was defined for each crank arm as the position where the crank arm was parallel to the plinth and the foot was closest to the hip (top dead center, 0°). Signals from the encoder were carried to a controller unit (MR310, Micronor, Inc.) via a fiber optic cable and sampled to a desktop computer at 2000 Hz (Spike 2, Cambridge Electronic Design, Ltd., UK).

Feasibility of passive pedaling

All subjects completed a familiarization session outside the fMRI environment to determine whether muscle activity could be minimized for passive pedaling (feasibility). Surface electrodes were placed bilaterally over tibialis anterior (TA), medial gastrocnemius (MG), rectus femoris (RF), biceps femoris (BF), and adductor magnus (AM). Subjects lay supine on a plinth with their feet secured to the pedaling device. Volitional and passive pedaling were performed. During volitional pedaling, subjects were asked to use voluntary muscle activity to pedal. During passive pedaling, a member of the study team moved the pedals. Subjects were instructed to relax their legs and avoid assisting the study personnel. Each subject was given multiple opportunities to successfully complete the task over approximately 15 minutes of testing. In subjects with

visible muscle activity, verbal cues were given during and after each trial about relaxing the active muscle(s). For example, if the medial gastrocnemius was active, subjects were given verbal feedback during and after the trial to focus on relaxing that muscle. As needed, another member of the study team provided manual support at the knees to prevent hip abduction and external rotation. Subjects wore solid ankle foot orthoses (AFOs) to stabilize the ankles and to minimize muscle activity in the dorsi- and plantar flexors. AFOs were also worn during the volitional condition.

For both passive and volitional pedaling, two trials of 30s duration were recorded. An auditory pacing cue was used to maintain the desired rate of 45 revolutions per minute (RPM). The order in which passive and volitional conditions were introduced was counterbalanced. We also recorded electromyography (EMG) during quiet rest. Surface EMG was recorded with a bipolar, differential amplification system (Bagnoli-8, Delsys, Inc., Natick, MA), band-pass filtered (20-450 Hz), amplified (1000X), and passed to a 16-bit analog to digital convertor (micro 1401 mk II, Cambridge Electronic Design, Ltd.). Signals were sampled to a desktop computer at 2000 Hz via data acquisition software (Spike 2, Cambridge Electronic Design, Ltd.).

Adequate minimization of muscle activity during passive pedaling was determined per the following criteria. If muscle contractions were visually apparent, subjects were considered unable to achieve passive pedaling. For subjects with no visually apparent muscle contractions, EMG activity was examined offline using MATLAB (R2015b, The Mathworks, Inc., Natick, MA). Signals recorded during pedaling were rectified, smoothed (4^{th} order Butterworth 10 Hz low-pass filter), referenced to crank position, and averaged across cycles. Subjects were considered able

to achieve passive pedaling if the mean EMG amplitude of each muscle was less than the mean + 4 SD of quiet rest. Using these criteria, subjects were classified as able (PASSIVE) or unable (NON-PASSIVE) to minimize lower limb muscle activity for passive pedaling. PASSIVE subjects were invited for fMRI.

fMRI procedures

Of the 24 subjects who could perform passive pedaling, fMRI data from 15 subjects (5 stroke, 10 control) were examined. Six subjects did not complete fMRI due to: claustrophobia (1 control), preexisting health conditions (1 stroke, 1 control), loss to follow-up (1 control), or bladder urgency (1 stroke, 1 control). One stroke subject had no medically confirmed evidence of stroke. One stroke subject's head movement exceeded requirements (> 4mm), and in one other stroke subject, no brain activation was detected with fMRI. See Table 4.1.

During fMRI, subjects lay supine on the scanner table with their feet secured to the pedals. The head was stabilized in the radiofrequency coil using a beaded vacuum pillow and foam padding. Chin and trunk straps were used to further reduce head and body movement. A strip of adhesive tape was placed on the forehead and secured to the outside of the coil to provide a sensory cue if the head moved. AFOs and manual support provided during familiarization were also applied during fMRI. Subjects performed passive and volitional pedaling in a block design consisting of 3 runs of each condition. Each run consisted of 18s of rest followed by 20s of pedaling and 20s of rest, repeated 5 times. Auditory cues were used to maintain a pedaling rate of 45 RPM and to cue subjects to pedal or rest. Auditory cues were provided during pedaling and rest segments

through MRI-compatible earbuds (model SRM 212, STAX, Ltd., Japan). Condition order was counterbalanced.

MRI data were obtained using a 3.0T MR scanner (General Electric Healthcare, Milwaukee, WI) and a single channel transmit/receive split head coil assembly (model 2376114, General Electric Healthcare). Functional images (T2*-weighted) were acquired using echoplanar imaging (repetition time (TR): 2000 ms, echo time (TE): 25 ms, flip angle: 77º, 36 contiguous slices in the sagittal plane, 64 x 64 matrix, 4 mm slice thickness, and field of view (FOV): 24 cm). The resolution of the images was 3.75 x 3.75 x 4 mm. Each run consisted of 109 TRs. Anatomical images (T1-weighted) were obtained half way through the scan session using a 3D fast spoiled GRASS pulse sequence (TR: 8.2 ms, TE: 3.2 ms, flip angle: 12°, 256 x 244 matrix, resolution: 1 mm^3, and FOV: 24 cm). Audio cues were synchronized with MR pulses using Presentation software (NeuroBehavioral Systems, Inc., Berkeley, CA).

Analysis of Functional NeuroImages (AFNI) software was used to process fMRI data. A detailed description of fMRI analysis methods is included in Appendix C. 3D images were temporally aligned, and the first 4 TRs from each run were removed. All runs from a single condition were concatenated and registered to the passive run adjacent to the anatomical scan. General linear modeling was used to fit a canonical hemodynamic response function (boxcar function convolved with a gamma function) to the measured blood-oxygenation-level dependent (BOLD) signal. Conventional fMRI signal processing for block designs, in which the entire BOLD signal is fit to a canonical function, may not be appropriate for detecting pedaling-related brain activation because limb and head motion may cause artifact (Mehta et al., 2009). To address this potential confound, we fit

only the rest portion of the BOLD time-series after pedaling stopped to the canonical function (Figure 4.1). This approach is justified because the termination of the BOLD signal is delayed with respect to the termination of behavior (DeYoe et al., 1994). Thus, data recorded during the rest period contains the end of the plateau portion of the BOLD signal, the declining phase of the BOLD signal, and baseline. This approach has been validated and used in prior work examining pedaling-related brain activation in individuals with and without stroke (Mehta et al., 2009, 2012; Promjunyakul et al., 2015). Head movement was used as a variable of no interest. Model fitting was performed in each subject's native coordinate system to avoid misregistration caused by conversion to standard space.

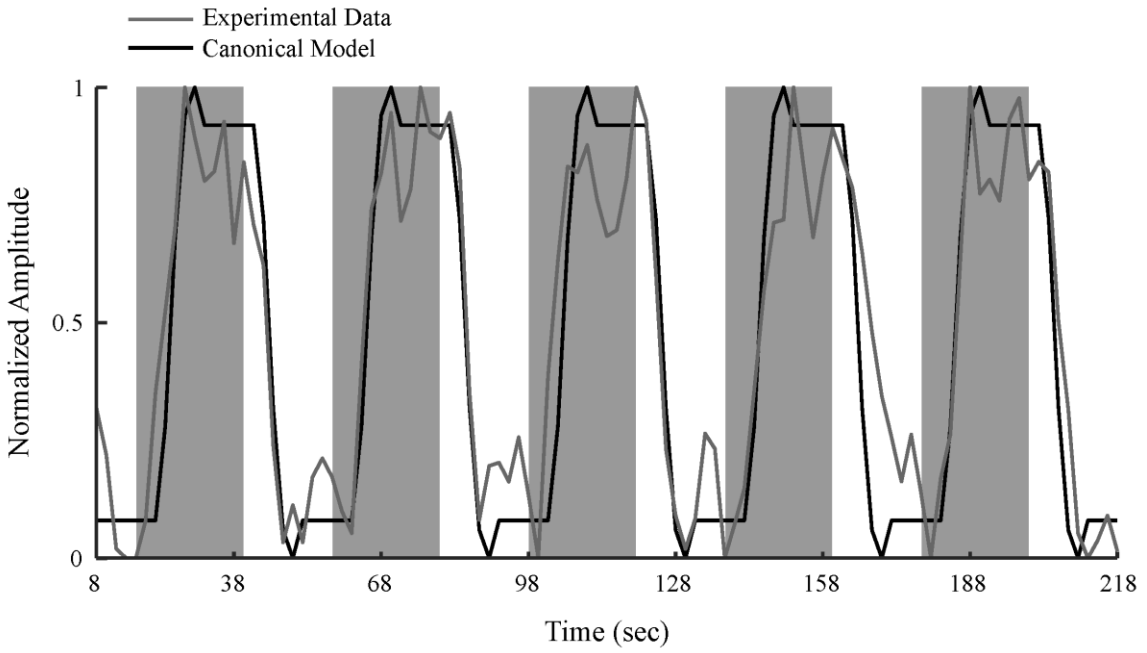

Figure 4.1 Delayed non-movement modeling technique. Experimental data from a single voxel in the sensorimotor cortex overlaid on the canonical hemodynamic response function. Gray shaded regions represent periods of time when the pedaling task was being performed, and white regions represent the rest periods. Data are shown for a single run with 5 pedaling blocks. The canonical hemodynamic response function (black line) was fit only to the portion of the BOLD response (gray line) obtained during rest periods. Note the delayed nature of the decline in the BOLD response associated with pedaling.

Noise smoothness was estimated using a spatial autocorrelation function, fit to a mixed model (Gaussian and mono-exponential functions), and used to blur functional data. To identify significantly active voxels at a familywise error rate of $P < 0.05$, we used Monte Carlo simulation to set an appropriate cluster size for a given individual voxel at $P < 0.005$. Voxels outside of the brain, negatively correlated voxels, and voxels with percent signal change greater than 10 were ignored.

Anatomical landmarks defined in native space on a subject-by-subject basis were used to circumscribe the primary motor and sensory cortices (M1S1), Brodmann's area 6 (BA6), and cerebellum (Cb) as previously described (Promjunyakul et al., 2015; Schmahmann et al., 1999; Wexler et al., 1997). These regions of interest (ROIs) were chosen because they were consistently activated across subjects. Quantitative measures of volume, intensity, and location of activation were extracted from each region and all regions combined. Volume was defined as the number of significantly active voxels in each region multiplied by voxel volume in microliters (μL). These values were also normalized to the anatomic volume of the region. Intensity was defined as the average percent signal change from baseline. Location of activation was measured with laterality index (LI), defined as the difference in volume between the damaged and undamaged sides (stroke) or left and right sides (control) as a proportion of total volume on both sides of the brain. Positive LI values indicated activation more towards the damaged hemisphere or the left hemisphere for stroke and control subjects respectively. In the Cb, LI was inverted. Location of activation was also measured by the center of mass (COM) of activation in M1S1. Group data were obtained by extracting the volume, intensity, and

LI values from ROIs defined in each subject's native space and averaging these values across all subjects.

Three types of head movement were estimated from volume registration performed in AFNI: 1) displacement – mean distance from registration point, 2) oscillation – mean variation around registration point, and 3) drift – change in position from start to the end of each trial. For all three types, movement was determined in the x (medial/lateral), y (anterior/posterior), and z (inferior/superior) directions. Calculations were performed separately for each subject and for each condition.

Statistical tests

Tests were performed in SPSS Statistics 22.0 (International Business Machines Corporation, NY). Effects were considered significant at $P < 0.05$.

Subject demographics

Descriptive characteristics between groups (control, stroke) were compared using Mann Whitney U (age, height, body mass index (BMI)), chi-square (sex), and independent t-tests (mass). Chi-square and independent t-tests were also used to determine whether subjects who were scanned and whose fMRI data were used in analysis were different from the entire group in terms of sex, hyperreflexia, paretic limb, stroke location, age, height, mass, BMI, time since stroke, walking velocity, and Fugl-Meyer score (total, motor, sensory, balance, range of motion, pain).

Feasibility of passive pedaling

In subjects who could perform passive pedaling, we examined the effect of condition on the mean EMG of each muscle; repeated measures analysis of variance (ANOVA) with 3 levels of condition (passive, volitional, rest) and 5 levels of muscle (TA, MG, RF, BF, AM) was used. When an effect of condition was detected, post-hoc pairwise comparisons were performed using Fischer's least significant difference. Data were collapsed across limbs, as we detected no significant between-limb differences ($P \geq 0.26$). Numerous post-hoc, exploratory analyses were used to identify factors associated with the ability to perform passive pedaling. Chi-square, Mann Whitney U, and independent t-tests were used to examine the effects of sex, hyperreflexia, group, age, mass, BMI, Fugl-Meyer scores, time since stroke, and walking velocity. Logistic regression was used to examine the predictive value of sex, group, age, mass, and BMI on the ability to perform passive pedaling. Tests were performed in control and stroke groups and, where appropriate, on the two groups combined.

Brain activation

Group and condition effects on brain activation volume, intensity, and LI of activation were examined using mixed effect ANOVA with 2 levels of condition (passive, volitional), 2 levels of group (stroke, control). and 3 levels of region (M1S1, BA6, and Cb). Normalized and non-normalized values for volume were examined. Effects of group and condition on COM were examined using mixed effect ANOVA with 2 levels of condition (passive, volitional) and 2 levels of group (stroke, control).

Pedaling rate, head motion

Group and condition effects on pedaling rate and head motion were examined using mixed effects ANOVA with 2 levels of condition (passive, volitional) and 2 levels of group (stroke, control). The ANOVA for head motion also used three levels of movement type (oscillation, drift, displacement) and three levels of movement direction (X, Y, Z).

4.3 Results

Subject demographics

Stroke and control groups were not different in age, height, BMI, or sex ($P \geq 0.07$). Mass was higher in stroke than control subjects ($P = 0.03$). For all characteristics examined, subjects involved in different steps of the study (familiarization, scanned, fMRI analysis) were not different from all subjects enrolled ($P \geq 0.18$). See Table 4.1.

Feasibility of passive pedaling

All enrolled subjects could perform volitional pedaling. However, only 53% of subjects [10 stroke (45%), 14 control (61%)] could adequately minimize lower limb muscle activity for passive pedaling. As suggested by the representative data in Figure 4.2A, subjects who could perform passive pedaling displayed a marked reduction in EMG during passive compared to volitional pedaling. They also showed no visually apparent, phase-dependent modulation of EMG amplitude during the passive condition. Moreover, the EMG observed during passive pedaling resembled that recorded during quiet rest (Figure 4.2B). These observations were apparent in all 5 muscles examined and

in both limbs of stroke and control subjects. Quantitative analyses of the EMG data support these conclusions. In subjects who could perform passive pedaling, mean (SD) EMG across muscles and groups decreased from 0.0106 (0.0569) mV during volitional pedaling to 0.0024 (0.0010) mV during passive pedaling ($P < 0.001$) and 0.0022 (0.0011) mV during quiet rest ($P < 0.001$).

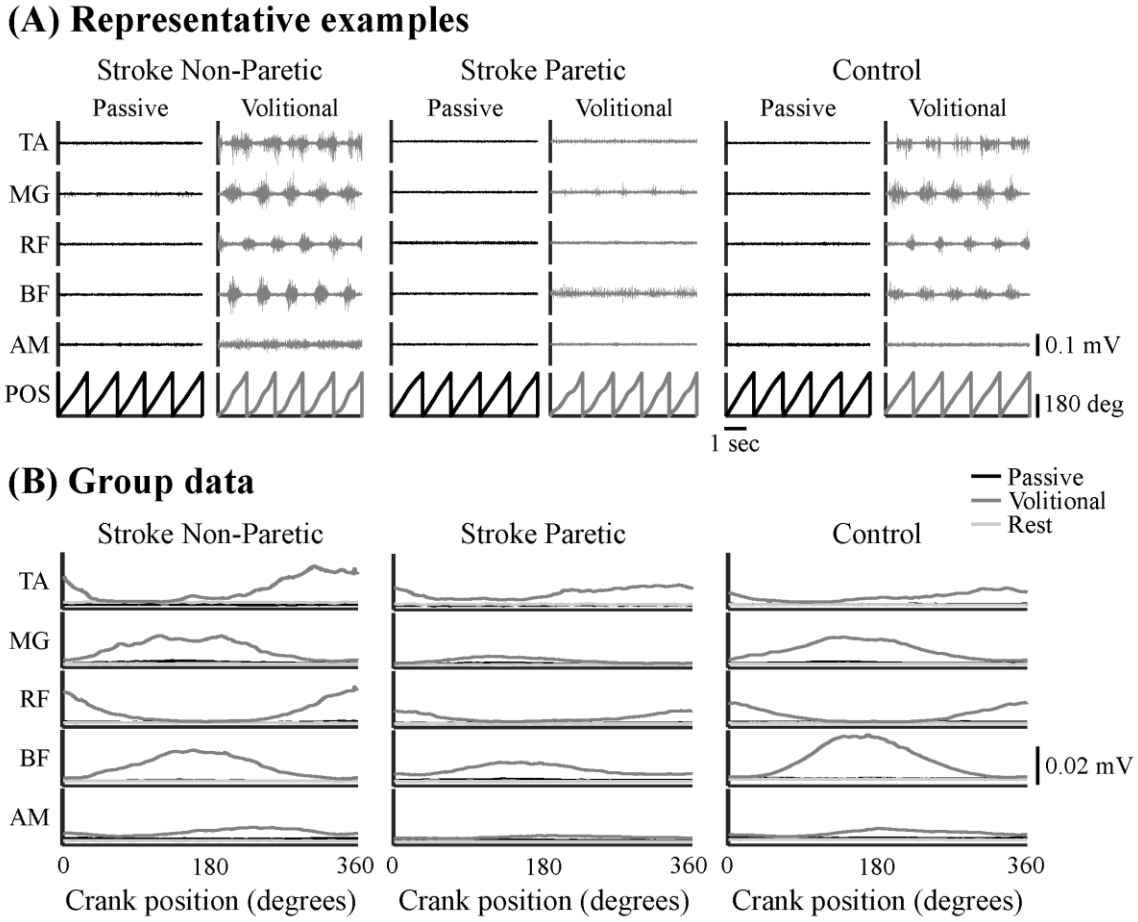

Figure 4.2. Muscle activity during passive and volitional pedaling in PASSIVE subjects: representative examples and group averages. (**A**) representative examples of EMG (raw, unprocessed) during passive and volitional pedaling in the non-paretic and paretic legs of one stroke subject and in the right leg of one control subject able to minimize muscle activity for passive pedaling. Data shown for 5 revolutions. (**B**) group average EMG (rectified, filtered, ensemble-averaged) for the non-paretic, paretic, and control limbs from all subjects able to minimize muscle activity during passive pedaling. TA, tibialis anterior; MG, medial gastrocnemius; RF, rectus femoris; BF, biceps femoris; AM, adductor magnus; POS, pedal position.

Most subjects who could not perform passive pedaling (20/21, (95%); 12 stroke, 8 control) displayed a pattern of EMG activity in one or more muscles that resembled the EMG during volitional pedaling (see Figure 4.3). These subjects could reduce, but not eliminate, pedaling-related muscle activity. Some subjects (5 stroke, 5 control) also displayed a relatively invariant level of EMG across the pedaling cycle that was greater than the mean + 4 SD of quiet rest. Because EMG amplitude in these muscles was not modulated across the pedaling cycle, we considered that these muscles were stabilizing their limbs during passive pedaling. Only one subject was considered NON-PASSIVE because she showed this type of muscle activity alone. A few subjects (1 stroke, 3 control) also displayed EMG during periods of apparent muscle lengthening. Hence, it appeared that in these muscles reflex-generated muscle activity could not be fully eliminated for passive pedaling.

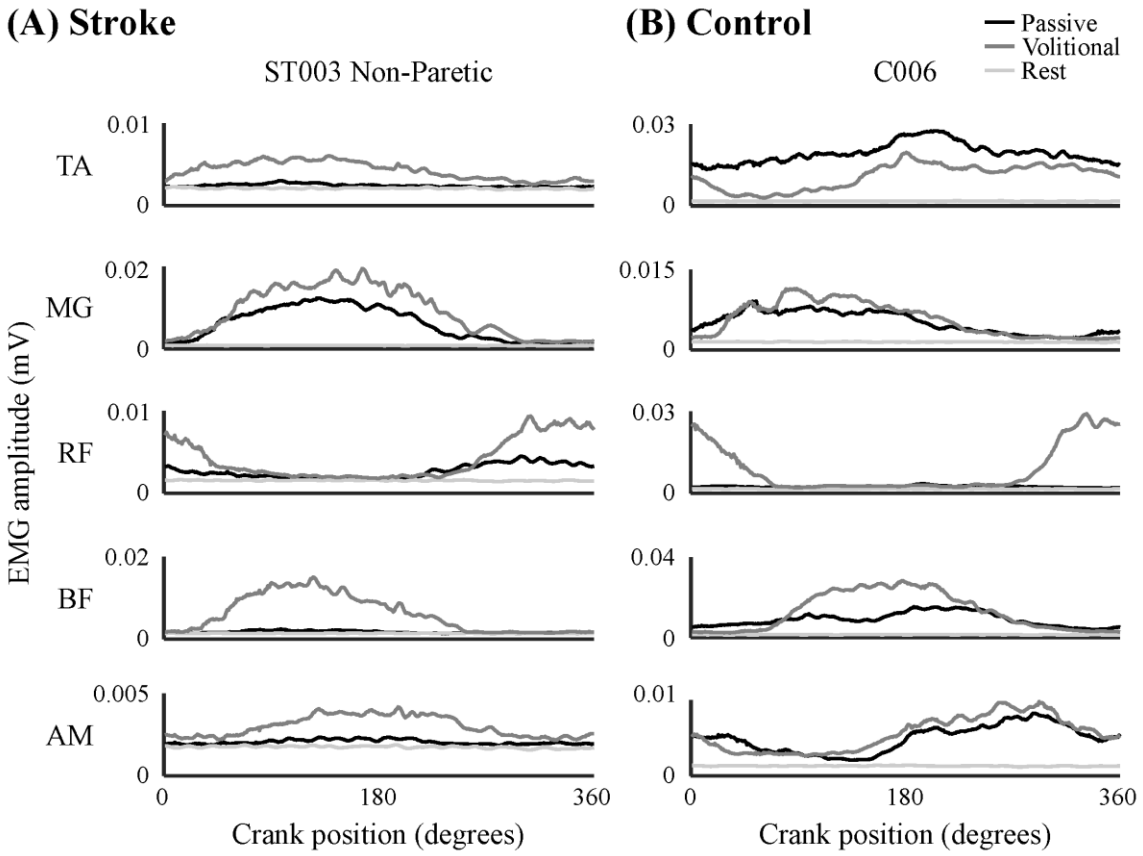

Figure 4.3. Representative examples of NON-PASSIVE stroke and control subjects. Examples from one stroke (**A**) and one control subject (**B**) who were classified as NON-PASSIVE. Data shown are EMG (processed, ensemble averaged) during passive pedaling that were similar as during volitional pedaling. MG, medial gastrocnemius; RF, rectus femoris; BF, biceps femoris; AM, adductor magnus.

Sex was the only descriptive variable that was significantly associated with the ability to perform passive pedaling. The proportion of females in the PASSIVE group (70%) was significantly higher than the proportion of males (36%) ($\chi^2 = 4.98$, $P = 0.03$), but there was no significant effect of group ($\chi^2 = 1.07$, $P = 0.30$). Logistic regression analysis showed that sex was the only variable to make a significant contribution to the prediction of passive pedaling ($R^2 = 0.15$, $P = 0.01$). Moreover, when age, group, BMI, and mass were forced into the regression, the F-value on the full model decreased and the *P*-value increased. This observation suggests that the addition of descriptive variables

other than sex had no positive effect and even impaired the relative predictive power of the model. Finally, as shown in Table 4.2, there were no significant differences between PASSIVE and NON-PASSIVE subjects with respect to age, mass, BMI, time since stroke, Fugl-Meyer scores, walking velocity, or hyperreflexia.

	PASSIVE	**NON-PASSIVE**	**t-value**	***P*-value**
All				
age	64 (9)	61 (14)	0.82	0.42
mass	79 (13)	85 (20)	-1.21	0.30
BMI	27 (4)	28 (6)	-0.28	0.78
Control				
age	63 (7)	61 (17)	0.44	0.67
mass	76 (12)	77 (16)	-0.09	0.93
BMI	27 (4)	25 (4)	1.08	0.29
Stroke				
age	64 (11)	60 (13)	0.68	0.50
mass	83 (14)	91 (21)	-1.11	0.28
BMI	28 (4)	30 (7)	-0.82	0.42
time since stroke	8 (3)	8 (5)	0.29	0.78
walking velocity	0.63 (0.34)	0.89 (0.38)	-1.53	0.15
Fugl-Meyer				
total	76 (8)	81 (9)	-1.28	0.22
motor	23 (6)	26 (5)	-0.97	0.35
sensory	9 (4)	10 (2)	-0.85	0.41
balance	7 (1)	8 (1)	-1.98	0.14
ROM	18 (2)	18 (2)	-0.31	0.76
Pain	20 (0)	20 (0)	0	>0.99
			χ^2	***P*-value**
hyperreflexia	8 (89%)	5 (56%)	2.49	0.11

Table 4.2. Differences between PASSIVE and NON-PASSIVE subjects. Data are shown for all subjects, the control group alone, and the stroke group alone. Values for age (years), mass (kg), and BMI (kg/m^2) are shown for both groups. Values for time since stroke (years), walking velocity (m/s), Fugl-Meyer scores, and hyperreflexia are also shown for the stroke group. Values for hyperreflexia are count (%). All other values are mean (SD).

Brain activation, passive vs. volitional

As illustrated by the examples in Figure 4.4, passive and volitional pedaling produced bilateral activation in M1S1, BA6, and Cb in both the stroke and control group. In most subjects, activation in BA6 was limited to the supplementary motor area, and activation in the Cb was limited to the vermis and lobules IV, V, and VIII. Regardless of group or region examined, there was no significant difference in brain activation volume, intensity, or LI for passive as compared to volitional pedaling. See Figure 4.5 and Table 4.3. Normalized brain activation volume ($P = 0.34$) and COM were also not different between conditions ($P = 0.14$).

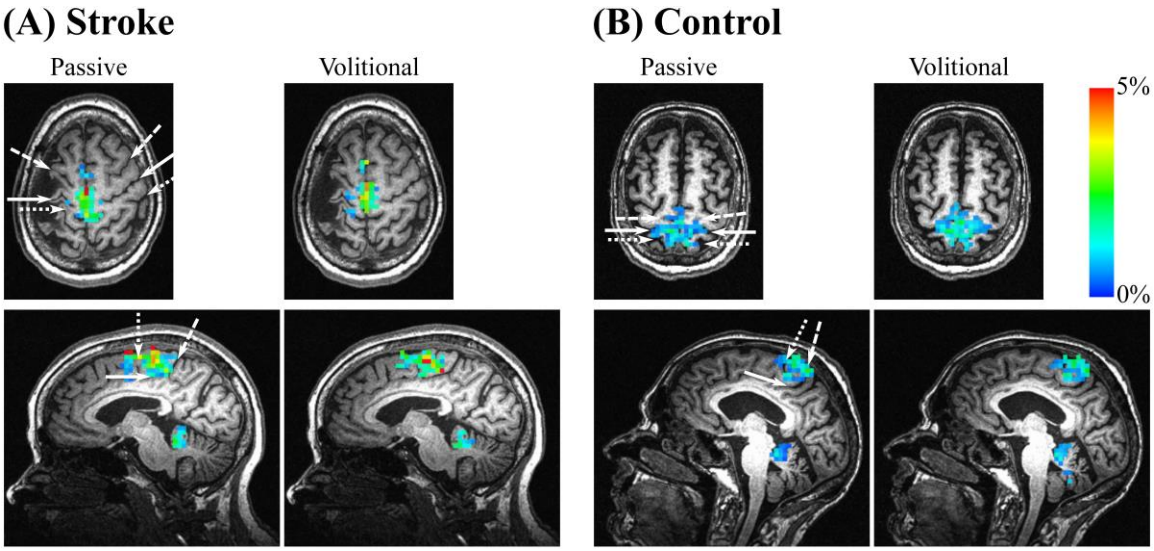

Figure 4.4. Representative examples of pedaling-related brain activation. fMRI activation during pedaling in a stroke (**A**) and control (**B**) subject. A single axial and sagittal slice is shown for each subject to demonstrate the brain activation during passive and volitional pedaling. The same slices are depicted for passive and volitional pedaling. Color scale represents percent signal change compared to rest (0-5%). White arrows indicate anatomical landmarks. In the axial plane: long dash, precentral sulcus; solid line, central sulcus; short dash, postcentral sulcus. In the sagittal plane: long dash, marginal sulcus; solid line, cingulate sulcus; short dash, paracentral sulcus.

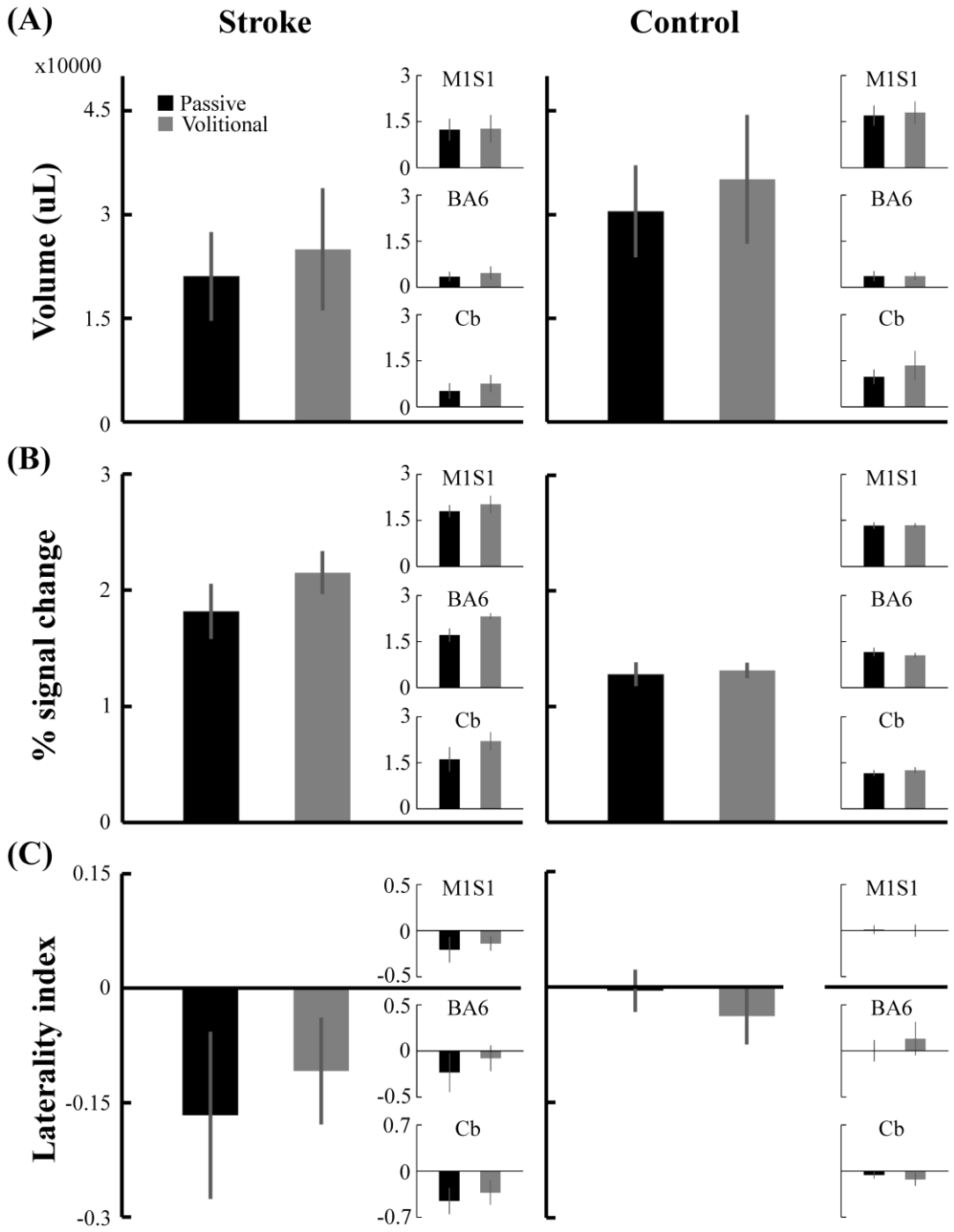

Figure 4.5. Group average pedaling-related brain activation for all active brain regions. Volume (**A**), intensity (**B**), and laterality index (**C**) of brain activation. Large bar graphs show activation values for all active brain regions. Inset bar graphs show activation values for the indicated region of interest. Each dependent variable was extracted from native space on a subject-by-subject basis and then averaged for each group and for each condition. Volume, intensity, and laterality index were similar for both groups when comparing passive and volitional pedaling. Error bars are SE. M1S1, primary motor and sensory cortices; BA6, Brodmann's area 6; Cb, cerebellum.

			Passive	Volitional		Passive	Volitional	P_g	P_c	$P_{g\,x\,c}$	$P_{c\,x\,r}$
Stroke	Volume	All regions	21,060 (14,382)	24,983 (19,766)	**Control**	30,459 (21,070)	35,094 (29,558)	0.41	0.46	0.95	0.61
		M1S1	12,396 (8,029)	12,711 (10,081)		16,996 (10,452)	17,947 (11,613)				
		BA6	3,478 (3,532)	4,689 (4,700)		3,670 (5,270)	3,642 (4,138)				
		Cb	5,186 (5,659)	7,583 (6,216)		9,793 (7,662)	13,506 (14,870)				
	Intensity	All regions	1.82 (0.53)	2.15 (0.41)		1.28 (0.33)	1.31 (0.21)	<0.001	0.13	0.13	0.30
		M1S1	1.80 (0.45)	2.03 (0.63)		1.33 (0.35)	1.34 (0.23)				
		BA6	1.71 (0.50)	2.32 (0.25)		1.16 (0.46)	1.05 (0.26)				
		Cb	1.61 (0.89)	2.21 (0.66)		1.16 (0.32)	1.26 (0.31)				
	LI	All regions	-0.22 (0.33)	-0.14 (0.21)		-0.01 (0.12)	-0.05 (0.15)	0.11	0.21	0.36	0.61
		M1S1	-0.21 (0.31)	-0.14 (0.17)		0.01 (0.15)	0.00 (0.21)				
		BA6	-0.23 (0.48)	-0.08 (0.31)		0.00 (0.37)	0.13 (0.57)				
		Cb	-0.45 (0.45)	-0.33 (0.42)		-0.06 (0.18)	-0.13 (0.31)				

Table 4.3. Pedaling-related brain activation during passive and volitional pedaling. Volume, intensity, and LI are shown for stroke and control during passive and volitional pedaling. *P*-values for each measure are from separate repeated measures GLM [between-subject factor of group (stroke, control), within-subject factors of condition (passive, volitional) and region (M1S1, BA6, and Cb)]. Values are Mean (SD). P_g – group effect; P_c – condition effect; $P_{g\,x\,c}$ – group*condition effect; $P_{c\,x\,r}$ – condition*region effect.

Brain activation, stroke vs. control

Regardless of the region or condition examined, there were no between-group differences (stroke vs. control) in activation volume or LI. Normalized brain activation volume was also not different between groups ($P = 0.55$). In contrast, the intensity of pedaling-related brain activation (collapsed across conditions) was higher in the stroke group as compared to controls for all active regions ($P < 0.001$). There were also no group*condition interactions (intensity: $P = 0.13$; volume: $P = 0.95$; LI: $P = 0.36$). See Table 4.3.

Pedaling rate, head motion

During fMRI, pedaling was performed at the desired rate, as shown by a mean (SD) rate of 45 (3) RPM that did not differ across conditions or groups ($P = 0.19$ condition, $P = 0.42$ group, $P = 0.38$ condition*group). During familiarization, pedaling rate was not different between groups (44.9 (1.8) RPM, $P = 0.08$). However, the rate of passive pedaling (44.2 (1.0)) was lower than the rate of volitional pedaling (45.6 (2.1)) with an effect size of 1.4 RPM and $P < 0.001$.

Head motion was successfully minimized during fMRI. Subjects included in fMRI analysis displayed 0.22 (0.20) mm of oscillation, 0.58 (0.64) mm of displacement, and 0.46 (0.52) mm of drift. Values did not differ across conditions or groups ($P = 0.19$ condition, $P = 0.62$ group, $P = 0.22$ condition*group).

4.4 Discussion

This study provides three novel discoveries with important implications for understanding neural control of leg movement after stroke. First, we found that passive pedaling did not reduce between-group differences (stroke vs. control) in pedaling-related brain activation. Second, brain activation in people with and without stroke was not significantly different between passive and volitional pedaling. Together, these observations suggest that altered volitional motor commands and pedaling performance are unlikely to account for reduced pedaling-related brain activation post-stroke, as reported by Promjunyakul et al. (2015). Instead, this phenomenon may be due to loss of structural connectivity among brain regions, exaggerated cortical inhibition, increased reliance on spinal and brainstem pathways for rhythmic leg movement, or poor sensorimotor integration. These mechanisms require further study. The lack of difference between brain activation during passive and volitional pedaling also suggests that sensory signals from the moving limbs make an important contribution to pedaling-related brain activation in people with and without stroke. Third, our data demonstrate that it is not uncommon for stroke and control subjects to have difficulty minimizing lower limb muscle activity for passive pedaling. Passive pedaling may require processes that are more developed in some individuals than others, such as: alteration of descending drive, inhibition of reflexes, and inhibition of pattern generating circuits.

Motivation and limitations

This study was motivated by our prior work demonstrating that the volume of pedaling-related brain activation is reduced in people post-stroke as compared to age-

matched controls (Promjunyakul et al., 2015). Unlike our prior work, the present study found no significant difference in pedaling-related brain activation volume between the stroke and control groups. The absence of a significant group effect on volume is a limitation and raises the possibility that there is no real reduction in pedaling-related brain activation volume after stroke. However, several pieces of evidence suggest otherwise. In the present study, the volume of activation across all regions was 29% lower in the stroke than in the control group. This reduction is consistent with the 27% reduction reported previously that reached statistical significance (Promjunyakul et al., 2015). Hence, it is likely that the lack of significance reported here was due to a small sample and low statistical power, not a true absence of a between-group difference. The intensity data provide further evidence that sampling may account for inconsistencies between studies. The present study found significantly higher pedaling-related brain activation intensity in the stroke as compared to the control group. In our prior publication (Promjunyakul et al., 2015), there was a trend toward higher intensity activation post-stroke that was not statistically significant. These observations suggest that inter-individual variation may have contributed to disparate results across studies. Larger samples would be useful in future work to increase statistical power and to better represent the full range of responses within the population. In this study, our sample was constrained by strict criteria for passive pedaling that was necessary for eliminating motor commands to pedal and minimizing between-group differences in pedaling performance. With these limitations in mind, we discuss the implications of our results in the sections that follow.

Influence of volitional motor commands and pedaling performance on brain activation post-stroke

Plausible explanations for reduced pedaling-related brain activation post-stroke are not limited to neuroplasticity. Altered volitional motor commands and pedaling performance may contribute. Unlike control subjects who use both limbs equally to pedal (Ambrosini, Ferrante, Ferrigno, Molteni, & Pedrocchi, 2012; Brown & Kautz, 1998), people with stroke typically exhibit an asymmetric pedaling strategy in which the non-paretic limb contributes more than half the work of pedaling (Brown & Kautz, 1998; Perell et al., 1998). This strategy is characterized by abnormal muscle activation patterns, kinetics, and kinematics that may be driven by volitional motor commands that are different from normal. These phenomena occur at the same time and may be inter-dependent with neuroplastic adaptations. Thus, it is difficult to separate the contributions of neuroplasticity, altered motor commands, and pedaling performance to changes in pedaling-related brain activation.

We are not the first to consider the effects of task performance on movement-related brain activation post-stroke. Levin et al. (2009) included this issue in a contemporary review highlighting the importance of altered movement patterns after stroke. Other commentaries and position papers have also included altered task performance as a limiting factor in the interpretation of fMRI data (Baron et al., 2004; Krakauer, 2007). To examine this issue, subjects performed passive and volitional pedaling while we examined brain activation with fMRI. Passive pedaling eliminated motor commands to pedal and minimized between-group differences in pedaling performance (e.g. muscle activity, kinematics, symmetry), providing insight into how

motor commands and pedaling performance may influence brain activation. We reasoned that if motor commands and pedaling performance have an important influence on brain activation post-stroke, then between-group differences in the volume, intensity, and/or location of brain activation would be reduced during passive as compared to volitional pedaling. Moreover, brain activation would be different during passive as compared to volitional pedaling.

Contrary to our prediction, our data suggest that motor commands and pedaling performance do not produce significant changes in brain activation post-stroke. Despite eliminating motor commands to pedal and minimizing between-group differences in muscle activity, kinematics, and symmetry, passive pedaling did not minimize differences in brain activation volume, intensity, or LI between the stroke and control group. On average, the volume of brain activation in the stroke group was 71% of control during volitional pedaling and 69% of control during passive pedaling. Intensity values for the stroke group were 164% of control during volitional and 142% of control during passive pedaling. For LI, values for the stroke and control groups were -0.14 and -0.05 during volitional pedaling and -0.22 and -0.01 during passive pedaling. Furthermore, we saw no significant difference in the volume, intensity, or LI of brain activation during passive as compared to volitional pedaling. We also found no evidence of a shift in the COM of activation when comparing passive to volitional pedaling. Taken together, these observations suggest that whether pedaling is performed volitionally or passively, brain activation remains largely unchanged. If such a robust manipulation of motor commands and pedaling performance does not alter brain activation, then less substantial differences in motor commands and pedaling performance, such as asymmetric work output, are

unlikely to explain stroke-related decreases in brain activation volume that have been described (Promjunyakul et al., 2015).

The absence of significant differences in brain activation between volitional and passive pedaling also suggests that sensory signals from the moving limbs make an important contribution to pedaling-related brain activation in people with and without stroke. This observation is consistent with a prior study from our lab that used fMRI to demonstrate that cortical activation in young adults without stroke was not different during passive and volitional pedaling (Mehta et al., 2012). Moreover, Christensen et al. (2000) recorded brain activation volume and peak regional cerebral blood flow (rCBF) with positron emission tomography (PET) during passive and volitional pedaling in adults without stroke. Despite differing from our study in imaging modality (PET vs. fMRI) and pedaling rate (60 vs. 45 RPM), Christensen's results are consistent with ours. They reported no between-condition differences in activation volume or peak rCBF in the primary sensory area, supplementary motor area, or the cerebellar vermis. The only significant difference between conditions was a 12-14% increase in rCBF in M1 during volitional as compared to passive pedaling. While not reaching statistical significance, the present paper and our prior work (Mehta et al., 2012) reveal a tendency for brain activation volume in M1 to be larger (13-14%) during volitional as compared to passive pedaling. Perhaps the lack of significance in our work is related to sample size or our use of mean intensity, not peak rCBF. Overall, the observations reported here provide further evidence that much of the brain activation during pedaling may not be related to the volitional commands or muscle activity, but rather to monitoring sensory information to respond to perturbations or to maintain, reinforce, or shape ongoing motor output.

A largely sensory contribution to pedaling-related brain activation, particularly for motor areas of the brain, may seem counterintuitive. However, many studies have found that brain activation in neurologically intact individuals is not different or minimally different during passive and volitional movements of the finger, hand, wrist, elbow, shoulder, toe, ankle, knee, or hip (Blatow et al., 2011; Boscolo Galazzo et al., 2014; Guzzetta et al., 2007; Kocak, Ulmer, Sahin Ugurel, Gaggl, & Prost, 2009; Onishi et al., 2013; Terumitsu, Ikeda, Kwee, & Nakada, 2009; Weiller et al., 1996). In people with stroke, passive and volitional movements of the finger and ankle are associated with the same brain activation (Alary et al., 1998; Enzinger et al., 2008). Other studies in humans support an influence of sensory input on brain activation. When anesthesia is used to block muscle afferent feedback during static and dynamic contractions, a large decrease in brain activation is observed in humans (Friedman, Friberg, Mitchell, & Secher, 1991; Friedman, Friberg, Payne, Mitchell, & Secher, 1992).

Alternatively, passive pedaling may engage different motor commands (e.g., commands to relax the legs) that produces a similar fMRI response as the volitional command to pedal. Similarly, because fMRI cannot distinguish between excitation and inhibition (Logothetis, 2008), volitional and passive pedaling may differentially activate excitatory and inhibitory circuits without changing total cortical activation measured with fMRI. For example, when individuals relax from a contraction, there is an increase in the magnitude of short-interval intracortical inhibition (SICI) (Motawar, Hur, Stinear, & Seo, 2012) but no change in cortical activation (Toma et al., 1999). During response inhibition, cortical excitability decreases and and SICI increases (Coxon, Stinear, & Byblow, 2006). Passive pedaling may involve analogous alterations in the balance of

cortical excitation and inhibition that decrease descending drive to spinal motor neurons without changing brain activation as measured with fMRI.

Limitations in the measurement properties of fMRI may have contributed to our results. Passive pedaling may induce enough neural activation to saturate the blood flow response such that additional neural activation caused by motor commands fails to increase the fMRI signal. Evidence for this hypothesis comes from Reddy et al. (2001) who found no difference in brain activation, as measured with fMRI, during volitional and passive finger movements in neurologically intact individuals. In people with sensory neuropathy, volitional movement produced activation that was indistinguishable from the neurologically intact group; while passive movement produced no measurable brain activation (Reddy et al., 2001). These observations suggest that both sensory and motor signals contribute to brain activation, but they do not have an additive effect on the fMRI signal.

Finally, our results could be influenced by a sample that does not represent the population. Forty-seven percent of our sample could not achieve passive pedaling according to our strict criteria; these subjects did not undergo fMRI. Individuals who could achieve passive pedaling might be different from those who could not. Specifically, they might be able to inhibit muscle activity through an active process. As discussed above, active inhibition may produce similar fMRI signals as volitional commands to pedal. Detracting from this explanation is prior work showing no difference in brain activation during passive and volitional movements (including pedaling) with minimal or non-existent criteria for achieving the passive condition (see below: *Minimizing muscle activity for passive pedaling*). These observations suggest that our results may generalize

to the broader population, including individuals who cannot completely relax for passive pedaling.

Explanations for reduced pedaling-related brain activation post-stroke

Finding no compelling evidence for altered motor commands and pedaling performance as an explanation for reduced brain activation post-stroke, we continue to consider alternative explanations. With respect to anatomical contributions, reduced pedaling-related brain activation volume could be caused by the loss of viable brain tissue, as all stroke survivors suffered tissue loss. However, no stroke survivors had lesions affecting the leg area of M1S1, and only one subject had a lesion affecting the cerebellum. Thus, as in our prior work, brain activation was lacking in apparently vital regions that are typically involved in pedaling (Promjunyakul et al., 2015). Therefore, stroke may cause a fundamental change in the structure or function of the brain. Below we consider several possibilities that could be tested in future work.

Reduced activation volume in anatomically intact brain regions could be explained by impaired white matter connectivity (Kalinosky, Schindler-Ivens, & Schmit, 2013; Zhang et al., 2016). All stroke subjects examined had some white matter damage, which could reduce the effects of signals from intact portions of the brain. Moreover, unless these signals find other pathways, intact brain regions may stop firing for lack of effects on their targets. Similarly, loss of structural connectivity could reduce the amount of sensory input reaching the cortex, which may be a major source of pedaling-related cortical activation, as discussed above (Christensen et al., 2000; Mehta et al., 2012). While plausible, these hypotheses require further study. Contrary to these assertions,

others have suggested that reduced connectivity among motor areas of the brain leads to over-activity of cortical tissue (Hamzei, Dettmers, Rijntjes, & Weiller, 2008).

Elevated cortical inhibition could also contribute to reduced pedaling-related brain activation volume post-stroke. Previous work has demonstrated reduced excitability of the lesioned hemisphere (Byrnes, Thickbroom, Phillips, Wilson, & Mastaglia, 1999; Liepert et al., 2001). Exaggerated inhibition could be intrinsic to the lesioned hemisphere, or it could be due to interhemispheric inhibition whereby transcallosal output from the undamaged hemisphere inhibits M1 of the damaged hemisphere (Murase et al., 2004; Traversa et al., 1998). These phenomena manifest as lateralized activation towards the intact side of the brain. Our data are in line with this explanation, as there was a tendency for lateralization of brain activation toward the undamaged cortex and Cb, although this observation did not reach statistical significance.

It is also possible that reduced pedaling-related brain activation volume after stroke is due to enhanced reliance on the spinal cord and/or brainstem for lower limb movement. Kautz et al. (2006) found that pedaling with one leg induces rhythmic muscle activity in the contralateral leg in both stroke and control subjects. There was a greater induction of activation in the contralateral, non-moving limb in stroke compared to control, particularly in those with greater impairments (Kautz et al., 2006). This result suggests that stroke survivors may have a greater reliance on spinal cord pathways for pedaling than controls. Perhaps the reduced cortical activation observed in stroke survivors is adequate for initiating pedaling, after which the maintenance of ongoing movement occurs in the brainstem and/or spinal cord. The result may be the

unsophisticated and inflexible pattern of leg movement that is characteristic of hemiparesis.

Finally, impaired somatosensory integration in the cortex may also contribute to reduced pedaling-related brain activation after stroke. During passive wrist movement, stroke survivors with severe sensory impairment have reduced somatosensory evoked responses as measured by electroencephalography (EEG) (Vlaar et al., 2017). Similarly, several studies have demonstrated that somatosensory evoked potentials are absent in stroke survivors who experience poor motor recovery (Feys, Van Hees, Bruyninckx, Mercelis, & De Weerdt, 2000; La Joie, Reddy, & Melvin, 1982). These studies suggest that there are impairments in the transmission of sensory information to the cortex or impairments in the cortical integration of sensory information after stroke. These deficits might result in decreased pedaling-related brain activation after stroke.

Minimizing muscle activity for passive pedaling

The other major discovery from this study was that a large proportion of subjects (55% stroke, 39% control) had difficulty minimizing lower limb muscle activity for passive pedaling. The proportion of subjects unable to perform passive pedaling was surprisingly large given that few prior studies excluded subjects for failing to perform a passive condition. Our rate of exclusion may be due to the complexity of the task; subjects were required to relax multiple muscles across multiple joints of both limbs. Most other studies of passive movement were limited to a single joint, did not record muscle activity, and/or did not provide quantitative measures of EMG (Alary et al., 1998; Blatow et al., 2011; Boscolo Galazzo et al., 2014; Christensen et al., 2000; Enzinger et

al., 2008; Guzzetta et al., 2007; Jain, Gourab, Schindler-Ivens, & Schmit, 2013; Kocak et al., 2009; Mehta et al., 2012; Onishi et al., 2013; Terumitsu et al., 2009; Weiller et al., 1996). Our criteria for minimizing muscle activity were rigorous, requiring the near absence of EMG. The presence of pedaling-related EMG despite instruction and effort to remain passive raises questions about the physiological mechanisms underlying ability to perform passive movement. There may be inter-individual differences in the ability to alter descending drive, inhibit spinal reflexes, or inhibit pattern generating activity.

To minimize muscle activity for passive pedaling, individuals may need to reduce excitatory descending drive to spinal motor neurons. The ability to do so may be mediated by intracortical inhibition, which may differ among individuals. Jain et al. (2013) and Yamaguchi et al. (2012) suggest that passive pedaling may require a greater level of intracortical inhibition than volitional pedaling. Using EEG, Jain et al. (2013) found that passive pedaling induced less beta desynchronization than volitional pedaling. As prior work has established an inverse relationship between beta desynchronization and intracortical inhibition (Takemi, Masakado, Liu, & Ushiba, 2013), this observation suggests that passive pedaling requires a higher level of intracortical inhibition than volitional pedaling. Yamaguchi et al. (2012) used TMS to evaluate intracortical inhibition before and after passive and volitional pedaling. They found that intracortical inhibition was the same before and after passive pedaling, but lower after volitional pedaling. Again, this observation suggests that passive pedaling may involve intracortical inhibition. Work from Coxon et al. (2006) and Motawar et al. (2012) provides further support for these conclusions. These authors have suggested that intracortical inhibition is important for relaxing from a volitional contraction or preventing a prepared movement.

Stretch reflexes may be responsible for residual EMG during passive pedaling. Typically, monosynaptic reflexes are dramatically reduced by both passive and volitional pedaling (Brooke et al., 1992; Brooke, Misiaszek, & Cheng, 1993; Fuchs et al., 2011; Larsen, Voight, & Grey, 2006; McIlroy, Collins, & Brooke, 1992; Motl, Knowles, & Dishman, 2003; S. Schindler-Ivens et al., 2008). The mechanism responsible for reflex suppression, presynaptic inhibition of primary afferent terminals (Brooke et al., 1992; McIlroy et al., 1992), may be better developed in some individuals than others. Indeed, group Ia reflex suppression during pedaling is severely reduced in some people with stroke, but near normal in other people with stroke (Fuchs et al., 2011; S. Schindler-Ivens et al., 2008). Even in able-bodied individuals, inhibition of Group Ia afferent input is affected by training (Nielsen, Crone, & Hultborn, 1993). Yet, it is unlikely that hyperexcitable reflexes significantly contribute to our results because few control (n = 3) and stroke (n = 1) subjects displayed EMG during lengthening phases of passive pedaling. Additionally, 20/21 (95%) of NON-PASSIVE subjects had at least one muscle that showed activation like that seen during volitional pedaling.

Some subjects may have difficulty suppressing sensory input that influences the pattern-generating circuits that contribute to rhythmic movement. It is well established that sensory input activates spinal pattern-generating circuits in non-human animals (Prochazka & Ellaway, 2012) and influences the timing and amplitude of human rhythmic motor output (Grey, Nielsen, Mazzaro, & Sinkjaer, 2007; Sinkjaer, Andersen, Ladouceur, Christensen, & Nielsen, 2000; Stephens & Yang, 1999; Verschueren, Swinnen, Desloovere, & Duysens, 2002; Yang, Stein, & James, 1991). To achieve passive pedaling, it may be necessary to suppress sensory input from muscle length,

velocity, or load receptors or to suppress the output of pattern-generating circuits influenced by these sensory signals. The ability to do so may vary among individuals as described above for monosynaptic reflex suppression. This mechanism could account for cases in which the muscle activation was reduced during passive as compared to volitional pedaling, but the pattern of EMG was the same across conditions. Ninety-five percent of subjects who were unable to achieve passive pedaling displayed this EMG pattern in at least one muscle.

Finally, we cannot rule out inter-individual differences in EMG signal detection as a possible explanation for differences in the ability to achieve passive pedaling. Fewer males than females could achieve passive pedaling. This finding may reflect better EMG signal detection in males, who typically have less body fat and more lean mass than women, including in the lower body (Power & Schulkin, 2008). However, post-hoc analyses of descriptive data suggest that differences in body composition may not explain the observed sex differences. We found no differences between males and females with respect to mass or BMI. Moreover, PASSIVE individuals had lower values for mass and BMI compared to NON-PASSIVE individuals. Additionally, our logistic regression analysis indicated that sex, but not mass or BMI, was related to ability to perform passive pedaling. Therefore, we cannot rule out the possibility that sex influences neuromuscular control of passive movement or inhibition of rhythmic movement. However, we are unaware of evidence of sex differences in the ability to alter descending drive, alter the excitability of spinal reflexes, or inhibit pattern generating circuits.

Additional limitations

Despite our strict criteria during passive pedaling, a limitation of this study is that EMG activity was not measured during the fMRI scanning session. Differences in environment between the familiarization and scanning session could lead to changes in the ability to perform passive pedaling. Consequently, the lack of difference between brain activation during passive and volitional pedaling may be a result of the presence of muscle activity during passive pedaling. However, we did not experience any evidence of muscle contraction during passive pedaling in the MRI scanner. Our fMRI results are limited by a small sample size, particularly in the stroke group where five subjects were included. The small sample increases the risk of Type II error and limits generalizability to the population. However, the strict criteria that resulted in the small sample also allowed us to maximize differences between volitional and passive pedaling and minimize between-group differences in motor commands and pedaling performance. The lack of visual or auditory biofeedback about muscle activity during passive pedaling may have contributed to the large number of individuals who were unsuccessful at the task. Future studies may benefit from more extensive training with biofeedback to help participants achieve passive pedaling.

Conclusion

This study found that between-group differences in brain activation were not reduced during passive as compared to volitional pedaling and that brain activation was not different between these conditions. These results suggest that factors besides altered volitional motor commands and pedaling performance may contribute to a reduction in

pedaling-related brain activation post-stroke, including: loss of structural connectivity, exaggerated cortical inhibition, increased reliance on spinal and brainstem pathways, or poor sensorimotor integration in the cortex. We cannot rule out Type II error as a factor in our results, and larger samples would be highly desirable for future studies. Additionally, this study tested the feasibility of minimizing muscle activity for passive pedaling. We found that a high proportion of both stroke and control subjects were unable to perform passive pedaling. This finding may reflect inter-individual and sex differences in the ability to alter descending drive, inhibit spinal reflexes, or inhibit pattern generating circuits.

CHAPTER 5: INTEGRATION OF RESULTS AND FUTURE DIRECTIONS

The purpose of this dissertation was to describe how compensation is related to motor function and brain activation during lower limb pedaling and identify elements that cause this behavior to persist chronically. This purpose was tailored to improve our understanding of long-term motor dysfunction after stroke and promote the development of more effective rehabilitation techniques. The preceding chapters provided novel information that may help address the problem of chronic compensation and long-term motor dysfunction. This chapter summarizes the main findings from this dissertation, describes future studies that would further advance this line of research, and discusses the implications of these findings for lower limb rehabilitation after stroke.

5.1 Summary of results

In Chapter 2, we evaluated muscle activation and pedaling performance when compensation was prevented with unilateral and bilateral uncoupled pedaling. We also determined whether paretic motor impairments, impaired interlimb coordination, or learned nonuse may contribute to compensation after stroke. Subjects performed conventional, unilateral, and bilateral uncoupled pedaling. Muscle activation and pedaling performance were measured. Compensation was measured as the percent mechanical work of pedaling performed by the paretic limb. We had different hypotheses for each of the possible contributors to compensation: 1) if paretic motor impairments contribute to compensation, then pedaling performance would deteriorate during unilateral pedaling with the paretic limb as compared to conventional pedaling; 2) if

impaired interlimb coordination contributes to compensation, then pedaling performance would deteriorate in both limbs during bilateral uncoupled as compared to conventional and unilateral pedaling; 3) if learned nonuse contributes to compensation, then paretic muscle activation would increase during unilateral and bilateral uncoupled pedaling, with minimal difference in performance as compared to conventional pedaling.

During conventional pedaling, we found evidence of compensation. Muscle activation was lower in the paretic limb, and the paretic limb produced less mechanical work than the non-paretic limb. During unilateral and bilateral uncoupled, muscle activity increased as compared to conventional pedaling. However, pedaling rate and smoothness were worse in the paretic limb during unilateral as compared to conventional pedaling. Furthermore, during bilateral uncoupled pedaling, pedaling rate and smoothness deteriorated further, and both the paretic and non-paretic limb had performance deficits. In addition, stroke survivors were unable to maintain the desired phasing between the pedals. These results suggest that both motor impairments in the paretic limb and impaired interlimb coordination may contribute to compensation. This hypothesis was supported by correlations of interlimb coordination and paretic motor impairments with the degree of compensation. When both variables were entered into a linear regression as independent factors, only interlimb coordination had a significant contribution to compensation. Overall, these findings suggest that impairment in interlimb coordination is the most likely contributor to compensation after stroke. Impaired interlimb coordination might occur because of altered control of several pathways important for interlimb coordination. We also found a relation between compensation and stroke

related motor function, suggesting that these findings are pertinent to the understanding of long term motor dysfunction after stroke.

In Chapter 3, we determined whether interlimb cutaneous reflex amplitude is altered during pedaling after stroke and whether alterations contribute to impaired interlimb coordination and compensation. Stroke and control subjects performed conventional pedaling while interlimb cutaneous reflexes were elicited with stimulation of the sural nerve of each limb. Interlimb reflex amplitude was quantified in both limbs at particular reflex latencies. Interlimb coordination and compensation were assessed during both pedaling and walking. Interlimb coordination was quantified as the ability to accurately and consistently maintain an antiphase relation between the limbs. Compensation was quantified as the contribution of the paretic limb to propulsion. We hypothesized that stroke survivors would have abnormalities in interlimb cutaneous reflex amplitude and that these abnormalities would be associated with interlimb coordination and compensation.

Contrary to our hypothesis, we found that interlimb cutaneous reflex amplitude was generally well conserved after stroke. However, there were some differences in reflex amplitude, most notably in bifunctional muscles at pedaling transitions. Furthermore, the few alterations in reflex amplitude were correlated with interlimb coordination and compensation during both pedaling and walking. These findings suggest that there are important alterations in the supraspinal and/or spinal control of interlimb sensory pathways that contribute to impaired interlimb coordination after stroke. Our results also have implications for the control of interlimb coordination through other neural pathways. In conjunction with the connection between interlimb coordination and

compensation found in Chapter 2, we found that alterations in interlimb reflexes and interlimb coordination were both correlated with compensation. This provides further evidence that abnormal control of interlimb coordination contributes to compensation. Finally, impairments were conserved across different locomotor tasks and correlated with stroke-related sensorimotor function.

In Chapter 4, we evaluated whether reduced pedaling-related brain activation after stroke can be explained by altered volitional motor commands and pedaling performance. To answer this question, stroke and control subjects performed volitional and passive pedaling during fMRI. Passive pedaling eliminated motor commands to pedal and minimized between-group differences in pedaling performance. Remaining differences in brain activation are likely reflective of neuroplastic changes, not acute alterations in brain activation related to task performance. Overall, this intervention was intended to provide insight into how brain activation might be affected by changes in motor commands and pedaling performance caused by compensation. We hypothesized that if motor commands and pedaling performance contribute to reduced pedaling-related brain activation post-stroke, then: 1) between-group differences would be reduced during passive as compared to volitional pedaling and 2) brain activation would be different between passive and volitional pedaling.

Contrary to our hypothesis, we found that between-group differences in pedaling-related brain activation were not reduced during passive pedaling. Likewise, brain activation was not different between passive and volitional pedaling for either stroke or control subjects. Therefore, it is unlikely that altered volitional motor commands and pedaling performance account for reduced pedaling-related brain activation after stroke.

Accordingly, it is also unlikely that motor compensation during pedaling accounts for reduced brain activation after stroke. Alternative mechanisms for reduced pedaling-related brain activation after stroke are: loss of structural connectivity among brain regions, exaggerated cortical inhibition, increased reliance on spinal and brainstem pathways for rhythmic leg movement, or poor sensorimotor integration. These mechanisms do not preclude the potential long-term neuroplastic effects of compensation. Specifically, the long-term use of compensatory movement patterns may have contributed to a fundamental change in how the brain is activated during movement.

Overall, this dissertation described how compensation is related to motor function and brain activation during lower limb pedaling and identified elements that cause this behavior to persist chronically. Our results suggest that instead of exhibiting deficits in pedaling performance because of an inability to coordinate movements between the limbs, stroke survivors may produce the mechanical work of pedaling primarily with the non-paretic limb. Abnormal control of interlimb sensory reflexes may contribute to impaired interlimb coordination and compensation after stroke; important changes in interlimb cutaneous reflexes were correlated with impaired interlimb coordination and compensation. However, interlimb reflexes were generally well preserved, so the control of interlimb coordination through other pathways such as descending supraspinal pathways may be important. Although compensation may help preserve pedaling performance, it also yields an underutilization of the motor ability of the paretic limb. Finally, despite its effects on muscle activity and motor performance, it is unlikely that compensation acutely causes reduced pedaling-related brain activation after stroke. Instead changes in brain activation might occur through other mechanisms or through

long-term use of compensatory movements. Across multiple chapters, we found a relation between compensation and stroke-related motor function. Thus, the findings from this dissertation are likely important for developing rehabilitation that reduces long term motor dysfunction after stroke.

5.2 Future studies

There is considerable potential for future investigation of how compensation is related to motor function and brain activation during lower limb pedaling and what elements cause this behavior to persist chronically. Some of these possibilities are discussed below.

Chapter 2 demonstrated that impairments in interlimb coordination may contribute to compensation. However, there was also evidence that motor impairments in the paretic limb are also relevant for compensation during pedaling. A regression analysis suggests that interlimb coordination is a more important contributing element, but the relative contribution of each element could be further explored. To help identify the relative contribution of each element, a training study could be performed. Stroke survivors could perform training with either unilateral or bilateral uncoupled pedaling. I would expect that unilateral pedaling training would preferentially address motor impairments in the paretic limb, while bilateral uncoupled training would preferentially address impairments in interlimb coordination. If motor impairments in the paretic limb contribute to compensation, then unilateral pedaling training should lead to a reduction in compensation. Conversely, if impaired interlimb coordination contributes to

compensation, then bilateral uncoupled pedaling training should lead to a reduction in compensation.

Chapter 3 identified some changes in interlimb reflex pathways that were related to impaired interlimb coordination and compensation. Because of the latency of the evoked responses, it is unclear whether these alterations in interlimb reflexes have a spinal or supraspinal path. It is important to identify the pathway involved to provide a potential target for rehabilitation. Therefore, we could evaluate the specific reflex pathway by using TMS or TES to condition interlimb cutaneous reflexes during pedaling after stroke. Supraspinal stimulation would be applied at multiple latencies following the application of cutaneous stimulation. MEPs would be evoked with TMS by applying electrical stimulation over the motor area of one cortical hemisphere or with TES by applying electrical stimulation at the level of the mastoid processes. It is thought that TMS activates pyramidal neurons indirectly, while TES directly stimulates pyramidal neurons. Consequently, the comparison of responses to these two types of stimulation provides insight into the involvement of the cortex. I would hypothesize that if cutaneous interlimb reflexes follow a supraspinal pathway, responses to stimulation would be enhanced with supraspinal stimulation at short latencies. Such a finding would suggest that supraspinal and cutaneous stimulation converge at a supraspinal level. In contrast, if cutaneous interlimb reflexes follow a spinal pathway, responses to stimulation would be enhanced with supraspinal stimulation at longer latencies. This would be suggestive of convergence at the motoneuronal or pre-motoneuronal level. The comparison of responses to TMS and TES could provide insight into whether a supraspinal pathway involves the motor cortex. One problem with the strategy of using TMS and TES to

evoke responses is that interlimb cutaneous reflexes likely involve both spinal and supraspinal pathways at different latencies. Shorter latency reflexes could alter motoneuronal excitability, complicating the interpretation of reflex responses conditioned with TMS or TES.

An alternative approach would be to use subthreshold TMS to test whether supraspinal input modulates the strength of spinal pathways for interlimb cutaneous reflexes. Subthreshold stimulation is thought to produce intracortical inhibition, which can block motor output from the cortex. Although the precise effects of subthreshold TMS are unclear, it might alter descending modulation of spinal pathways. Therefore, subthreshold TMS could be applied following the application of cutaneous stimulation at latencies that would modulate the path of spinal pathways. I would hypothesize that if cutaneous interlimb reflexes follow a spinal pathway that is modulated by descending input, responses to stimulation would be altered when subthreshold TMS is applied at an appropriate latency.

Although Chapter 3 highlights some changes in interlimb sensory reflex pathways, these pathways were generally well conserved in the stroke group. Future studies could evaluate other pathways that might be involved in interlimb coordination impairments after stroke. Specifically, we could investigate whether altered ipsilateral projections from supraspinal areas might contribute to impaired interlimb coordination after stroke. Ipsilateral descending supraspinal projections may be enhanced after stroke to help restore function in the paretic limb (Jankowska & Edgley, 2006). After stroke, there is evidence that motor signals associated with activation of the non-paretic limb contribute to impaired interlimb coordination (Kautz & Patten, 2005; Rogers et al., 2011).

There are a few primary ways to test whether ipsilateral descending supraspinal pathways contribute to impaired interlimb coordination. First, we could elicit ipsilateral MEPs with TMS and TES during pedaling after stroke. TMS and TES should evoke measurable responses in both limbs, but for the purpose of this question, the analysis would focus on the limb ipsilateral to the stimulated hemisphere. Based on previous findings, I would hypothesize that if abnormal ipsilateral supraspinal projections contribute to impaired interlimb coordination after stroke, then altered responses to stimulation would be correlated with worse interlimb coordination. Comparison of the responses to TES and TMS would provide insight into whether the cortex is involved in impaired interlimb coordination after stroke. As mentioned above, similar information could be obtained through the application of subthreshold TMS. Using this paradigm, I would hypothesize that changes in the background EMG evoked by subthreshold TMS would be correlated with worse interlimb coordination.

One problem with the strategy of using TMS and TES to evoke responses is that the portion of the motor cortex with the greatest leg representation is located medially. Consequently, because of spatial limitations, TMS and TES stimulate neurons in both hemispheres going to both limbs. MEPs measured in one limb would reflect both ipsilateral and contralateral descending signals. Responses would only partly represent the phenomenon of interest. This problem is also relevant for the proposed studies to test whether interlimb cutaneous reflexes have a supraspinal pathway. One strategy to address this issue was used by Madhavan et al. (2010). Instead of merely evaluating MEP amplitude, they evaluated the ratio of evoked ipsilateral to contralateral responses.

Essentially, this is a method for measuring the ipsilateral response, while accounting for a concurrent contralateral response.

In Chapter 4, we found that it is unlikely that altered volitional motor commands and pedaling performance account for reduced pedaling-related brain activation after stroke. However, there are potential issues with the use of passive pedaling as a paradigm to answer this question because the task has no motor component. Other methods could be used to more directly test the relation between compensation and brain activation. Subjects could perform bilateral uncoupled pedaling while brain activation is measured during fMRI. Bilateral uncoupled pedaling provides a method to manipulate compensation while also maintaining much of the sensorimotor components of conventional pedaling. I would hypothesize that if compensation explains reduced pedaling-related brain activation post-stroke, then between-group differences would be reduced during bilateral uncoupled as compared to conventional pedaling. I would also predict that brain activation during bilateral uncoupled as compared to conventional pedaling would be increased in the stroke group, but similar in the control group. I tested this strategy in a small pilot study detailed in Appendix D.

Alternatively, the degree of compensation (mechanical work asymmetry) could be manipulated during pedaling via volition or via manipulation of the pedaling device. Brain activation would be measured during fMRI. Asymmetries in mechanical work could be elicited in controls and improved symmetry could be elicited in the stroke group. I would hypothesize that if compensation explains reduced pedaling-related brain activation post-stroke, then between-group differences would be reduced when mechanical work symmetry is similar between groups. Brain activation would increase

when stroke survivors pedaled more symmetrically and decrease when control subjects pedaled more asymmetrically. I tested strategies to manipulate the mechanical work symmetry outside of the fMRI scanner, as detailed in Appendix E.

Finally, subjects could perform unilateral pedaling while brain activation is measured during fMRI. Unilateral pedaling could be performed to simulate the more unilateral pedaling style employed by stroke survivors exhibiting compensation. I would hypothesize that if compensation explains reduced pedaling-related brain activation post-stroke, then between-group differences would be reduced during unilateral as compared to conventional pedaling. I would also predict that brain activation during unilateral as compared to conventional pedaling would be similar in the stroke group, but lower in the control group. This hypothesis is supported by findings from Arand (2013), which demonstrated a trend for reduced brain activation in M1S1 during unilateral as compared to conventional pedaling. However, brain activation measurements during unilateral pedaling in stroke survivors would need to be obtained to fully test the hypothesis.

5.3 Implications for lower limb rehabilitation

The results from this dissertation have implications for lower limb rehabilitation after stroke. Compensation may contribute to long-term motor dysfunction after stroke; results from Chapter 2 and Chapter 3 demonstrate a relation between compensation and stroke-related sensorimotor function, as measured by the Fugl Meyer Assessment of the lower extremity. We found evidence that interlimb coordination may contribute to the chronic persistence of compensation. Interlimb sensory reflexes may reflect impairments in the supraspinal and/or spinal control of interlimb coordination. Additionally, although

it is unlikely that compensation acutely accounts for altered pedaling-related brain activation after stroke, compensation may elicit long-term neuroplastic effects that cause a fundamental change in how the brain is activated during movement. Thus, the results from this dissertation provide several potential intervention points that could be exploited with rehabilitation efforts.

First, rehabilitative interventions could aim to prevent compensation, increasing use of the paretic limb. In Chapter 2, we found that preventing compensation during unilateral and bilateral uncoupled pedaling caused muscle activation to increase in the paretic limb. Thus, this strategy can facilitate the use of unused paretic motor ability. In the upper limb, the prevention of compensation is one of the hallmark characteristics of constraint-induced movement therapy (CIMT). This therapy has been successful at improving motor performance and increasing spontaneous use of the paretic upper limb (Miltner et al., 1999; Taub et al., 1993; Wolf et al., 1989). There have been similar efforts to prevent compensation during movements of the lower limb. Splinting and unilateral step training have improved paretic limb use (Kahn & Hornby, 2009; Numata et al., 2008). Treadmill walking with mediolateral corrective forces to the pelvis (to enhance paretic limb loading) leads to increased paretic muscle activity (C. J. Hsu, Kim, Roth, Rymer, & Wu, 2017). Another strategy has been to use shoe wedge inserts to enhance loading and use of the paretic limb. Several studies have found that training with this approach improves paretic limb weight bearing, mobility, gait symmetry, and gait velocity (Aruin, Rao, Sharma, & Chaudhuri, 2012; Yu et al., 2015).

As apparent from these previous strategies, efforts to prevent compensation have been both unilateral and bilateral. It is unclear whether unilateral or bilateral movements

would be more effective at improving paretic motor function. In the upper limb, bilateral movements are more successful at improving the kinematics of reaching than unilateral movements (Mudie & Matyas, 2000). Bilateral training might be more effective because it enhances activation of the paretic limb through ipsilateral and contralateral pathways. Additionally, bilateral movements would be the most functionally relevant if rehabilitation aims to improve locomotion. However, some investigators have found no additional benefit of bilateral over unilateral training (Lewis & Byblow, 2004).

Although there is evidence that preventing compensation can reduce lower limb motor dysfunction in chronic stroke, this strategy may not address the elements that contributed to compensation. Namely, as suggested in this dissertation, impaired interlimb coordination might result in compensation as a strategy to prevent deficits in motor performance. Consistent with this explanation, Chapter 2 demonstrates that pedaling performance declines when compensation is prevented. Thus, rehabilitative strategies that attempt to modulate interlimb coordination might be more successful at reducing lower limb motor dysfunction. One such strategy that has been explored is split-belt treadmill walking. When neurologically intact humans walk on a split-belt treadmill (the belt under each limb moves at a different velocity), coordination between limbs is adaptable (Dietz et al., 1994; Reisman et al., 2005). This finding raises the possibility that split-belt treadmill walking could be used to improve interlimb coordination in patient populations and indirectly reduce compensation. Studies using this technique in stroke survivors have found that walking on a split-belt treadmill can increase plantarflexor force in the paretic limb, decrease plantarflexor force in the non-paretic limb, and improve symmetry of stance time (Lauzière et al., 2014; Reisman, McLean, Keller,

Danks, & Bastian, 2013; Reisman, Wityk, Silver, & Bastian, 2007). The effects of split-belt treadmill walking may also be achieved through other interventions such as acoustic pacing and foot positioning guidance (Finley, Long, Bastian, & Torres-Oviedo, 2015; Roerdink et al., 2007). Similar to findings during walking, altering the relative pedal position can elicit adaptation in the phasing of muscle activity in stroke survivors (Alibiglou & Brown, 2011). However, it is unclear whether these interventions can transfer between tasks and/or elicit long-term changes in gait. For example, effects from split-belt treadmill walking can transfer to overground walking but are only marginally maintained over long term evaluation (Reisman et al., 2013; Reisman, Wityk, Silver, & Bastian, 2009).

As detailed in Chapter 3, alterations in interlimb cutaneous reflexes may contribute to impairments in interlimb coordination and reflect alterations in the supraspinal and/or spinal control of interlimb coordination through other pathways. Efforts to restore more typical control of interlimb reflexes could provide an alternative method for improving lower limb motor function. One potential way to restore more typical interlimb reflex responses in the lower limb after stroke is to exploit the influence of the upper limb on the lower limb. E.P Zehr and colleagues have conducted an expansive analysis of how motor behavior in the lower limb is affected by movements of the upper limb. Cutaneous stimulation of the upper and lower limb elicits descending and ascending interlimb reflexes, which are phase modulated during walking (Haridas & Zehr, 2003; Zehr, Collins, & Chua, 2001; Zehr & Haridas, 2003; Zehr & Loadman, 2012). Quadrupedal influences, particularly during locomotion, are likely achieved through long propriospinal pathways and evolutionarily conserved (Zehr et al., 2016).

The degree of phase modulation of cutaneous reflexes during pedaling with the lower limb is enhanced when the upper limb also performs rhythmic pedaling (Balter & Zehr, 2007). In other words, movement of the upper limb may affect the reflex excitability and modulation pattern in the lower limb. The interrelation between the upper limb and lower limb has been exploited to suppress hyperactive reflex responses. Rhythmic arm cycling suppresses H-reflex and stretch amplitude in the paretic and non-paretic soleus (Barzi & Zehr, 2008; Mezzarane et al., 2014). This raises the possibility that simultaneous arm and leg pedaling could be used to modulate abnormal cutaneous reflexes after stroke and potentially improve motor function. Although, cyclical flexion and extension simultaneously performed by the upper and lower limb acutely impairs motor performance, long term interventions have been more successful (Garry, van Steenis, & Summers, 2005; Lewis & Byblow, 2004). Klarner and colleagues (2016a, 2016b) found that five weeks of combined arm and leg cycling leads to neuroplastic changes in the amplitude of cutaneous and stretch reflexes, increases paretic muscle activity, and improves walking ability. Overall, this is a promising strategy that could be beneficial for stroke rehabilitation.

In Chapter 4, we found that it is unlikely that motor compensation during pedaling accounts for reduced brain activation after stroke. Instead, brain activation changes may be related to neuroplastic changes such as loss of brain structural connectivity, exaggerated cortical inhibition, increased reliance on spinal and brainstem pathways for rhythmic leg movement, or poor sensorimotor integration. Tools that elicit adaptive neuroplasticity may be beneficial in reversing these changes. Anodal transcranial direct current stimulation (tDCS) and repetitive TMS (rTMS) are two tools that have been used

to modulate cortical excitability for a period of time after stimulation (Di Pino et al., 2014). These noninvasive brain stimulation techniques have been used to correct imbalanced hemispheric excitability and/or to prime neural circuitry before lower limb motor training. When applied in stroke survivors as the sole intervention, tDCS and rTMS improve walking velocity and lower extremity motor function (Chang, Kim, & Park, 2015; Chieffo et al., 2014; Rastgoo et al., 2016). When paired with treadmill-based locomotor training, rTMS improves walking velocity (Kakuda et al., 2013). Similarly, tDCS enhances control of ankle tracking movements and walking improvements from robotic-assisted gait training (Madhavan, Weber, & Stinear, 2011; Seo et al., 2017). Thus, noninvasive brain stimulation techniques may aid stroke rehabilitation by addressing imbalances in cortical excitability or by enhancing the effects of motor training. However, these techniques are still relatively new, and more information about stimulation parameters and effects is needed to ensure optimal application.

Most of the rehabilitative efforts discussed have focused on preventing compensation, improving interlimb coordination, or modulating reflex amplitude in isolation. A strategy that combines aspects of each of these approaches might provide the greatest benefit. Accordingly, our research lab has initiated a clinical trial that combines several of these strategies to improve motor function after stroke. We have designed a mechanically decoupled bike with motors attached to each crank arm. Subjects will train on this bike, and compensation will be prevented with bilateral uncoupled pedaling. During training, the motorized system will provide external torque to aid in the maintenance of an antiphase relation between the pedals. Over time, as interlimb coordination improves, the amount of assistance needed to maintain an antiphase relation

between the pedals will decrease. Overall, this rehabilitative approach aims to enhance muscle activation in the paretic limb by preventing compensation while also addressing one of the potential causes of compensation—impaired interlimb coordination. We plan to explore the effect of this intervention on brain activation and interlimb sensory reflex pathways. In the future, we could add simultaneous upper limb pedaling to aid in the elicitation of neuroplastic changes in interlimb cutaneous reflexes or use noninvasive brain stimulation to prime the brain before training and/or address interhemispheric imbalances.

This dissertation described how compensation is related to motor function and brain activation during lower limb pedaling and identified impaired interlimb coordination as one element that may cause this behavior to persist chronically. By achieving this purpose, this work has identified rehabilitative targets and improved our understanding of long-term locomotor dysfunction after stroke. Hopefully the implementation of a combination of rehabilitative approaches that address the targets identified in this dissertation will lead to improved locomotor function after stroke.

BIBLIOGRAPHY

Alary, F., Doyon, B., Loubinoux, I., Carel, C., Boulanouar, K., Ranjeva, J. P., . . . Chollet, F. (1998). Event-related potentials elicited by passive movements in humans: characterization, source analysis, and comparison to fMRI. *Neuroimage, 8*(4), 377-390. doi:10.1006/nimg.1998.0377

Alaverdashvili, M., Foroud, A., Lim, D. H., & Whishaw, I. Q. (2008). "Learned baduse" limits recovery of skilled reaching for food after forelimb motor cortex stroke in rats: a new analysis of the effect of gestures on success. *Behav Brain Res, 188*(2), 281-290. doi:10.1016/j.bbr.2007.11.007

Alibiglou, L., & Brown, D. A. (2011). Relative temporal leading or following position of the contralateral limb generates different aftereffects in muscle phasing following adaptation training post-stroke. *Exp Brain Res, 211*(1), 37-50. doi:10.1007/s00221-011-2644-9

Alibiglou, L., López-Ortiz, C., Walter, C. B., & Brown, D. A. (2009). Bilateral limb phase relationship and its potential to alter muscle activity phasing during locomotion. *J Neurophysiol, 102*(5), 2856-2865. doi:10.1152/jn.00211.2009

Allen, J. L., Kautz, S. A., & Neptune, R. R. (2011). Step length asymmetry is representative of compensatory mechanisms used in post-stroke hemiparetic walking. *Gait Posture, 33*(4), 538-543. doi:10.1016/j.gaitpost.2011.01.004

Allen, J. L., Kautz, S. A., & Neptune, R. R. (2013). The influence of merged muscle excitation modules on post-stroke hemiparetic walking performance. *Clin Biomech (Bristol, Avon), 28*(6), 697-704. doi:10.1016/j.clinbiomech.2013.06.003

Allen, J. L., Kautz, S. A., & Neptune, R. R. (2014). Forward propulsion asymmetry is indicative of changes in plantarflexor coordination during walking in individuals with post-stroke hemiparesis. *Clin Biomech (Bristol, Avon), 29*(7), 780-786. doi:10.1016/j.clinbiomech.2014.06.001

Allred, R. P., & Jones, T. A. (2008). Maladaptive effects of learning with the less-affected forelimb after focal cortical infarcts in rats. *Exp Neurol, 210*(1), 172-181. doi:10.1016/j.expneurol.2007.10.010

Allred, R. P., Maldonado, M. A., Hsu And, J. E., & Jones, T. A. (2005). Training the "less-affected" forelimb after unilateral cortical infarcts interferes with functional

recovery of the impaired forelimb in rats. *Restor Neurol Neurosci, 23*(5-6), 297-302.

Ambrosini, E., Ferrante, S., Ferrigno, G., Molteni, F., & Pedrocchi, A. (2012). Cycling induced by electrical stimulation improves muscle activation and symmetry during pedaling in hemiparetic patients. *IEEE Trans Neural Syst Rehabil Eng, 20*(3), 320-330. doi:10.1109/TNSRE.2012.2191574

Arand, B. (2013). *Supraspinal control of unilateral locomotor performance : an FMRI study using a custom pedaling device (Unpublished master's thesis).* (Master's Thesis), Marquette University, Milwaukee, WI. Retrieved from http://epublications.marquette.edu/theses_open/223

Arasaki, K., Igarashi, O., Ichikawa, Y., Machida, T., Shirozu, I., Hyodo, A., & Ushijima, R. (2006). Reduction in the motor unit number estimate (MUNE) after cerebral infarction. *J Neurol Sci, 250*(1-2), 27-32. doi:10.1016/j.jns.2006.06.024

Aruin, A. S., Rao, N., Sharma, A., & Chaudhuri, G. (2012). Compelled body weight shift approach in rehabilitation of individuals with chronic stroke. *Top Stroke Rehabil, 19*(6), 556-563. doi:10.1310/tsr1906-556

Balter, J. E., & Zehr, E. P. (2007). Neural coupling between the arms and legs during rhythmic locomotor-like cycling movement. *J Neurophysiol, 97*(2), 1809-1818. doi:10.1152/jn.01038.2006

Baron, J. C., Cohen, L. G., Cramer, S. C., Dobkin, B. H., Johansen-Berg, H., Loubinoux, I., . . . Recovery, F. I. W. o. N. a. S. (2004). Neuroimaging in stroke recovery: a position paper from the First International Workshop on Neuroimaging and Stroke Recovery. *Cerebrovasc Dis, 18*(3), 260-267.

Barzi, Y., & Zehr, E. P. (2008). Rhythmic arm cycling suppresses hyperactive soleus H-reflex amplitude after stroke. *Clin Neurophysiol, 119*(6), 1443-1452. doi:10.1016/j.clinph.2008.02.016

Benjamin, E. J., Blaha, M. J., Chiuve, S. E., Cushman, M., Das, S. R., Deo, R., . . . Subcommittee, A. H. A. S. C. a. S. S. (2017). Heart Disease and Stroke Statistics-2017 Update: A Report From the American Heart Association. *Circulation, 135*(10), e146-e603. doi:10.1161/CIR.0000000000000485

Berger, W., Dietz, V., & Quintern, J. (1984). Corrective reactions to stumbling in man: neuronal co-ordination of bilateral leg muscle activity during gait. *J Physiol, 357*, 109-125.

Biernaskie, J., & Corbett, D. (2001). Enriched rehabilitative training promotes improved forelimb motor function and enhanced dendritic growth after focal ischemic injury. *J Neurosci, 21*(14), 5272-5280.

Blatow, M., Reinhardt, J., Riffel, K., Nennig, E., Wengenroth, M., & Stippich, C. (2011). Clinical functional MRI of sensorimotor cortex using passive motor and sensory stimulation at 3 Tesla. *J Magn Reson Imaging, 34*(2), 429-437. doi:10.1002/jmri.22629

Bohannon, R. W., & Andrews, A. W. (1995). Limb muscle strength is impaired bilaterally after stroke. *Journal of Physical Therapy Science, 7*, 7.

Bohannon, R. W., & Larkin, P. A. (1985). Lower extremity weight bearing under various standing conditions in independently ambulatory patients with hemiparesis. *Phys Ther, 65*(9), 1323-1325.

Bonita, R., & Beaglehole, R. (1988). Recovery of motor function after stroke. *Stroke, 19*(12), 1497-1500.

Boscolo Galazzo, I., Storti, S. F., Formaggio, E., Pizzini, F. B., Fiaschi, A., Beltramello, A., . . . Manganotti, P. (2014). Investigation of brain hemodynamic changes induced by active and passive movements: a combined arterial spin labeling-BOLD fMRI study. *J Magn Reson Imaging, 40*(4), 937-948. doi:10.1002/jmri.24432

Bosnell, R. A., Kincses, T., Stagg, C. J., Tomassini, V., Kischka, U., Jbabdi, S., . . . Johansen-Berg, H. (2011). Motor practice promotes increased activity in brain regions structurally disconnected after subcortical stroke. *Neurorehabil Neural Repair, 25*(7), 607-616. doi:10.1177/1545968311405675

Bowden, M. G., Balasubramanian, C. K., Neptune, R. R., & Kautz, S. A. (2006). Anterior-posterior ground reaction forces as a measure of paretic leg contribution in hemiparetic walking. *Stroke, 37*(3), 872-876. doi:10.1161/01.STR.0000204063.75779.8d

Brandstater, M. E., de Bruin, H., Gowland, C., & Clark, B. M. (1983). Hemiplegic gait: analysis of temporal variables. *Arch Phys Med Rehabil, 64*(12), 583-587.

Briere, A., Lauziere, S., Gravel, D., & Nadeau, S. (2010). Perception of weight-bearing distribution during sit-to-stand tasks in hemiparetic and healthy individuals. *Stroke, 41*(8), 1704-1708. doi:10.1161/STROKEAHA.110.589473

Brooke, J. D., Cheng, J., Collins, D. F., McIlroy, W. E., Misiaszek, J. E., & Staines, W. R. (1997). Sensori-sensory afferent conditioning with leg movement: gain control in spinal reflex and ascending paths. *Prog Neurobiol, 51*(4), 393-421.

Brooke, J. D., McIlroy, W. E., & Collins, D. F. (1992). Movement features and H-reflex modulation. I. Pedalling versus matched controls. *Brain Res, 582*(1), 78-84.

Brooke, J. D., McIlroy, W. E., Staines, W. R., Angerilli, P. A., & Peritore, G. F. (1999). Cutaneous reflexes of the human leg during passive movement. *J Physiol, 518 (Pt 2)*, 619-628.

Brooke, J. D., Misiaszek, J. E., & Cheng, J. (1993). Locomotor-like rotation of either hip or knee inhibits soleus H reflexes in humans. *Somatosens Mot Res, 10*(4), 357-364.

Brown, D. A., & Kautz, S. A. (1998). Increased workload enhances force output during pedaling exercise in persons with poststroke hemiplegia. *Stroke, 29*(3), 598-606.

Brown, D. A., Kautz, S. A., & Dairaghi, C. A. (1997). Muscle activity adapts to anti-gravity posture during pedalling in persons with post-stroke hemiplegia. *Brain, 120 (Pt 5)*, 825-837.

Brown, D. A., & Kukulka, C. G. (1993). Human flexor reflex modulation during cycling. *J Neurophysiol, 69*(4), 1212-1224.

Burdett, R. G., Borello-France, D., Blatchly, C., & Potter, C. (1988). Gait comparison of subjects with hemiplegia walking unbraced, with ankle-foot orthosis, and with Air-Stirrup brace. *Phys Ther, 68*(8), 1197-1203.

Bury, S. D., & Jones, T. A. (2002). Unilateral sensorimotor cortex lesions in adult rats facilitate motor skill learning with the "unaffected" forelimb and training-induced dendritic structural plasticity in the motor cortex. *J Neurosci, 22*(19), 8597-8606.

Butt, S. J., Lebret, J. M., & Kiehn, O. (2002). Organization of left-right coordination in the mammalian locomotor network. *Brain Res Brain Res Rev, 40*(1-3), 107-117.

Byrnes, M. L., Thickbroom, G. W., Phillips, B. A., Wilson, S. A., & Mastaglia, F. L. (1999). Physiological studies of the corticomotor projection to the hand after subcortical stroke. *Clin Neurophysiol, 110*(3), 487-498.

Calancie, B. (1991). Interlimb reflexes following cervical spinal cord injury in man. *Exp Brain Res, 85*(2), 458-469.

Calautti, C., & Baron, J. C. (2003). Functional neuroimaging studies of motor recovery after stroke in adults: a review. *Stroke, 34*(6), 1553-1566. doi:10.1161/01.STR.0000071761.36075.A6

Calautti, C., Leroy, F., Guincestre, J. Y., & Baron, J. C. (2001). Dynamics of motor network overactivation after striatocapsular stroke: a longitudinal PET study using a fixed-performance paradigm. *Stroke, 32*(11), 2534-2542.

Calautti, C., Leroy, F., Guincestre, J. Y., Marié, R. M., & Baron, J. C. (2001). Sequential activation brain mapping after subcortical stroke: changes in hemispheric balance and recovery. *Neuroreport, 12*(18), 3883-3886.

Cao, Y., D'Olhaberriague, L., Vikingstad, E. M., Levine, S. R., & Welch, K. M. (1998). Pilot study of functional MRI to assess cerebral activation of motor function after poststroke hemiparesis. *Stroke, 29*(1), 112-122.

Carey, L. M., Abbott, D. F., Egan, G. F., Bernhardt, J., & Donnan, G. A. (2005). Motor impairment and recovery in the upper limb after stroke: behavioral and neuroanatomical correlates. *Stroke, 36*(3), 625-629. doi:10.1161/01.STR.0000155720.47711.83

Carmichael, S. T., Wei, L., Rovainen, C. M., & Woolsey, T. A. (2001). New patterns of intracortical projections after focal cortical stroke. *Neurobiol Dis, 8*(5), 910-922. doi:10.1006/nbdi.2001.0425

Carson, R. G. (2005). Neural pathways mediating bilateral interactions between the upper limbs. *Brain Res Brain Res Rev, 49*(3), 641-662. doi:10.1016/j.brainresrev.2005.03.005

Carter, A. R., Astafiev, S. V., Lang, C. E., Connor, L. T., Rengachary, J., Strube, M. J., . . . Corbetta, M. (2010). Resting interhemispheric functional magnetic resonance imaging connectivity predicts performance after stroke. *Ann Neurol, 67*(3), 365-375. doi:10.1002/ana.21905

Carter, A. R., Patel, K. R., Astafiev, S. V., Snyder, A. Z., Rengachary, J., Strube, M. J., . . . Corbetta, M. (2012). Upstream dysfunction of somatomotor functional connectivity after corticospinal damage in stroke. *Neurorehabil Neural Repair, 26*(1), 7-19. doi:10.1177/1545968311411054

Castro, A. J. (1977). Limb preference after lesions of the cerebral hemisphere in adult and neonatal rats. *Physiol Behav, 18*(4), 605-608.

Chang, M. C., Kim, D. Y., & Park, D. H. (2015). Enhancement of Cortical Excitability and Lower Limb Motor Function in Patients With Stroke by Transcranial Direct Current Stimulation. *Brain Stimul, 8*(3), 561-566. doi:10.1016/j.brs.2015.01.411

Chen, G., & Patten, C. (2008). Joint moment work during the stance-to-swing transition in hemiparetic subjects. *J Biomech, 41*(4), 877-883. doi:10.1016/j.jbiomech.2007.10.017

Chen, G., Patten, C., Kothari, D. H., & Zajac, F. E. (2005). Gait differences between individuals with post-stroke hemiparesis and non-disabled controls at matched speeds. *Gait Posture, 22*(1), 51-56. doi:10.1016/j.gaitpost.2004.06.009

Chen, H. Y., Chen, S. C., Chen, J. J., Fu, L. L., & Wang, Y. L. (2005). Kinesiological and kinematical analysis for stroke subjects with asymmetrical cycling movement patterns. *J Electromyogr Kinesiol, 15*(6), 587-595. doi:10.1016/j.jelekin.2005.06.001

Chieffo, R., De Prezzo, S., Houdayer, E., Nuara, A., Di Maggio, G., Coppi, E., . . . Leocani, L. (2014). Deep repetitive transcranial magnetic stimulation with H-coil on lower limb motor function in chronic stroke: a pilot study. *Arch Phys Med Rehabil, 95*(6), 1141-1147. doi:10.1016/j.apmr.2014.02.019

Chollet, F., DiPiero, V., Wise, R. J., Brooks, D. J., Dolan, R. J., & Frackowiak, R. S. (1991). The functional anatomy of motor recovery after stroke in humans: a study with positron emission tomography. *Ann Neurol, 29*(1), 63-71. doi:10.1002/ana.410290112

Chou, L. W., Palmer, J. A., Binder-Macleod, S., & Knight, C. A. (2013). Motor unit rate coding is severely impaired during forceful and fast muscular contractions in individuals post stroke. *J Neurophysiol, 109*(12), 2947-2954. doi:10.1152/jn.00615.2012

Christensen, L. O., Johannsen, P., Sinkjaer, T., Petersen, N., Pyndt, H. S., & Nielsen, J. B. (2000). Cerebral activation during bicycle movements in man. *Exp Brain Res, 135*(1), 66-72.

Christensen, L. O., Morita, H., Petersen, N., & Nielsen, J. (1999). Evidence suggesting that a transcortical reflex pathway contributes to cutaneous reflexes in the tibialis anterior muscle during walking in man. *Exp Brain Res, 124*(1), 59-68.

Cirstea, M. C., & Levin, M. F. (2000). Compensatory strategies for reaching in stroke. *Brain, 123 (Pt 5)*, 940-953.

Clark, D. J., Neptune, R. R., Behrman, A. L., & Kautz, S. A. (2016). Locomotor Adaptability Task Promotes Intense and Task-Appropriate Output From the Paretic Leg During Walking. *Arch Phys Med Rehabil, 97*(3), 493-496. doi:10.1016/j.apmr.2015.10.081

Clark, D. J., Ting, L. H., Zajac, F. E., Neptune, R. R., & Kautz, S. A. (2010). Merging of healthy motor modules predicts reduced locomotor performance and muscle coordination complexity post-stroke. *J Neurophysiol, 103*(2), 844-857. doi:10.1152/jn.00825.2009

Cleland, B., Gelting, T., Arand, B., Struhar, J., & Schindler-Ivens, S. (2016). Split-crank pedaling reveals residual lower limb motor capacity after stroke. In: Society for Neuroscience National Meeting. San Diego, CA.

Cleland, B., & Schindler-Ivens, S. (2015). Reduced pedaling related brain activation volume post-stroke does not depend on task performance. In: Society for Neuroscience National Meeting. Chicago, IL.

Coxon, J. P., Stinear, C. M., & Byblow, W. D. (2006). Intracortical inhibition during volitional inhibition of prepared action. *J Neurophysiol, 95*(6), 3371-3383. doi:10.1152/jn.01334.2005

Cramer, S. C., Nelles, G., Benson, R. R., Kaplan, J. D., Parker, R. A., Kwong, K. K., . . . Rosen, B. R. (1997). A functional MRI study of subjects recovered from hemiparetic stroke. *Stroke, 28*(12), 2518-2527.

Crone, C., Johnsen, L. L., Biering-Sørensen, F., & Nielsen, J. B. (2003). Appearance of reciprocal facilitation of ankle extensors from ankle flexors in patients with stroke or spinal cord injury. *Brain, 126*(Pt 2), 495-507.

Cruz, E. G., Waldinger, H. C., & Kamper, D. G. (2005). Kinetic and kinematic workspaces of the index finger following stroke. *Brain, 128*(Pt 5), 1112-1121. doi:10.1093/brain/awh432

Dancause, N., Barbay, S., Frost, S. B., Plautz, E. J., Chen, D., Zoubina, E. V., . . . Nudo, R. J. (2005). Extensive cortical rewiring after brain injury. *J Neurosci, 25*(44), 10167-10179. doi:10.1523/JNEUROSCI.3256-05.2005

De Marchis, C., Ambrosini, E., Schmid, M., Monticone, M., Pedrocchi, A., Ferrigno, G., . . . Ferrante, S. (2015). Neuro-mechanics of muscle coordination during recumbent pedaling in post-acute stroke patients. *Conf Proc IEEE Eng Med Biol Soc, 2015*, 246-249. doi:10.1109/EMBC.2015.7318346

Delwaide, P. J., & Crenna, P. (1984). Cutaneous nerve stimulation and motoneuronal excitability. II: Evidence for non-segmental influences. *J Neurol Neurosurg Psychiatry, 47*(2), 190-196.

Den Otter, A. R., Geurts, A. C., Mulder, T., & Duysens, J. (2006). Gait recovery is not associated with changes in the temporal patterning of muscle activity during treadmill walking in patients with post-stroke hemiparesis. *Clin Neurophysiol, 117*(1), 4-15. doi:10.1016/j.clinph.2005.08.014

Den Otter, A. R., Geurts, A. C., Mulder, T., & Duysens, J. (2007). Abnormalities in the temporal patterning of lower extremity muscle activity in hemiparetic gait. *Gait Posture, 25*(3), 342-352. doi:10.1016/j.gaitpost.2006.04.007

Desrosiers, J., Malouin, F., Bourbonnais, D., Richards, C. L., Rochette, A., & Bravo, G. (2003). Arm and leg impairments and disabilities after stroke rehabilitation: relation to handicap. *Clin Rehabil, 17*(6), 666-673. doi:10.1191/0269215503cr662oa

DeYoe, E. A., Bandettini, P., Neitz, J., Miller, D., & Winans, P. (1994). Functional magnetic resonance imaging (FMRI) of the human brain. *J Neurosci Methods, 54*(2), 171-187.

Di Pino, G., Pellegrino, G., Assenza, G., Capone, F., Ferreri, F., Formica, D., . . . Di Lazzaro, V. (2014). Modulation of brain plasticity in stroke: a novel model for neurorehabilitation. *Nat Rev Neurol, 10*(10), 597-608. doi:10.1038/nrneurol.2014.162

Dickstein, R., Hocherman, S., Amdor, G., & Pillar, T. (1993). Reaction and movement times in patients with hemiparesis for unilateral and bilateral elbow flexion. *Phys Ther, 73*(6), 374-380; discussion 381-375.

Dietz, V. (2003). Spinal cord pattern generators for locomotion. *Clin Neurophysiol, 114*(8), 1379-1389.

Dietz, V., & Berger, W. (1984). Interlimb coordination of posture in patients with spastic paresis. Impaired function of spinal reflexes. *Brain, 107 (Pt 3)*, 965-978.

Dietz, V., Horstmann, G. A., & Berger, W. (1989). Interlimb coordination of leg-muscle activation during perturbation of stance in humans. *J Neurophysiol, 62*(3), 680-693.

Dietz, V., Müller, R., & Colombo, G. (2002). Locomotor activity in spinal man: significance of afferent input from joint and load receptors. *Brain, 125*(Pt 12), 2626-2634.

Dietz, V., Quintern, J., Boos, G., & Berger, W. (1986). Obstruction of the swing phase during gait: phase-dependent bilateral leg muscle coordination. *Brain Res, 384*(1), 166-169.

Dietz, V., & Schrafl-Altermatt, M. (2016). Control of functional movements in healthy and post-stroke subjects: Role of neural interlimb coupling. *Clin Neurophysiol, 127*(5), 2286-2293. doi:10.1016/j.clinph.2016.02.014

Dietz, V., Zijlstra, W., & Duysens, J. (1994). Human neuronal interlimb coordination during split-belt locomotion. *Exp Brain Res, 101*(3), 513-520.

Dobkin, B. H., Firestine, A., West, M., Saremi, K., & Woods, R. (2004). Ankle dorsiflexion as an fMRI paradigm to assay motor control for walking during rehabilitation. *Neuroimage, 23*(1), 370-381. doi:10.1016/j.neuroimage.2004.06.008

Donelan, J. M., Kram, R., & Kuo, A. D. (2002). Mechanical work for step-to-step transitions is a major determinant of the metabolic cost of human walking. *J Exp Biol, 205*(Pt 23), 3717-3727.

Dong, Y., Winstein, C. J., Albistegui-DuBois, R., & Dobkin, B. H. (2007). Evolution of FMRI activation in the perilesional primary motor cortex and cerebellum with

rehabilitation training-related motor gains after stroke: a pilot study. *Neurorehabil Neural Repair, 21*(5), 412-428. doi:10.1177/1545968306298598

Duncan, P. W., Goldstein, L. B., Horner, R. D., Landsman, P. B., Samsa, G. P., & Matchar, D. B. (1994). Similar motor recovery of upper and lower extremities after stroke. *Stroke, 25*(6), 1181-1188.

Duysens, J. (1977). Reflex control of locomotion as revealed by stimulation of cutaneous afferents in spontaneously walking premammillary cats. *J Neurophysiol, 40*(4), 737-751. doi:10.1152/jn.1977.40.4.737

Duysens, J., & Loeb, G. E. (1980). Modulation of ipsi- and contralateral reflex responses in unrestrained walking cats. *J Neurophysiol, 44*(5), 1024-1037.

Duysens, J., Loeb, G. E., & Weston, B. J. (1980). Crossed flexor reflex responses and their reversal in freely walking cats. *Brain Res, 197*(2), 538-542.

Duysens, J., & Pearson, K. G. (1976). The role of cutaneous afferents from the distal hindlimb in the regulation of the step cycle of thalamic cats. *Exp Brain Res, 24*, 245-255.

Duysens, J., & Stein, R. B. (1978). Reflexes induced by nerve stimulation in walking cats with implanted cuff electrodes. *Exp Brain Res, 32*(2), 213-224.

Duysens, J., Tax, A. A., Trippel, M., & Dietz, V. (1992). Phase-dependent reversal of reflexly induced movements during human gait. *Exp Brain Res, 90*(2), 404-414.

Duysens, J., Tax, A. A., Trippel, M., & Dietz, V. (1993). Increased amplitude of cutaneous reflexes during human running as compared to standing. *Brain Res, 613*(2), 230-238.

Duysens, J., Tax, A. A., van der Doelen, B., Trippel, M., & Dietz, V. (1991). Selective activation of human soleus or gastrocnemius in reflex responses during walking and running. *Exp Brain Res, 87*(1), 193-204.

Duysens, J., Trippel, M., Horstmann, G. A., & Dietz, V. (1990). Gating and reversal of reflexes in ankle muscles during human walking. *Exp Brain Res, 82*(2), 351-358.

Eidelberg, E., Story, J. L., Meyer, B. L., & Nystel, J. (1980). Stepping by chronic spinal cats. *Exp Brain Res, 40*(3), 241-246.

Eng, J. J., Winter, D. A., & Patla, A. E. (1994). Strategies for recovery from a trip in early and late swing during human walking. *Exp Brain Res, 102*(2), 339-349.

English, C., McLennan, H., Thoirs, K., Coates, A., & Bernhardt, J. (2010). Loss of skeletal muscle mass after stroke: a systematic review. *Int J Stroke, 5*(5), 395-402. doi:10.1111/j.1747-4949.2010.00467.x

Enoka, R. M. (2008). *Neuromechanics of Human Movement* (4th ed.). Champaign, IL: Human Kinetics.

Enzinger, C., Dawes, H., Johansen-Berg, H., Wade, D., Bogdanovic, M., Collett, J., . . . Matthews, P. M. (2009). Brain activity changes associated with treadmill training after stroke. *Stroke, 40*(7), 2460-2467. doi:10.1161/STROKEAHA.109.550053

Enzinger, C., Johansen-Berg, H., Dawes, H., Bogdanovic, M., Collett, J., Guy, C., . . . Matthews, P. M. (2008). Functional MRI correlates of lower limb function in stroke victims with gait impairment. *Stroke, 39*(5), 1507-1513. doi:10.1161/STROKEAHA.107.501999

Feeney, D. M., & Baron, J. C. (1986). Diaschisis. *Stroke, 17*(5), 817-830.

Feys, H., Van Hees, J., Bruyninckx, F., Mercelis, R., & De Weerdt, W. (2000). Value of somatosensory and motor evoked potentials in predicting arm recovery after a stroke. *J Neurol Neurosurg Psychiatry, 68*(3), 323-331.

Finley, J. M., & Bastian, A. J. (2017). Associations Between Foot Placement Asymmetries and Metabolic Cost of Transport in Hemiparetic Gait. *Neurorehabil Neural Repair, 31*(2), 168-177. doi:10.1177/1545968316675428

Finley, J. M., Long, A., Bastian, A. J., & Torres-Oviedo, G. (2015). Spatial and Temporal Control Contribute to Step Length Asymmetry During Split-Belt Adaptation and Hemiparetic Gait. *Neurorehabil Neural Repair, 29*(8), 786-795. doi:10.1177/1545968314567149

Forssberg, H., & Grillner, S. (1973). The locomotion of the acute spinal cat injected with clonidine i.v. *Brain Res, 50*(1), 184-186.

Forssberg, H., Grillner, S., Halbertsma, J., & Rossignol, S. (1980). The locomotion of the low spinal cat. II. Interlimb coordination. *Acta Physiol Scand, 108*(3), 283-295. doi:10.1111/j.1748-1716.1980.tb06534.x

Forssberg, H., Grillner, S., & Rossignol, S. (1975). Phase dependent reflex reversal during walking in chronic spinal cats. *Brain Res, 85*(1), 103-107.

Forssberg, H., Grillner, S., & Rossignol, S. (1977). Phasic gain control of reflexes from the dorsum of the paw during spinal locomotion. *Brain Res, 132*(1), 121-139.

Fox, P. T., & Raichle, M. E. (1986). Focal physiological uncoupling of cerebral blood flow and oxidative metabolism during somatosensory stimulation in human subjects. *Proc Natl Acad Sci U S A, 83*, 1140-1144.

Friedman, D. B., Friberg, L., Mitchell, J. H., & Secher, N. H. (1991). Effect of axillary blockade on regional cerebral blood flow during static handgrip. *J Appl Physiol (1985), 71*(2), 651-656.

Friedman, D. B., Friberg, L., Payne, G., Mitchell, J. H., & Secher, N. H. (1992). Effects of axillary blockade on regional cerebral blood flow during dynamic hand contractions. *J Appl Physiol (1985), 73*(5), 2120-2125.

Friel, K. M., & Nudo, R. J. (1998). Recovery of motor function after focal cortical injury in primates: compensatory movement patterns used during rehabilitative training. *Somatosens Mot Res, 15*(3), 173-189.

Frontera, W. R., Grimby, L., & Larsson, L. (1997). Firing rate of the lower motoneuron and contractile properties of its muscle fibers after upper motoneuron lesion in man. *Muscle Nerve, 20*(8), 938-947.

Fuchs, D. P., Sanghvi, N., Wieser, J., & Schindler-Ivens, S. (2011). Pedaling alters the excitability and modulation of vastus medialis H-reflexes after stroke. *Clin Neurophysiol, 122*(10), 2036-2043. doi:10.1016/j.clinph.2011.03.010

Garry, M. I., van Steenis, R. E., & Summers, J. J. (2005). Interlimb coordination following stroke. *Hum Mov Sci, 24*(5-6), 849-864. doi:10.1016/j.humov.2005.10.005

Gauthier, L., & Rossignol, S. (1981). Contralateral hindlimb responses to cutaneous stimulation during locomotion in high decerebrate cats. *Brain Res, 207*(2), 303-320.

Gemperline, J. J., Allen, S., Walk, D., & Rymer, W. Z. (1995). Characteristics of motor unit discharge in subjects with hemiparesis. *Muscle Nerve, 18*(10), 1101-1114. doi:10.1002/mus.880181006

Geurts, A. C., de Haart, M., van Nes, I. J., & Duysens, J. (2005). A review of standing balance recovery from stroke. *Gait Posture, 22*(3), 267-281. doi:10.1016/j.gaitpost.2004.10.002

Gharbawie, O. A., & Whishaw, I. Q. (2006). Parallel stages of learning and recovery of skilled reaching after motor cortex stroke: "oppositions" organize normal and compensatory movements. *Behav Brain Res, 175*(2), 249-262. doi:10.1016/j.bbr.2006.08.039

Giuliani, C. A., & Smith, J. L. (1987). Stepping behaviors in chronic spinal cats with one hindlimb deafferented. *J Neurosci, 7*(8), 2537-2546.

Gracies, J. M. (2005). Pathophysiology of spastic paresis. I: Paresis and soft tissue changes. *Muscle Nerve, 31*(5), 535-551. doi:10.1002/mus.20284

Gray, V. L., Pollock, C. L., Wakeling, J. M., Ivanova, T. D., & Garland, S. J. (2015). Patterns of muscle coordination during stepping responses post-stroke. *J Electromyogr Kinesiol, 25*(6), 959-965. doi:10.1016/j.jelekin.2015.09.003

Grefkes, C., Eickhoff, S. B., Nowak, D. A., Dafotakis, M., & Fink, G. R. (2008). Dynamic intra- and interhemispheric interactions during unilateral and bilateral hand movements assessed with fMRI and DCM. *Neuroimage, 41*(4), 1382-1394. doi:10.1016/j.neuroimage.2008.03.048

Grefkes, C., Nowak, D. A., Eickhoff, S. B., Dafotakis, M., Küst, J., Karbe, H., & Fink, G. R. (2008). Cortical connectivity after subcortical stroke assessed with functional magnetic resonance imaging. *Ann Neurol, 63*(2), 236-246. doi:10.1002/ana.21228

Grey, M. J., Nielsen, J. B., Mazzaro, N., & Sinkjaer, T. (2007). Positive force feedback in human walking. *J Physiol, 581*(Pt 1), 99-105. doi:10.1113/jphysiol.2007.130088

Grillner, S., & Zangger, P. (1979). On the central generation of locomotion in the low spinal cat. *Exp Brain Res, 34*(2), 241-261.

Grillner, S., & Zangger, P. (1984). The effect of dorsal root transection on the efferent motor pattern in the cat's hindlimb during locomotion. *Acta Physiol Scand, 120*(3), 393-405. doi:10.1111/j.1748-1716.1984.tb07400.x

Guzzetta, A., Staudt, M., Petacchi, E., Ehlers, J., Erb, M., Wilke, M., . . . Cioni, G. (2007). Brain representation of active and passive hand movements in children. *Pediatr Res, 61*(4), 485-490. doi:10.1203/pdr.0b013e3180332c2e

Halbertsma, J. M. (1983). The stride cycle of the cat: the modelling of locomotion by computerized analysis of automatic recordings. *Acta Physiol Scand Suppl, 521*, 1-75.

Hall, A. L., Peterson, C. L., Kautz, S. A., & Neptune, R. R. (2011). Relationships between muscle contributions to walking subtasks and functional walking status in persons with post-stroke hemiparesis. *Clin Biomech (Bristol, Avon), 26*(5), 509-515. doi:10.1016/j.clinbiomech.2010.12.010

Hamzei, F., Dettmers, C., Rijntjes, M., & Weiller, C. (2008). The effect of cortico-spinal tract damage on primary sensorimotor cortex activation after rehabilitation therapy. *Exp Brain Res, 190*(3), 329-336. doi:10.1007/s00221-008-1474-x

Han, C. E., Kim, S., Chen, S., Lai, Y. H., Lee, J. Y., Osu, R., . . . Schweighofer, N. (2013). Quantifying arm nonuse in individuals poststroke. *Neurorehabil Neural Repair, 27*(5), 439-447. doi:10.1177/1545968312471904

Haridas, C., & Zehr, E. P. (2003). Coordinated interlimb compensatory responses to electrical stimulation of cutaneous nerves in the hand and foot during walking. *J Neurophysiol, 90*(5), 2850-2861. doi:10.1152/jn.00531.2003

Harris, M. L., Polkey, M. I., Bath, P. M., & Moxham, J. (2001). Quadriceps muscle weakness following acute hemiplegic stroke. *Clin Rehabil, 15*(3), 274-281.

Heeger, D. J., & Ress, D. (2002). What does fMRI tell us about neuronal activity? *Nat Rev Neurosci, 3*(2), 142-151. doi:10.1038/nrn730

Hendricks, H. T., van Limbeek, J., Geurts, A. C., & Zwarts, M. J. (2002). Motor recovery after stroke: a systematic review of the literature. *Arch Phys Med Rehabil, 83*(11), 1629-1637.

Hermens, H. J., Freriks, B., Disselhorst-Klug, C., & Rau, G. (2000). Development of recommendations for SEMG sensors and sensor placement procedures. *J Electromyogr Kinesiol, 10*(5), 361-374.

Hirschberg, G. G., & Nathanson, M. (1952). Electromyographic recording of muscular activity in normal and spastic gaits. *Arch Phys Med Rehabil, 33*(4), 217-225.

Hoffman, D. S., & Strick, P. L. (1995). Effects of a primary motor cortex lesion on step-tracking movements of the wrist. *J Neurophysiol, 73*(2), 891-895.

Hsiao, H., Awad, L. N., Palmer, J. A., Higginson, J. S., & Binder-Macleod, S. A. (2015). Contribution of Paretic and Nonparetic Limb Peak Propulsive Forces to Changes in Walking Speed in Individuals Poststroke. *Neurorehabil Neural Repair*. doi:10.1177/1545968315624780

Hsiao, H., Awad, L. N., Palmer, J. A., Higginson, J. S., & Binder-Macleod, S. A. (2016). Contribution of Paretic and Nonparetic Limb Peak Propulsive Forces to Changes in Walking Speed in Individuals Poststroke. *Neurorehabil Neural Repair, 30*(8), 743-752. doi:10.1177/1545968315624780

Hsu, A. L., Tang, P. F., & Jan, M. H. (2003). Analysis of impairments influencing gait velocity and asymmetry of hemiplegic patients after mild to moderate stroke. *Arch Phys Med Rehabil, 84*(8), 1185-1193.

Hsu, C. J., Kim, J., Roth, E. J., Rymer, W. Z., & Wu, M. (2017). Forced Use of the Paretic Leg Induced by a Constraint Force Applied to the Nonparetic Leg in Individuals Poststroke During Walking. *Neurorehabil Neural Repair, 31*(12), 1042-1052. doi:10.1177/1545968317740972

Huettel, S. A., Song, A. W., & McCarthy, G. (2009). *Functional magnetic resonance imaging* (2nd ed.). Sunderland, Mass.: Sinauer Associates.

Hyngstrom, A., Onushko, T., Chua, M., & Schmit, B. D. (2010). Abnormal volitional hip torque phasing and hip impairments in gait post stroke. *J Neurophysiol, 103*(3), 1557-1568. doi:10.1152/jn.00528.2009

Jain, S., Gourab, K., Schindler-Ivens, S., & Schmit, B. D. (2013). EEG during pedaling: evidence for cortical control of locomotor tasks. *Clin Neurophysiol, 124*(2), 379-390. doi:10.1016/j.clinph.2012.08.021

Jankowska, E., & Edgley, S. A. (2006). How can corticospinal tract neurons contribute to ipsilateral movements? A question with implications for recovery of motor functions. *Neuroscientist, 12*(1), 67-79. doi:10.1177/1073858405283392

Johansen-Berg, H., Dawes, H., Guy, C., Smith, S. M., Wade, D. T., & Matthews, P. M. (2002). Correlation between motor improvements and altered fMRI activity after rehabilitative therapy. *Brain, 125*(Pt 12), 2731-2742.

Johnson, M., Paranjape, R., Strachota, E., Tchekanov, G., & McGuire, J. (2011). Quantifying learned non-use after stroke using unilateral and bilateral steering tasks. *IEEE Int Conf Rehabil Robot, 2011*, 5975457. doi:10.1109/ICORR.2011.5975457

Jones, T. A., Kleim, J. A., & Greenough, W. T. (1996). Synaptogenesis and dendritic growth in the cortex opposite unilateral sensorimotor cortex damage in adult rats: a quantitative electron microscopic examination. *Brain Res, 733*(1), 142-148.

Jones, T. A., & Schallert, T. (1994). Use-dependent growth of pyramidal neurons after neocortical damage. *J Neurosci, 14*(4), 2140-2152.

Jonkers, I., Delp, S., & Patten, C. (2009). Capacity to increase walking speed is limited by impaired hip and ankle power generation in lower functioning persons post-stroke. *Gait Posture, 29*(1), 129-137. doi:10.1016/j.gaitpost.2008.07.010

Jørgensen, H. S., Nakayama, H., Raaschou, H. O., & Olsen, T. S. (1995). Recovery of walking function in stroke patients: the Copenhagen Stroke Study. *Arch Phys Med Rehabil, 76*(1), 27-32.

Jørgensen, L., & Jacobsen, B. K. (2001). Changes in muscle mass, fat mass, and bone mineral content in the legs after stroke: a 1 year prospective study. *Bone, 28*(6), 655-659.

Kahn, J. H., & Hornby, T. G. (2009). Rapid and long-term adaptations in gait symmetry following unilateral step training in people with hemiparesis. *Phys Ther, 89*(5), 474-483. doi:10.2522/ptj.20080237

Kakuda, W., Abo, M., Watanabe, S., Momosaki, R., Hashimoto, G., Nakayama, Y., . . . Yoshida, H. (2013). High-frequency rTMS applied over bilateral leg motor areas combined with mobility training for gait disturbance after stroke: a preliminary study. *Brain Inj, 27*(9), 1080-1086. doi:10.3109/02699052.2013.794973

Kalinosky, B. T., Schindler-Ivens, S., & Schmit, B. D. (2013). White matter structural connectivity is associated with sensorimotor function in stroke survivors. *Neuroimage Clin, 2*, 767-781. doi:10.1016/j.nicl.2013.05.009

Kato, M. (1988). Longitudinal myelotomy of lumbar spinal cord has little effect on coordinated locomotor activities of bilateral hindlimbs of the chronic cats. *Neurosci Lett, 93*(2-3), 259-263.

Kato, M., Murakami, S., Yasuda, K., & Hirayama, H. (1984). Disruption of fore- and hindlimb coordination during overground locomotion in cats with bilateral serial hemisection of the spinal cord. *Neurosci Res, 2*(1-2), 27-47.

Kautz, S. A., & Brown, D. A. (1998). Relationships between timing of muscle excitation and impaired motor performance during cyclical lower extremity movement in post-stroke hemiplegia. *Brain, 121 (Pt 3)*, 515-526.

Kautz, S. A., Brown, D. A., Van der Loos, H. F., & Zajac, F. E. (2002). Mutability of bifunctional thigh muscle activity in pedaling due to contralateral leg force generation. *J Neurophysiol, 88*(3), 1308-1317.

Kautz, S. A., Duncan, P. W., Perera, S., Neptune, R. R., & Studenski, S. A. (2005). Coordination of hemiparetic locomotion after stroke rehabilitation. *Neurorehabil Neural Repair, 19*(3), 250-258. doi:10.1177/1545968305279279

Kautz, S. A., & Neptune, R. R. (2002). Biomechanical determinants of pedaling energetics: internal and external work are not independent. *Exerc Sport Sci Rev, 30*(4), 159-165.

Kautz, S. A., & Patten, C. (2005). Interlimb influences on paretic leg function in poststroke hemiparesis. *J Neurophysiol, 93*(5), 2460-2473. doi:10.1152/jn.00963.2004

Kautz, S. A., Patten, C., & Neptune, R. R. (2006). Does unilateral pedaling activate a rhythmic locomotor pattern in the nonpedaling leg in post-stroke hemiparesis? *J Neurophysiol, 95*(5), 3154-3163. doi:10.1152/jn.00951.2005

Kim, C. M., & Eng, J. J. (2003). Symmetry in vertical ground reaction force is accompanied by symmetry in temporal but not distance variables of gait in persons with stroke. *Gait Posture, 18*(1), 23-28.

Kim, Y. H., You, S. H., Kwon, Y. H., Hallett, M., Kim, J. H., & Jang, S. H. (2006). Longitudinal fMRI study for locomotor recovery in patients with stroke. *Neurology, 67*(2), 330-333. doi:10.1212/01.wnl.0000225178.85833.0d

Klarner, T., Barss, T. S., Sun, Y., Kaupp, C., Loadman, P. M., & Zehr, E. P. (2016a). Exploiting Interlimb Arm and Leg Connections for Walking Rehabilitation: A Training Intervention in Stroke. *Neural Plast, 2016*, 1517968. doi:10.1155/2016/1517968

Klarner, T., Barss, T. S., Sun, Y., Kaupp, C., Loadman, P. M., & Zehr, E. P. (2016b). Long-Term Plasticity in Reflex Excitability Induced by Five Weeks of Arm and Leg Cycling Training after Stroke. *Brain Sci, 6*(4). doi:10.3390/brainsci6040054

Klein, C. S., Brooks, D., Richardson, D., McIlroy, W. E., & Bayley, M. T. (2010). Voluntary activation failure contributes more to plantar flexor weakness than antagonist coactivation and muscle atrophy in chronic stroke survivors. *J Appl Physiol (1985), 109*(5), 1337-1346. doi:10.1152/japplphysiol.00804.2009

Klein, C. S., Power, G. A., Brooks, D., & Rice, C. L. (2013). Neural and muscular determinants of dorsiflexor weakness in chronic stroke survivors. *Motor Control, 17*(3), 283-297.

Kloter, E., Wirz, M., & Dietz, V. (2011). Locomotion in stroke subjects: interactions between unaffected and affected sides. *Brain, 134*(Pt 3), 721-731. doi:10.1093/brain/awq370

Knutsson, E., & Richards, C. (1979). Different types of disturbed motor control in gait of hemiparetic patients. *Brain, 102*(2), 405-430.

Kocak, M., Ulmer, J. L., Sahin Ugurel, M., Gaggl, W., & Prost, R. W. (2009). Motor homunculus: passive mapping in healthy volunteers by using functional MR imaging--initial results. *Radiology, 251*(2), 485-492. doi:10.1148/radiol.2512080231

Krakauer, J. W. (2007). Avoiding performance and task confounds: multimodal investigation of brain reorganization after stroke rehabilitation. *Exp Neurol, 204*(2), 491-495. doi:10.1016/j.expneurol.2006.12.026

Krasovsky, T., Lamontagne, A., Feldman, A. G., & Levin, M. F. (2013). Reduced gait stability in high-functioning poststroke individuals. *J Neurophysiol, 109*(1), 77-88. doi:10.1152/jn.00552.2012

La Joie, W. J., Reddy, N. M., & Melvin, J. L. (1982). Somatosensory evoked potentials: their predictive value in right hemiplegia. *Arch Phys Med Rehabil, 63*(5), 223-226.

Lamont, E. V., & Zehr, E. P. (2006). Task-specific modulation of cutaneous reflexes expressed at functionally relevant gait cycle phases during level and incline walking and stair climbing. *Exp Brain Res, 173*(1), 185-192. doi:10.1007/s00221-006-0586-4

Lamontagne, A., Richards, C. L., & Malouin, F. (2000). Coactivation during gait as an adaptive behavior after stroke. *J Electromyogr Kinesiol, 10*(6), 407-415.

Landin, S., Hagenfeldt, L., Saltin, B., & Wahren, J. (1977). Muscle metabolism during exercise in hemiparetic patients. *Clin Sci Mol Med, 53*(3), 257-269.

Larsen, B., Voight, M., & Grey, M. J. (2006). Changes in the soleus stretch reflex at different pedaling frequencies and crank loads during pedaling. *Motor Control, 10*(3), 265-279.

Lauzière, S., Miéville, C., Betschart, M., Duclos, C., Aissaoui, R., & Nadeau, S. (2014). Plantarflexion moment is a contributor to step length after-effect following walking on a split-belt treadmill in individuals with stroke and healthy individuals. *J Rehabil Med, 46*(9), 849-857. doi:10.2340/16501977-1845

Levin, M. F., Kleim, J. A., & Wolf, S. L. (2009). What do motor "recovery" and "compensation" mean in patients following stroke? *Neurorehabil Neural Repair, 23*(4), 313-319. doi:10.1177/1545968308328727

Lewis, G. N., & Byblow, W. D. (2004). Neurophysiological and behavioural adaptations to a bilateral training intervention in individuals following stroke. *Clin Rehabil, 18*(1), 48-59.

Li, X., Wang, Y. C., Suresh, N. L., Rymer, W. Z., & Zhou, P. (2011). Motor unit number reductions in paretic muscles of stroke survivors. *IEEE Trans Inf Technol Biomed, 15*(4), 505-512. doi:10.1109/TITB.2011.2140379

Liepert, J., Uhde, I., Gräf, S., Leidner, O., & Weiller, C. (2001). Motor cortex plasticity during forced-use therapy in stroke patients: a preliminary study. *J Neurol, 248*(4), 315-321.

Lin, P. Y., Chen, J. J., & Lin, S. I. (2013). The cortical control of cycling exercise in stroke patients: an fNIRS study. *Hum Brain Mapp, 34*(10), 2381-2390. doi:10.1002/hbm.22072

Lin, P. Y., Yang, Y. R., Cheng, S. J., & Wang, R. Y. (2006). The relation between ankle impairments and gait velocity and symmetry in people with stroke. *Arch Phys Med Rehabil, 87*(4), 562-568. doi:10.1016/j.apmr.2005.12.042

Logothetis, N. K. (2008). What we can do and what we cannot do with fMRI. *Nature, 453*(7197), 869-878. doi:10.1038/nature06976

Luft, A. R., Forrester, L., Macko, R. F., McCombe-Waller, S., Whitall, J., Villagra, F., & Hanley, D. F. (2005). Brain activation of lower extremity movement in chronically impaired stroke survivors. *Neuroimage, 26*(1), 184-194. doi:10.1016/j.neuroimage.2005.01.027

Lukacs, M. (2005). Electrophysiological signs of changes in motor units after ischaemic stroke. *Clin Neurophysiol, 116*(7), 1566-1570. doi:10.1016/j.clinph.2005.04.005

Lukács, M., Vécsei, L., & Beniczky, S. (2008). Large motor units are selectively affected following a stroke. *Clin Neurophysiol, 119*(11), 2555-2558. doi:10.1016/j.clinph.2008.08.005

Madhavan, S., Rogers, L. M., & Stinear, J. W. (2010). A paradox: after stroke, the non-lesioned lower limb motor cortex may be maladaptive. *Eur J Neurosci, 32*(6), 1032-1039. doi:10.1111/j.1460-9568.2010.07364.x

Madhavan, S., Weber, K. A., 2nd, & Stinear, J. W. (2011). Non-invasive brain stimulation enhances fine motor control of the hemiparetic ankle: implications for rehabilitation. *Exp Brain Res, 209*(1), 9-17. doi:10.1007/s00221-010-2511-0

Marque, P., Simonetta-Moreau, M., Maupas, E., & Roques, C. F. (2001). Facilitation of transmission in heteronymous group II pathways in spastic hemiplegic patients. *J Neurol Neurosurg Psychiatry, 70*(1), 36-42.

Marshall, R. S., Perera, G. M., Lazar, R. M., Krakauer, J. W., Constantine, R. C., & DeLaPaz, R. L. (2000). Evolution of cortical activation during recovery from corticospinal tract infarction. *Stroke, 31*(3), 656-661.

Matsuyama, K., Mori, F., Nakajima, K., Drew, T., Aoki, M., & Mori, S. (2004). Locomotor role of the corticoreticular-reticulospinal-spinal interneuronal system. *Prog Brain Res, 143*, 239-249. doi:10.1016/S0079-6123(03)43024-0

Mayo, N. E., Wood-Dauphinee, S., Ahmed, S., Gordon, C., Higgins, J., McEwen, S., & Salbach, N. (1999). Disablement following stroke. *Disabil Rehabil, 21*(5-6), 258-268.

Mayo, N. E., Wood-Dauphinee, S., Cote, R., Durcan, L., & Carlton, J. (2002). Activity, participation, and quality of life 6 months poststroke. *Arch Phys Med Rehabil, 83*(8), 1035-1042.

McComas, A. J., Sica, R. E., Upton, A. R., & Aguilera, N. (1973). Functional changes in motoneurones of hemiparetic patients. *J Neurol Neurosurg Psychiatry, 36*(2), 183-193.

McIlroy, W. E., Collins, D. F., & Brooke, J. D. (1992). Movement features and H-reflex modulation. II. Passive rotation, movement velocity and single leg movement. *Brain Res, 582*(1), 85-93.

Mehrholz, J., Thomas, S., & Elsner, B. (2017). Treadmill training and body weight support for walking after stroke. *Cochrane Database Syst Rev, 8*, CD002840. doi:10.1002/14651858.CD002840.pub4

Mehta, J. P., Verber, M. D., Wieser, J. A., Schmit, B. D., & Schindler-Ivens, S. M. (2009). A novel technique for examining human brain activity associated with pedaling using fMRI. *J Neurosci Methods, 179*(2), 230-239. doi:10.1016/j.jneumeth.2009.01.029

Mehta, J. P., Verber, M. D., Wieser, J. A., Schmit, B. D., & Schindler-Ivens, S. M. (2012). The effect of movement rate and complexity on functional magnetic resonance signal change during pedaling. *Motor Control, 16*(2), 158-175.

Meijer, R., Plotnik, M., Zwaaftink, E. G., van Lummel, R. C., Ainsworth, E., Martina, J. D., & Hausdorff, J. M. (2011). Markedly impaired bilateral coordination of gait in post-stroke patients: Is this deficit distinct from asymmetry? A cohort study. *J Neuroeng Rehabil, 8*, 23. doi:10.1186/1743-0003-8-23

Mezzarane, R. A., Nakajima, T., & Zehr, E. P. (2014). After stroke bidirectional modulation of soleus stretch reflex amplitude emerges during rhythmic arm cycling. *Front Hum Neurosci, 8*, 136. doi:10.3389/fnhum.2014.00136

Mileva, K., Green, D. A., & Turner, D. L. (2004). Neuromuscular and biomechanical coupling in human cycling: modulation of cutaneous reflex responses to sural nerve stimulation. *Exp Brain Res, 158*(4), 450-464. doi:10.1007/s00221-004-1922-1

Miltner, W. H., Bauder, H., Sommer, M., Dettmers, C., & Taub, E. (1999). Effects of constraint-induced movement therapy on patients with chronic motor deficits after stroke: a replication. *Stroke, 30*(3), 586-592.

Mirka, G. A. (1991). The quantification of EMG normalization error. *Ergonomics, 34*(3), 343-352. doi:10.1080/00140139108967318

Miyai, I., Yagura, H., Hatakenaka, M., Oda, I., Konishi, I., & Kubota, K. (2003). Longitudinal optical imaging study for locomotor recovery after stroke. *Stroke, 34*(12), 2866-2870. doi:10.1161/01.STR.0000100166.81077.8A

Miyai, I., Yagura, H., Oda, I., Konishi, I., Eda, H., Suzuki, T., & Kubota, K. (2002). Premotor cortex is involved in restoration of gait in stroke. *Ann Neurol, 52*(2), 188-194. doi:10.1002/ana.10274

Morita, H., Crone, C., Christenhuis, D., Petersen, N. T., & Nielsen, J. B. (2001). Modulation of presynaptic inhibition and disynaptic reciprocal Ia inhibition during voluntary movement in spasticity. *Brain, 124*(Pt 4), 826-837.

Motawar, B., Hur, P., Stinear, J., & Seo, N. J. (2012). Contribution of intracortical inhibition in voluntary muscle relaxation. *Exp Brain Res, 221*(3), 299-308. doi:10.1007/s00221-012-3173-x

Motl, R. W., Knowles, B. D., & Dishman, R. K. (2003). Acute bouts of active and passive leg cycling attenuate the amplitude of the soleus H-reflex in humans. *Neurosci Lett, 347*(2), 69-72.

Mudie, M. H., & Matyas, T. A. (2000). Can simultaneous bilateral movement involve the undamaged hemisphere in reconstruction of neural networks damaged by stroke? *Disabil Rehabil, 22*(1-2), 23-37.

Murase, N., Duque, J., Mazzocchio, R., & Cohen, L. G. (2004). Influence of interhemispheric interactions on motor function in chronic stroke. *Ann Neurol, 55*(3), 400-409. doi:10.1002/ana.10848

Nadeau, S., Gravel, D., Arsenault, A. B., & Bourbonnais, D. (1999). Plantarflexor weakness as a limiting factor of gait speed in stroke subjects and the compensating role of hip flexors. *Clin Biomech (Bristol, Avon), 14*(2), 125-135.

Nakayama, H., Jørgensen, H. S., Raaschou, H. O., & Olsen, T. S. (1994). Compensation in recovery of upper extremity function after stroke: the Copenhagen Stroke Study. *Arch Phys Med Rehabil, 75*(8), 852-857.

Napieralski, J. A., Butler, A. K., & Chesselet, M. F. (1996). Anatomical and functional evidence for lesion-specific sprouting of corticostriatal input in the adult rat. *J Comp Neurol, 373*(4), 484-497. doi:10.1002/(SICI)1096-9861(19960930)373:4<484::AID-CNE2>3.0.CO;2-Y

Nelles, G., Spiekermann, G., Jueptner, M., Leonhardt, G., Müller, S., Gerhard, H., & Diener, H. C. (1999). Reorganization of sensory and motor systems in hemiplegic stroke patients. A positron emission tomography study. *Stroke, 30*(8), 1510-1516.

Neptune, R. R., & van den Bogert, A. J. (1998). Standard mechanical energy analyses do not correlate with muscle work in cycling. *J Biomech, 31*(3), 239-245.

Newham, D. J., & Hsiao, S. F. (2001). Knee muscle isometric strength, voluntary activation and antagonist co-contraction in the first six months after stroke. *Disabil Rehabil, 23*(9), 379-386.

Nielsen, J., Crone, C., & Hultborn, H. (1993). H-reflexes are smaller in dancers from The Royal Danish Ballet than in well-trained athletes. *Eur J Appl Physiol Occup Physiol, 66*(2), 116-121.

Nielsen, J., Petersen, N., & Fedirchuk, B. (1997). Evidence suggesting a transcortical pathway from cutaneous foot afferents to tibialis anterior motoneurones in man. *J Physiol, 501 (Pt 2)*, 473-484.

Noble, J. W., Eng, J. J., & Boyd, L. A. (2014). Bilateral motor tasks involve more brain regions and higher neural activation than unilateral tasks: an fMRI study. *Exp Brain Res, 232*(9), 2785-2795. doi:10.1007/s00221-014-3963-4

Nudo, R. J., & Milliken, G. W. (1996). Reorganization of movement representations in primary motor cortex following focal ischemic infarcts in adult squirrel monkeys. *J Neurophysiol, 75*(5), 2144-2149.

Numata, K., Murayama, T., Takasugi, J., & Oga, M. (2008). Effect of modified constraint-induced movement therapy on lower extremity hemiplegia due to a higher-motor area lesion. *Brain Inj, 22*(11), 898-904. doi:10.1080/02699050802425436

O'Sullivan, S. B., Schmitz, T. J., & Fulk, G. D. (2014). *Physical rehabilitation* (6th ed.). Philadelphia: F.A. Davis Co.

Olney, S. J., Griffin, M. P., Monga, T. N., & McBride, I. D. (1991). Work and power in gait of stroke patients. *Arch Phys Med Rehabil, 72*(5), 309-314.

Olney, S. J., Monga, T. N., & Costigan, P. A. (1986). Mechanical energy of walking of stroke patients. *Arch Phys Med Rehabil, 67*(2), 92-98.

Olney, S. J., & Richards, C. (1996). Hemiparetic gait following stroke. Part I: Characteristics. *Gait & Posture., 4*(2), 136-148.

Onishi, H., Sugawara, K., Yamashiro, K., Sato, D., Suzuki, M., Kirimoto, H., . . . Kameyama, S. (2013). Neuromagnetic activation following active and passive finger movements. *Brain Behav, 3*(2), 178-192. doi:10.1002/brb3.126

Onushko, T., & Schmit, B. D. (2007). Reflex response to imposed bilateral hip oscillations in human spinal cord injury. *J Neurophysiol, 98*(4), 1849-1861. doi:10.1152/jn.00461.2007

Palmer, J. A., Zarzycki, R., Morton, S. M., Kesar, T. M., & Binder-Macleod, S. A. (2017). Characterizing differential post-stroke corticomotor drive to the dorsi- and plantarflexor muscles during resting and volitional muscle activation. *J Neurophysiol*, jn.00393.02016. doi:10.1152/jn.00393.2016

Patterson, K. K., Parafianowicz, I., Danells, C. J., Closson, V., Verrier, M. C., Staines, W. R., . . . McIlroy, W. E. (2008). Gait asymmetry in community-ambulating stroke survivors. *Arch Phys Med Rehabil, 89*(2), 304-310. doi:10.1016/j.apmr.2007.08.142

Perell, K. L., Gregor, R. J., & Scremin, A. M. E. (1998). Lower limb cycling mechanics in subjects with unilateral cerebrovascular accidents. *Journal of Applied Biomechanics, 14*, 158-179.

Peterson, C. L., Hall, A. L., Kautz, S. A., & Neptune, R. R. (2010). Pre-swing deficits in forward propulsion, swing initiation and power generation by individual muscles during hemiparetic walking. *J Biomech, 43*(12), 2348-2355. doi:10.1016/j.jbiomech.2010.04.027

Pierrot-Deseilligny, E., & Burke, D. J. (2012). *The circuitry of the human spinal cord : spinal and corticospinal mechanisms of movement*. Cambridge, England ; New York: Cambridge University Press.

Pijnappels, M., Van Wezel, B. M., Colombo, G., Dietz, V., & Duysens, J. (1998). Cortical facilitation of cutaneous reflexes in leg muscles during human gait. *Brain Res, 787*(1), 149-153.

Platts, M. M., Rafferty, D., & Paul, L. (2006). Metabolic cost of over ground gait in younger stroke patients and healthy controls. *Med Sci Sports Exerc, 38*(6), 1041-1046. doi:10.1249/01.mss.0000222829.34111.9c

Plotnik, M., Giladi, N., & Hausdorff, J. M. (2007). A new measure for quantifying the bilateral coordination of human gait: effects of aging and Parkinson's disease. *Exp Brain Res, 181*(4), 561-570. doi:10.1007/s00221-007-0955-7

Power, M. L., & Schulkin, J. (2008). Sex differences in fat storage, fat metabolism, and the health risks from obesity: possible evolutionary origins. *Br J Nutr, 99*(5), 931-940. doi:10.1017/S0007114507853347

Prochazka, A., & Ellaway, P. (2012). Sensory systems in the control of movement. *Compr Physiol, 2*(4), 2615-2627. doi:10.1002/cphy.c100086

Promjunyakul, N. O., Schmit, B. D., & Schindler-Ivens, S. M. (2015). A novel fMRI paradigm suggests that pedaling-related brain activation is altered after stroke. *Front Hum Neurosci, 9*, 324. doi:10.3389/fnhum.2015.00324

Qü, M., Buchkremer-Ratzmann, I., Schiene, K., Schroeter, M., Witte, O. W., & Zilles, K. (1998). Bihemispheric reduction of GABAA receptor binding following focal cortical photothrombotic lesions in the rat brain. *Brain Res, 813*(2), 374-380.

Raasch, C. C., & Zajac, F. E. (1999). Locomotor strategy for pedaling: muscle groups and biomechanical functions. *J Neurophysiol, 82*(2), 515-525.

Raja, B., Neptune, R. R., & Kautz, S. A. (2012). Coordination of the non-paretic leg during hemiparetic gait: expected and novel compensatory patterns. *Clin Biomech (Bristol, Avon), 27*(10), 1023-1030. doi:10.1016/j.clinbiomech.2012.08.005

Rastgoo, M., Naghdi, S., Nakhostin Ansari, N., Olyaei, G., Jalaei, S., Forogh, B., & Najari, H. (2016). Effects of repetitive transcranial magnetic stimulation on lower extremity spasticity and motor function in stroke patients. *Disabil Rehabil, 38*(19), 1918-1926. doi:10.3109/09638288.2015.1107780

Reddy, H., Floyer, A., Donaghy, M., & Matthews, P. M. (2001). Altered cortical activation with finger movement after peripheral denervation: comparison of active and passive tasks. *Exp Brain Res, 138*(4), 484-491.

Rehme, A. K., Eickhoff, S. B., Rottschy, C., Fink, G. R., & Grefkes, C. (2012). Activation likelihood estimation meta-analysis of motor-related neural activity after stroke. *Neuroimage, 59*(3), 2771-2782. doi:10.1016/j.neuroimage.2011.10.023

Rehme, A. K., Fink, G. R., von Cramon, D. Y., & Grefkes, C. (2011). The role of the contralesional motor cortex for motor recovery in the early days after stroke assessed with longitudinal FMRI. *Cereb Cortex, 21*(4), 756-768. doi:10.1093/cercor/bhq140

Reisman, D. S., Block, H. J., & Bastian, A. J. (2005). Interlimb coordination during locomotion: what can be adapted and stored? *J Neurophysiol, 94*(4), 2403-2415. doi:10.1152/jn.00089.2005

Reisman, D. S., McLean, H., Keller, J., Danks, K. A., & Bastian, A. J. (2013). Repeated split-belt treadmill training improves poststroke step length asymmetry. *Neurorehabil Neural Repair, 27*(5), 460-468. doi:10.1177/1545968312474118

Reisman, D. S., Wityk, R., Silver, K., & Bastian, A. J. (2007). Locomotor adaptation on a split-belt treadmill can improve walking symmetry post-stroke. *Brain, 130*(Pt 7), 1861-1872. doi:10.1093/brain/awm035

Reisman, D. S., Wityk, R., Silver, K., & Bastian, A. J. (2009). Split-belt treadmill adaptation transfers to overground walking in persons poststroke. *Neurorehabil Neural Repair, 23*(7), 735-744. doi:10.1177/1545968309332880

Rice, M. S., & Newell, K. M. (2001). Interlimb coupling and left hemiplegia because of right cerebral vascular accident. *The Occupational Therapy Journal of Research, 21*(1), 12-28.

Riley, N. A., & Bilodeau, M. (2002). Changes in upper limb joint torque patterns and EMG signals with fatigue following a stroke. *Disabil Rehabil, 24*(18), 961-969. doi:10.1080/0963828021000007932

Rinehart, J. K., Singleton, R. D., Adair, J. C., Sadek, J. R., & Haaland, K. Y. (2009). Arm use after left or right hemiparesis is influenced by hand preference. *Stroke, 40*(2), 545-550. doi:10.1161/STROKEAHA.108.528497

Roby-Brami, A., & Bussel, B. (1987). Long-latency spinal reflex in man after flexor reflex afferent stimulation. *Brain, 110 (Pt 3)*, 707-725.

Roerdink, M., Geurts, A. C., de Haart, M., & Beek, P. J. (2009). On the relative contribution of the paretic leg to the control of posture after stroke. *Neurorehabil Neural Repair, 23*(3), 267-274. doi:10.1177/1545968308323928

Roerdink, M., Lamoth, C. J., Kwakkel, G., van Wieringen, P. C., & Beek, P. J. (2007). Gait coordination after stroke: benefits of acoustically paced treadmill walking. *Phys Ther, 87*(8), 1009-1022. doi:10.2522/ptj.20050394

Rogers, L. M., Stinear, J. W., Lewis, G. N., & Brown, D. A. (2011). Descending control to the nonparetic limb degrades the cyclic activity of paretic leg muscles. *Hum Mov Sci, 30*(6), 1225-1244. doi:10.1016/j.humov.2011.03.001

Rosenfalck, A., & Andreassen, S. (1980). Impaired regulation of force and firing pattern of single motor units in patients with spasticity. *J Neurol Neurosurg Psychiatry, 43*(10), 907-916.

Ryan, A. S., Buscemi, A., Forrester, L., Hafer-Macko, C. E., & Ivey, F. M. (2011). Atrophy and intramuscular fat in specific muscles of the thigh: associated weakness and hyperinsulinemia in stroke survivors. *Neurorehabil Neural Repair, 25*(9), 865-872. doi:10.1177/1545968311408920

Ryan, A. S., Dobrovolny, C. L., Smith, G. V., Silver, K. H., & Macko, R. F. (2002). Hemiparetic muscle atrophy and increased intramuscular fat in stroke patients. *Arch Phys Med Rehabil, 83*(12), 1703-1707. doi:10.1053/apmr.2002.36399

Sanchez, N., Acosta, A. M., Lopez-Rosado, R., Stienen, A. H. A., & Dewald, J. P. A. (2017). Lower Extremity Motor Impairments in Ambulatory Chronic Hemiparetic Stroke: Evidence for Lower Extremity Weakness and Abnormal Muscle and Joint Torque Coupling Patterns. *Neurorehabil Neural Repair, 31*(9), 814-826. doi:10.1177/1545968317721974

Sawaki, L., Butler, A. J., Leng, X., Wassenaar, P. A., Mohammad, Y. M., Blanton, S., . . . Wittenberg, G. F. (2008). Constraint-induced movement therapy results in increased motor map area in subjects 3 to 9 months after stroke. *Neurorehabil Neural Repair, 22*(5), 505-513. doi:10.1177/1545968308317531

Schaechter, J. D., Kraft, E., Hilliard, T. S., Dijkhuizen, R. M., Benner, T., Finklestein, S. P., . . . Cramer, S. C. (2002). Motor recovery and cortical reorganization after constraint-induced movement therapy in stroke patients: a preliminary study. *Neurorehabil Neural Repair, 16*(4), 326-338. doi:10.1177/154596830201600403

Schiene, K., Bruehl, C., Zilles, K., Qü, M., Hagemann, G., Kraemer, M., & Witte, O. W. (1996). Neuronal hyperexcitability and reduction of GABAA-receptor expression in the surround of cerebral photothrombosis. *J Cereb Blood Flow Metab, 16*(5), 906-914. doi:10.1097/00004647-199609000-00014

Schindler-Ivens, S., Arand, B., & Cleland, B. (2016). An MRI-compatible, split-crank pedaling device to prevent motor compensation after stroke. In: Society for Neuroscience National Meeting. San Diego, CA.

Schindler-Ivens, S., Brown, D. A., & Brooke, J. D. (2004). Direction-dependent phasing of locomotor muscle activity is altered post-stroke. *J Neurophysiol, 92*(4), 2207-2216. doi:10.1152/jn.01207.2003

Schindler-Ivens, S., Brown, D. A., Lewis, G. N., Nielsen, J. B., Ondishko, K. L., & Wieser, J. (2008). Soleus H-reflex excitability during pedaling post-stroke. *Exp Brain Res, 188*(3), 465-474. doi:10.1007/s00221-008-1373-1

Schmahmann, J. D., Doyon, J., McDonald, D., Holmes, C., Lavoie, K., Hurwitz, A. S., . . . Petrides, M. (1999). Three-dimensional MRI atlas of the human cerebellum in proportional stereotaxic space. *Neuroimage, 10*(3 Pt 1), 233-260. doi:10.1006/nimg.1999.0459

Schrafl-Altermatt, M., & Dietz, V. (2016). Cooperative hand movements in post-stroke subjects: Neural reorganization. *Clin Neurophysiol, 127*(1), 748-754. doi:10.1016/j.clinph.2015.07.004

Seo, H. G., Lee, W. H., Lee, S. H., Yi, Y., Kim, K. D., & Oh, B. M. (2017). Robotic-assisted gait training combined with transcranial direct current stimulation in chronic stroke patients: A pilot double-blind, randomized controlled trial. *Restor Neurol Neurosci, 35*(5), 527-536. doi:10.3233/RNN-170745

Sharafi, B., Hoffmann, G., Tan, A. Q., & Y, Y. D. (2016). Evidence of impaired neuromuscular responses in the support leg to a destabilizing swing phase perturbation in hemiparetic gait. *Exp Brain Res, 234*(12), 3497-3508. doi:10.1007/s00221-016-4743-0

Shield, A., & Zhou, S. (2004). Assessing voluntary muscle activation with the twitch interpolation technique. *Sports Med, 34*(4), 253-267.

Shirota, C., Jansa, J., Diaz, J., Balasubramanian, S., Mazzoleni, S., Borghese, N. A., & Melendez-Calderon, A. (2016). On the assessment of coordination between upper extremities: towards a common language between rehabilitation engineers, clinicians and neuroscientists. *J Neuroeng Rehabil, 13*(1), 80. doi:10.1186/s12984-016-0186-x

Sinkjaer, T., Andersen, J. B., Ladouceur, M., Christensen, L. O., & Nielsen, J. B. (2000). Major role for sensory feedback in soleus EMG activity in the stance phase of walking in man. *J Physiol, 523 Pt 3*, 817-827.

Skilbeck, C. E., Wade, D. T., Hewer, R. L., & Wood, V. A. (1983). Recovery after stroke. *J Neurol Neurosurg Psychiatry, 46*(1), 5-8.

Sousa, A. S., Silva, A., Santos, R., Sousa, F., & Tavares, J. M. (2013). Interlimb coordination during the stance phase of gait in subjects with stroke. *Arch Phys Med Rehabil, 94*(12), 2515-2522. doi:10.1016/j.apmr.2013.06.032

Sousa, A. S., & Tavares, J. M. (2015). Interlimb Coordination During Step-to-Step Transition and Gait Performance. *J Mot Behav, 47*(6), 563-574. doi:10.1080/00222895.2015.1023391

Steenbergen, B., Hulstijn, W., de Vries, A., & Berger, M. (1996). Bimanual movement coordination in spastic hemiparesis. *Exp Brain Res, 110*(1), 91-98.

Stephens, M. J., & Yang, J. F. (1999). Loading during the stance phase of walking in humans increases the extensor EMG amplitude but does not change the duration of the step cycle. *Exp Brain Res, 124*(3), 363-370.

Sterr, A., Freivogel, S., & Schmalohr, D. (2002). Neurobehavioral aspects of recovery: assessment of the learned nonuse phenomenon in hemiparetic adolescents. *Arch Phys Med Rehabil, 83*(12), 1726-1731. doi:10.1053/apmr.2002.35660

Stroemer, R. P., Kent, T. A., & Hulsebosch, C. E. (1995). Neocortical neural sprouting, synaptogenesis, and behavioral recovery after neocortical infarction in rats. *Stroke, 26*(11), 2135-2144.

Stubbs, P. W., Nielsen, J. F., Sinkjær, T., & Mrachacz-Kersting, N. (2012). Short-latency crossed spinal responses are impaired differently in sub-acute and chronic stroke patients. *Clin Neurophysiol, 123*(3), 541-549. doi:10.1016/j.clinph.2011.07.033

Sunderland, A., & Tuke, A. (2005). Neuroplasticity, learning and recovery after stroke: a critical evaluation of constraint-induced therapy. *Neuropsychol Rehabil, 15*(2), 81-96. doi:10.1080/09602010443000047

Swinnen, S. P., & Duysens, J. (2004). *Neuro-behavioral determinants of interlimb coordination : a multidisciplinary approach*. Boston: Kluwer Academic.

Szameitat, A. J., Shen, S., Conforto, A., & Sterr, A. (2012). Cortical activation during executed, imagined, observed, and passive wrist movements in healthy volunteers and stroke patients. *Neuroimage, 62*(1), 266-280. doi:10.1016/j.neuroimage.2012.05.009

Takemi, M., Masakado, Y., Liu, M., & Ushiba, J. (2013). Event-related desynchronization reflects downregulation of intracortical inhibition in human primary motor cortex. *J Neurophysiol, 110*(5), 1158-1166. doi:10.1152/jn.01092.2012

Taub, E. (1976). Movement in nonhuman primates deprived of somatosensory feedback. *Exerc Sport Sci Rev, 4*, 335-374.

Taub, E. (2012). The behavior-analytic origins of constraint-induced movement therapy: an example of behavioral neurorehabilitation. *Behav Anal, 35*(2), 155-178.

Taub, E., Miller, N. E., Novack, T. A., Cook, E. W., Fleming, W. C., Nepomuceno, C. S., . . . Crago, J. E. (1993). Technique to improve chronic motor deficit after stroke. *Arch Phys Med Rehabil, 74*(4), 347-354.

Taub, E., Uswatte, G., Mark, V. W., & Morris, D. M. (2006). The learned nonuse phenomenon: implications for rehabilitation. *Eura Medicophys, 42*(3), 241-256.

Taub, E., Uswatte, G., & Pidikiti, R. (1999). Constraint-Induced Movement Therapy: a new family of techniques with broad application to physical rehabilitation--a clinical review. *J Rehabil Res Dev, 36*(3), 237-251.

Tax, A. A., Van Wezel, B. M., & Dietz, V. (1995). Bipedal reflex coordination to tactile stimulation of the sural nerve during human running. *J Neurophysiol, 73*(5), 1947-1964.

Terumitsu, M., Ikeda, K., Kwee, I. L., & Nakada, T. (2009). Participation of primary motor cortex area 4a in complex sensory processing: 3.0-T fMRI study. *Neuroreport, 20*(7), 679-683. doi:10.1097/WNR.0b013e32832a1820

Ting, L. H., Kautz, S. A., Brown, D. A., & Zajac, F. E. (2000). Contralateral movement and extensor force generation alter flexion phase muscle coordination in pedaling. *J Neurophysiol, 83*(6), 3351-3365.

Ting, L. H., Raasch, C. C., Brown, D. A., Kautz, S. A., & Zajac, F. E. (1998). Sensorimotor state of the contralateral leg affects ipsilateral muscle coordination of pedaling. *J Neurophysiol, 80*(3), 1341-1351.

Toma, K., Honda, M., Hanakawa, T., Okada, T., Fukuyama, H., Ikeda, A., . . . Shibasaki, H. (1999). Activities of the primary and supplementary motor areas increase in preparation and execution of voluntary muscle relaxation: an event-related fMRI study. *J Neurosci, 19*(9), 3527-3534.

Traversa, R., Cicinelli, P., Pasqualetti, P., Filippi, M., & Rossini, P. M. (1998). Follow-up of interhemispheric differences of motor evoked potentials from the 'affected' and 'unaffected' hemispheres in human stroke. *Brain Res, 803*(1-2), 1-8.

Trompetto, C., Marinelli, L., Mori, L., Pelosin, E., Currà, A., Molfetta, L., & Abbruzzese, G. (2014). Pathophysiology of spasticity: implications for neurorehabilitation. *Biomed Res Int, 2014*, 354906. doi:10.1155/2014/354906

Tseng, S. C., & Morton, S. M. (2010). Impaired interlimb coordination of voluntary leg movements in poststroke hemiparesis. *J Neurophysiol, 104*(1), 248-257. doi:10.1152/jn.00906.2009

Turns, L. J., Neptune, R. R., & Kautz, S. A. (2007). Relationships between muscle activity and anteroposterior ground reaction forces in hemiparetic walking. *Arch Phys Med Rehabil, 88*(9), 1127-1135. doi:10.1016/j.apmr.2007.05.027

Van Wezel, B. M., Ottenhoff, F. A., & Duysens, J. (1997). Dynamic control of location-specific information in tactile cutaneous reflexes from the foot during human walking. *J Neurosci, 17*(10), 3804-3814.

Vanzetta, I., & Grinvald, A. (1999). Increased cortical oxidative metabolism due to sensory stimulation: implications for functional brain imaging. *Science, 286*(5444), 1555-1558.

Vega-González, A., & Granat, M. H. (2005). Continuous monitoring of upper-limb activity in a free-living environment. *Arch Phys Med Rehabil, 86*(3), 541-548. doi:10.1016/j.apmr.2004.04.049

Verschueren, S. M., Swinnen, S. P., Desloovere, K., & Duysens, J. (2002). Effects of tendon vibration on the spatiotemporal characteristics of human locomotion. *Exp Brain Res, 143*(2), 231-239. doi:10.1007/s00221-001-0987-3

Vlaar, M. P., Solis-Escalante, T., Dewald, J. P. A., van Wegen, E. E. H., Schouten, A. C., Kwakkel, G., . . . consortium, D. E. (2017). Quantification of task-dependent cortical activation evoked by robotic continuous wrist joint manipulation in chronic hemiparetic stroke. *J Neuroeng Rehabil, 14*(1), 30. doi:10.1186/s12984-017-0240-3

von Schroeder, H. P., Coutts, R. D., Lyden, P. D., Billings, E., & Nickel, V. L. (1995). Gait parameters following stroke: a practical assessment. *J Rehabil Res Dev, 32*(1), 25-31.

Wade, D. T., Wood, V. A., & Hewer, R. L. (1985). Recovery after stroke--the first 3 months. *J Neurol Neurosurg Psychiatry, 48*(1), 7-13.

Ward, N. S., Brown, M. M., Thompson, A. J., & Frackowiak, R. S. (2003a). Neural correlates of motor recovery after stroke: a longitudinal fMRI study. *Brain, 126*(Pt 11), 2476-2496. doi:10.1093/brain/awg245

Ward, N. S., Brown, M. M., Thompson, A. J., & Frackowiak, R. S. (2003b). Neural correlates of outcome after stroke: a cross-sectional fMRI study. *Brain, 126*(Pt 6), 1430-1448.

Weiller, C., Chollet, F., Friston, K. J., Wise, R. J., & Frackowiak, R. S. (1992). Functional reorganization of the brain in recovery from striatocapsular infarction in man. *Ann Neurol, 31*(5), 463-472. doi:10.1002/ana.410310502

Weiller, C., Jüptner, M., Fellows, S., Rijntjes, M., Leonhardt, G., Kiebel, S., . . . Thilmann, A. F. (1996). Brain representation of active and passive movements. *Neuroimage, 4*(2), 105-110. doi:10.1006/nimg.1996.0034

Wexler, B. E., Fulbright, R. K., Lacadie, C. M., Skudlarski, P., Kelz, M. B., Constable, R. T., & Gore, J. C. (1997). An fMRI study of the human cortical motor system response to increasing functional demands. *Magn Reson Imaging, 15*(4), 385-396.

Wolf, S. L., Lecraw, D. E., Barton, L. A., & Jann, B. B. (1989). Forced use of hemiplegic upper extremities to reverse the effect of learned nonuse among chronic stroke and head-injured patients. *Exp Neurol, 104*(2), 125-132.

Yamaguchi, T., Fujiwara, T., Liu, W., & Liu, M. (2012). Effects of pedaling exercise on the intracortical inhibition of cortical leg area. *Exp Brain Res, 218*(3), 401-406. doi:10.1007/s00221-012-3026-7

Yang, J. F., & Stein, R. B. (1990). Phase-dependent reflex reversal in human leg muscles during walking. *J Neurophysiol, 63*(5), 1109-1117.

Yang, J. F., Stein, R. B., & James, K. B. (1991). Contribution of peripheral afferents to the activation of the soleus muscle during walking in humans. *Exp Brain Res, 87*(3), 679-687.

Yu, W. H., Liu, W. Y., Wong, A. M., Wang, T. C., Li, Y. C., & Lien, H. Y. (2015). Effect of forced use of the lower extremity on gait performance and mobility of post-acute stroke patients. *J Phys Ther Sci, 27*(2), 421-425. doi:10.1589/jpts.27.421

Zamparo, P., Francescato, M. P., De Luca, G., Lovati, L., & di Prampero, P. E. (1995). The energy cost of level walking in patients with hemiplegia. *Scand J Med Sci Sports, 5*(6), 348-352.

Zehr, E. P. (2005). Neural control of rhythmic human movement: the common core hypothesis. *Exerc Sport Sci Rev, 33*(1), 54-60.

Zehr, E. P., Barss, T. S., Dragert, K., Frigon, A., Vasudevan, E. V., Haridas, C., . . . Sun, Y. (2016). Neuromechanical interactions between the limbs during human locomotion: an evolutionary perspective with translation to rehabilitation. *Exp Brain Res, 234*(11), 3059-3081. doi:10.1007/s00221-016-4715-4

Zehr, E. P., Collins, D. F., & Chua, R. (2001). Human interlimb reflexes evoked by electrical stimulation of cutaneous nerves innervating the hand and foot. *Exp Brain Res, 140*(4), 495-504. doi:10.1007/s002210100857

Zehr, E. P., & Haridas, C. (2003). Modulation of cutaneous reflexes in arm muscles during walking: further evidence of similar control mechanisms for rhythmic human arm and leg movements. *Exp Brain Res, 149*(2), 260-266. doi:10.1007/s00221-003-1377-9

Zehr, E. P., Hesketh, K. L., & Chua, R. (2001). Differential regulation of cutaneous and H-reflexes during leg cycling in humans. *J Neurophysiol, 85*(3), 1178-1184.

Zehr, E. P., Hundza, S. R., & Vasudevan, E. V. (2009). The quadrupedal nature of human bipedal locomotion. *Exerc Sport Sci Rev, 37*(2), 102-108. doi:10.1097/JES.0b013e31819c2ed6

Zehr, E. P., Komiyama, T., & Stein, R. B. (1997). Cutaneous reflexes during human gait: electromyographic and kinematic responses to electrical stimulation. *J Neurophysiol, 77*(6), 3311-3325.

Zehr, E. P., & Loadman, P. M. (2012). Persistence of locomotor-related interlimb reflex networks during walking after stroke. *Clin Neurophysiol, 123*(4), 796-807. doi:10.1016/j.clinph.2011.07.049

Zehr, E. P., Loadman, P. M., & Hundza, S. R. (2012). Neural control of rhythmic arm cycling after stroke. *J Neurophysiol, 108*(3), 891-905. doi:10.1152/jn.01152.2011

Zehr, E. P., & Stein, R. B. (1999). What functions do reflexes serve during human locomotion? *Prog Neurobiol, 58*(2), 185-205.

Zhang, Y., Li, K. S., Ning, Y. Z., Fu, C. H., Liu, H. W., Han, X., . . . Zou, Y. H. (2016). Altered structural and functional connectivity between the bilateral primary motor cortex in unilateral subcortical stroke: A multimodal magnetic resonance imaging study. *Medicine (Baltimore), 95*(31), e4534. doi:10.1097/MD.0000000000004534

APPENDIX A: SUPPLEMENT TO CHAPTER 2

This appendix is a supplement to Chapter 2. Included is additional results and the analysis code used to evaluate dependent measures of interest.

A.1 Additional results

Figure A.1 provides group ensemble averaged velocity traces from control participants and stroke participants from each of the subgroups identified during bilateral uncoupled pedaling. Conventional, unilateral, and bilateral uncoupled pedaling are shown.

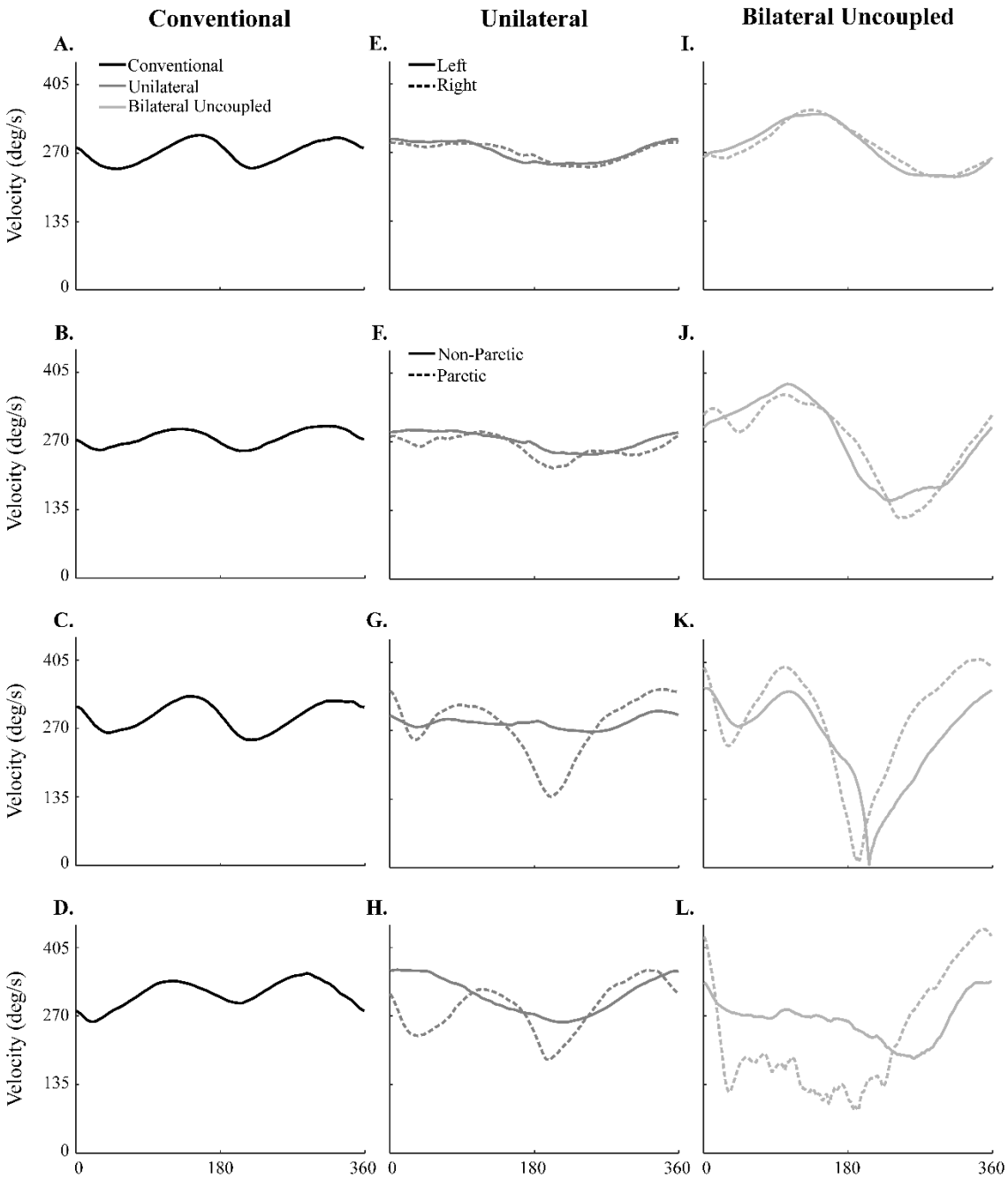

Figure A.1. Group velocity data from control participants and each stroke subgroup. Group ensemble average velocity data are shown for A-D) conventional (black lines), E-H) unilateral (dark gray lines), and I-L) bilateral uncoupled (light gray lines) pedaling for control participants (top row) and for each stroke subgroup as defined during bilateral uncoupled pedaling: the stroke subgroup who displayed an exaggerated version of the control strategy (2nd row), the stroke subgroup where one limb stopped pedaling while the other advanced the crank (3rd row), and the stroke subgroup with no evidence of a reciprocal, alternating strategy between limbs (4th row). Data are shown for both the left and right limb of control participants and the paretic and non-paretic limb of participants with stroke. For conventional pedaling, data are only shown for one limb because they were mechanically coupled. For unilateral pedaling, data for each leg are shown together despite being from different conditions.

A.2 Analysis methods

Matlab scripts and functions (presented in order of use)

Matlab script or function	Purpose
Data Collection Script	Parent script that calls different functions for processing.
AllDataInputter	Takes data file and outputs position, velocity, and EMG.
posrel	Calculates the time relative position and velocity.
Dependent Measures Script	Outputs dependent measures used in this study

***Data Collection Script for Stroke Subjects*:** this script will process position, velocity, acceleration, and torque signals. The outputs of this script are saved to the subject's individual folder.

```
clear
%Adjust these inputs to reflect the characteristics of each subject.
global side emg_gain P_leg
path = 'C:\Users\clela\Documents\_SSI_Lab\Split Crank\Stroke Subjects\ST017\Day 2\';
S_n = 'ST017'; %subject number
D_n = '2'; %day number
P_leg = 'R'; %Define which leg is the P leg
R_n = '2'; %run number (1 or 2). These are determined by whether M or NM was 1st
L_lvl = 'M'; %load level for BC condition
B_lvl_np = '8'; %band level - NP leg
B_lvl_p = '6'; %band level - P leg
emg_gain=1000;
%%%%%%%%%%%%%%%%%%%%%%%%%%%%%%%%%%%%%%%%%%%
% Creates the file names that we will need to access the needed data.
BC_file = ['SC ',S_n,'_',D_n,'_BC_',L_lvl,'_',R_n,'.txt']; %Bilateral Coupled
Un_NP_file = ['SC ',S_n,'_',D_n,'_NP_',B_lvl_np,'_',R_n,'.txt']; %Unilateral NP Leg
Un_P_file = ['SC ',S_n,'_',D_n,'_P_',B_lvl_p,'_',R_n,'.txt']; %Unilateral P Leg
BUC_file = ['SC ',S_n,'_',D_n,'_BUC_',R_n,'.txt']; %Bilateral Uncoupled
%%%%%%%%%%%%%%%%%%%%%%%%%%%%%%%%%%%%%%%%%%%
%This first portion of the script will output 9 variables calculated in AllDataInputter:
%1) & 2) newcycle = the locations where new revolutions begin (L and R).
%3)  pos = the position trace transformed to degrees. 1 = time, 2 = L pos, 3 = R pos
%4) wave_cumm = cumulative position trace 1 = L pos, 2 = R pos
%5) vel = velocity. 1 = time, 2 = L vel, 3 = R vel
%5) accel = acceleration. 1 = time, 2 = L accel, 3 = R accel
%6) vel_bins = velocity binned into 360 degrees. 1 = L vel, 2 = R vel
%7) accel_bins = acceleration binned into 360 degrees. 1 = L accel, 2 = R accel
%8) emg_bins = EMG. 1 = NP TA, 2 = NP MG, 3 = NP RF, 4 = NP BF, 5 = P TA, 6 =
```

```
%P MG, 7 = P RF, 8 = P BF;
%Bilateral Coupled
side = 'Both';
[ncBcNP,ncBcP,pBc,cpBc,vBc,aBc,vBc_bins,vBc_std,aBc_bins,aBc_std,eBc_bins,...
   eBc_std,tBc_bins,tBc_std]=AllDataInputter(path,BC_file);
%Unilateral
side = 'Non-Paretic';
[ncUnNPnp,ncUnNPp,pUnNP,cpUnNP,vUnNP,aUnNP,vUnNP_bins,vUnNP_std,aUnNP
_bins,...
   aUnNP_std,eUnNP_bins,eUnNP_std,tUnNP_bins,tUnNP_std]...
   =AllDataInputter(path,Un_NP_file);
side = 'Paretic';
[ncUnPnp,ncUnPp,pUnP,cpUnP,vUnP,aUnP,vUnP_bins,vUnP_std,aUnP_bins,aUnP_std,
...
   eUnP_bins,eUnP_std,tUnP_bins,tUnP_std]...
   =AllDataInputter(path,Un_P_file);
%Bilateral Uncoupled
side = 'Both';
[ncBuNP,ncBuP,pBu,cpBu,vBu,aBu,vBu_bins,vBu_std,aBu_bins,aBu_std,eBu_bins,...
   eBu_std,tBu_bins,tBu_std]...
   =AllDataInputter(path,BUC_file);
%%%%%%%%%%%%%%%%%%%%%%%%%%%%%%%%%%%%%%%%%%%%%%%%%%%%%%%%
%Calculate time relative position and velocity using function pos_rel.
Bu_av_rev_np=[];Bu_av_rev_p=[];Bu_av_revs_np=[];Bu_av_revs_p=[];...
   Bu_av_vel_np=[];Bu_av_vel_p=[];Bu_av_vels_np=[];Bu_av_vels_p=[];
for i = [1,4,5,7:22,24,25]
   [Bu_av_rev_np(:,:,i),Bu_av_rev_p(:,:,i),Bu_av_revs_np{i},Bu_av_revs_p{i},...
      Bu_av_vel_np(:,:,i),Bu_av_vel_p(:,:,i),Bu_av_vels_np{i},Bu_av_vels_p{i}]...
      = pos_rel(cpBu{i},vBu{i},ncBuNP{i},ncBuP{i});
end
```

function AllDataInputter: this function will input from the file, process the data, and output the desired variables listed above.

```
function [newcyclel,newcycler,pos,wave_cumm,vel,accel, vel_std,...
        accel_std,emg_bins,emg_std] = AllDataInputter(path,file)
%% Import and preliminary setup of data.
% Load data file. Then determine how many variables are included in the file.
global side emg_gain P_leg
input=importdata([path file],'\t');
[~,n]=size(input.data);
bin_size=1;
newcycler=[];newcyclel=[];pos=[];wave_cumm=[];vel=[];accel=[];vel_bins=[];
vel_std=[];accel_bins=[];accel_std=[];emg_bins=[];emg_std=[];
tq_std=[];wave4=[];
```

```
%Input all data from each side. Here we input the position, EMG, and TQ data. Velocity
data is not inputted because the optical encoders cannot detect negative velocities.
Instead, we will calculate velocity and acceleration from the position trace.
wave = input.data(:,[1 4 2]); %time & pos
wave(:,2) = abs(wave(:,2)-max(wave(:,2))); %Flip the left position trace so it is the same
direction as the right leg.
wave3 = input.data(:,[10 11 12 13 6 7 8 9]); %EMG
if n == 15 %If the file has this many variables, TQ was collected.
   wave4 = input.data(:,[15 14]); %TQ
end
%If the paretic leg is the left leg, we are going to swap the left and right signals. This puts
it so the NP leg is always the first column, and the P leg is always the second column.
if P_leg == 'L'
   wave(:,[3,2])=wave(:,[2,3]);
   wave3(:,[5,6,7,8,1,2,3,4])=wave3(:,[1,2,3,4,5,6,7,8]);
   if isempty(wave4)==0
      wave4(:,[2,1])=wave4(:,[1,2]);
   end
end
%Bad point elimination. Find points in the position trace that are not too close or distant
from the previous point (mistakes). These points are kept. This is performed for both
sides or just one side, depending on what the condition is. Corrects problems found at the
pedaling anterior transition.
if strcmp(side,'Both') || strcmp(side,'Left') || strcmp(side,'Non-Paretic')
   len = length(wave(:,2));
   diffs = abs(wave(2:len,2)-wave(1:len-1,2));
   mwave = diffs>.05 & diffs<4.9;
   locs = find(mwave);
   wave(locs,2) = 0;
end
if strcmp(side,'Both') || strcmp(side,'Right') || strcmp(side,'Paretic')
   len2 = length(wave(:,3));
   diffs2 = abs(wave(2:len2,3)-wave(1:len2-1,3));
   mwave2 = diffs2>.05 & diffs2<4.9;
   locs2 = find(mwave2);
   wave(locs2,3) = 0;
end
%Determine when new revolutions occur.
pos=wave(:,1);
if strcmp(side,'Both') || strcmp(side,'Left') || strcmp(side,'Non-Paretic')
   for i=1:size(wave(:,2),1)-1
      if (abs(wave(i,2)-wave(i+1,2)))>.1
         newcyclel=[newcyclel;i+1];
      end
   end
   %Convert volts to degrees
```

```
    wave(:,2) = wave(:,2)+min(wave(:,2));
    wave(:,2) = wave(:,2)/max(wave(:,2))*359;
    pos1(:,1) = round(wave(:,2)); %rounded degrees
    pos(:,2)=pos1;
    pos(:,3)=0;
end
if strcmp(side,'Both') || strcmp(side,'Right') || strcmp(side,'Paretic')
    for i=1:size(wave(:,3),1)-1
        if (abs(wave(i,3)-wave(i+1,3)))>.1
            newcycler=[newcycler;i+1];
        end
    end
    wave(:,3) = wave(:,3)+min(wave(:,3));
    wave(:,3) = wave(:,3)/max(wave(:,3))*359;
    pos2(:,1) = round(wave(:,3));
    pos(:,3)=pos2;
end
%%%%%%%%%%%%%%%%%%%%%%%%%%%%%%%%%%%%%%%%%%%%%%%%
% Calculate velocity and acceleration from position trace. First, we create a cumulative
position trace. This works by using the markers of when new cycles begin. Every time we
get to a data point in the position trace where a new cycle begins, we add the cumulative
position from the point before that, and so on until we reach the end of the pos trace.
wave_cumm=zeros(length(wave),2);
ntr=length(newcycler);ntl=length(newcyclel);
if strcmp(side,'Both') || strcmp(side,'Left') || strcmp(side,'Non-Paretic')
    wave_cumm(1:newcyclel(1)-1,1)=wave(1:newcyclel(1)-1,2)-wave(1,2); %The
    %beginning values are taken directly from the pos trace.
    for i = 1:ntl
        if i<ntl && wave(newcyclel(i),2)<300
            wave_cumm(newcyclel(i):(newcyclel(i+1)-
            1),1)=wave(newcyclel(i):(newcyclel(i+1)-1),2)...
                +wave_cumm((newcyclel(i)-1),1);
        elseif i<ntl && wave(newcyclel(i),2)>=300
            wave_cumm(newcyclel(i):(newcyclel(i+1)-1),1)=wave_cumm((newcyclel(i)-
            1),1)...
                -(360-wave(newcyclel(i):(newcyclel(i+1)-1),2));
        elseif i==ntl && wave(newcyclel(i),2)<300 %If we reach the last marker of a cycle,
then we add it on
            wave_cumm(newcyclel(i):length(wave),1)=wave(newcyclel(i):length(wave),2)...
                +wave_cumm((newcyclel(i)-1),1);
        elseif i==ntl && wave(newcyclel(i),2)>=300
            wave_cumm(newcyclel(i):length(wave),1)=wave_cumm((newcyclel(i)-1),1)...
                -(360-wave(newcyclel(i):length(wave),2));
        end
    end
end
```

```
if strcmp(side,'Both') || strcmp(side,'Right') || strcmp(side,'Paretic')
    wave_cumm(1:newcycler(1)-1,2)=wave(1:newcycler(1)-1,3)-wave(1,3);
    for i = 1:ntr
        if i<ntr && wave(newcycler(i),3)<300
            wave_cumm(newcycler(i):(newcycler(i+1)-
            1),2)=wave(newcycler(i):(newcycler(i+1)-1),3)...
                +wave_cumm((newcycler(i)-1),2);
        elseif i<ntr && wave(newcycler(i),3)>=300
            wave_cumm(newcycler(i):(newcycler(i+1)-1),2)=wave_cumm((newcycler(i)-
            1),2)...
                -(360-wave(newcycler(i):(newcycler(i+1)-1),3));
        elseif i==ntr && wave(newcycler(i),3)<300
            wave_cumm(newcycler(i):length(wave),2)=wave(newcycler(i):length(wave),3)...
                +wave_cumm((newcycler(i)-1),2);
        elseif i==ntr && wave(newcycler(i),3)>=300
            wave_cumm(newcycler(i):length(wave),2)=wave_cumm((newcycler(i)-1),2)...
                -(360-wave(newcycler(i):length(wave),3));
        end
    end
end
%Calculate velocity.
vel1=zeros(length(wave_cumm),2);
for j=[1 2]
    for i=2:(length(wave_cumm)-1)
        vel1(i,j)= ((wave_cumm(i+1,j)-wave_cumm(i-1,j))/(2*0.0005));
    end
end
%Follow this up by filtering at a very low frequency to reveal the basic shape for the
velocity. 20 Hz filter.
[b,a] = butter(2,20/(2000/2), 'low');
vel(:,1)=pos(:,1);
for i=[1 2]
    vel(:,i+1)=filtfilt(b,a,vel1(:,i));
end
%This will then determine the acceleration from the calculated velocity trace.
accel=zeros(length(vel),3);
accel(:,1)=pos(:,1);
for j=[2 3]
    for i=2:(length(vel)-1)
        accel(i,j) = ((vel(i+1,j)-vel(i-1,j))/(2*0.0005));
    end
end
%%%%%%%%%%%%%%%%%%%%%%%%%%%%%%%%%%%%%%%%%%%%%%%%%%%%%%%%%%%%
%% Process EMG data
[~,NoEMGch]=size(wave3);
```

```
%First, this will convert the EMG values to mV.  Then it will take each EMG channel
and detrend, or set the DC component of the signal to 0. Then it takes the absolute value
to remove negative portions of the signal.
[b,a] = butter(4,25/(2000/2),'low'); %25 Hz LPF.
for i = 1:NoEMGch;
   wave3(:,i) = wave3(:,i).*1000/emg_gain;
   wave3(:,i) = detrend(wave3(:,i));
   wave3(:,i) = abs(wave3(:,i));
   wave3(:,i) = filtfilt(b,a,wave3(:,i));
end
%EMG binning
emg_bins=zeros(360,NoEMGch);emg_std=zeros(360,NoEMGch);
if strcmp(side,'Left') || strcmp(side,'Non-Paretic')
   for i = 1:NoEMGch
      tempemg = wave3(:,i);
      for d = 0:bin_size:359
         emgmask = pos(:,2)==d; %Locations in the data where the degree is 1-360
         bin = tempemg.*emgmask; %Multiply by mask, values not in this degree are 0
         emg_bins(d+1,i) = sum(bin)/(length(find(bin))); %Takes the total value divided
         by the number of indices with a nonzero value (average value at that degree)
         emg_std(d+1,i) = std(bin(find(bin)));
      end
   end
   for k = 5:8
      emg_bins(:,k)=circshift(emg_bins(:,k),180,1);
      emg_std(:,k)=circshift(emg_std(:,k),180,1);
   end
elseif strcmp(side,'Right') || strcmp(side,'Paretic')
   for i = 1:NoEMGch
      tempemg = wave3(:,i);
      for d = 0:bin_size:359
         emgmask = pos(:,3)==d;
         bin = tempemg.*emgmask;
         emg_bins(d+1,i) = sum(bin)/(length(find(bin)));
         emg_std(d+1,i) = std(bin(find(bin)));
      end
   end
   for k = 1:4
      emg_bins(:,k)=circshift(emg_bins(:,k),180,1);
      emg_std(:,k)=circshift(emg_std(:,k),180,1);
   end
elseif strcmp(side,'Both')
   for i = 1:(NoEMGch/2)
      tempemg = wave3(:,i);
      tempemg2 = wave3(:,i+4);
      for d = 0:bin_size:359
```

```
            emgmask = pos(:,2)==d;
            emgmask2 = pos(:,3)==d;
            bin = tempemg.*emgmask;
            bin2 = tempemg2.*emgmask2;
            emg_bins(d+1,i) = sum(bin)/(length(find(bin)));
            emg_bins(d+1,i+4) = sum(bin2)/(length(find(bin2)));
            emg_std(d+1,i) = std(bin(find(bin)));
            emg_std(d+1,i+4) = std(bin2(find(bin2)));
        end
    end
end
```

function pos_rel: this function determines the average, time relative, position and velocity trace for the ipsilateral limb. It also determines what the contralateral limb was doing the average revolution of the ipsilateral limb. Essentially, the script uses the cumulative position trace and transition markers to determine where every revolution has occurred. It then splits up all acceptable revolutions into 500 relative data points.

```
function [av_rev_np,av_rev_p,av_revs_np,av_revs_p,av_vel_np,av_vel_p,...
    av_vels_np,av_vels_p] = pos_rel(cpos,vel,trans_np,trans_p)
%The cumulative position trace starts at 0. So, we need to use the index of when the first transition point is to determine where 0 degrees actually is for each leg. This extracts only data points from the cumulative position trace that lie between the first and last transition markers.Before and after these markers should not contain a full revolution, so they are discarded.
cp_np=cpos(trans_np(1):(trans_np(end)-1),:);
vel_np=vel(trans_np(1):(trans_np(end)-1),2:3);
cp_p=cpos(trans_p(1):(trans_p(end)-1),:);
vel_p=vel(trans_p(1):(trans_p(end)-1),2:3);
%The first data point for each leg is the first 0 degree position. So, the value at this location is subtracted from all points to shift the values down to their real position.
cp_np(:,1)=cp_np(:,1)-cp_np(1,1);
cp_p(:,2)=cp_p(:,2)-cp_p(1,2);
%For the contralateral limb, it is a bit more complicated. We find the first transition point larger than the first transition point for the ipsilateral limb. This is subtracted from all data points, which would create a negative number, so 360 is added.
for i = 1:length(trans_p)
    if trans_p(i)>trans_np(1)
        cp_np(:,2)=cp_np(:,2)-cpos(trans_p(i),2)+360;
        break
    end
end
for i = 1:length(trans_np)
    if trans_np(i)>trans_p(1)
        cp_p(:,1)=cp_p(:,1)-cpos(trans_np(i),1)+360;
```

```
        break
    end
end
%Using the position at this first position point, we fill find the index where the position first reaches +360 degrees from that point. Regardless of what happens between 0 and +360, we know that a full revolution has occurred at this point. After we reach +360, a new revolution has started, even if the subject pedals backwards. %We then use multiples of 360 to split up the data into every individual revolution.
revs_np=[];rev=360;k=1;m=1;
for j = 1:(length(cp_np)-1)
   if cp_np(j,1) < rev*k && cp_np(j+1,1) > rev*k
      revs_np{k}=cp_np(m:j,:);
      vels_np{k}=vel_np(m:j,:);
      k=k+1;
      m=j+1;
   end
end
revs_p=[];rev=360;k=1;m=1;
for j = 1:(length(cp_p)-1)
    if cp_p(j,2) < rev*k && cp_p(j+1,2) > rev*k
       revs_p{k}=cp_p(m:j,:);
       vels_p{k}=vel_p(m:j,:);
       k=k+1;
       m=j+1;
    end
end
%Bring every revolution to a 0-360 range by subtracting the offset at the start of the revolution. This will also take care of backwards pedaling by turning those positions into negative degrees. For the contralateral leg, it's more complicated. We have to determine how many degrees have been completed since the last revolution. Then, we adjust for if the position went past 360 degrees. This makes it so that the starting position for the contralateral leg is going to be non-zero, but will be < 360.
revs_np_adj=[];revs_np_adj{1}=revs_np{1};
for n=2:length(revs_np)
    revs_np_adj{n}(:,1)=revs_np{n}(:,1)-360*(n-1);
    diff=revs_np{n}(1,2)-revs_np{n-1}(1,2);
    newang=revs_np_adj{n-1}(1,2)+diff;
    if newang < 360
       revs_np_adj{n}(1,2)=newang;
       revs_np_adj{n}(2:end,2)=revs_np{n}(2:end,2)-(revs_np{n}(1,2)-newang);
    elseif newang > 360
       newang2=newang;
       while newang2 > 360
          newang2=newang2-360;
       end
       revs_np_adj{n}(1,2)=newang2;
```

```
        revs_np_adj{n}(2:end,2)=revs_np{n}(2:end,2)-(revs_np{n}(1,2)-newang2);
    end
end
revs_p_adj=[];revs_p_adj{1}=revs_p{1};
for n=2:length(revs_p)
    revs_p_adj{n}(:,2)=revs_p{n}(:,2)-360*(n-1);
    diff=revs_p{n}(1,1)-revs_p{n-1}(1,1);
    newang=revs_p_adj{n-1}(1,1)+diff;
    if newang < 360
        revs_p_adj{n}(1,1)=newang;
        revs_p_adj{n}(2:end,1)=revs_p{n}(2:end,1)-(revs_p{n}(1,1)-newang);
    elseif newang > 360
        newang2=newang;
        while newang2 > 360
            newang2=newang2-360;
        end
        revs_p_adj{n}(1,1)=newang2;
        revs_p_adj{n}(2:end,1)=revs_p{n}(2:end,1)-(revs_p{n}(1,1)-newang2);
    end
end
%Now, for every revolution, we determine how long the revolution was, and what is
1/500th of the revolution. We can then break up each revolution into 500 relative points.
temp=[];temp2=[];temp3=[];temp4=[];
for i=1:length(revs_np_adj)
    tt=length(revs_np_adj{i}); %total number of points for the cycle of interest.
    pp=tt/500; %The interval of time that represents 1/500th of that cycle.
    for k=1:500
        temp{i}(:,k)=revs_np_adj{i}(((k-1)*pp+1):k*pp,1);
        temp2{i}(:,k)=revs_np_adj{i}(((k-1)*pp+1):k*pp,2);
        temp3{i}(:,k)=vels_np{i}(((k-1)*pp+1):k*pp,1);
        temp4{i}(:,k)=vels_np{i}(((k-1)*pp+1):k*pp,2);
    end
end
temp5=[];temp6=[];temp7=[];temp8=[];
for i=1:length(revs_p_adj)
    tt=length(revs_p_adj{i});
    pp=tt/500;
    for k=1:500
        temp5{i}(:,k)=revs_p_adj{i}(((k-1)*pp+1):k*pp,2);
        temp6{i}(:,k)=revs_p_adj{i}(((k-1)*pp+1):k*pp,1);
        temp7{i}(:,k)=vels_p{i}(((k-1)*pp+1):k*pp,2);
        temp8{i}(:,k)=vels_p{i}(((k-1)*pp+1):k*pp,1);
    end
end
%Find the average position at all 500 relative data points, for each revolution
individually, to determine what each revolution looked like for that person.
```

```
for j=1:length(temp)
   av_revs_np(j,:,1)=mean(temp{j},1);
   av_revs_np(j,:,2)=mean(temp2{j},1);
   av_vels_np(j,:,1)=mean(temp3{j},1);
   av_vels_np(j,:,2)=mean(temp4{j},1);
end
for j=1:length(temp5)
   av_revs_p(j,:,2)=mean(temp5{j},1);
   av_revs_p(j,:,1)=mean(temp6{j},1);
   av_vels_p(j,:,2)=mean(temp7{j},1);
   av_vels_p(j,:,1)=mean(temp8{j},1);
end
%Average across each revolution to find a representative revolution.
av_rev_np(:,:)=mean(av_revs_np,1);
av_rev_p(:,:)=mean(av_revs_p,1);
av_vel_np(:,:)=mean(av_vels_np,1);
av_vel_p(:,:)=mean(av_vels_p,1);
```

Dependent Measures Script: outputs dependent measures used in this study.

```
%%%%%%%%%%%%%%%%%%%%%%%%%%%%%%%%%%%%%%%%%%%%
%Extract mean, std, max, min, and modulation index from EMG. Output is sent to an
array. Rows are 1) mean, 2) SD, 3) max, 4) min, 5) modulation index. Columns are
muscle activity for 1) BC, 2) UN, and 3) BU.
emg{1}=eBc_bins(:,:);
emg{2}(:,1:4)=eUnNP_bins(:,1:4);
emg{2}(:,5:8)=eUnP_bins(:,5:8);
emg{3}=eBu_bins(:,:);
for i = 1:3
   stroke_evalues{1,i}=mean(emg{i}(:,:));
   stroke_evalues{2,i}=std(emg{i}(:,:));
   stroke_evalues{3,i}=max(emg{i}(:,:));
   stroke_evalues{4,i}=min(emg{i}(:,:));
   stroke_evalues{5,i}=(max(emg{i}(:,:))-min(emg{i}(:,:)))./max(emg{i}(:,:))*100;
end
%%%%%%%%%%%%%%%%%%%%%%%%%%%%%%%%%%%%%%%%%%%%
%Calculate PCI
for i = [1,4,5,7:22,24,25]
   BU{i}=abs(pBu{i}(:,2)-pBu{i}(:,3)); %Subtract pedal positions
   for j=1:length(BU{i}) %Correction for circularity of values. Minimum absolute diff.
      if BU{i}(j,1)>180
         BU{i}(j,1)=360-BU{i}(j,1);
      end
   end
   phase_acc(i,1)=((mean(abs(BU_rev{i}-180)))/180)*100; %Phase accuracy
   phase_con(i,1)=std(BU_rev{1,i})/mean(BU_rev{1,i})*100; %Phase consistency
```

```
    pci(i,1)= phase_con(i,1) + phase_acc(i,1);
end
%%%%%%%%%%%%%%%%%%%%%%%%%%%%%%%%%%%%%%%%%%%%
%Calculate mean and COV of velocity from the relative traces.
for k=[1,4,5,7:22,24,25]
    vel(k,1)=mean(Bc_av_vel_l(:,1,k));
    vel(k,2)=mean(Bc_av_vel_r(:,2,k));
    vel(k,3)=mean(Un_av_vel_l(:,1,k));
    vel(k,4)=mean(Un_av_vel_r(:,2,k));
    vel(k,5)=mean(Bu_av_vel_l(:,1,k));
    vel(k,6)=mean(Bu_av_vel_r(:,2,k));
    cov(k,1)=(std(Bc_av_vel_np(:,1,k))/mean(Bc_av_vel_np(:,1,k)))*100;
    cov(k,2)=(std(Bc_av_vel_p(:,2,k))/mean(Bc_av_vel_p(:,2,k)))*100;
    cov(k,3)=(std(Un_av_vel_np(:,1,k))/mean(Un_av_vel_np(:,1,k)))*100;
    cov(k,4)=(std(Un_av_vel_p(:,2,k))/mean(Un_av_vel_p(:,2,k)))*100;
    cov(k,5)=(std(Bu_av_vel_np(:,1,k))/mean(Bu_av_vel_np(:,1,k)))*100;
    cov(k,6)=(std(Bu_av_vel_p(:,2,k))/mean(Bu_av_vel_p(:,2,k)))*100;
end
```

APPENDIX B: SUPPLEMENT TO CHAPTER 3

This appendix is a supplement to Chapter 3. Included are additional results that may be of interest. Also included is a detailed description of the methods used to evoke and analyze interlimb cutaneous reflexes.

B.1 Additional results

Introduction

As briefly described in Chapter 3, I collected information on walking in stroke survivors. Some additional analyses and results from walking trials were not included in that chapter. We also collected some information about symmetry of standing. These analyses are included here to provide further characterization of walking and standing after stroke.

Methods

Subjects performed two 60 second quiet standing trials. Subjects were asked to stand quietly with their arms at their sides while ground reaction force data were acquired from both belts of a split belt instrumented treadmill (FIT, Bertec Corporation, OH, USA). Mean GRFz was determined for each limb. As described, subjects also performed walking trials a self-selected comfortable walking speed. Two 60 second trials were performed. Bilateral ground reaction forces in the vertical (GRFz), anterior/posterior (GRFx), and left/right (GRFy) directions were measured with force plates under each belt. Subjects wore a safety harness with no body-weight support. Although encouraged

to walk without support, subjects were permitted to use handrails as needed to ensure safety. As detailed in Chapter 3, we measured interlimb coordination with PCI and measured propulsive and braking forces. In addition, we assessed step, stance, and swing times for each limb. Heel strike and toe-off events were identified as when GRFz exceeded or fell below 15 N. Using heel strike and toe-off event times, we calculated step, stance, and swing times for each limb. Step time was defined as the time between consecutive ipsilateral and contralateral heel strikes. Stance time was defined as the time between ipsilateral heel strikes and toe-offs. Swing time was defined as the time between ipsilateral toe-offs and heel strikes. Symmetry was calculated for step, stance, and swing times and for GRFz during standing trials:

$$\text{Symmetry (\%)} = \frac{\text{paretic}}{\text{non-paretic}} \times 100\%$$

A value of 100% represents equality between limbs.

Statistics

Step, stance, and swing times and GRFz were compared between limbs with paired t-tests and Wilcoxon signed rank test. Symmetry values were compared with 100% using one sample t-tests. The relation of symmetry values for stance and swing times and GRFz with dependent measures from Chapter 3 were performed with Pearson and Spearman correlations. Dependent measures for correlations were: $PCI_{walking}$, $PCI_{pedaling}$, $\%Propulsion_{walking}$, $\%Propulsion_{pedaling}$, $FM_{LEtotal}$, $FM_{LEmotor}$, Berg Balance

score, self-selected walking velocity, and interlimb cutaneous reflex amplitude for muscle-position combinations that had within or between group differences.

Results

Standing and walking data were analyzed from a subset of stroke survivors (n = 15). Data were excluded from 7 subjects because of loss to follow-up (n = 3), safety limitations that precluded treadmill walking (n = 3), and equipment malfunction (n = 1). Standing data were also available from one additional subject who experienced an equipment malfunction during walking trials. During static standing trials, ground reaction force (GRFz) was lower ($P = 0.02$) under the paretic limb [395 (101) N, 44%] than the non-paretic limb [499 (128) N, 56%].

During walking, an average of 80 (30) steps were analyzed per subject. Data were excluded from one significant outlier. For reference, group average GRF in the vertical and anterior/posterior directions are shown in Figure B.1. Step time was longer ($P = 0.002$) in the non-paretic [0.80 (0.19) s] than the paretic limb [0.69 (0.13) s]. Stance time was shorter ($P = 0.001$) in the paretic [1.02 (0.21) s] than the non-paretic limb [1.11 (0.24) s]. Swing time was longer ($P = 0.001$) in the paretic [0.46 (0.13) s] than the non-paretic [0.37 (0.09) s] limb. Correspondingly, the step, stance, and swing time symmetry values were different from 100% ($P \leq 0.002$).

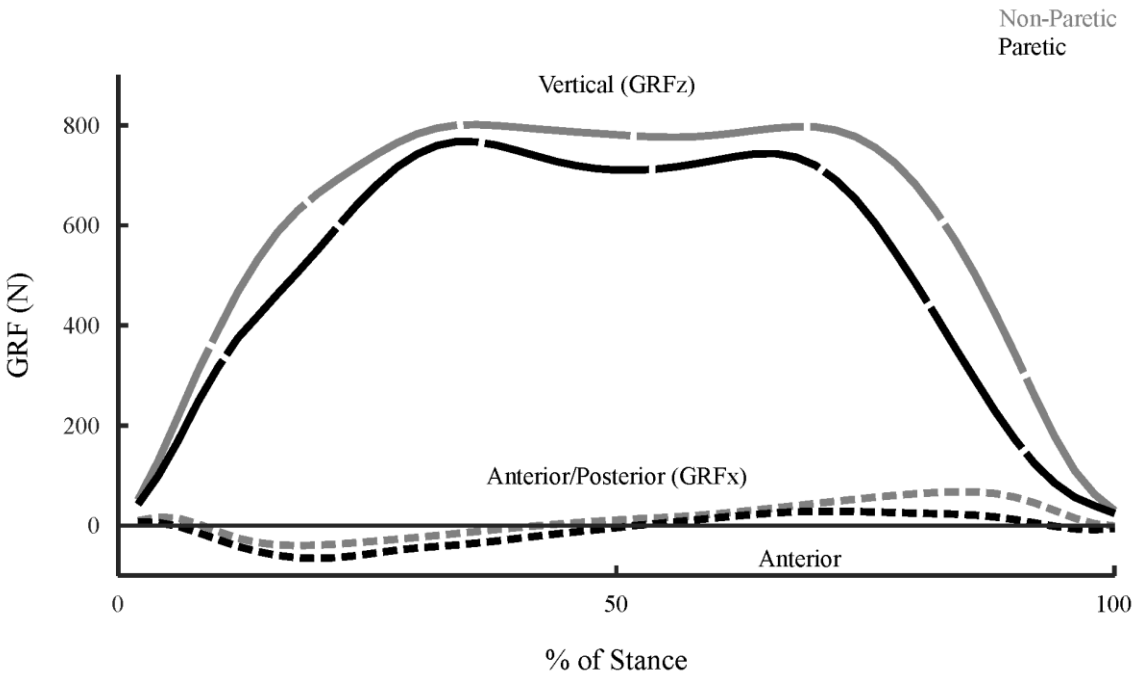

Figure B.1. Group average ground reaction force in the vertical and anterior/posterior directions. GRFz values (long dash) and GRFx values (short dash) are shown for the average paretic (black) and non-paretic (medium gray) limbs from 0 – 100% of the stance phase. Note that the paretic limb produced lower GRFz values, more posterior GRFx, and less anterior GRFx. These differences are all consistent with the existence of compensation.

Shorter stance and longer swing times in the paretic limb were correlated with larger $PCI_{pedaling}$ ($R^2 \geq 0.28$, $P < 0.05$) and $PCI_{walking}$ ($R^2 \geq 0.76$, $P < 0.001$), smaller $\%Propulsion_{pedaling}$ ($R^2 \geq 0.30$, $P \leq 0.04$) and $\%Propulsion_{walking}$ ($R^2 \geq 0.52$, $P \leq 0.003$), smaller interlimb cutaneous reflexes in the paretic ST at the anterior transition ($R^2 \geq 0.46$, $P \leq 0.01$), and lower $FM_{LEtotal}$ and $FM_{LEmotor}$ ($R^2 \geq 0.27$, $P < 0.05$). GRFz during quiet standing was not correlated with any dependent measures.

Discussion

These results confirm what has been found previously. Stroke survivors have a longer swing time and shorter stance time in the paretic limb as compared to the non-paretic limb and controls (Brandstater et al., 1983; G. Chen et al., 2005; A. L. Hsu et al.,

2003; C. M. Kim & Eng, 2003; Olney et al., 1991; von Schroeder et al., 1995). These kinematic asymmetries are correlated with kinetic asymmetries (C. M. Kim & Eng, 2003; Olney & Richards, 1996). Altered swing and stance times in the paretic limb likely occur to reduce the amount of time the paretic limb must support the body (i.e. maintain balance) and to allow more ground contact time for the non-paretic limb, which produces the majority of the propulsive power.

The unique findings from these additional analyses were that individuals with greater asymmetries in stance and swing times had worse interlimb coordination, greater abnormalities in interlimb cutaneous reflexes, and more stroke-related disability. Relations with compensation and interlimb coordination were significant for both pedaling and walking. Because of the strong correlation of stance and swing symmetry with PCI, it is likely that asymmetry values provide an alternative measure of interlimb coordination. This is not surprising because both stance and swing times are calculated with heel strike times, which also forms the basis for PCI.

Given that stance and swing symmetry are alternative measures of interlimb coordination, these results support the relation of interlimb coordination with compensation and interlimb cutaneous reflexes. As with other dependent measures, reflex abnormality in ST near the anterior transition had the strongest relation with asymmetry values, reinforcing the importance of interlimb reflexes in bifunctional muscles at transition phases of pedaling. These results also support the finding that interlimb coordination and compensation are related across different locomotor tasks. In contrast, our measure of compensation during standing was not related to compensation, interlimb coordination, or reflexes from a locomotor task. Thus, although compensation is also

present during quiet standing, this form of the phenomenon likely has different proximal causes.

B.2 Stimulation methods for interlimb cutaneous reflexes

Included in this section is the Spike script used to elicit interlimb cutaneous reflexes during pedaling.

Spike functions (presented in order of use)

Spike function	**Purpose**
Variable definition	Defines variables before use.
InitVariables	Establishes subject type.
EstStartPoint	Defines subject and stimulation characteristics.
DoToolbar	Sets up interactive toolbar.
Idle	Calculates velocity, sends information to trigger stimulation.
Quit	Toolbar button to quit data collection.
Start	Toolbar button to start sampling.
Stop	Toolbar button to stop sampling.
InitSample	Reads trial information to prepare to start.
Setup	Dialogue to enter stimulation information.
Angles	Randomizes stimulation angle.
CR_Sequencer	Sends signal to stimulate

Variable definition: sets up all variables used in Spike.

```
var daten$, fpath$, newdir$, v, v2%, v1%, ret, ret1, vh%, v10%, ok%, ok2%, code%,
        dummy[15], eTime, gdec, st%, len%, grpmax%;
var sortkey%; 'Randomize w/in groups or the PASS/STIM trials w/in an angle.
var ntrial%, nptrial; 'Number of STIM trials/angle.
var nptrial%; 'Number of PASS trials/angle.
var pt; 'Percentage of trials that are PASS trials.
var passorstim%; 'Whether CURRENT trial is a PASS or STIM trial.
var nang%; 'Number of total angles (max: 15).
var ang[15]; 'Stores the angles to be tested (e.g. [0 90 180 270...]).
var gfa%[15]; 'Tells which group each angle (1-15) comes from (e.g. [1 1 1 1 0 0 0 0 0 0
                0 0 0 0 0]. 4 angles all in group 1.
var napgr%[15]; 'Number of angles/group, of index [] (e.g. [4 0 0 0 0 0 0 0 0 0 0 0 0 0 0].
```

```
                    Group 1 has 4 angles, other groups have 0.
var rannum[1500]; 'Store 1500 values that are randomized and used to randomize angle,
                    PASS/STIM, and leg.
var angind%[1500]; 'Angle index # from 'ang' (e.g. [0 0 0 0 1 1 1 1...]. 4 stims @ index 0
                    (0 degrees), 4 stims @ index 1 (90 degrees))...
var angtr[1500]; 'Angle @ which to stim. Combines 'angind' and 'ang' (e.g. [0 0 0 0 90 90
                    90 90...])
var numb%[1500]; 'Trial/index w/in each angle (e.g. [0 1 2 3 0 1 2 3...]) 0-3rd trial @ 0
                    degrees, followed by 0-3rd trial @ 90 degrees.
var stim$[1500]; 'Whether trial is PASS or STIM (e.g. ["Stim" "Pass" "Stim" "Stim"...]
var leg$[1500]; 'Whether each trial is 'R' or 'L' leg.
var angler%, anglel%; 'What is the CURRENT angle to be stimulated next for R or L
var v1max%, v1min%; 'max and min angle values of v1% for a group.
var stype$[2], stype1$; 'Subject type: "Control" or "Stroke"
var stype%; 'Subject type: 0 = Control, 1 = Stroke
var snumb%; 'Subject code number.
var numleg% := 2; 'Number of legs to be stimulated.
var sTime; 'The last time we looked at the idle routine
var first% := 0; 'variable to keep track of 1st pass through Idle routine with
SampleSeqVar(5) set
var time2 := 0; 'variable to store the relative time to when SampleSeqVar(5) is set to 1
var initial% := 0; 'which sample sequence, initial =0 or matching with EMC =1
var datai%; 'stores view handle for the data file in the initial sample sets
var vgrp%; 'used to pass selected group number for initial trials
var vind%; 'used to pass the angle index for intial trials
var angrange:= 3; 'range of angle over which to match
var lastTopTime := 0; 'Time of last top of crank
var lastIdleTime := 0; 'Maxtime at last call to idle function
var ttChan% := 1; 'Chan number of crank top times. In other words the R_POS channel.
InitVariables(); 'Before interacting with any buttons set the options for subject type.
EstStartPoint(); 'Then determine if the sampling protocol has already been determined
                    and saved in a .txt file, or if a new protocol should be created.
HideAll(); 'Hide all toolbars etc
ToolbarVisible(1); 'Make toolbar visible always
DoToolbar(); 'Make the Toolbar visible so buttons can be interacted with.
RestoreAll(); 'Put all toolbars back in view.
halt;
```

Func InitVariables()*:* this function is called from the main program and establishes the values for some of the arrays used in defining the characteristics of the subject and the testing. Essentially, it is providing options for forced choice options throughout the script.

```
stype$[0] := "Control";
stype$[1] := "Stroke";
```

```
end;
```

Func EstStartPoint(): this function is called from the main program and creates an interaction with the user to first determine whether this is a new case or a pre-existing case. A pre-existing case means that the sampling protocol has already been selected for that subject. If it is a pre-existing case, the user selects the .txt file which defines that case. The global variables then used by many of the functions are initialized. The values of the global variables are displayed in the Log file. Note that the Log file is cleared before showing the values for the case.

```
v10% :=1;
ret := Query("Start with pre-existing case?");
if ret then 'If testing parameters have been defined, load the file and variables.
        v10% := 0;
        ret1 := FileOpen("",8); 'If 'Yes' is selected, then open a dialog box to load a .txt.
        if ret1<0 then 'If 'No' is selected, then Idle the system and end this if statement.
                Halt;
        endif;
        Read(ntrial%,sortkey%,nptrial%,pt); 'load global variables that define the
sampling protocol.
        Read(stype1$,snumb%);
        Read(gfa%[]);
        Read(ang[]);
        Read(angtr[]);
        Read(numb%[]);
        Read(angind%[]);
        Read(stim$[]);
   Read(leg$[]);
        FileClose();
        for v1% := 0 to 14      do 'This sets the number of angles in each group.
                docase
      case  gfa%[v1%]=1 then 'If angle is from group 1
                        napgr%[0] := napgr%[0] + 1; ‘Add to the count of angles in grp 1.
      case  gfa%[v1%]=2 then
                        napgr%[1] := napgr%[1] + 1;
      case  gfa%[v1%]=3 then
                        napgr%[2] := napgr%[2] + 1;
      case  gfa%[v1%]=4 then
                        napgr%[3] := napgr%[3] + 1;
      case  gfa%[v1%]=5 then
                        napgr%[4] := napgr%[4] + 1;
      case  gfa%[v1%]=6 then
                        napgr%[5] := napgr%[5] + 1;
      case  gfa%[v1%]=7 then
                        napgr%[6] := napgr%[6] + 1;
```

```
        case  gfa%[v1%]=8 then
                        napgr%[7] := napgr%[7] + 1;
        case  gfa%[v1%]=9 then
                        napgr%[8] := napgr%[8] + 1;
        case  gfa%[v1%]=10 then
                        napgr%[9] := napgr%[9] + 1;
        case  gfa%[v1%]=11 then
                        napgr%[10] := napgr%[10] + 1;
        case  gfa%[v1%]=12 then
                        napgr%[11] := napgr%[11] + 1;
        case  gfa%[v1%]=13 then
                        napgr%[12] := napgr%[12] + 1;
        case  gfa%[v1%]=14 then
                        napgr%[13] := napgr%[13] + 1;
        case  gfa%[v1%]=15 then
                        napgr%[14] := napgr%[14] + 1;
                endcase;
          next;
          nang% := ArrSum(napgr%[]);
          FrontView(LogHandle());
          EditSelectAll();
          EditClear();
          PrintLog("Number Trials/Angle = %d\n",ntrial%);
          PrintLog("Number Passes/Angle = %d\n",nptrial%);
          PrintLog("Number of Angles = %d\n",nang%);
          PrintLog("%s\n",stype1$);
          'Use the string variable to create the variable with actual values.
          if stype1$="Control" then
                  stype% := 0;
          else
                  stype% := 1;
          endif;

          PrintLog("Group\tAngle\tStimulate\tAngle Trial\tAngle Index\tLeg\n");
          for v := 0 to numleg%*nang%*(ntrial%+nptrial%)-1 do
                  PrintLog("%d\t%3.0f\t%s\t\t%d\t\t%d\t\t%s\n",
gfa%[angind%[v]],angtr[v], stim$[v], numb%[v], angind%[v], leg$[v]);
          next;
          FrontView(LogHandle());
          WindowVisible(3);
endif;
end;
```

proc DoToolbar(): this procedure sets up the Toolbar from which different operations are run. The number shows which toolbar button it is, in parentheses is the text shown on the toolbar, and the rest is the function that is called when the button is pressed.

```
ToolbarSet(0,"",Idle%); 'Call Idle%() which communicates with synchronization file.
ToolbarSet(1,"&Quit",Quit%); 'Set up toolbar buttons
ToolbarSet(2,"&Sample Start", Start%); 'Begin sampling.
ToolbarSet(3,"&Sample Stop", Stop%); 'Stop sampling.
ToolbarSet(4,"Initialize Sample", InitSample%); 'Identify group and other specifics
                                                    before data collection.
ToolbarSet(5,"Setup", Setup%); 'This button is the setup for the sampling.
ToolbarEnable(3,0); 'Disable "Sample stop" button
ToolbarEnable(2,0); 'Disable "Sample start" button
Toolbar("Press SAMPLE START to commence sampling", 1023); 'Wait here until quit is
                                                              pressed
end;
```

func Idle%(): the Idle routine calculates the cadence during pedaling and passes information about stimulation to the synchronization file. Variable initial% defines which phase.

```
var interval := 0;
var nextT := 0;
'This section is essentially so we can calculate and display the cadence during pedaling. It
also places a mark in a memory channel every time there is a TDC. 120 RPM is the limit
that this script can work to detect revolutions. Otherwise it will miss every other
revolution.
if ViewKind(datai%) = 0 then 'If the view is the time view.
        View(datai%); 'Don't change the view
        eTime := Maxtime(); 'The current time is the maximum time in the file.
   if (lastIdleTime < eTime) and (eTime > lastTopTime+0.5) then 'If current time is
                                    greater than the last idle time, and 0.5 s from the last TDC
                MemImport(ttChan%, 1, lastIdleTime, eTime, 3, 0.5, 0.1); 'Puts a mark in
        the memory channel as long as the value > 0.1 and is 0.5 s from the last mark.
                nextT := NextTime(ttChan%, lastTopTime); 'From the memory channel,
                                                set the next time as the last TDC time.
                if nextT > 0 then 'If the current TDC is not at the same time as the one
                                        before (we are still sampling)
                        interval := nextT - lastTopTime; 'Calculate the time between marks
        if interval > 0 then
                                    ToolBarText(Print$("Cadence = %8g RPM",
60.0/interval)); 'This calculates and displays the cadence.
        endif;
        lastTopTime := nextT; 'Set the last TDC time as the one we just dealt with.
                endif;
```

```
        endif;
    lastIdleTime := eTime; 'Also reset the last IdleTime
endif;
'This section passes stimulation information to the synchronization script and then
activates one of the synchronization buttons to allow stimulation.
if ViewKind(datai%) = 0 then 'If the view is in the time view
    View(datai%); 'Don't change the view
    if SampleStatus()=2 then 'If sampling is in progress
       if vind%=v1min% or (vind%>v1min% and SampleSeqVar(5)=1) then 'If this is the
first angle, OR it is a later angle in the group and we have been sampling already.
        if first%=0 then 'If this is the first pass through the Idle function.
            time2 := Seconds(); 'This is the time when we first pass through Idle function.
            first% := 1; 'Mark that we have passed through the Idle function once.
        endif;
        if vind% = v1max% + 1 then 'If finished all the angles in the group of interest
            Yield(1);
            Stop%(); 'Then stop sampling
            initial% := 0; 'Not sampling
            Message("Initial Sampling Done"); 'Give message that stopped sampling
            PrintLog("Angle Index = %d\n",vgrp%)
        endif
        if vind%=v1min% or ((Seconds()-time2) > 3.7) then 'If we are on the first angle
        OR it is longer than 3.7 seconds since we first passed through the Idle function.
            if stim$[vind%] = "Pass" then 'If the index for this trial is "Pass"
                code% := angind%[vind%]*10; 'Set code% value
                passorstim% := 0; 'Set stimtype to PASS
            else
                code% := angind%[vind%]*10 + 1; 'Otherwise set code
                passorstim% := 1; 'And set stimtype to STIM
            endif;
            if leg$[vind%] = "L" then
                anglel% := (32767/2)-angtr[vind%]*32767/720;
                SampleSeqVar(2,anglel%); 'Send this angle to the sequencer
                SampleSeqVar(4,passorstim%); 'Set the stimtype to Pass or Stim
                SampleSeqVar(6,code%); 'Set the marker channel.
                SampleSeqVar(5,0); 'Whether Spike is sampling
                SampleKey("L");
            else
                angler% := angtr[vind%]*32767/720; 'angle specified.
                SampleSeqVar(2,angler%); 'Send this angle to the sequencer
                SampleSeqVar(4,passorstim%); 'Set the stimtype to Pass or Stim
                SampleSeqVar(6,code%); 'Set the marker channel.
                SampleSeqVar(5,0); 'Whether Spike is sampling
                SampleKey("R");
            endif
            Seconds(0);
```

```
            first% := 0;
            vind% := vind% + 1;
          endif;
        endif;
    endif
endif;
return 1;
end;
```

func Quit%(): quit Spike

```
SampleStop(); 'Stop sampling
return 0; 'leave toolbar
end;
```

func Start%(): start sampling

```
SampleStart(); 'Start sampling
ToolbarEnable(5,0); 'Disable "Initial Sample" button
ToolbarEnable(3,1); 'Enable "Sample stop" button
ToolbarEnable(2,0); 'Disable "Sample start" button
ToolbarEnable(1,0); 'Disable "Quit" button
ToolbarText("Press SAMPLE STOP to stop sampling");
return 1;
end;
```

func Stop%(): stop sampling

```
var grp$;
var vx%,vset$;
SampleStop(); 'Stop sampling
if (datai%>0) and 'if no data in file, stop will close it
   (ViewKind(datai%) <> 0) then datai% := 0
endif;
if datai%>0 then View(datai%);
   grp$:=Str$(vgrp%);
endif;
ToolbarEnable(5,1); 'Enable "Init Sample" button
ToolbarEnable(3,0); 'Disable "Sample Stop" button
ToolbarEnable(1,1); 'Enable "Quit" button
ToolbarText("Choose Next step -");
initial% := 0;
return 1;
```

```
end;
```

Func InitSample%(): setup sampling characteristics

```
var ok%, v5%, grp$, grpmax%, vi%;
'Debug();
grpmax% := 0;
repeat
   grpmax% := grpmax% +1;
until nang%-ArrSum(napgr%[0:grpmax%]) = 0; 'This determines # of groups.
'ok% := FileOpen("C:\Users\1106clelanb\Desktop\Stimulation
Practice\BTC_2016.s2c",6);
'PrintLog("Code1 = %d\n", ok%);
vgrp% := 1;
DlgCreate("Select Group",0,0,60,7.5); 'Prompt for selecting the group.
DlgInteger(1,"Group Number", 1,grpmax%); 'Select group from which angles will be
selected
DlgReal(2,"Angle Range (+/- degrees)",1,50); 'Select the angle range
ok% := DlgShow(vgrp%,angrange);
v1min% := 0;
if vgrp% > 1 then 'If we are a group other than group 1
      v1min% := v1min% + (ntrial%+nptrial%)*ArrSum(napgr%[0:(vgrp%-
1)])*numleg%; This determines which angle position is the first for that group.
endif;
v1max% := v1min% + (ntrial%+nptrial%)*napgr%[vgrp%-1]*numleg% - 1; 'Determine
the angle position that will be last for the group.
PrintLog("v1min=  %d\n",v1min%);
vind% := v1min%; 'Initial angle.
time2 := 0;
first% := 0;
Seconds(0);
initial% := 2;
if ok%=1 then
        datai% := FileNew(0,1); 'Open up the data file window
   ttChan% := memChan(2);
   ChanShow(ttChan%);
        PrintLog("Code2 = %d\n", vh%);
        '*****************************************************************
        DrawMode(-1,2); 'Set draw mode to lines
        Window(0,0,100,100); 'Make data window in top bit of screen
        WindowVisible(3); 'Make the window visible and full size
        XRange(0,15); 'Show 15 seconds of data
        '*****************************************************************
        ToolbarEnable(3,0); 'Disable "Sample stop" button
        ToolbarEnable(2,1); 'Enable "Sample start" button
```

```
        ToolbarText("Press SAMPLE START to commence sampling");
endif;
return 1;
end;
```

Func Setup%(): creates a dialogue for the user to specify or modify the sampling protocol. The starting point is specified by the func EstStartPoint as either new or a user-selected pre-exisiting case. After specifying number of trials per angle, percentage PASS trials, the method to randomize, subject, and subject number, the user calls a sub-dialogue to actually specify the angles. The specification of the angles is handled in the func Angles%.

```
v10% := 0;
FrontView(LogHandle());
EditSelectAll();
EditClear();
DlgCreate("Front Page",0,0,120,20);
DlgInteger(1,"Number Trials/Angle",3,100,40); '3 - 100 trials per angle
DlgInteger(2,"Percentage Pass Trials", 0,100,40); '0 - 100 % pass trials
DlgList(3,"SortKey","Sort P/S in Angle|Sort Group",2,40);
DlgList(4,"Subject",stype$[],2,34); 'Control or stroke subject
DlgInteger(5,"Subject Number",0,99,40); 'Subject # from 0 - 99
for v1% := 6 to 20 do 'Sets up 15 boxes for angles
        DlgLabel(v1%,Print$("Angles in Group %d", v1%-5),60,v1%-5); 'Angles from
        DlgInteger(v1%+15, 3, 0, 15, 100, v1%-5); '0-15 angles is the max per group
next;
DlgButton(1,"&Angles",Angles%); 'Opens sub-dialogue to enter specific angle
'DlgAllow(0x3ff,0,Change%);
'stype1$ := "1"; 'DlgValue$(6);
ok% := DlgShow(ntrial%,pt,sortkey%,stype%,snumb%,dummy[],napgr%[]);
return 1; 'This leaves toolbar active
end;
```

Func Angles%(): this function is called from the button "Angles" in the dialog and provides the user with an interface to specify the angles for the case. It creates a random order over all the angles and the pass/stim input and then prints the resulting case to the Log file. Note that the Log file is not cleared before writing this data.

```
var grp:=1, v%:=0, v4%:=0, v3%:=0, v7%:=0, v6%:=0, numang%:=0, end%:=0;
var fpset% := 2; specifying path setting - "2" lets user set directory, "1" creates a
                    directory
for v% := 0 to 14  do
        napgr%[v%] := DlgValue(v%+21); 'Set  napgr[0:1:14] to the values from input
                spaces [26:1:40], (where the user types in the # of angles in each group).
```

```
next;
nang% := ArrSum(napgr%[]); 'The total # of angles is equal to the sum of the array. This
                                    is equal to the # of angles/group * # of groups
if nang%>15 then 'The # of angles is limited to 15, if more give a warning.
        Message("Number Angles Limited to 15")  ;
        nang% := 15; 'Set the total # of angles to 15.
endif;
for v% := 0 to 14 do
        if nang%-ArrSum(napgr%[0:v%+1]) < 0 then 'correction if negative number
      napgr%[v%] := nang% - ArrSum(napgr%[0:v%]); 'Make it a positive number
        endif;
next;
v% := 0;
gdec := napgr%[v%];

'This section creates the variable gfa, which tells which group each angle, in order, is
coming from.
repeat
   if gdec=0 then 'If there are no angles in a group, then move to the next and set gdec.
      v% := v% + 1;
      gdec := napgr%[v%];
      grp := grp + 1; 'Record which group number is the first to actually have angles.
   else
      gfa%[v4%] := grp; 'Sets the first entry of gfa as group number that first has angles.
      gdec := gdec - 1;
      v4% := v4% + 1;
   endif;
until v% = 14; 'Stop when we reach the end of the possible number of groups.
DlgCreate("Angles", 0,0,80,17);
ntrial% := DlgValue(1); 'Number of trials per angle
pt := DlgValue(2); 'Percentage of pass trials.
sortkey% := DlgValue(3); 'Sort based on some criteria.
stype1$ := DlgValue$(4); 'Control or stroke subject
snumb% := DlgValue(5); 'Subject number
nptrial := (pt/(100-pt))*ntrial%; 'Calculate the number of pass trials
nptrial% := trunc(nptrial); 'Removes a fraction so it is an integer
v1% := nang%; 'Set v1 to be the number of angles.
for v := 2 to v1%+1 do 'This creates the dialog where the specific angles can be defined.
        DlgReal(v-1,Print$("Grp %d Trigger Angle (degrees)", gfa%[v-2]), 0, 360);
next;
ok2% := DlgShow(ang[]); 'ang stores the angles after being typed into the dialog
PrintLog("Number Trials/Angle = %d\n",ntrial%);
PrintLog("Number Passes/Angle = %d\n",nptrial%);
PrintLog("Number of Angles = %d\n",nang%);
PrintLog("Sort Key = %d\n",sortkey%);
PrintLog("Legs = %d\n",numleg%);
```

```
'Create random arrays to allow sorting of other variables.
Rand(rannum[]); 'Creates random numbers in a 1500 element array
for v := numleg%*nang%*(ntrial%+nptrial%) to 1499 do 'From # of trials to 1499
   rannum[v] := 1.5; 'set the unused indices to 1.5
next;
'Determine the number of groups.
grpmax% := 0;
repeat
   grpmax% := grpmax% +1;
until nang%-ArrSum(napgr%[0:grpmax%]) = 0; 'Find the number of groups
'This section creates arrays specifying what angles we are stimulating at, how groups are
ordered, and the number of pass/stim trials. After doing this, it then randomizes within an
angle or within a group.
for v3% := 1 to grpmax% do
   v7% := v6%;
   v6% := v6%+napgr%[v3%-1];
   for v% := v7% to (v6%-1) do 'index 0 to (# of angles - 1)
      for v2% := 0 to numleg%-1 do 'If we are testing 2 legs, double the trials
         for v4% := 0 to ntrial%-1 do 'index 0 to (# of trials - 1)
            stim$[(ntrial%+nptrial%)*v%*numleg%+(ntrial%+nptrial%)*v2%+v4%] :=
"Stim"; 'Stim for these trials
            angtr[(ntrial%+nptrial%)*v%*numleg%+(ntrial%+nptrial%)*v2%+v4%] :=
ang[v%]; 'The angle at which to stim.
            angind%[(ntrial%+nptrial%)*v%*numleg%+(ntrial%+nptrial%)*v2%+v4%]
:= v%; 'Angle index # from ang
            numb%[(ntrial%+nptrial%)*v%*numleg%+(ntrial%+nptrial%)*v2%+v4%] :=
v4%+v2%*(ntrial%+nptrial%); 'Trial number within each angle.
            if v2% = 0 then
               leg$[(ntrial%+nptrial%)*v%*numleg%+(ntrial%+nptrial%)*v2%+v4%] :=
"L";
            else
               leg$[(ntrial%+nptrial%)*v%*numleg%+(ntrial%+nptrial%)*v2%+v4%] :=
"R";
            endif;
         next;
         for v4% := ntrial% to ntrial% + nptrial%-1 do       '3 - 5
            stim$[(ntrial%+nptrial%)*v%*numleg%+(ntrial%+nptrial%)*v2%+v4%] :=
"Pass";     'Pass for these trials.
            angtr[(ntrial%+nptrial%)*v%*numleg%+(ntrial%+nptrial%)*v2%+v4%] :=
ang[v%];    'The angle at which to pass
            angind%[(ntrial%+nptrial%)*v%*numleg%+(ntrial%+nptrial%)*v2%+v4%]
:= v%;       'Angle index # from ang
            numb%[(ntrial%+nptrial%)*v%*numleg%+(ntrial%+nptrial%)*v2%+v4%] :=
v4%+v2%*(ntrial%+nptrial%);  'Trial number within each angle.
            if v2% = 0 then
```

```
            leg$[(ntrial%+nptrial%)*v%*numleg%+(ntrial%+nptrial%)*v2%+v4%] :=
"L";
         else
            leg$[(ntrial%+nptrial%)*v%*numleg%+(ntrial%+nptrial%)*v2%+v4%] :=
"R";
         endif;
      next;
   next;
next;

if sortkey% = 1 then 'If we are sorting the pass/stim trials within an angle.
   if grpmax% > 1 then
      st% := 0;
      for v% :=0 to grpmax%-1 do
         len% := ((ntrial%+nptrial%)*numleg%*napgr%[v%]-1);
         ArrSort(rannum[st%:len%], 0, leg$[st%:len%], angtr[st%:len%],
stim$[st%:len%], numb%[st%:len%], angind%[st%:len%]); 'Sort
         numang% := numang%+napgr%[v%];
         st% := numang%*(ntrial% + nptrial%)*numleg%; 'Move to the next indices to
sort those also.
      next;
   else
      ArrSort(rannum, 0, angtr, stim$, numb%, angind%, leg$);
   endif
else
endif;
'PrintLog("Angle\tStimulate\n");
'for v := 0 to nang%*(ntrial%+nptrial%)-1 do
'PrintLog("%3.0f\t%s\t%d\t%d\n", angtr[v], stim$[v], numb%[v], angind%[v]);
'next;
PrintLog("Group\tAngle\tStimulate\n");
for v := 0 to numleg%*nang%*(ntrial%+nptrial%)-1 do
   PrintLog("%d\t%3.0f\t%s\t\t%d\t\t%d\t\t%s\n", gfa%[angind%[v]],angtr[v], stim$[v],
numb%[v], angind%[v], leg$[v]); 'group #, angle, pass/stim, the original position of these
parameters before randomization, ang index.
next;
FrontView(LogHandle());
WindowVisible(3);
'This section determines where to save the created sampling characteristics.
if fpset% = 1 then 'If we want to create a new directory
   ok% := FilePathSet("C:\\Spike5",0,1);
   if ok% then
      Message("Directory Not Created");
   endif;
   ok% := FilePathSet("C:\\Spike5\\Experiments",0,1);
```

```
   if ok% then
      Message("Directory1 Not Created");
   endif;
   fpath$ := FilePath$();
   ok% := FilePathSet(Print$("%s\%s_Marquette", fpath$),0,1);
   if ok% then
      Message("Directory2 Not Created");
   endif;
   fpath$ := FilePath$();
   ok% := FilePathSet(Print$("%s\%s", fpath$, stype1$),0,1);
   if ok% then
      Message("Directory4 Not Created");
   endif;
   daten$ := Date$(2,2,1,0,"+");
   daten$ := Print$("%s%s%s", Mid$(daten$,1,2), Mid$(daten$,4,2), Mid$(daten$,7,2));
   'daten$ := "010106";
   fpath$ := FilePath$();
   newdir$ := Print$("%s\%s%s_%s", fpath$, Mid$(stype1$,1,1),
Mid$(Str$(100+snumb%,3),2,2), daten$);
   PrintLog("%s\n", newdir$);
   ok% := FilePathSet(Print$("%s\%s%s_%s", fpath$, Mid$(stype1$,1,1),
Mid$(Str$(100+snumb%,3),2,2), daten$),0,1);
   if ok% then
      Message("Directory5 Not Created");
   endif;
else
   ok% := FilePathSet("");
   if ok% then
      Message("Directory6 Not Created");
   endif;
endif;
'Saving the .txt file with the specified characteristics.
ret :=FileNew(1);
daten$ := Date$(2,2,1,0,"+");
daten$ := Print$("%s%s%s", Mid$(daten$,1,2), Mid$(daten$,4,2), Mid$(daten$,7,2));
FileSaveAs(Print$("%s%s_%s.txt", Mid$(stype1$,1,1),
Mid$(Str$(100+snumb%,3),2,2),daten$));
Print("%d,%d,%d,%f\n",ntrial%,sortkey%,nptrial%,pt);
Print("\"%s\",%d,\n",stype1$,snumb%);
Print("%d\n",gfa%[]);
Print("%f\n",ang[]);
Print("%f\n",angtr[]);
Print("%d\n",numb%[]);
Print("%d\n",angind%[]);
for v :=0 to 1499 do
   Print("\"%s\",",stim$[v]);
```

```
next;
Print("\n");
for v :=0 to 1499 do
   Print("\"%s\",",leg$[v]);
next;
FileSave();
FileClose();
end;
var gFloat%[20]; 'global for floating window states
```

CR_Sequencer: sends signals to stimulator

```
        SET     0.333 1 0    ;Sets clock tick time - 0.5 ms/step | 5V scale | 0 offset
        VAR   V1             ;Initialize variables V1,V3,V5,V6 to 0. V1 stores results.
        VAR   V2             ;V2 is the angle where the stimulation should occur.
        VAR   V3             ;V3 stores results in this sequencer.
        VAR   V4             ;V4 stimulation is 0=PASS or 1=STIM.
        VAR   V5             ;Whether Spike is sampling or not.
        VAR   V6             ;Marker channel for when events happen.
        DIGOUT [......00]
        HALT                ;Stops sequencer until something happens
;============== R is Cutaneous Stimulation during forward pedaling==========
      'R  CHAN   V1,1          ;Will look at value from channel 1, R_POS, set V1 as that.
LOOPA:     MOV    V3,V1,-100     ;Subtract 100 (~0.015s) from V1, save as V3.
        CHAN   V1,1          ;Resample R_POS channel.
        BGT    V1,V3,LOOPA     ;If new (V1) is greater than previous (V3), keep looking
LOOPB:     CHAN   V1,1          ;After LOOPA is complete (pass TDC), sample angle
        BLT    V1,V2,LOOPB     ;After finding zero, find the angle-point for triggering
        BLT    V4,1,LBL1      ;Check to see if STIM or PASS
        DIGOUT [......10]     ;trigger from output channel 0.
        DIGOUT [......00]     ;reset
        MARK   V6            ;Makes a digital mark that a stim trial occurred.
        DELAY  6             ;hold on for 1 ms
        DIGOUT [......10]     ;trigger from output channel 0.
        DIGOUT [......00]     ;reset
        DELAY  7             ;hold on for 1 ms
        DIGOUT [......10]     ;trigger from output channel 0.
        DIGOUT [......00]     ;reset
        DELAY  7             ;hold on for 1 ms
        DIGOUT [......10]     ;trigger from output channel 0.
        DIGOUT [......00]     ;reset
        DELAY  7             ;hold on for 1 ms
        DIGOUT [......10]     ;trigger from output channel 0.
        DIGOUT [......00]     ;resetDIGOUT [......01]
        JUMP   LBL2
```

```
LBL1:      DIGOUT [......00]     ;Completed step if it is a pass trial. No stim.
           MARK   V6             ;Makes a digital mark that a pass trial occurred.
           JUMP   LBL2           ;Go to LBL2.
LBL2:      DELAY  20             ;Wait 10 ms
           DIGOUT [......00]     ;Reset the outputs to be zero.
           DELAY  400            ;Wait 200 ms.
           MOVI   V5,1           ;Let Spike know to stop sampling. Set V5 to 1.
           HALT                  ;Stop and wait for something else to happen.
;============== L is Cutaneous Stimulation during forward pedaling==========
      'L  CHAN   V1,3            ;Will look at value from channel 3, L_POS, set V1 as that.
LOOPC:     MOV    V3,V1,100      ;Subtract 100 (~0.015s) from V1 and save as V3.
           CHAN   V1,3           ;Resample L_POS channel.
           BLT    V1,V3,LOOPC    ;If new (V1) is less than previous (V3), keep looking
LOOPD:     CHAN   V1,3           ;After LOOPC is complete (pass TDC), sample angle
           BGT    V1,V2,LOOPD    ;After finding zero, find the angle-point for triggering
           BLT    V4,1,LBL3      ;Check to see if STIM or PASS
           DIGOUT [......01]     ;trigger from output channel 0.
           DIGOUT [......00]     ;reset
           MARK   V6             ;Makes a digital mark that a stim trial occurred.
           DELAY  6              ;hold on for 1 ms
           DIGOUT [......01]     ;trigger from output channel 0.
           DIGOUT [......00]     ;reset
           DELAY  7              ;hold on for 1 ms
           DIGOUT [......01]     ;trigger from output channel 0.
           DIGOUT [......00]     ;reset
           DELAY  7              ;hold on for 1 ms
           DIGOUT [......01]     ;trigger from output channel 0.
           DIGOUT [......00]     ;reset
           DELAY  7              ;hold on for 1 ms
           DIGOUT [......01]     ;trigger from output channel 0.
           DIGOUT [......00]     ;resetDIGOUT [......01]
           JUMP   LBL4
LBL3:      DIGOUT [......00]     ;Completed step if it is a pass trial. No stim.
           MARK   V6             ;Makes a digital mark that a pass trial occurred.
           JUMP   LBL4           ;Go to LBL2.
LBL4:      DELAY  20             ;Wait 10 ms
           DIGOUT [......00]     ;Reset the outputs to be zero.
           DELAY  400            ;Wait 200 ms.
           MOVI   V5,1           ;Let Spike know to stop sampling. Set V5 to 1.
           HALT                  ;Stop and wait for something else to happen.
;============== EL: 5 pulses @ 300 Hz ========================
      'E  DIGOUT [......01]      ;trigger from output channel 0.
           DIGOUT [......00]     ;reset
           MARK   V6             ;Makes a digital mark that a stim trial occurred.
           DELAY  6              ;hold on for 1 ms
           DIGOUT [......01]     ;trigger from output channel 0.
```

```
        DIGOUT [......00]     ;reset
        DELAY  7              ;hold on for 1 ms
        DIGOUT [......01]     ;trigger from output channel 0.
        DIGOUT [......00]     ;reset
        DELAY  7              ;hold on for 1 ms
        DIGOUT [......01]     ;trigger from output channel 0.
        DIGOUT [......00]     ;reset
        DELAY  7              ;hold on for 1 ms
        DIGOUT [......01]     ;trigger from output channel 0.
        DIGOUT [......00]     ;resetDIGOUT [......01]
        HALT
;============== ER: 5 pulses @ 300 Hz ========================
    'F  DIGOUT [......10]     ;trigger from output channel 0.
        DIGOUT [......00]     ;reset
        MARK   V6             ;Makes a digital mark that a stim trial occurred.
        DELAY  6              ;hold on for 1 ms
        DIGOUT [......10]     ;trigger from output channel 0.
        DIGOUT [......00]     ;reset
        DELAY  7              ;hold on for 1 ms
        DIGOUT [......10]     ;trigger from output channel 0.
        DIGOUT [......00]     ;reset
        DELAY  7              ;hold on for 1 ms
        DIGOUT [......10]     ;trigger from output channel 0.
        DIGOUT [......00]     ;reset
        DELAY  7              ;hold on for 1 ms
        DIGOUT [......10]     ;trigger from output channel 0.
        DIGOUT [......00]     ;resetDIGOUT [......01]
        HALT
```

B.3 Analysis methods

Matlab scripts and functions and their purposes

Matlab scripts and functions	**Purpose**
CutaneousAnalysis	Parent script that calls functions.
cr_norm	Inputs Spike data and calculates EMG and cutaneous reflexes.

CutaneousAnalysis: parent script for cutaneous reflex data.

```
clear
global emg_gain
emg_gain = 10000;
```

```
P_leg = 'L';
NP_leg = 'R';
path = 'C:\Users\clela\Documents\_SSI_Lab\Electrophysiology\Subjects\S01\';
temp = strsplit(path,'\'); subject = char(temp(:,8));
file = ['EP_S01_1_01.txt';'EP_S01_1_02.txt';'EP_S01_1_03.txt';'EP_S01_1_05.txt'];
%file = 'EP_S11_1_03.txt';
log = ['S01_081517.TXT'];
[angles,devs,crs_avg,bemg_avg,post,pre,vel,emg]=cutaneous_reflex(path,file,log);
```

function cr_norm: inputs Spike data and calculates EMG and cutaneous reflexes.

```
function [lEarly,lLate,rEarly,rLate] = cr_norm(path,file,log)
global emg_gain
data_length=0;ang_order=[];ps_order=[];leg_order=[];devs=[];emark=[];estim=[];emg=[]
;pos=[];
input2 = importdata([path log],'\t'); %Testing characteristics
ang_order_adj = str2double(strsplit(input2{5,1},',')); %Order of angles
ps_order = strsplit(input2{8,1},','); %Whether each angle was PASS/STIM
leg_order = strsplit(input2{9,1},','); %L/R leg
%%%%%%%%%%%%%%%%%%%%%%%%%%%%%%%%%%%%%%%%%%%%%%%%%%%%%%%%%%%%%%%%
for h=1:size(file)
   input = importdata([path file(h,:)],'\t'); %All data
   emark = [emark;input.data(:,2)]; %STIM marker to either leg (from sequencer)
   emg = [emg;input.data(:,[21,20,19,18,17,16,15,14,13,12,11,10,9,8,7,6])]; %EMG
         %[LTA,LSOL,LMG,LVM,LRF,LVL,LMHAM,LLHAM,RTA,RSOL,RMG,RV
         M,RRF,RVL,RMHAM,RLHAM]
   pos = [pos;input.data(:,[25,27])]; %Time and crank position
   estim = [estim;input.data(:,[5,4])]; %Time and STIM marker (from stimulator)
   data_length=[data_length;length(emg)];
end
[~,NoEMGch]=size(emg); %Number of EMG channels.
%%%%%%%%%%%%%%%%%%%%%%%%%%%%%%%%%%%%%%%%%%%%%%%%%%%%%%%%%%%%%%%%
%% Processing position data
%Flip the left position trace to the same direction as the right leg.
pos(:,1) = abs(pos(:,1)-max(pos(:,1)));
%Bad point elimination. Points in the position trace that are not too close or distant from
the previous point (mistakes) are kept. This section also goes through and determines
when each new revolution occurred.
newcyclel=[];newcycler=[];
for p=1:(length(data_length)-1)
   for j = 1:2
      diffs=[];mwave=[];locs=[];
      diffs = abs(pos((data_length(p)+2):data_length(p+1),j)-
pos((data_length(p)+1):(data_length(p+1)-1),j));
      mwave = diffs>.05 & diffs<4.9;
```

```
        locs = find(mwave)+data_length(p)+1;
        pos(locs,j) = 0;
        %Find where new revolutions occur.
        for i=(data_length(p)+1):(data_length(p+1)-1)
            if j == 1
                if (abs(pos(i,j)-pos(i+1,j)))>.1
                    newcyclel=[newcyclel;i+1];
                end
            elseif j == 2
                if (abs(pos(i,j)-pos(i+1,j)))>.1
                    newcycler=[newcycler;i+1];
                end
            end
        end
    end
end
%Convert volts to degrees
for k=1:2
    pos(:,k) = pos(:,k)/5*360;
end
%Split position traces and new revs into each trial.
pos_trial=[];estim_trial=[];ncr_trial=[];ncl_trial=[];
for r = 1:(length(data_length)-1)
    pos_trial{r}=pos((data_length(r)+1):data_length(r+1),:);
    estim_trial{r}=estim((data_length(r)+1):data_length(r+1),:);
    emg_trial{r}=emg((data_length(r)+1):data_length(r+1),:);
    for q = 1:length(newcycler)
        if newcycler(q) > (data_length(r)+1) && newcycler(q) <= data_length(r+1)
            try
                ncr_trial{r}=[ncr_trial{r};(newcycler(q)-data_length(r))];
            catch
                ncr_trial{r}=(newcycler(q)-data_length(r));
            end
        end
    end
    for v = 1:length(newcyclel)
        if newcyclel(v) > (data_length(r)+1) && newcyclel(v) <= data_length(r+1)
            try
                ncl_trial{r}=[ncl_trial{r};(newcyclel(v)-data_length(r))];
            catch
                ncl_trial{r}=(newcyclel(v)-data_length(r));
            end
        end
    end
end
%Markers of when PASS/STIM occurred.
```

```
stims_start = find(emark(:,1)==1);
%Determine the unique angles that were stimulated.
angles = unique(ang_order(1,1:length(stims_start)));
%%%%%%%%%%%%%%%%%%%%%%%%%%%%%%%%%%%%%%%%%%%%%%%%%%%%
%% Process the EMG before averaging. The processing performed here is to remove the
gain (values will be in mV), detrend, apply a 60 Hz notch filter, and take the absolute
value.
Design a notch filter at 60 Hz.
d = designfilt('bandstopiir','FilterOrder',2,'HalfPowerFrequency1',59,...
   'HalfPowerFrequency2',61,'DesignMethod','butter','SampleRate',2000);
%Apply processing to EMG data.
emg = emg*(1000/emg_gain);
for p=1:(length(data_length)-1)
   for i = 1:16
      emg((data_length(p)+1):data_length(p+1),i) = ...
         detrend(emg((data_length(p)+1):data_length(p+1),i));
      emg((data_length(p)+1):data_length(p+1),i) = ...
         filtfilt(d,emg((data_length(p)+1):data_length(p+1),i));
   end
end
emg = abs(emg); %Take the absolute value
%Split emg traces into each trial.
emg_trial=[];
for r = 1:(length(data_length)-1)
   emg_trial{r}=emg((data_length(r)+1):data_length(r+1),:);
end
%This long section goes through the left and right leg and finds complete revolutions
where EMG is not potentially contaminated by the application of an electrical stimulus
either to that revolution or to the revolution immediately preceding it. The EMG from
these revolutions is saved so we can determine the phasing.
emg_nostiml=[];emg_nostimr=[];pos_nostiml=[];pos_nostimr=[];
for p=1:(length(data_length)-1)
   for w = 1:(length(ncl_trial{p})-1)
      if w == 1
         if sum(sum(estim_trial{p}(1:(ncl_trial{p}(1)-1),:)))<1 ...
               && sum(sum(estim_trial{p}(ncl_trial{p}(1):(ncl_trial{p}(2)-1),:)))<1
            try
               emg_nostiml=[emg_nostiml;emg_trial{p}(1:(ncl_trial{p}(1)-1),1:8)];
               pos_nostiml=[pos_nostiml;pos_trial{p}(1:(ncl_trial{p}(1)-1),1)];
            catch
               emg_nostiml=emg_trial{p}(1:(ncl_trial{p}(1)-1),1:8);
               pos_nostiml=pos_trial{p}(1:(ncl_trial{p}(1)-1),1);
            end
         end
      elseif w > 1 && w < (length(ncl_trial{p})-1)
         if sum(sum(estim_trial{p}(ncl_trial{p}(w):(ncl_trial{p}(w+1)-1),:)))<1 ...
```

```
            && sum(sum(estim_trial{p}(ncl_trial{p}(w-1):(ncl_trial{p}(w)-1),:)))<1
          try

emg_nostiml=[emg_nostiml;emg_trial{p}(ncl_trial{p}(w):(ncl_trial{p}(w+1)-1),1:8)];
            pos_nostiml=[pos_nostiml;pos_trial{p}(ncl_trial{p}(w):(ncl_trial{p}(w+1)-
1),1)];
          catch
            emg_nostiml=emg_trial{p}(ncl_trial{p}(w):(ncl_trial{p}(w+1)-1),1:8);
            pos_nostiml=pos_trial{p}(ncl_trial{p}(w):(ncl_trial{p}(w+1)-1),1);
          end
        end
      elseif w == (length(ncl_trial{p})-1)
        if sum(sum(estim_trial{p}(ncl_trial{p}(w):end,:)))<1 ...
            && sum(sum(estim_trial{p}(ncl_trial{p}(w-1):(ncl_trial{p}(w)-1),:)))<1
          try
            emg_nostiml=[emg_nostiml;emg_trial{p}(ncl_trial{p}(w):end,1:8)];
            pos_nostiml=[pos_nostiml;pos_trial{p}(ncl_trial{p}(w):end,1)];
          catch
            emg_nostiml=emg_trial{p}(ncl_trial{p}(w):end,1:8);
            pos_nostiml=pos_trial{p}(ncl_trial{p}(w):end,1);
          end
        end
      end
    end
    for y = 1:(length(ncr_trial{p})-1)
      if y == 1
        if sum(sum(estim_trial{p}(1:(ncr_trial{p}(1)-1),:)))<1 ...
            && sum(sum(estim_trial{p}(ncr_trial{p}(1):(ncr_trial{p}(2)-1),:)))<1
          try
            emg_nostimr=[emg_nostimr;emg_trial{p}(1:(ncr_trial{p}(1)-1),9:16)];
            pos_nostimr=[pos_nostimr;pos_trial{p}(1:(ncr_trial{p}(1)-1),2)];
          catch
            emg_nostimr=emg_trial{p}(1:(ncr_trial{p}(1)-1),9:16);
            pos_nostimr=pos_trial{p}(1:(ncr_trial{p}(1)-1),2);
          end
        end
      elseif y > 1 && y < (length(ncr_trial{p})-1)
        if sum(sum(estim_trial{p}(ncr_trial{p}(y):(ncr_trial{p}(y+1)-1),:)))<1 ...
            && sum(sum(estim_trial{p}(ncr_trial{p}(y-1):(ncr_trial{p}(y)-1),:)))<1
          try

emg_nostimr=[emg_nostimr;emg_trial{p}(ncr_trial{p}(y):(ncr_trial{p}(y+1)-1),9:16)];
            pos_nostimr=[pos_nostimr;pos_trial{p}(ncr_trial{p}(y):(ncr_trial{p}(y+1)-
1),2)];
          catch
            emg_nostimr=emg_trial{p}(ncr_trial{p}(y):(ncr_trial{p}(y+1)-1),9:16);
```

```
                pos_nostimr=pos_trial{p}(ncr_trial{p}(y):(ncr_trial{p}(y+1)-1),2);
            end
        end
    elseif y == (length(ncr_trial{p})-1)
        if sum(sum(estim_trial{p}(ncr_trial{p}(y):end,:)))<1 ...
                && sum(sum(estim_trial{p}(ncr_trial{p}(y-1):(ncr_trial{p}(y)-1),:)))<1
            try
                emg_nostimr=[emg_nostimr;emg_trial{p}(ncr_trial{p}(y):end,9:16)];
                pos_nostimr=[pos_nostimr;pos_trial{p}(ncr_trial{p}(y):end,2)];
            catch
                emg_nostimr=emg_trial{p}(ncr_trial{p}(y):end,9:16);
                pos_nostimr=pos_trial{p}(ncr_trial{p}(y):end,2);
            end
        end
    end
end
%Perform EMG binning
emg_bins=zeros(360,NoEMGch);emg_std=zeros(360,NoEMGch);
for d = 0:359
    tempposl=round(pos_nostiml);tempposr=round(pos_nostimr);
    emgmask = tempposl==d;%Finds the locations in the data where the degree is 0-359
    emgmask2 = tempposr==d;
    bin = emg_nostiml.*emgmask;%Multiply by mask, values not in this degree are 0
    bin2 = emg_nostimr.*emgmask2;
    for f = 1:8
        emg_bins(d+1,f) = sum(bin(:,f))./(length(find(bin(:,f)))); %Takes the total value...
        emg_bins(d+1,(f+8)) = sum(bin2(:,f))./(length(find(bin2(:,f)))); %divided by the
            number of indices with a nonzero value (average value at that degree)
        emg_std(d+1,f) = std(bin(find(bin(:,f))));
        emg_std(d+1,(f+8)) = std(bin2(find(bin2(:,f))));
    end
end
%% Extraction of EMG from relevant time periods around stimulation.
%Extract the 250 ms after the stimulus.
post = zeros(500,16,length(stims_start));phase = zeros(500,2,length(stims_start));
for j = 1:length(stims_start)
    post(:,:,j) = emg((stims_start(j)):(stims_start(j)+499),1:16);
    phase(:,:,j) = pos((stims_start(j)):(stims_start(j)+499),:);
end
%% Average PASS/STIM response and background EMG.
%Sort pre-stimulus and post-stimulus responses based upon whether it was from a PASS
or STIM trial, which leg received stimulation, and the angle.
for i = 1:length(stims_start)
    try
```

```
        r=size(crs.(leg_order{i}(2)).(ps_order{i}(2:5)).(strcat('angle',sprintf('%d',ang_ord
        er_adj(i)))),3)+1;
    catch
        r=1;
    end
crs.(leg_order{i}(2)).(ps_order{i}(2:5)).(strcat('angle',sprintf('%d',ang_order_adj(i))))(:,:,
r)=post(:,:,i);
phasep.(leg_order{i}(2)).(ps_order{i}(2:5)).(strcat('angle',sprintf('%d',ang_order_adj(i))))
(:,:,r)=phase(:,:,i);
end
%Average across trials w/in leg, PASS/STIM, and degree. Determine position for every
data point included in the cutaneous reflex interval.
for k=['L' 'R']
    for j = 1:length(angles)
        crs_avg.(sprintf('%s',k)).Stim.(strcat('angle',sprintf('%d',angles(j))))(:,:,:)=...
            mean(crs.(sprintf('%s',k)).Stim.(strcat('angle',sprintf('%d',angles(j)))),3);
        crs_avg.(sprintf('%s',k)).Pass.(strcat('angle',sprintf('%d',angles(j))))(:,:,:)=...
            mean(crs.(sprintf('%s',k)).Pass.(strcat('angle',sprintf('%d',angles(j)))),3);
        phase_avg.(sprintf('%s',k)).(strcat('angle',sprintf('%d',angles(j))))(:,:,:)=...
            (mean(phasep.(sprintf('%s',k)).Stim.(strcat('angle',sprintf('%d',angles(j)))),3)+...
            mean(phasep.(sprintf('%s',k)).Pass.(strcat('angle',sprintf('%d',angles(j)))),3))./2;
    end
end
%Subtract STIM and PASS trials
for k=['L' 'R']
    for j = 1:length(angles)
        crs_avg.(sprintf('%s',k)).Diff.(strcat('angle',sprintf('%d',angles(j))))=...
            crs_avg.(sprintf('%s',k)).Stim.(strcat('angle',sprintf('%d',angles(j))))-...
            crs_avg.(sprintf('%s',k)).Pass.(strcat('angle',sprintf('%d',angles(j))));
    end
end
%Round angles for every data point.
for k=['L' 'R']
    for j = 1:length(angles)
        for g = 1:500
            phase_avg.(sprintf('%s',k)).(strcat('angle',sprintf('%d',angles(j))))(g,1) =...
                round(phase_avg.(sprintf('%s',k)).(strcat('angle',sprintf('%d',angles(j))))(g,1));
            if phase_avg.(sprintf('%s',k)).(strcat('angle',sprintf('%d',angles(j))))(g,1)==0
                phase_avg.(sprintf('%s',k)).(strcat('angle',sprintf('%d',angles(j))))(g,1)=360;
            end
            phase_avg.(sprintf('%s',k)).(strcat('angle',sprintf('%d',angles(j))))(g,2) =...
                round(phase_avg.(sprintf('%s',k)).(strcat('angle',sprintf('%d',angles(j))))(g,2));
            if phase_avg.(sprintf('%s',k)).(strcat('angle',sprintf('%d',angles(j))))(g,2)==0
                phase_avg.(sprintf('%s',k)).(strcat('angle',sprintf('%d',angles(j))))(g,2)=360;
            end
        end
```

```
   end
end
%Set the stimulus artifact to 0.
crs_avg_stim=crs_avg;
for j = 1:length(angles)
   crs_avg.L.Norm.(strcat('angle',sprintf('%d',angles(j))))(1:130,:)=0;
   crs_avg.L.Diff.(strcat('angle',sprintf('%d',angles(j))))(1:130,:)=0;
   crs_avg.L.Stim.(strcat('angle',sprintf('%d',angles(j))))(1:130,:)=0;
   crs_avg.L.Pass.(strcat('angle',sprintf('%d',angles(j))))(1:130,:)=0;
   crs_avg.R.Norm.(strcat('angle',sprintf('%d',angles(j))))(1:130,:)=0;
   crs_avg.R.Diff.(strcat('angle',sprintf('%d',angles(j))))(1:130,:)=0;
   crs_avg.R.Stim.(strcat('angle',sprintf('%d',angles(j))))(1:130,:)=0;
   crs_avg.R.Pass.(strcat('angle',sprintf('%d',angles(j))))(1:130,:)=0;
end
%Take the mean reflex (subtracted) and divide by the mean from the pass trial.
for j=['L' 'R']
   for i=1:length(angles)
      crs_avg.(sprintf('%s',j)).EarlyN.(strcat('angle',sprintf('%d',angles(i))))...
=mean(crs_avg.(sprintf('%s',j)).Diff.(strcat('angle',sprintf('%d',angles(i))))(131:300,:));
      crs_avg.(sprintf('%s',j)).LateN.(strcat('angle',sprintf('%d',angles(i))))...
=mean(crs_avg.(sprintf('%s',j)).Diff.(strcat('angle',sprintf('%d',angles(i))))(300:500,:));
      pass.(sprintf('%s',j)).Early.(strcat('angle',sprintf('%d',angles(i))))...
=mean(crs_avg.(sprintf('%s',j)).Pass.(strcat('angle',sprintf('%d',angles(i))))(131:300,:));
      pass.(sprintf('%s',j)).Late.(strcat('angle',sprintf('%d',angles(i))))...
=mean(crs_avg.(sprintf('%s',j)).Pass.(strcat('angle',sprintf('%d',angles(i))))(300:500,:));
      crs_avg.(sprintf('%s',j)).EarlyNorm.(strcat('angle',sprintf('%d',angles(i))))...
         =(crs_avg.(sprintf('%s',j)).EarlyN.(strcat('angle',sprintf('%d',angles(i)))))./...
         pass.(sprintf('%s',j)).Early.(strcat('angle',sprintf('%d',angles(i))))).*100;
      crs_avg.(sprintf('%s',j)).LateNorm.(strcat('angle',sprintf('%d',angles(i))))...
         =(crs_avg.(sprintf('%s',j)).LateN.(strcat('angle',sprintf('%d',angles(i)))))./...
         pass.(sprintf('%s',j)).Late.(strcat('angle',sprintf('%d',angles(i))))).*100;
   end
end
%Put in Excel Output form
angles2=circshift(angles,3);lEarly=[];rEarly=[];lLate=[];rLate=[];
for i=1:length(angles2)
   lEarly=[lEarly crs_avg.R.EarlyNorm.(strcat('angle',sprintf('%d',angles2(i))))(:,1:8)];
   rEarly=[rEarly crs_avg.L.EarlyNorm.(strcat('angle',sprintf('%d',angles2(i))))(:,9:16)];
   lLate=[lLate crs_avg.R.LateNorm.(strcat('angle',sprintf('%d',angles2(i))))(:,1:8)];
   rLate=[rLate crs_avg.L.LateNorm.(strcat('angle',sprintf('%d',angles2(i))))(:,9:16)];
end
```

APPENDIX C: SUPPLEMENT TO CHAPTER 4

This appendix is a supplement to Chapter 4. Included are additional results that may be of interest. Also included is a detailed description of fMRI analysis methods, including the analysis code used.

C.1 Additional results

Figure C.1 provides fMRI images from all stroke subjects included in the fMRI analysis. (A & B) are the same control and stroke subjects displayed in Figure 4.4.

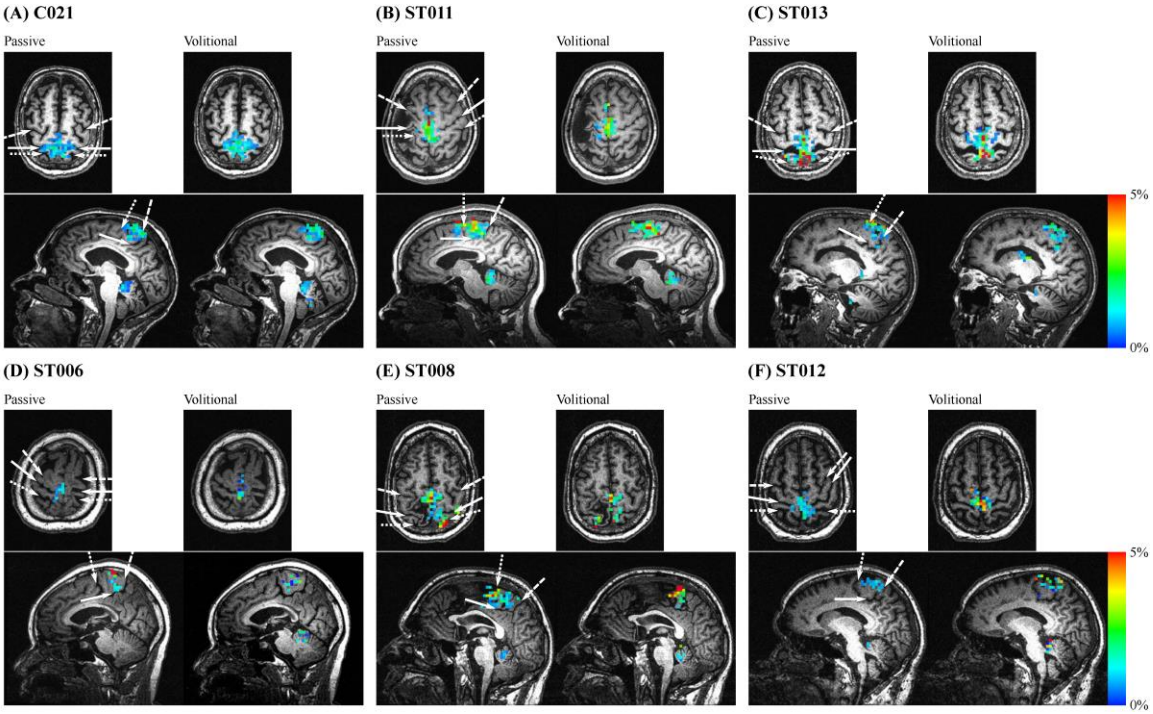

Figure C.1. Representative examples of pedaling-related brain activation from all stroke and one control subject. fMRI activation during pedaling in a control (**A**) and all stroke (**B** – **F**) subjects. A single axial and sagittal slice is shown for each subject to demonstrate the brain activation during passive and volitional pedaling. Color scale represents percent signal change compared to rest (0-5%). White arrows indicate anatomical landmarks. In the axial plane: long dash – precentral sulcus, solid line – central sulcus, short dash – postcentral sulcus. In the sagittal plane: long dash – marginal sulcus, solid line – cingulate sulcus, short dash – paracentral sulcus.

C.2 fMRI analysis methods

AFNI functions and purposes (presented in order of use)

AFNI function	**Purpose**
to3d	Converts 2D DICOM data into 3D image datasets
3dTshift	Time shifts voxels from different runs so they have the same temporal origin. To do this, the function detrends the data and interpolates to the new time grid.
3dToutcount	Counts the number of outliers at each time point in the 3D dataset.
3dTcat	Concatenates 3D time series from each run into one dataset. As part of the process, the first 4 TRs from each run is ignored to avoid the effects of non-steady state magnetization.
3dvolreg	Registers functional scans to the first point of the passive scan closest in time to the anatomical scan. In so doing, this function corrects for and outputs information about small head movements.
3dSkullStrip	Extracts brain tissue from T1 images and excludes the skull, surrounding tissue, and non-physiological space.
3dDeconvolve	Runs a multiple linear regression fitting the 3D time series to the expected hemodynamic response function. Head movement parameters outputted from 3dvolreg are included as variables of no interest.
3dFWHMx	Estimates the smoothness of the dataset using a spatial auto-correlation function fit to a mixed model consisting of a Gaussian and mono-exponential function.
3dClustSim	Estimates a cluster size where the familywise probability of a false positive is < 0.05. This is done using a Monte Carlo simulation.
psc.pedal	Computes percent signal change.
3dmerge.maskout	Applies clustering and thresholding to data. Also applies the brain mask from 3dSkullStrip and discards intensities > abs(10%).

masksize	Creates individual ROI masks from manual definition and changes the resolution to match the functional data.
ROImeasures	Calculates the mean intensity and volume within each ROI.

to3d

```
#!/bin/csh %This specifies the folder where the code for to3d is located.
#if (0) then %Change directory to the anatomical folder.
cd anat
to3d \
-prefix anat \ %Create 3D datasets from MRI images. These are then saved.
*MRDC*
mv *anat* ../
#endif
#*********************************************************************#
cd .. %Go through functional datasets and produce 3D datasets.
cd biped
set conditions = (pedal1 pedal2 pedal3)
foreach condition ( $conditions )
 echo $condition
 cd $condition
 to3d \
 -prefix $condition \
 -time:zt 36 109 2000 alt+z \ %Details about functional data.
 *MRDC*
mv *orig* ../
cd ..
end
#endif
#*************************************************************#
# zt means that slices are input with the z-axis first (space), and then the t-axis (time).
# 36 is the number of points in the z-direction (number of slices).
# 109 is the number of points in the t-direction (# of TRs)
# 2000 is the TR in milliseconds
# The overall time of the scan is then 109 * 2000 = 218,000 ms = 218 s = 3 min. 38 sec.
# alt+z shows that slices were gathered in the +z direction (this is because slices are 2D
that are spread out in time)
#*************************************************************#
cd ..
cd pass
set conditions = (pedal1 pedal2 pedal3)
foreach condition ( $conditions )
```

```
 echo $condition
 cd $condition
 to3d \
 -prefix $condition \
 -time:zt 36 109 2000 alt+z \
 *MRDC*
mv *orig* ../
 cd ..
end
#endif
cd ..
```

3dTshift

```
#!/bin/csh
set conditions = (pedal1 pedal2 pedal3) %Different runs for each condition.
foreach condition ( $conditions )
 echo $condition
 3dTshift \
 -verb \ %Prints messages while the program runs.
 -tzero 0 \ %Align each slice to the time offset = 0
 -prefix $condition.tshift \
 -ignore 4 \ %Ignore the first 4 TRs to avoid the effects of non-steady state magnetization
 -heptic \ %Interpolation with 7th order Lagrange polynomial interpolation.
 $condition+orig
end
```

3dToutcount: To determine whether a voxel is an outlier at a certain timepoint, the trend and median absolute deviation (MAD) of each time series from this trend are calculated. Points that are far away are labeled outliers.

```
#!/bin/csh
set runs = (pedal1.tshift pedal2.tshift pedal3.tshift)
foreach run ( $runs )
 3dToutcount \
 -automask \ %Automatically creates the mask for which outliers are counted.
 $run+orig \
 > $run.outcount
end
```

3dTcat

```
#!/bin/csh
#if (0) then
#rm *tshift.cat*
#*********************************************************************#
# three runs
3dTcat \
pedal1.tshift+orig'[4..108]' \ %Ignore the first 4 TRs
pedal2.tshift+orig'[4..108]' \
pedal3.tshift+orig'[4..108]' \
-prefix pedal.tshift.cat
#endif
```

3dvolreg: this function uses iterated linearized weighted least squares modeling to make each sub-brick as similar to the base brick as possible. Motion parameters outputted are roll, pitch, yaw, dS (inferior/superior), dL (left/right), and dP (anterior/posterior).

```
#!/bin/csh
set runs = (pedal.tshift.cat)
#*********************************************************************#
#Run by using 1 ref-point. The zero point of the passive run that is closest to the anat.
#if (0) then
foreach run ($runs)
 3dvolreg \
 -heptic \ %Uses heptic polynomial interpolation
 -prefix $run.volreg \
 -base 'pedal.reg+orig[108]' \ %Sets the base brick from the input dataset. Set to 0 if run is
                                after anatomical, or 108 if run is before anatomical.
 -dfile $run.volreg.dfile \ %Save the motion parameters.
 -1Dfile $run.volreg.1Dfile \
 $run+orig
end
#endif

#if (0) then
# Rerun volreg to see the effect of volreg from the data with 1 ref-point
foreach run ($runs) %Performed for visualization only. Files produced are not used later
 3dvolreg \
 -heptic \
 -prefix $run.volreg.twice \
 -base 'pedal.reg+orig[108]' \
 -dfile $run.volreg.twice.dfile \
 -1Dfile $run.volreg.twice.1Dfile \
 $run.volreg+orig
```

```
end
#endif
```

3dSkullStrip: the basic steps are 1) preprocessing the volume to remove large artifacts, 2) expands a sphere until it encompasses the brain tissue, and 3) creates masks based on where the brain tissue is located.

```
#!/bin/csh
#if (0) then
# Making a skull strip from anatomical image %Detect the skull
3dSkullStrip \
-input anat+orig \
-push_to_edge \ %Push to the edge to avoid drop-out.
-blur_fwhm 4 \ %Blur dataset with a Gaussian function with FWHM of 4 mm
-ld 50 \ %Controls the density of the surface.
-prefix anat_pedal_strip_PTE_mesh
#endif

#if (0) then
# Making a mask using the skull-strip
3dcalc \
-a anat_pedal_strip_PTE_mesh+orig \
-expr "step(a-1500)" \ %Extract voxels greater than 1 after subtracting 1500.
-prefix anat_pedal_strip_1500_PTE_mesh
#endif

#if (0) then
# Changing the sample size of anatomical to functional scan size (b/c the resolution of the anatomical is different from functional scan)
3dfractionize \
-template pedal.tshift.cat+orig
-input anat_pedal_strip_1500_PTE_mesh+orig \
-prefix anat_pedal_strip_1500_PTE_mesh_bigvoxels
#endif

#if (0) then
# Making the fractionized file to be a mask for Alphasim
3dcalc \
-a anat_pedal_strip_1500_PTE_mesh_bigvoxels+orig \
-expr "step(a)" \ %Voxels with value >0 are selected for a mask to be used in Alphasim.
-prefix anat_pedal_strip_1500_PTE_mesh_bigvoxels.mask
#endif
```

3dDeconvolve: prior to running this function, outliers detected in 3dToutcount were manually censored, by changing the value in the censor file. Note that the name of this function is a misnomer.

```
#!/bin/csh
#*****************************************************
3dDeconvolve \
-float \
-input pedal.tshift.cat.volreg+orig \
-concat concat.pedal.315 \ %File noting location where runs were concatenated.
-polort A \ %Polynomial size is automatically chosen by the program.
-num_stimts 7 \ %Number of input stimulus time series.
-censor Mcensor315.1D \ %Censor file indicating which time series values are included
                        in the regression.
-stim_file 1 Mcanonical315.1D \ %Canonical model for the regression.
-stim_minlag 1 0 \ %Minimum and maximum time lag.
-stim_maxlag 1 0 \
-stim_label 1 pedal \ %The label for the stimulus.
-stim_file 2 pedal.tshift.cat.volreg.1Dfile'[0]' -stim_base 2 -stim_label 2 roll \
%The next 6 inputs are head movement parameters included in the baseline model.
-stim_file 3 pedal.tshift.cat.volreg.1Dfile'[1]' -stim_base 3 -stim_label 3 pitch \
-stim_file 4 pedal.tshift.cat.volreg.1Dfile'[2]' -stim_base 4 -stim_label 4 yaw \
-stim_file 5 pedal.tshift.cat.volreg.1Dfile'[3]' -stim_base 5 -stim_label 5 dS \
-stim_file 6 pedal.tshift.cat.volreg.1Dfile'[4]' -stim_base 6 -stim_label 6 dL \
-stim_file 7 pedal.tshift.cat.volreg.1Dfile'[5]' -stim_base 7 -stim_label 7 dP \
-fitts pedal.tshift.cat.decon.fitts_censor.modify \ %Full model time series fit to the input.
-errts pedal.tshift.cat.decon.errts_censor.modify \ %Residual error time series from the
                                                    full model fit to the input.
-fout \ %F-statistics
-tout \ %T-statistics
-bout \ %baseline coefficients
-full_first \ %Full model statistics are first in the bucket file
-bucket pedal.tshift.cat.decon.bucket_censor.modify %Output file
csh pedal.REML_cmd
```

3dFWHMx: note that the name of this function is a misnomer as data smoothness is not accurately estimated with a pure FWHM Gaussian function.

```
set maxlags = (15)
if (0) then
 3dFWHMx \
 -dset pedal.tshift.cat.decon.errts_censor.modify+orig \ #Input is the error terms from the
                                                          GLM
 -mask anat_pedal_strip_1500_PTE_mesh_bigvoxels.mask+orig \ #Use mask from
                                                             3dSkullStrip
```

```
 -acf \ #Autocorrelation function to determine blurring
 -out -
endif
```

3dClustSim: function parameters from 3dFWHMx are used in this function. Multiple cluster sizes are output based on various parameters. I chose 1-sided thresholding (the upper tail of the probability determines the threshold) and third-nearest neighbor clustering (voxels in a cluster can be touching at the faces, edges, or corners). To determine the minimum cluster size (mL), this is then multiplied by the size of one cluster.

```
if (0) then
 3dClustSim \
 -quiet \
 -mask anat_pedal_strip_1500_PTE_mesh_bigvoxels.mask+orig \
 -acf 0.950063 1.99365 19.5741 \ #function parameters from 3dFWHMx.
 -pthr 0.005 \ #Threshold probability for individual voxels.
 -iter 2000 \ #2000 simulations
#Alpha = 0.05   #of Cl = 5.0  x 56.25 = 281.25 #Familywise error rate of 0.05.
                                                Calculation of minimum cluster size.
endif
```

psc.pedal

```
#!/bin/csh
set runs = (pedal.tshift.cat)
foreach run ($runs)
3dcalc \
-fscale \ #scale so max value is 1, and minimum value is 0
#a, b, and c are baseline coefficients for each run from regression.
-a $run.decon.bucket_censor.modify+orig'[1]' \ #function parameters from 3dFWHMx.
-b $run.decon.bucket_censor.modify+orig'[7]' \
-c $run.decon.bucket_censor.modify+orig'[13]' \
-d pedal.tshift.cat.decon.bucket_censor.modify+orig'[19]' \
-expr "100 * (d/((a+b+c)/3)) * step( 1 - abs( (d/((a+b+c)/3)) ) )" \
-prefix $run.decon.bucket_censor.modify.PSC
end
#*************************************************************************#
# Putting coef and stat data together
#*************************************************************************#
foreach run ($runs)
 3dbuc2fim \
 -prefix $run.decon.bucket_censor.modify.PSC.stat \
 $run.decon.bucket_censor.modify.PSC+orig'[0]'\
 $run.decon.bucket_censor.modify_REML+orig'[2]'
```

```
end
```

3dmerge.maskout

```
#!/bin/csh
set runs = (pedal.tshift.cat)
# From csh.3dmerge.noneg.maskout.pedal
rm *AUC*
foreach run ($runs)
3dmerge \
 -1thresh 2.85 \ %t-stat threshold for individual voxels
 -1clust 6.6 393.8 \ %Clusters with connection radius of 6.6 mm, and clusters must have
                        the minimum size determined with 3dClustSim
 -1dindex 0 \ %Sub-brick 0 is the data source
 -1tindex 1 \ %Sub-brick 1 is threshold source
 -prefix $run.decon.bucket_censor.modify.PSC_AUC_thresh.stat \
 $run.decon.bucket_censor.modify.PSC.stat+orig
end

foreach run ($runs)
3dcalc \
 -a $run.decon.bucket_censor.modify.PSC_AUC_thresh.stat+orig \ %Applies parameters
 -b anat_pedal_strip_1500_PTE_mesh_bigvoxels.mask+orig \ %Applies brain mask
 -expr "step(b)*a" \
 -prefix $run.decon.bucket_censor.modify.PSC.STAT.MASK
end
#***************************
foreach run ($runs)
3dcalc \
 -a $run.decon.bucket_censor.modify.PSC.STAT.MASK+orig'[0]' \ %Only keeps
                                                        intensities between -10 to 10%
 -expr "a*within(a,-10,10) " \
 -prefix $run.decon.bucket_censor.modify.PSC.STAT.MASK_outlier
end
```

masksize: note that ROImask was created by manually outlining the regions of interest (i.e. M1 right, M1 left, S1 right, S1 left, BA6 right, BA6 left, Cb right, and Cb left) with corresponding values (1:8). I have only shown one example instead of including all. Below that, smaller ROIs are combined into large ROIs. I have also only shown one example.

```
#*************************************************************************#
# Performed for M1R, M1L, S1R, S1L, A6R, A6L, CbR, CbL
#*************************************************************************#
```

```
#!/bin/csh
3dcalc \
-a ROImask+orig \
-expr "and(step(a-0),step((0+2)-a))" \ %Only keeps values corresponding to the
                                        ROImask. Both places that have “0” iterate up to 7
                                        or (region value – 1)
-prefix M1R+orig %prefix changes with region.
#***********************************************************************#
# Combines ROIs. Performed for M1a, S1a, A6a, Cba, M1S1R, M1S1L, M1S1a,
M1S1A6R, M1S1A6L, M1S1A6a
#***********************************************************************#
3dcalc \
-a M1R+orig \
-b M1L+orig \
-expr "step(a+b)" \
-prefix M1a+orig
#***********************************************************************#
# Changing the resolution of the anat masks to the functional scan
#***********************************************************************#
set areas = (M1R M1L S1R S1L A6R A6L CbR CbL M1a S1a A6a Cba M1S1R M1S1L
M1S1a M1S1A6R M1S1A6L M1S1A6a)
foreach area ($areas)
   3dfractionize \
   -template pedal.reg+orig \
   -input "$area"+orig \
   -prefix "$area"_low+orig
end
```

ROImeasures

```
#!/bin/csh
# draw the activation maps in each ROI
set areas = (M1R M1L S1R S1L A6R A6L CbR CbL M1a S1a A6a Cba M1S1R M1S1L
M1S1a M1S1A6R M1S1A6L M1S1A6a)
foreach area ($areas)

3dcalc \
-a pedal.tshift.cat.decon.bucket_censor.modify.PSC.STAT.MASK_outlier+orig \
-b "$area"_low+orig \
-expr "step(b)*a" \ %Multiply each ROImask by data that has been thresholded,
                    clustered, had the brain masked out, and been intensity thresholded
-prefix "$area"_PSMO+orig

3dBrickStat \ %Calculate volume and mean
 -volume \
```

```
 -mean \
 -positive \ %Only include positively correlated voxels
 "$area"_PSMO+orig \
 >"$area"_PSMOmeasures.txt

end
```

APPENDIX D: BILATERAL UNCOUPLED PEDALING DURING fMRI

D.1 Introduction

Chapter 4 of this dissertation aimed to determine whether reduced pedaling-related brain activation post-stroke can be explained by compensation (altered volitional motor commands and pedaling performance). In that chapter, I tested brain activation during volitional and passive pedaling. Passive pedaling eliminated motor commands to pedal and minimized between-group differences in pedaling performance. Thus, passive pedaling was used to provide insight into how compensation might be related to pedaling-related brain activation. We hypothesized that if volitional motor commands and pedaling performance contribute to reduced pedaling-related brain activation post-stroke, then: 1) between-group differences would be reduced during passive as compared to volitional pedaling and 2) brain activation would be different between passive and volitional pedaling. In contrast to this hypothesis, we found that between-group differences were maintained during passive pedaling and that brain activation was not different between passive and volitional pedaling.

Although the results from Chapter 4 do not support a relation between compensation and brain activation, there are limitations to the use of passive pedaling to address this aim. Passive pedaling does not alter motor commands in the same way as the asymmetrical pedaling associated with compensation. Instead, passive pedaling removes motor commands to pedal and may involve the engagement of different motor commands, such as those to prevent muscle activation during movement. These

differences make passive pedaling a fundamentally different task, and potentially limit the insight into the relation between compensation and brain activation.

To determine whether reduced pedaling-related brain activation post-stroke can be explained by compensation, a more suitable experimental approach might be to more explicitly manipulate the degree of compensation and measure brain activation. Accordingly, we sought to apply one of the manipulations of compensation used in Chapter 2 during fMRI. Specifically, subjects performed bilateral uncoupled pedaling on our custom pedaling device. We hypothesized that if compensation explains reduced pedaling-related brain activation post-stroke, then: 1) between-group differences would be reduced during bilateral uncoupled as compared to volitional pedaling and 2) brain activation would be different between bilateral uncoupled and volitional pedaling. Ultimately, we were unable to test these hypotheses because excessive head motion obscured detection of brain activation. This appendix details the methods and results from this pilot study.

D.2 Methods

Subjects

Five stroke survivors were tested once, and two were tested on multiple occasions. These participants were a subset of those involved in the procedures described in Chapter 2. In addition, two young control subjects were tested. In total, there were 11 scanning sessions. All provided written informed consent in accordance with the Declaration of Helsinki and the Institutional Review Boards at Marquette University and the Medical College of Wisconsin.

Procedures

All participants performed conventional and bilateral uncoupled pedaling on a custom-designed, split-crank pedaling device (Figure 2.1) during a setup and fMRI scanning session. Briefly, the crankshaft of this pedaling device can be split, allowing each half of the bike to function independently. When the crankshaft is split, elastic loads applied through an eccentric pulley system help simulate the contribution of the contralateral leg to angular rotation. During conventional pedaling, subjects pedaled with both legs while the crankshaft halves were coupled with the pedals in an antiphase orientation. During bilateral uncoupled pedaling, the coupler was removed, and subjects pedaled bilaterally while maintaining an antiphase relation between the pedals.

Elastic and frictional loads used during pedaling were determined during the setup session described in Chapter 2. Briefly, the setup session was used to determine an elastic load on the eccentric pulley system that best approximated the contribution of the contralateral limb. Subjects performed unilateral pedaling against up to six loads. Elastic load for each limb was selected using criteria to determine the best match with conventional pedaling. See Chapter 2 for additional details on the device or protocol for the setup session.

After completing the entirety of the experiment described in Chapter 2, some subjects participated in an additional fMRI scanning session. These subjects were selected based upon their perceived ability to minimize head and body movement. During in lab testing, the experimenters observed the degree of head and body movement that occurred during conventional and bilateral uncoupled pedaling and invited those with the

least movement to participate in a scanning session. Two subjects were tested on a second occasion after the experimental protocol had been optimized.

Procedures followed during the fMRI scanning session approximated those described in Chapter 4. Subjects lay supine on the backboard of the bike with their feet secured to the pedals. Head and body stabilization were achieved with a beaded vacuum pillow, foam padding, chin and trunk straps, and adhesive tape placed on the forehead. Subjects performed conventional and bilateral uncoupled pedaling in a block design consisting of 3 runs of each condition. Some subjects also performed 3 runs of unilateral pedaling with the left and right leg (n = 1), with the paretic leg (n = 4), and with the non-paretic leg (n = 2). Each run consisted of 18s of rest followed by 20s of pedaling and 20s of rest, repeated 5 times. Auditory cues were used to maintain a pedaling rate of 45 RPM and to cue subjects to pedal or rest. Auditory cues were provided during both pedaling and rest segments through MRI-compatible earbuds (model SRM 212, STAX, Ltd., Japan).

MRI data were obtained using a 3.0T MR scanner (General Electric Healthcare, Milwaukee, WI) and a single channel transmit/receive split head coil assembly (model 2376114, General Electric Healthcare). Functional images (T2*-weighted) were acquired using echoplanar imaging (repetition time (TR): 2000 ms, echo time (TE): 25 ms, flip angle: 77º, 36 contiguous slices in the sagittal plane, 64 x 64 matrix, 4 mm slice thickness, and field of view (FOV): 24 cm). The resolution of the images was 3.75 x 3.75 x 4 mm. Each run consisted of 109 TRs. Anatomical images (T1-weighted) were obtained using a 3D fast spoiled GRASS pulse sequence (TR: 8.2 ms, TE: 3.2 ms, flip angle: 12°, 256 x 244 matrix, resolution: 1 mm^3, and FOV: 24 cm). Audio cues were

synchronized with MR pulses using Presentation software (NeuroBehavioral Systems, Inc., Berkeley, CA). Rotary optical encoders (MR318, Micronor, Inc., Newbury Park, CA) recorded the pedaling position of each crankshaft, and fiber optic cables carried these signals to controller units (MR310, Micronor, Inc.). Position signals were sampled at 2000 Hz with a 16-bit analog-to-digital convertor and data acquisition software (micro 1401 mk II, Spike 2, Cambridge Electronic Designs, UK). To obtain pedaling velocity, position data were low pass filtered at 20 Hz, and the derivative was computed.

Analysis of Functional NeuroImages (AFNI) software was used to process fMRI data. 3D images were temporally aligned, and the first 4 TRs from each run were removed. All runs from a single condition were concatenated and registered to the bilateral uncoupled pedaling run adjacent to the anatomical scan. General linear modeling was used to fit a canonical hemodynamic response function (boxcar function convolved with a gamma function) to the measured blood-oxygenation-level dependent (BOLD) signal after pedaling stopped (Figure 4.1). Head movement was used as a variable of no interest. Model fitting was performed in each subject's native coordinate system to avoid misregistration caused by conversion to standard space. Noise smoothness was estimated using a spatial autocorrelation function, fit to a mixed model (Gaussian and mono-exponential functions), and used to blur functional data. To identify significantly active voxels at a familywise error rate of $P < 0.05$, we used Monte Carlo simulation to set an appropriate cluster size for a given individual voxel at $P < 0.005$. Voxels outside of the brain, negatively correlated voxels, and voxels with percent signal change greater than 10 were ignored. Head movement parameters were estimated.

D.3 Results

Representative images from all stroke and control subjects are shown in Figure D.1 and D.2 respectively. For every testing session, brain activation during conventional pedaling occurred in expected areas, including the primary motor and sensory cortices (M1S1), the supplementary motor area (SMA), and cerebellum (Cb). In contrast, during bilateral uncoupled pedaling, 8/9 stroke survivors and 1/2 control subjects had no detectable brain activation or a large reduction in brain activation. The stark drop in brain activation during this condition was considered to be not likely the result of actual task-related differences in brain activation.

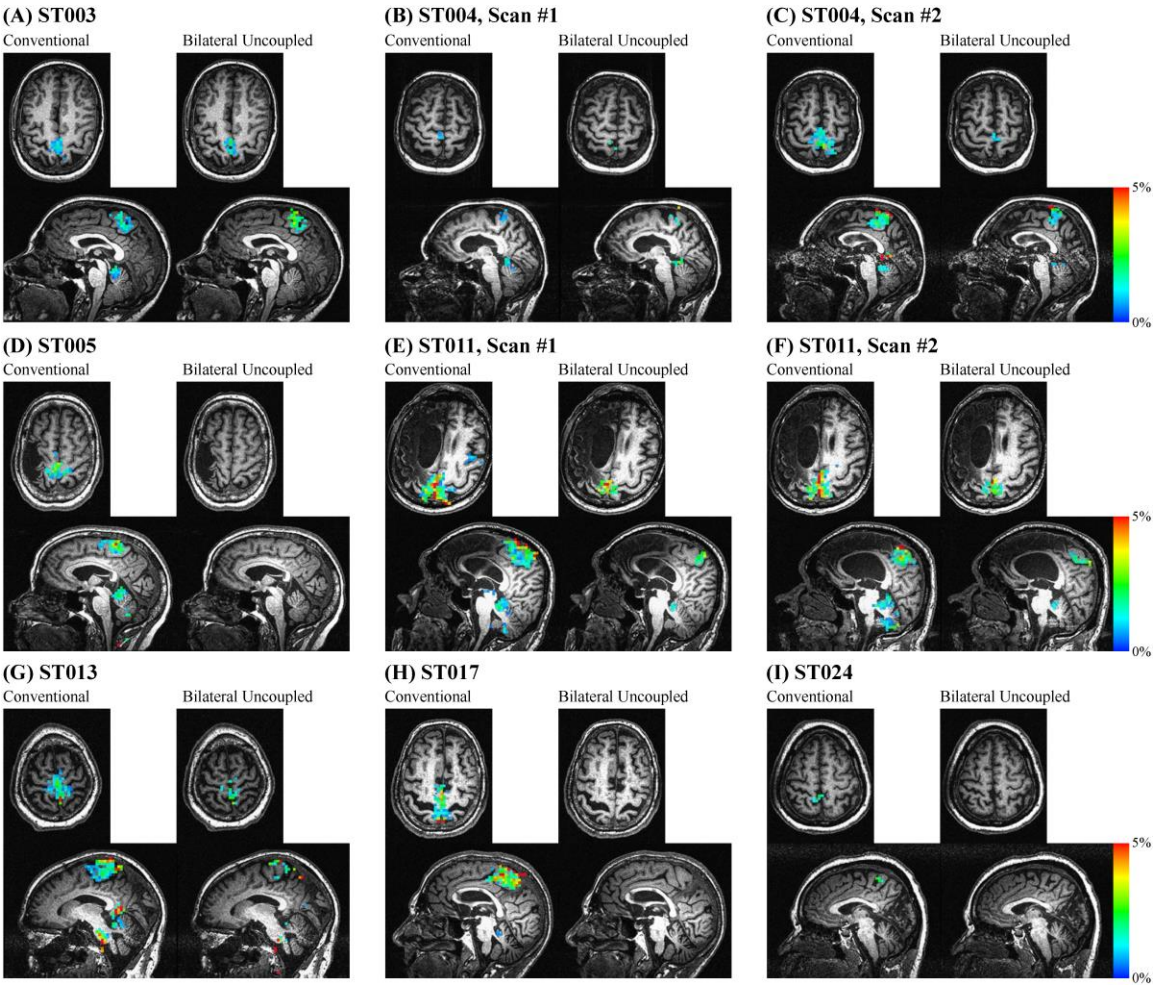

Figure D.1. Pedaling-related brain activation from all stroke subjects. fMRI activation during conventional and bilateral uncoupled pedaling. A single axial and sagittal slice is shown for each subject. Color scale represents percent signal change compared to rest (0-5%). In 8/9 of the subjects (B-I), brain activation was absent or markedly reduced during bilateral uncoupled as compared to conventional pedaling.

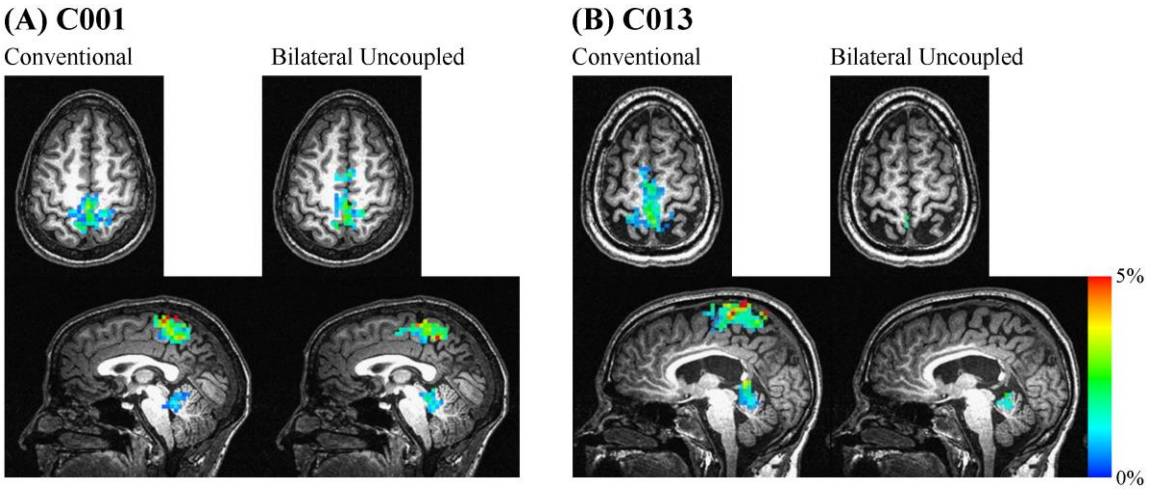

Figure D.2. Pedaling-related brain activation from both control subjects. fMRI activation during conventional and bilateral uncoupled pedaling. A single axial and sagittal slice is shown for both subjects. Color scale represents percent signal change compared to rest (0-5%). In one subject (B), brain activation was absent during bilateral uncoupled pedaling.

There are several issues that were detected during scanning and during processing that likely contributed to the absence or drop in brain activation during bilateral uncoupled pedaling. First, during four scanning sessions, scanning was automatically terminated by scanner software because of excessive movement of the scanning bed upon which the pedaling device rested. In all cases, this error occurred during or before the bilateral uncoupled pedaling condition. We determined that excessive body movement caused this excessive scanning bed movement. In the first subjects with whom we experienced this problem, we immediately restarted the scan. However, with later subjects, we reset the scanner positioning before resuming the scan. Additionally, after identifying this problem, we took proactive measures to secure the scanning bed to the entire scanning apparatus. In subjects where the scanner was not repositioned, we found a distinctive shift in the location of brain activation anteriorly during data processing (for example, see Figure D.3 A).

In five scanning sessions that showed a marked decline in brain activation, the scanning bed did not move. In these sessions, we evaluated the degree of head movement during scanning. During data processing, we detected several signs of misregistration resulting from excessive head movement, including the appearance of clusters of activation in non-brain regions or at the edges of the brain ("halo" effect). In these sessions, there was an average inferior-superior displacement of 3.0 (0.8) mm. We reasoned that this large amount of head movement led to our inability to detect an appropriate extent of brain activation during bilateral uncoupled pedaling.

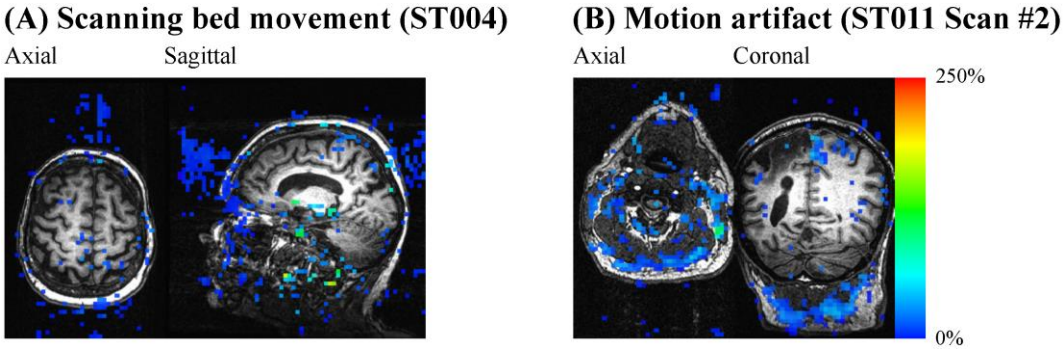

Figure D.3. Examples of misregistration of brain activation. Erroneous fMRI signal resulting from A) scanning bed movement and B) motion artifact. Color scale represents percent signal change compared to rest. Images show activation maps during an intermediate step of data processing. Specifically, data has been temporally aligned, concatenated, registered, modeled, and thresholded. Clustering and other voxel exclusion steps were performed after this intermediate step. Scanning bed movement led to the appearance of a large cluster anterior to the skull. Motion artifact led to the appearance of clusters in non-brain regions or at the edges of the brain ("halo" effect).

D.4 Discussion

Our results demonstrate that excessive head and body movement during bilateral uncoupled pedaling make it difficult to obtain realistic brain activation maps. 82% of the scanning sessions performed were marred by excessive movement of the scanning bed and/or of the head and body. Of the two successful scans, one was performed in one of

the highest functioning stroke survivors (lower extremity Fugl Meyer score of 92 out of 96), and the other was performed in a highly motivated control subject (the author of this dissertation, BTC). Based on these findings, we determined that obtaining sufficient fMRI data during bilateral uncoupled pedaling is not feasible in a substantial sample. Consequently, we discontinued data collection.

APPENDIX E: ASYMMETRICAL PEDALING

E.1 Introduction

Chapter 4 of this dissertation aimed to determine whether reduced pedaling-related brain activation post-stroke can be explained by compensation (altered volitional motor commands and pedaling performance) by comparing brain activation during volitional and passive pedaling. Appendix D addressed the same aim by comparing brain activation during conventional and bilateral uncoupled pedaling. Passive pedaling may provide limited insight into the relation between compensation and brain activation because motor commands during this task are fundamentally different from those during volitional pedaling. As described in Appendix D, excessive head and body movement during bilateral uncoupled pedaling made it unfeasible to measure brain activation during this task.

Because of the limitations of each of these approaches, I developed alternative strategies to address the relation between compensation and brain activation. Using the custom pedaling device (Figure 2.1), I sought to manipulate the degree of mechanical work symmetry during pedaling and measure brain activation. In stroke survivors, device manipulation would make mechanical work more symmetrical between the legs. In control subjects, device manipulation would make mechanical work asymmetrical. Taken together, device manipulation would make mechanical work symmetry more similar between the stroke and control group. We hypothesized that if compensation explains reduced pedaling-related brain activation post-stroke, then: 1) between-group differences would be reduced during pedaling with altered symmetry as compared to volitional

pedaling and 2) brain activation would be different between pedaling with altered symmetry and volitional pedaling. However, during protocol development, we encountered several setbacks in implementing these strategies. Ultimately, we were unable to test these hypotheses because of issues with achieving and measuring alterations in mechanical work symmetry. This appendix details the methods and results from this pilot study.

E.2 Methods

For all pilot work included in this appendix, testing was performed on four young control subjects. Thus, device manipulation aimed to make mechanical work asymmetrical between the limbs—decrease positive work and increase negative work in one limb. For this purpose, I tested three strategies during conventional pedaling: unilateral manipulation of eccentric loading, unilateral application of ankle foot orthoses (AFOs), and volitional production of asymmetry by the subject. The measurement of forces applied to each crank arm was critical to determining the symmetry (or asymmetry) of mechanical work production. For this purpose, non-magnetic strain gauges were affixed to both sides of the long axis of each crank arm (Figure E.1). These strain gauges measured forces applied perpendicularly to the crankshaft (bending), which rotate the crankshaft.

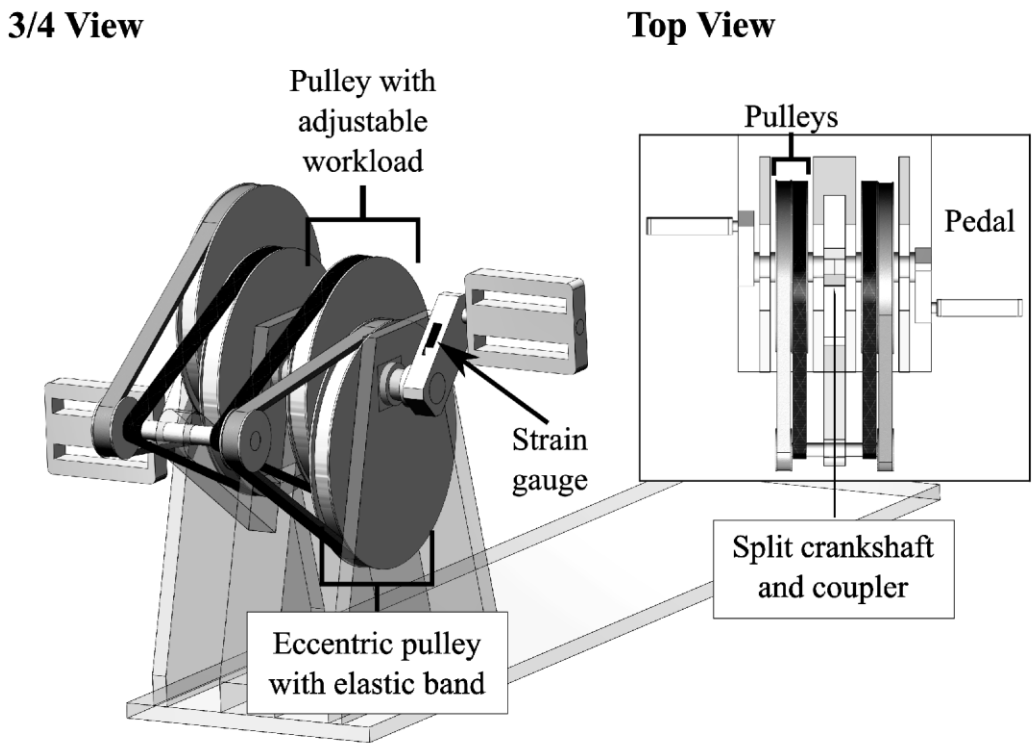

Figure E.1. Pedaling device with a split crankshaft and strain gauges. Depicted is the same device shown in Figure 2.1, but with strain gauges affixed to both sides of each crankshaft (only one is shown). The top view depicts the split crankshaft and coupler. For this testing, the coupler was in place to allow conventional pedaling. The ¾ view depicts the pulley systems of the pedaling device. A pulley with adjustable workload was used to provide frictional resistance. An eccentric pulley system with elastic bands was used to apply additional loading to one limb during conventional pedaling.

The first strategy I used to produce asymmetrical mechanical work production was the unilateral application of eccentric loading during conventional pedaling. As discussed in Chapter 2, during the downstroke of pedaling, an elastic band was stretched by the eccentric pulley, applying a resistive load. Energy stored in the elastic band during the downstroke was released during the upstroke to help return the leg towards the body. In our previous usage, the eccentric pulley was used when the split crankshaft was uncoupled (i.e. unilateral and bilateral uncoupled pedaling). Conversely, during this pilot testing, we applied the eccentric loading unilaterally during conventional pedaling. Theoretically, we expected that the unilateral application of eccentric loading would

increase the resistance during the downstroke of the ipsilateral limb (and thus increase positive work) and aid the return of the ipsilateral limb during the upstroke (and thus decrease negative work). In the contralateral limb, the resistance during the downstroke should be decreased, and the resistance during the upstroke should be increased. Thus, we expected that this would elicit asymmetry by manipulating the work production of both limbs in opposite directions. Subjects performed three trials of conventional pedaling with different levels of unilateral eccentric loading.

The second strategy I used to produce asymmetrical mechanical work production was to apply an AFO unilaterally. AFOs were used in Chapter 4 to help reduce muscle activation during passive pedaling. Additionally, from personal experience, the perceived effect of an AFO applied unilaterally is to restrict the ability to produce force with the ipsilateral limb. Theoretically, we expected that the unilateral application of eccentric loading would decrease the positive work production of the ipsilateral limb during downstroke, and there would be a compensatory increase in the net work production of the contralateral limb. Subjects performed two trials of conventional pedaling with an AFO on the right and left leg.

The third strategy I used to produce asymmetrical mechanical work production was to ask subjects to pedal asymmetrically using their volitional effort. Subjects were told to try to pedal primarily with the right leg and minimize use of the left leg. Essentially, they were asked to produce volitional pedaling with the right leg and passive pedaling with the left leg. Theoretically, we expected that subjects would be able to pedal in this manner, yielding asymmetrical mechanical work production between the limbs.

Subjects performed two trials of volitional asymmetrical pedaling—one with volitional pedaling in the right leg and one with volitional pedaling in the left leg.

For each of these strategies, subjects performed 60 second pedaling bouts. The pedaling position of the coupled crankshaft was measured with rotary optical encoders (MR318, Micronor, Inc., Newbury Park, CA). Fiber optic cables carried position signals to controller units (MR310, Micronor, Inc.). For each crank arm, the zero position was defined as where the crank arm was parallel to the plinth and the foot was closest to the hip (top dead center, 0°). The amount of force applied to each crank arm was measured with the custom designed strain gauges affixed to each crank arm. Fiber optic cables carried force signals to custom controller units. Position and force signals were sampled at 2000 Hz with a 16-bit analog-to-digital convertor and data acquisition software (micro 1401 mk II, Spike 2, Cambridge Electronic Designs, UK). Forces were converted to torque, ensemble averaged, and crank referenced.

The strain gauges used to measure torques were custom-designed and had not been previously used. Consequently, we went through procedures to calibrate and test the accuracy and consistency of these gauges. We also developed procedures to allow us to consider only the portion of the torque not caused by external factors (i.e. non-zero baseline, gravity, and off-axis strain).

E.3 Results

Asymmetrical pedaling strategies

Torque profiles resulting from each strategy for producing asymmetrical mechanical work production are shown in Figure E.2. (A and B) show torque profiles

resulting from unilateral application of eccentric loading. This strategy generally resulted in an increase in positive work in the ipsilateral limb, but also a concomitant increase in negative work. In the contralateral limb, positive work decreased, but negative work also decreased. As shown in Figure E.2. (B), this effect generally scaled with the amplitude of eccentric loading. Figure E.2 (C) shows torque profiles resulting from unilateral application of an AFO. This strategy had little effect on the torque produced by either limb. The effect that did occur was an increase in the positive work produced by each limb, and no change in the negative work. Figure E.2 (D) shows torque profiles resulting from asymmetrical pedaling through volitional effort. Generally, this strategy increased the positive work and decreased the negative work in the ipsilateral limb. In the contralateral limb, positive work decreased, and negative work increased.

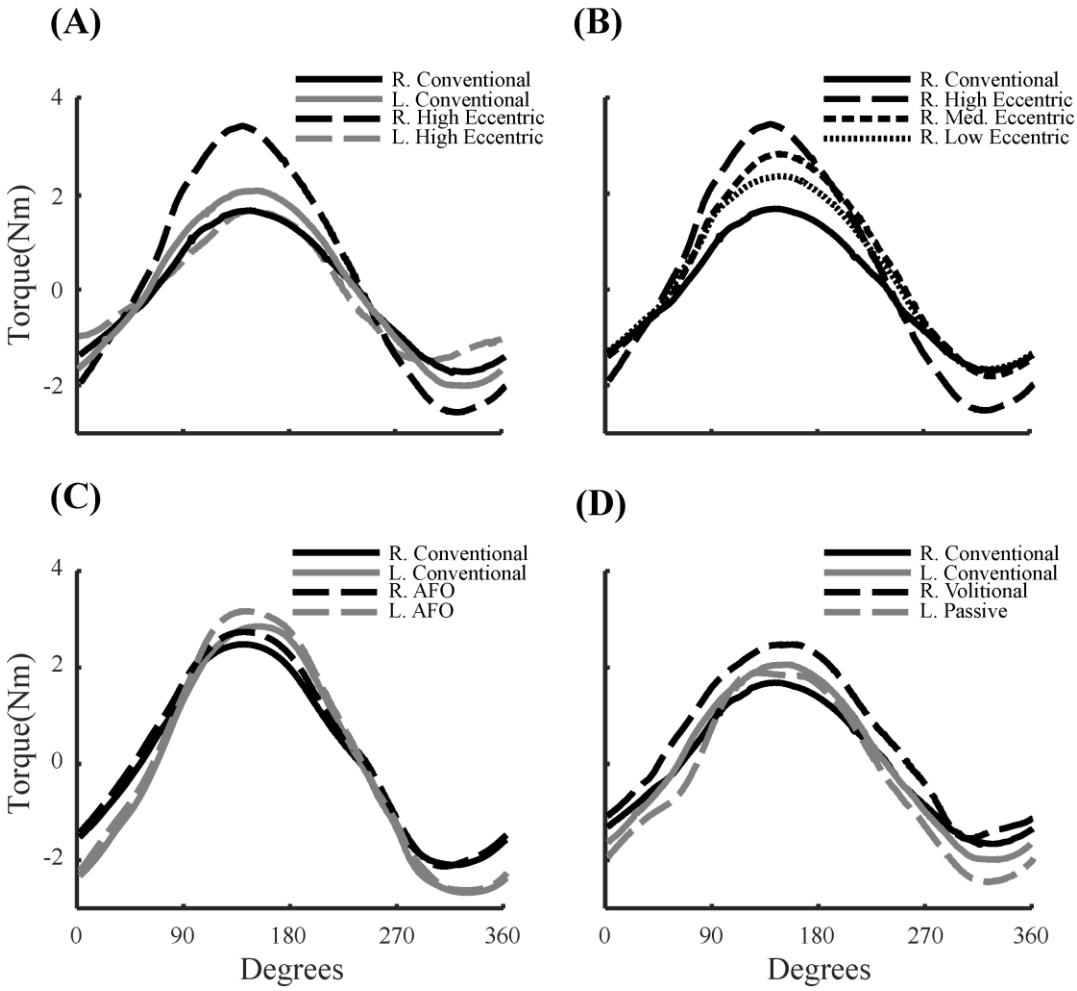

Figure E.2. Torque profiles of methods to produce asymmetric loading. In all subfigures, torque produced by both legs during conventional pedaling is represented by solid lines. (A) Torque produced when a high eccentric load was applied to the right side of the bike (long dash). Both positive and negative work increased in the ipsilateral limb and decreased in the contralateral limb. (B) Torque produced when a high (long dash), medium (medium dash), and low (short dash) eccentric load was applied to the right side of the bike. The changes in mechanical work scaled with the amplitude of loading. (C) Torque produced when an AFO was worn on the right leg (long dash). Positive work increased in both the ipsilateral and contralateral limb, and negative work was unaffected. (D) Torque produced when the subjects were asked to pedal with the right leg and relax the left leg (long dash). Positive work increased, and negative work decreased in the ipsilateral limb. Positive work decreased, and negative work increased in the contralateral limb.

E.4 Discussion

Overall, the most effective strategy for producing asymmetrical pedaling in controls was to ask them to pedal asymmetrically. This strategy led to increased positive work and decreased negative work in the ipsilateral limb, and vice versa in the contralateral limb. The application of unilateral eccentric loading was effective at increasing the positive work in the ipsilateral limb and decreasing the positive work in the contralateral limb. But, this strategy also increased negative work in the ipsilateral limb and decreased negative work in the contralateral limb. Consequently, this strategy was not able to reproduce the torque profiles generally seen in stroke survivors (Kautz & Brown, 1998). The application of and AFO unilaterally had the smallest effect, and generally increased positive work of both limbs.

Although we found that volitional asymmetric pedaling could produce asymmetrical pedaling as desired, problems with our measurement device made this strategy unfeasible. The major problem we experienced that led to the abandonment of this project were issues with the accuracy and reliability of the strain gauges on the pedaling device. This was a requirement for demonstrating that our acute manipulations of the pedaling device actually altered work symmetry. In order to optimize our measurements, we accounted for the portion of the strain gauge signal resulting from a non-zero baseline, the effects of gravity, and deformations of the strain gauges caused by compression or lengthening of the long axis of the strain gauge. These procedures are detailed in the master's project of Sam Wojcinski.

However, after accounting for these factors, there was a large amount of within-session variability in strain gauge output. As a result, changes in torque associated with

any of the interventions were within the 95% confidence interval of the nominal conventional pedaling condition. A full description of the problems associated with this high amount of variability are beyond the scope of this appendix. Briefly, one of the primary problems was that current to the strain gauges was not constant and dropped steadily throughout an experiment. Because of our inability to demonstrate a change in the pedaling work performed by each limb, this pilot project was abandoned. In the future, improvements in the strain gauge system and relevant circuitry may reduce variability and allow a continuation of this project.